Study on Pharmacokinetic and Nanocarrier Formulation Approaches for Improving the Oral Bioavailability of Tenofovir Disoproxil Fumarate in the Effective Treatment of HIV/AIDS

THESIS

Submitted in partial fulfilment

of the requirements for the degree of

DOCTOR OF PHILOSOPHY

by

SHAILENDER JOSEPH

ID. No. 2011PHXF019H

Under the Supervision of

Prof. PUNNA RAO RAVI

BITS Pilani

Pilani | Dubai | Goa | Hyderabad

BIRLA INSTITUTE OF TECHNOLOGY AND SCIENCE

PILANI (RAJASTHAN) INDIA

2017

BIRLA INSTITUTE OF TECHNOLOGY AND SCIENCE

PILANI (RAJASTHAN)

CERTIFICATE

This is to certify that the thesis entitled **"Study on Pharmacokinetic and Nanocarrier Formulation Approaches for Improving the Oral Bioavailability of Tenofovir Disoproxil Fumarate in the Effective Treatment of HIV/AIDS"** submitted by **SHAILENDER JOSEPH**, ID.No:2011PHXF019H for award of Ph.D. Degree of the institute embodies original work done by him under my supervision.

Date: **Signature in full of the Supervisor**_____

Name in capital Block letters: **Prof. PUNNA RAO RAVI**

Designation : Associate Professor

ACKNOWLEDGEMENT

The constant support and guidance provided by my mentor and guide, Prof. Punna Rao Ravi, Associate Professor, Department of Pharmacy, BITS-Pilani, Hyderabad Campus is the reason why I was able to take up the current thesis work and successfully complete it. The work was quite challenging and there were many situations where I felt that I have hit a wall. It was at moments like these that the technical advises and guidance provided by my guide helped me overcome such obstacles. Under him the learning, creative thinking and troubleshooting abilities that I gained were phenomenal. However, there is still a long way for me to go to reach to a place where he currently is, but, I hope to reach there someday. I was able to freely interact with him without any inhibitions because of his ability to break the hierarchies and create an atmosphere of equality, this greatly helped me and also my work because the discussions we had were honest and creative. Apart from his boundless enthusiasm coupled and sharp intellectual abilities he also has a very strict and uncompromising moral and ethical code of conduct which is a very rare quality and I hope to imbibe that in me in due course of time. It has been a great honour and privilege for me to be working under him, for which I am grateful.

It is my duty to express my sincere thanks to the Chancellor, BITS-Pilani for providing necessary infrastructural support to carry out my research work. I am thankful to Prof. Souvik Bhattacharyya, Vice Chancellor, BITS-Pilani for facilitating my research work at the institute. I am also thankful to Prof. G. Sundar, Director, BITS-Pilani, Hyderabad Campus for his support during the course of my stay at this campus. I am thankful to Prof S.K. Verma, Dean, Academic Research Division, BITS-Pilani, and Prof. Vidya Rajesh, Professor-in-charge, Academic Research (PhD Program) division, BITS-Pilani, Hyderabad Campus., for their co-operation and encouragement at every stage of this research work.

I am thankful to Dr. D. Sriram, Head, Department of Pharmacy for providing me with all the laboratory facilities and moral support during the course of my stay at the campus.

My special thanks to my doctoral advisory committee members (DAC) Dr. V Vamsi Krishna Venuganti and Dr. Swati Biswas for their unconditional and constant support. Both of them never hesitated to help and provide critical input whenever I needed.

I sincerely acknowledge the help provided by other faculty members, Prof. P. Yogeeswari, Prof. Sajeli Begum, Dr. Arti Dhar, Dr. Balaram Ghosh and Dr. Onkar Kulkarni for sharing their vast experience and technical knowledge with me at needy times.

I am also grateful to the non-teaching staff, Mrs. Saritha, Mr. Rajesh, Mr. Ramu, Mr. Srinivas and Mrs. Rekha for their support in maintaining the supply of chemicals, glassware and animals during the course of my research work.

I very grateful to my colleagues and friends, Ms. Avantika Dalvi, Mrs. Rimpy Diwan, Ms. Ekta Prasanthi, Mr. Chandra Teja Uppuluri and many others for their invaluable support, encouragement and help at all times. They have been extremely patient and bearing with me and have helped in gaining a lot through mutual exchange of knowledge. Their constructive criticism and technical inputs have been invaluable for my work. I also thank my seniors Dr. Aditya N. Murty, Dr. Rahul Vats and Dr. Praveen Kumar Mandapalli who provided a lot of support and guidance during their stay in BITS-Pilani, Hyderabad Campus.

The undergraduate and postgraduate students of pharmacy department deserve a special mention here. I cannot forget the help rendered by our students, Ms. Shruthi Antireddy, Ms. Keerthi Priya Odapalli, Ms. Srividya Myneni, Ms. Mrinalini Reddy, Ms. Paramita Saha, Mr. Uday Sai Ranjan, Mr. Shaik Ashiff and Mr. Karthik Bhattiprolu.

I acknowledge the help of Council for Scientific and Industrial Research (CSIR) for providing independent Senior Research Fellowship (SRF) to pursue doctoral studies.

I would like to thank Prof. R.N. Saha, Director, BITS-Pilani, Dubai Campus, he was my B.Pharm and M.Pharm project guide and played a very crucial role in identifying my interests and in choosing my career path.

A special thanks to Dr. Shrikant Y Charde and Dr. Meghana Charde, who were always concerned about my thesis work. They provided a lot of encouragement and positivity to me at very testing times which helped me come out my inertia and move forward.

I would also like to thank Dr. Vimal Bhanot and Dr. Surekha Bhanot who have been my life guides since my B.Pharm. My interaction with them has expanded my horizons which also helped me to have an out of the box approach to the challenges that I faced during my PhD. Their daughter Dr. Disha Bhanot is like elder sister to me, she provided a lot emotional support and guidance to me at several occasions. Her husband Dr. Debabrata Das has always been a well-wisher and a source of inspiration to me.

As Albert Einstein puts it “It is the supreme art of the teacher to awaken joy in creative expression and knowledge”. Hence, I would like to take this opportunity to thank all my teachers and activists right from my schooling for awakening this joy in me.

This section would be incomplete without thanking my family for their unwavering support throughout this period. My heartfelt thanks to my parents, Mr. Tony Joseph and Mrs. G. Renuka Devi for being pillars of my life and for providing me with moral support at all times. Even though they do not have the technical know-how of my field they still tried their best to listen and understand my problems so that I can clearly define my challenges which greatly helped me to develop an approach to overcome them. I also thank my younger brother Mr. Shashidhar C Joseph who is autistic and Ms. Arunima (daughter of Prof. Shrikant Y Charde), they always made me forget the difficulties of life and forced me to be present in the current moment and cherish it!

Shailender Joseph

List of Tables

List of Figures

List of Abbreviations and Symbols	
%RSD	Percentage relative standard deviation
%TDF remaining	The percentage of TDF remaining to be metabolized
%TMF formed	The percentage of TMF formed when compared to control (i.e. free TDF)
°C	Degree Celsius
µg	Micro gram
µL	Micro litre
µm	Micro meter
µM	Micro molar
2θ	X-ray scattering angle
A	Area
Å	Angstrom
ADME	Absorption, distribution, metabolism and elimination
AIDS	Acquired immune deficiency syndrome
ANOVA	Analysis of variance
AUC	Area under the curve
$AUC_{0\text{-}6h}$	Area under the curve for 0 to 6 hours
AUC_{Total}	Total area under the curve
BBD	Box-behnken design
BBJ	Blueberry juice
BCJ	Black cherry juice
CBJ	Cranberry juice
C_{crit}	Critical value of Cochran's C test
CD4	Cluster of differentiation 4
C-EL	Cremophor EL
CES	Carboxylesterase
C_{expt}	Experimental value of Cochran's C test

CGJ	Concord grape juice
CI	Confidence interval
CLs	Clearance
cm	Centimetre
C_{max}	Maximum plasma concentration
CO_2	Carbon dioxide
cps	Centipoise
CPZ	Chlorpromazine
CS	Chitosan
CS NPs	Chitosan based nanoparticles
CYP	Cytochrome P450
DCM	Dichloromethane
DMSO	Dimethyl sulfoxide
DNA	Deoxyribonucleic acid
DoE	Design of experiments
DPBS	Dulbecco's phosphate-buffered saline
DSC	Differential scanning calorimetry
EE%	Entrapment efficiency
ER	Endoplasmic reticulum
F_{abs}	Absolute bioavailability
FJs	Fruit juices
F_{rel}	Relative bioavailability
g	Gram
GAA	Glacial acetic acid
Gag	Group-specific antigen
Gag-pol	Group-specific antigen polyprotein
h	Hours

HAART	Highly active antiretroviral therapy
HIV	Human immunodeficiency virus
HPLC	High-performance liquid chromatography
HQC	High quality control
IAEC	Institutional animal ethics committee
ICH	International council of harmonization
ip	Intraperitoneal
IV	Intravenous
J	Flux
kDa	Kilo Dalton
kg	Kilogram
kV	Kilo volts
L	Litre
LDL	Low-density lipoprotein
LLE	Liquid-liquid extraction
LOD	Limit of detection
Log P	Logarithm of partition coefficient
LOQ	Limit of quantitation
LQC	Lower quality control
M	Molarity
m/z	Mass to charge ratio
MDR	Multiple drug resistance
mg	Milligram
min	Minute
mL	Millilitre
mM	Millimolar
mm	Millimetre

mol	Moles
MQC	Middle quality control
MRP-2	Multidrug resistance-associated protein 2
MRT	Mean residence time
ms	Millisecond
MS-MS	Tandem mass spectrometry
MTT	3-(4,5-dimethylthiazol-2-yl)-2,5-diphenyltetrazolium bromide
mV	Millivolts
MWCO	Molecular weight cut off
n	Number of replicates
NaCl	Sodium chloride
ng	Nanogram
nm	Nanometer
NPs	Nanoparticles
NtRI	Nucleotide reverse transcriptase inhibitors
NYS	Nystatin
O/O	Oil in oil
O/W	Oil in water
O_2	Oxygen
OJ	Orange juice
PBD	Placket-Burmann design
P_{cal}	Calculated *P* value
P_{crit}	Critical *P* value
PDI	Polydispersity index
pH	Potential of hydrogen
PJ	Pomegranate juice
PLGA	Poly(lactic-co-glycolic acid) – lactide:glycolate::50:50

pmol	Pico moles
PS	Particle size
PVA	Polyvinyl alcohol
pXRD	Powder X-ray diffraction
R^2	Regression coefficient
RGFJ	Ruby red grapefruit juice
RH	Relative humidity
RNA	Ribonucleic acid
rpm	Rotations per minute
s	Slope
SD	Standard deviation
SLLE	Salting out-assisted liquid-liquid extraction
STPP	Sodium tripolyphosphate
$T_{1/2}$	Elimination half life
TDF	Tenofovir disoproxil fumarate
TDF loaded CS NPs	Tenofovir disoproxil fumarate loaded chitosan nanoparticles
TDF loaded PLGA NPs	Tenofovir disoproxil fumarate loaded PLGA nanoparticles
T_{max}	Time taken to reach maximum plasma concentration
TMF	Monoester form of tenofovir
TNF	Tenofovir
USP	United States Pharmacopoeia
UV	Ultraviolet
v/v	Volume by volume
Vit E TPGS	d-α-Tocopheryl polyethylene glycol 1000 succinate
Vss	Volume of distribution
W/O	Water in oil
w/v	Weight by volume

$W_{free\ TDF}$	Amount of TDF determined in the filtrate
WHO	World health organization
$W_{total\ TDF}$	Amount of TDF added during the preparation of NPs
σ	Standard deviation of the intercepts

Abstract

Tenofovir disoproxil fumarate (TDF) is the only FDA approved nucleotide reverse transcriptase inhibitor. It is an integral part of highly active anti-retroviral therapy used in the treatment of HIV-AIDS. TDF is a diester prodrug of tenofovir (TNF), it exhibits low oral bioavailability (~ 25%) and high inter-patient variability in humans due to its susceptibility to esterases present in the GIT. The esterases convert TDF to its monoester form (TMF) which has relatively poor absorption characteristics, this leads to a decrease in the overall oral bioavailability of TDF. The objective of this work was to explore the pharmacokinetic and nanocarrier formulation approaches that can be used for enhancing the oral bioavailability of TDF.

In order to achieve the broader objective of this work, analytical methods were developed for TDF, TMF and TNF and bioanalytical method was developed for TNF. These methods were validated for accurate and precise estimation of the analyte in both bulk formulations, *in vitro* release studies samples and biological samples. The applicability of the bioanalytical method for conducting pharmacokinetic studies was also established.

The role of intestinal esterases on the absorption process of TDF was evaluated. The esterase inhibition capacity of fruit juices (FJs) rich in ester linkages and pharmaceutical excipients (having ester bonds) was performed *in vitro* by incubating TDF with each FJ and excipient in the intestinal washings. The *ex vivo* everted gut sac model was also used to evaluate the absorption enhancement capacity of these FJs and excipients. Single dose oral pharmacokinetic studies were performed by concomitant administration of TDF with each of the selected FJs and excipients. The *in vitro* and *ex vivo* studies showed that cremophor-EL and all FJs prevented the metabolism of TDF with grapefruit juice (GFJ) having the highest level of inhibition. Further, the permeability flux of the TMF was significantly increased by cranberry

juice (CBJ) pomegranate juice (PJ), GFJ and ruby red grapefruit juice (RGFJ). The *in vivo* studies also showed that these four FJs significantly enhanced the oral bioavailability of TDF with GFJ and PJ having the most prominent impact. These results indicate that the prevention of the metabolic conversion of TDF to its monoester form is crucial in increasing the oral absorption of TDF.

In the nanocarrier formulation approaches, chitosan and PLGA based polymeric nanoparticles were developed for improving the oral delivery of TDF. Manufacturing conditions for the formulations were optimized using design of experiments approach. Hybrid designs were used to get a better understanding of the factors affecting properties of nanoparticles like particle size and drug entrapment efficiency. The interaction effect of the critical process/formulation factors on the responses was also evaluated which was later used to develop an optimized formulation. The Optimized formulations were subjected to extensive physical characterization studies and pharmacokinetic evaluation (after oral administration) of the nanoparticles was also performed in male Wistar rats. Further, mechanistic studies in the presence of various cell uptake inhibitors like Chlorpromazine and Nystatin were performed to decipher the mechanisms involved in the intestinal uptake of these nanocarriers.

In both the cases, the developed nanocarrier systems were stable under accelerated conditions. A significant improvement in oral bioavailability of TDF was noticed. However, PLGA based nanoparticles showed a higher degree of oral absorption enhancement of TDF when compared to CS based nanoparticles. The significant improvement in oral bioavailability was attributed to protection of entrapped TDF from intestinal esterase metabolism and improvement in both active and passive uptake of TDF from the GIT.

Chapter 1

Introduction

1. Introduction

1.1 Human immunodeficiency virus and AIDS

Human immunodeficiency virus (HIV) is a lentivirus (genus) that belongs to retroviridae family (Barasa, 2011), this virus when infects an individual causes acquired immunodeficiency syndrome (AIDS). It is a condition in which the immune system fails progressively making the individual susceptible to life threatening opportunistic infections and cancers (Jayaraman & Shah, 2008). This infection occurs by transfer of body fluids like blood, semen, vaginal fluid, pre-ejaculate and breast milk; in these fluids, the virus is present as free virus particles and also in the infected cells (Hilleman, 1995).

This virus brings about the autodestructive immune response of the host immune system by mainly targeting helper T cells (specifically CD4+ T cells of the blood and lymphoid tissues), macrophages and dendritic cells. HIV virus is characterized into two subtypes HIV-1 and HIV-2, of which, the former is more virulent, infective and widespread (Hilleman, 1995).

1.2 Life cycle of HIV

The process of HIV infection (fig. 1.1) begins when the surface envelope glycoprotein gp120 of the virion binds to CD4 cells and interacts with the coreceptor. A membrane fusion reaction is triggered by the transmembrane envelope glycoprotein gp41. This glycoprotein is present between the lipid bilayer of the virion and the host cell plasma membrane. The fusion of the virion and the cell membrane cause the release of the viral core into the cytoplasm. The viral core uncoats and releases a high-molecular-weight complex (referred to as preintegration complex) which is reported to consist of Gag proteins p17 matrix, p7 nucleocapsid, the pol-encoded enzymes i.e. integrase and reverse transcriptase, and the viral protein R. Also, during this uncoating process, reverse transcription of the viral ribonucleic acid (RNA) to generate a double-stranded deoxyribonucleic acid (DNA) is completed. The preintegration complex is

transported across the nuclear membrane where the nucleus, the viral DNA integrates into the host cell chromosome, this process is catalyzed by integrase.

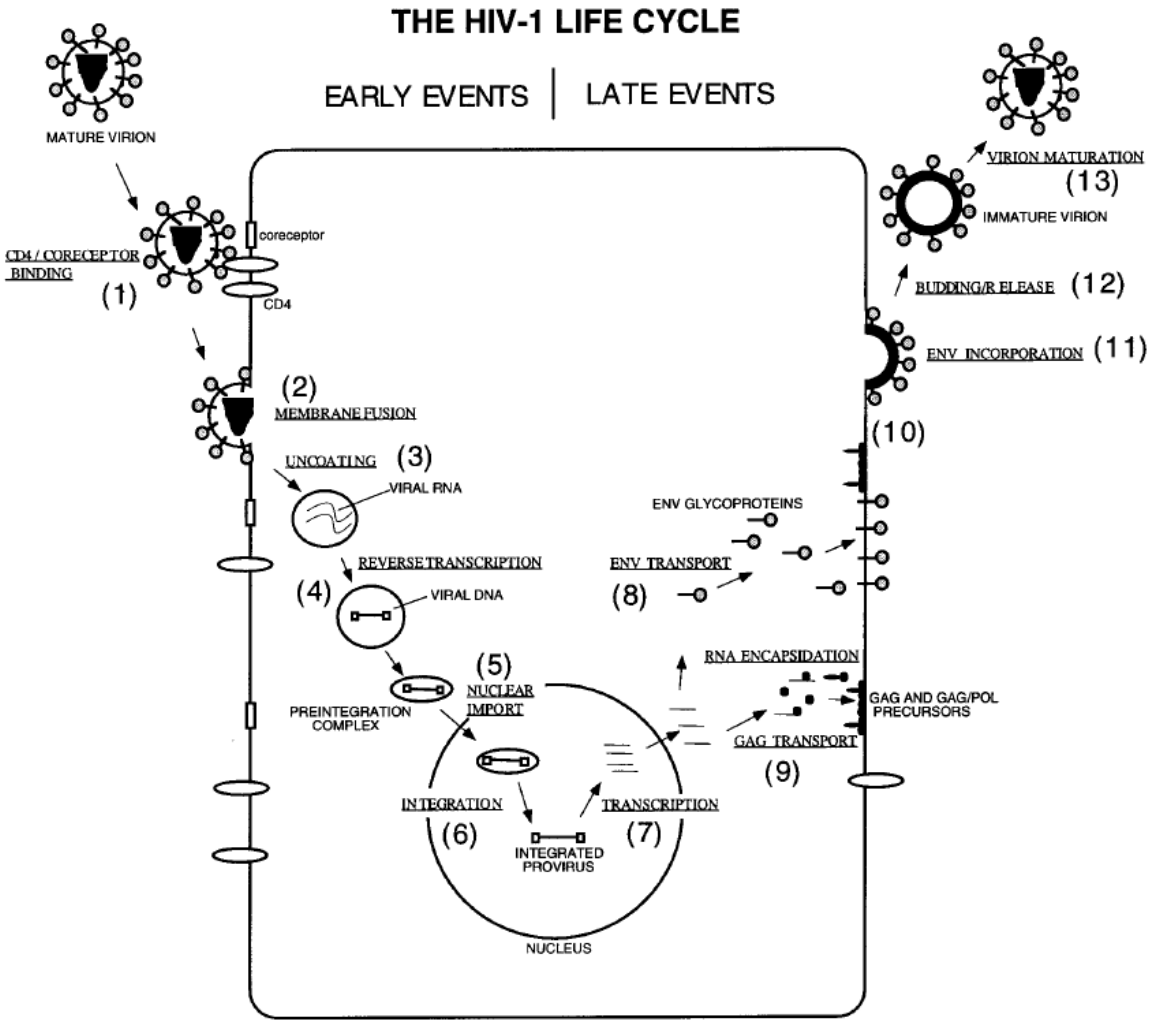

Fig. 1.1: Life cycle of HIV-I. Figure source: Freed, E. O. (1998). HIV-1 Gag Proteins: Diverse Functions in the Virus Life Cycle. *Virology*, *251*(1), 1–15.

The integrated viral DNA is called as the provirus and this acts as a template for the synthesis of viral RNAs, which are then transported to the cytoplasm. This leads to the synthesis of envelope glycoproteins in the endoplasmic reticulum which are transported to the plasma membrane via the secretory pathway. The Gag and Gag-pol polyprotein precursors are synthesized and transported to the plasma membrane. During this process, the Gag precursor recruits two copies of the single-stranded viral RNA genome, interacts with the Gag-pol

precursor, and assembles into structures which look like dense patches lining the inner face of the plasma membrane. The assembled Gag protein complex induces membrane curvature, leading to the formation of a bud. During budding, the viral envelop glycoproteins are incorporated into the nascent particles. The budding process is completed when the particle pinches off from the plasma membrane. The viral protease cleaves the Gag and Gag-pol polyprotein precursors to the mature Gag and Pol proteins. Protease cleavage leads to core condensation and the generation of a mature, infectious virion which is now capable of initiating a new round of infection (Freed, 1998; Rambaut, Posada, Crandall, & Holmes, 2004).

1.3 Prevalence of HIV-AIDS

Globally, 36.7 million people are infected with HIV by 2015 and 2.1 million people were newly infected with HIV in 2015 alone (table 1.1).

Table 1.1: Global prevalence of HIV-AIDS: Figure source: (UNAIDS/WHO AIDS epidemic update: 2016).

	People living with HIV (all ages)–in millions		New HIV infections (all ages)–in millions	
	2010	2015	2010	2015
Global	33.3 (30.9–36.1)	36.7 (34.0–39.8)	2.2 (2.0–2.5)	2.1 (1.8–2.4)
Asia and Pacific	4.7 (4.1–4.5)	5.1 (4.4–5.9)	0.31 (0.27–0.36)	0.3 (0.24–0.38)
Eastern and southern Africa	17.2 (16.1–18.5)	19.0 (17.7–20.5)	1.1 (1.0–1.2)	0.96 (0.83–1.1)
Eastern Europe and central Asia	1.0 (0.95–1.1)	1.5 (1.4–1.7)	0.12 (0.11–0.13)	0.19 (0.17–0.2)
Latin America and the Carribean	1.8 (1.5–2.1)	2.0 (1.7–2.3)	0.1 (0.086–0.12)	0.1 (0.086–0.12)
Middle East and North Africa	0.19 (0.15–0.24)	0.23 (0.16–0.33)	0.02 (0.015–0.029)	0.021 (0.012–0.037)
Western and central Africa	6.3 (5.2–7.7)	6.5 (5.3–7.8)	0.45 (0.35–0.56)	0.41 (0.31–0.53)
Western and central Europe and North America	2.1 (1.9–2.3)	2.4 (2.2–2.7)	0.092 (0.089–0.097)	0.091 (0.089–0.097)

Asia, home to 60% of world's population is only second to Sub-Saharan Africa in terms of the number of people living with HIV. In Asia, by the end of 2015, 5.1 million people were living

with this infection; India alone accounts for 49% of these people which comes to approximately 2.1 million. Among them, only 35% are reported to be receiving antiretroviral therapy. World Health Organization (WHO) puts India in the concentrated category. The spread of HIV in India has been uneven. The highest HIV prevalence rates are found in Andhra Pradesh, Maharashtra, Tamil Nadu and Karnataka in the south; and Manipur and Nagaland in the north-east (UNAIDS/WHO AIDS epidemic update: 2016).

1.4 Current treatment methods for HIV-AIDS

Most of the antiretroviral drugs work by targeting critical viral proteins at different stages of the viral life cycle (fig. 1.2). These drugs majorly belong to four categories which are as follows:

1.4.1 Nucleoside/nucleotide reverse transcriptase inhibitors

They are the analogs of naturally occurring deoxynucleosides/nucleotides but lack the 3'-hydroxyl group on the sugar moiety. These analogs are phosphorylated into their active triphosphate form by cellular kinases, the active form when incorporated in the growing viral DNA chain terminates the synthesis of the viral DNA thereby inhibiting the reverse transcription process (Kumari & Singh, 2012). This class of drugs consists of zidovudine, stavudine, didanosine, zalcitabine, lamivudine, abacavir, tenofovir etc.

1.4.2 Non-nucleoside reverse transcriptase inhibitors

This class of compounds, unlike the nucleoside/nucleotide reverse transcriptase inhibitors, interacts with reverse transcriptase by non-competitively binding to its allosteric site. This binding causes a conformational change in the structure of reverse transcriptase and disrupts the catalytic site of the enzyme (Temesgen, Warnke, & Kasten, 2006). Drugs like nevirapine, efavirenz and delavirdine belong to this class.

1.4.3 Protease inhibitors

Protease inhibitors act by inhibiting the HIV-1 protease. This enzyme is responsible for the cleavage of large polypeptides into functional proteins which allows the maturation of HIV virion, this process occurs in the final stages of the viral life cycle. Hence, inhibition of protease enzymes leads to the release of nonfunctional and harmless viral particles thereby, preventing the propagation of the virus into new cells (Phillips, 1996). Members of this class of drugs include nelfinavir, ritonavir, saquinavir, indinavir, lopinavir and amprenavir.

1.4.4 Entry/Fusion inhibitors

Fusion inhibitors target this process of fusion that takes place between glycoprotein gp 120 of the virion and the CD4+ receptor present on the host cell. Hence, they inhibit the entry of the viral capsid into the host cell (Esté & Cihlar, 2010). Currently, maraviroc and enfuvirtide are the only fusion inhibitors in the market but, other potential members of this class are in development.

1.4.5 Integrase inhibitors

This is a relatively newer class of compounds, which are also known as standard transfer integrase inhibitors. These molecules inhibit the activity of the integrase enzyme which is responsible for integrating the viral DNA strand into the host chromosome (McColl & Chen, 2010). Currently, dolutegravir, elvitegravir and raltegravir are the three integrase inhibitors in the market. However, there are few more molecules (bictegravir, cabotegravir etc.,) that are undergoing clinical trials.

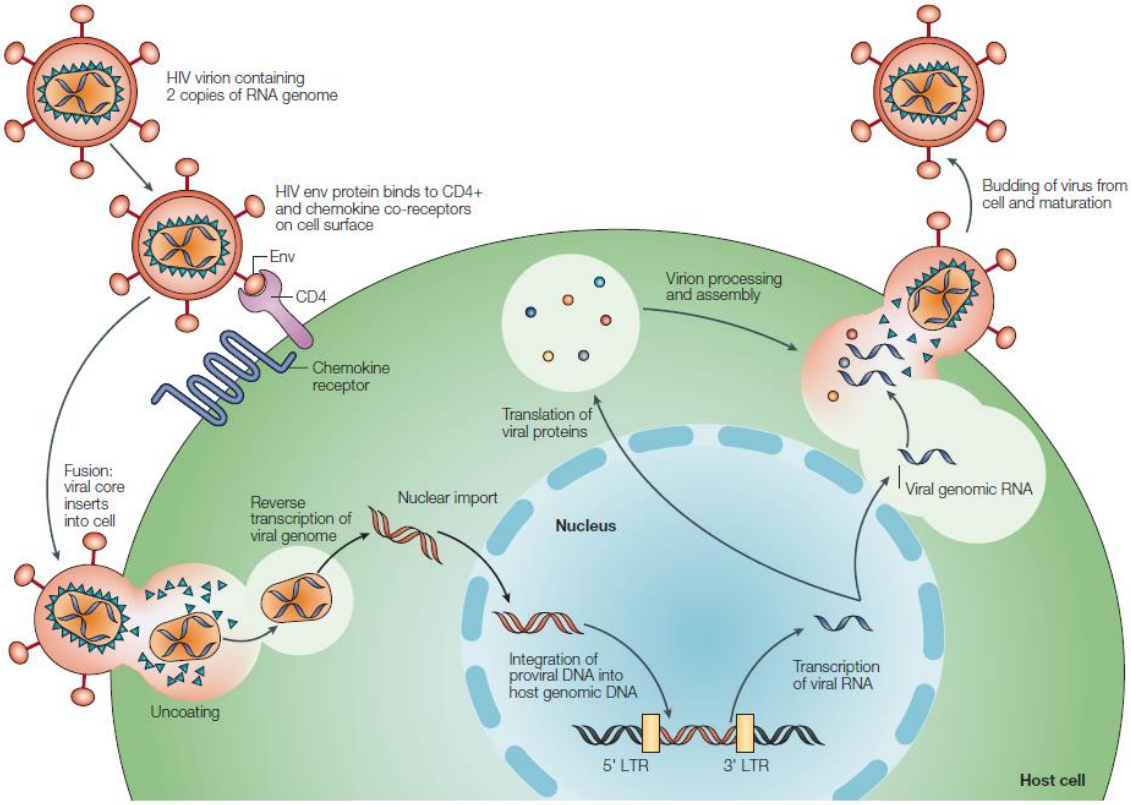

Fig. 1.2: Different target sites for antiretroviral drugs during the life cycle of HIV. Figure source: Rambaut, A et al. (2004). The causes and consequences of HIV evolution. *Nature Reviews Genetics*, *5*(1), 52–61.

The most effective treatment is observed when the dosage regimens consists a combination of drugs belonging to different classes. These regimens usually constitute nucleoside/nucleotide reverse transcriptase inhibitors with either a non-nucleoside reverse transcriptase inhibitors or protease inhibitor.

1.5 Challenges of HIV-AIDS therapy

Development of an effective drug delivery approach for the treatment of HIV/AIDS is a global challenge. The conventional drug delivery approaches including Highly Active Anti-Retroviral Therapy (HAART) have increased the life span of the HIV/AIDS patient (Hogg et al., 1997; Miller & Hodder, 2014; Montaner et al., 2014). However, eradication of HIV is still not possible with these approaches due to some limitations. The most important problem with

HIV/AIDS therapy today is development of multi-drug resistance (MDR) against antiretroviral agents used during the course of therapy, which leads to poor clinical outcomes (Pierson, McArthur, & Siliciano, 2000; Vyas, Shah, & Amiji, 2006; Wong, Chattopadhyay, Wu, & Bendayan, 2010).

Several antiretroviral drugs like TDF, lopinavir, saquinavir, darunavir, maraviroc etc., suffer from different drawbacks when administered through oral route using conventional formulations. These drugs are reported to have poor oral bioavailability, variable drug absorption etc. The possible reasons attributed to these drawbacks could be high ionization, high rate of gut wall/first-pass metabolism and drug efflux via different efflux pumps like P-gp (Lee & Sinko, 1999). In the treatment of HIV/AIDS patient's compliance to the dosage regimen is very important as it involves long-term management of the disease. Additionally, being a chronic therapy, patient non-compliance to the dosage regimen is common. Heavy pill burden due to low oral bioavailability and high clearance and high costs involved in the therapy cause patient non-compliance with existing conventional formulations. Also, poor accessibility of the drugs into the viral reservoirs, associated side effects due to multiple dosage regimens and drug interactions makes the treatment less effective and causes increased patient mortality (Temesgen et al., 2006).

1.6 Intestinal esterases: an overview

One of the critical factors affecting the oral bioavailability of many drugs are the enzymes that are present in the small intestine (Gavhane & Yadav, 2012). Among them, the most predominant and important ones are those belonging to the class of Cytochrome P 450 and esterases. The ester bonds present in various drugs (procaine penicillin) and prodrugs (Adefovir dipivoxil, TDF) are susceptible to esterases, hence, intestinal hydrolysis plays an important role in the pharmacokinetics and pharmacodynamics of such drugs (Masaki, Hashimoto, & Imai,

2007). Among the various esterases present, it has been observed that carboxylesterase (CES) and more specifically CES1 isozyme hCE1 and CES2 isozyme hCE2 are most prevalent in the intestine (Crow, Bittles, Borazjani, Potter, & Ross, 2012; Taketani, Shii, Ohura, Ninomiya, & Imai, 2007).

CES is a glycoprotein consisting of about 550 amino acid residues and its molecular weight is about 60 kDa. Most of the CESs are located in the membranes of the endoplasmic reticulum (ER) through the binding of four amino acid residues at their C-terminal (HEXL) with KDEL receptor. CESs act by binding to its substrate at the substrate binding site and forms a tetrahedral intermediate between the Ser, Glu and His moieties of the enzyme with the carboxyl group of the substrate, this intermediate is further stabilized with low barrier hydrogen bonding with Gly moieties (fig. 1.3). This complex then interacts with a water molecule giving rise to the active metabolite (in-case of a prodrug) or inactive metabolite (Imai & Ohura, 2010; Satoh & Hosokawa, 2006; Yang, Aloysius, Inoyama, Chen, & Hu, 2011).

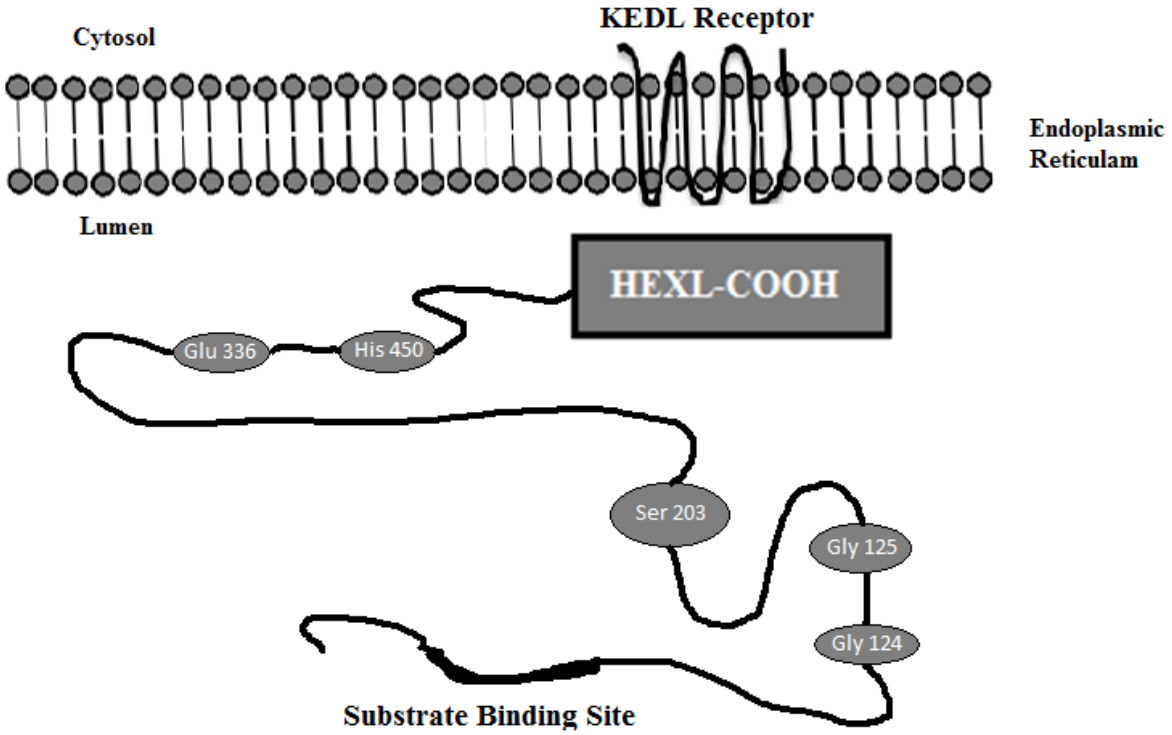

Fig. 1.3: A sketch depicting the critical parts of the CES enzyme involved in the hydrolysis of a CES substrate.

1.7 Approaches for absorption enhancement of esterase substrates

The oral bioavailability of esterase substrates is greatly limited, due to the lumenal and gut-wall metabolism. This has led to the exploration of different approaches by various research groups to increase the oral absorption of such drug molecules. The methods used can be broadly classified into two approaches which are as follows:

1.7.1 Pharmacokinetic approach

Many published works are available for the synthesis of novel CES inhibitors (Wadkins et al., 2004; Wheelock, Severson, & Hammock, 2001; Young et al., 2010). Also, few published works have used such novel CES inhibitors to enhance the bioavailability of the substrates of CES. Among them the most prominent one is that of Van Gelder et al. (2000, 2002) who in a series of published works showed that the bioavailability of ester prodrug of tenofovir (TNF) was enhanced significantly with the help of strawberry extract and a defined ester mixture which gave a 7 fold and 6 fold increase of TNF absorption in the *in situ* perfusion model of rat respectively. Another noticeable work was by the group Li et al. (2007, 2007 (a)), who worked with grapefruit juice (GFJ) and various extracts of GFJ to enhance the bioavailability of ester prodrugs of lovastatin and enalapril. These prodrugs when co-administered with GFJ gave a 82% and 279% increase in the area under the curve (AUC) in rat plasma respectively, co-administration of lovastatin with kaemferol and naringin (extracts of GFJ) increased the AUC by 171% and 159% respectively and for enalapril it was 18% and 68% respectively.

1.7.2 Formulation approach

There are different unique uptake pathways along the oral route other than passive diffusion. Many novel drug delivery systems capitalize on such active uptake mechanisms and transport drugs having poor absorption properties. Nanoparticles (NPs) have been extensively utilized in enhancing the oral bioavailability of different classes of drugs having poor permeation

properties (Akhtar, Rizvi, & Kar, 2012; Dudhani & Kosaraju, 2010; Mittal, Sahana, Bhardwaj, & Ravi Kumar, 2007; Modi, Joshi, & Sawant, 2013). The drugs that are susceptible to degradation when exposed to gut wall enzymes or those that have extensive first part metabolism have better metabolic stability when incorporated into polymeric NPs as the polymer used acts as a barrier which prevents the entry of such metabolic enzymes (Ravi, Vats, Balija, Adapa, & Aditya, 2014; Ravi, Vats, Dalal, Gadekar, & N, 2015). The unique uptake mechanisms of NPs further hinder this metabolic process and are very useful for transporting drugs like TDF into systemic circulation. Lymphoidal uptake either via chylomicrons or via M cells into Peyer's patches is one such uptake mechanism that is reported to act on NPs (Ravi, Vats, Dalal, & Murthy, 2014). It has also been reported that NPs are taken up into the enterocytes via endocytosis (fig. 1.4) majorly through clathrin or caveolae mediated pathways (Hillaireau & Couvreur, 2009; Plapied, Duhem, des Rieux, & Préat, 2011).

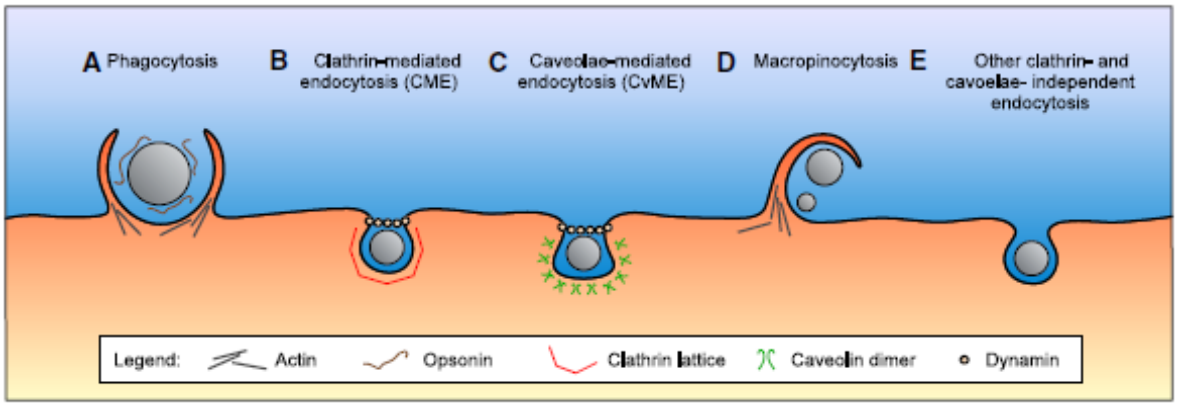

Fig. 1.4: Endocytic uptake pathways of NPs. Figure source: Hillaireau, H., & Couvreur, P. (2009). Nanocarriers' entry into the cell: relevance to drug delivery. *Cellular and Molecular Life Sciences : CMLS*, *66*(17), 2873–96.

Clathrin is triskelion molecule and when a ligand interacts with the transmembrane protein of this route, it leads to the polymerization of clathrin to form 'clathrin coated pits' that engulf the ligand. This pit further invaginates and gets cleaved to form a vesicle (Brodsky, 1988; Plapied et al., 2011; Snoeck, Goddeeris, & Cox, 2005). Caveolae mediated endocytosis takes place via

the flask-shaped invaginations. This cave like structure is primarily coated with caveolin (a dimeric protein) and is enriched with cholesterol and sphingolipids. When compared to clathrin mediated endocytosis internalization along this route is slow and is regulated by a more complex signaling pathway (Anderson, 1998; Hillaireau & Couvreur, 2009).

1.8 Drug profile: tenofovir disoproxil fumarate

TDF (fig. 1.5a) is chemically known as [(R)-2[[bis[[(isopropoxycarbonyl)oxy]methoxy]phosphinyl]methoxy]propyl]adenine fumarate. It is a white to off-white, crystalline powder that contains TDF not less than 98.5% percent and not more than 101.0%. It is a prodrug of TNF (fig. 1.5b) whose IUPAC name is ({[(2R)-1-(6-amino-9H-purin-9-yl)propan-2-yl]oxy}methyl)phosphonic acid.

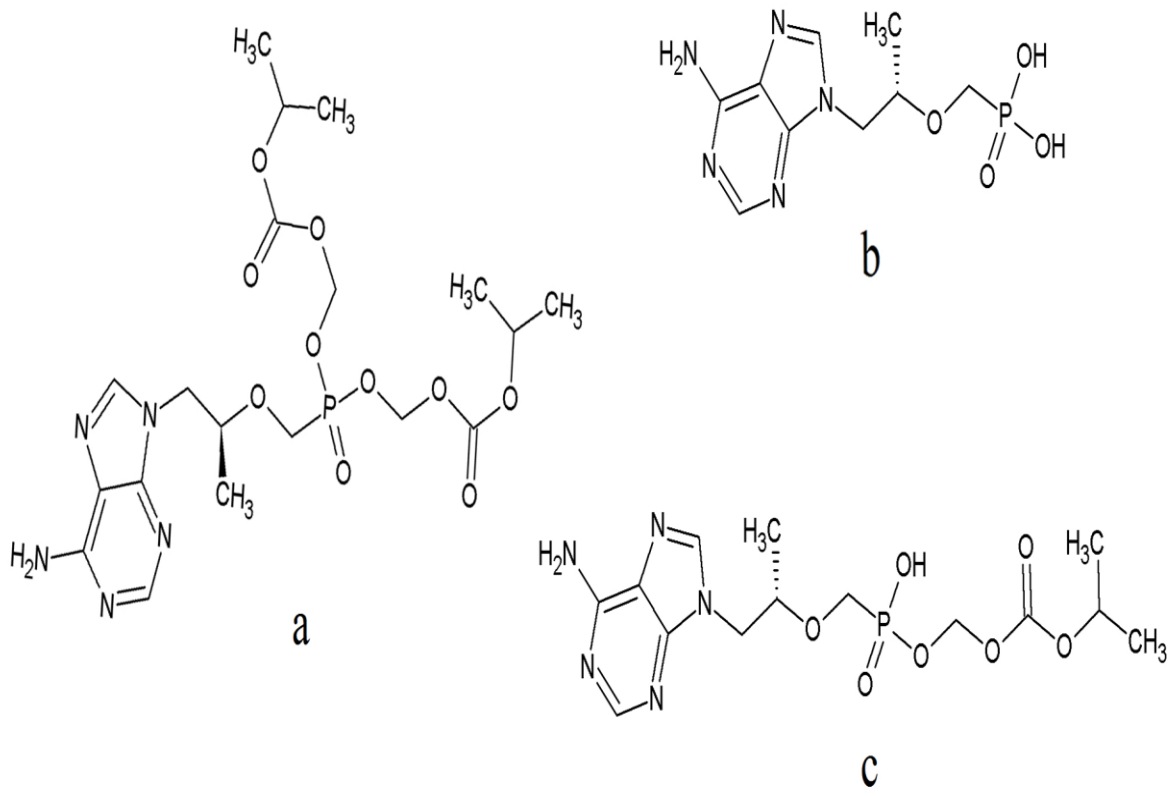

Fig. 1.5: Structure of (a) tenofovir disoproxil fumarate (TDF), (b) tenofovir (TNF) and (c) tenofovir monoester (TMF).

1.8.1 Physicochemical properties

The physicochemical properties of TDF are discussed in the following table:

Table 1.2: Physicochemical properties of TDF

Parameter	Description
Drug Name	Tenofovir disoproxil fumarate
Category	Nucleotide reverse transcriptase inhibitor
Therapeutic class	Antiretroviral
Chemical class	Adenosine monophosphate analog
Chemical name	[(R)-2[[bis[[(isopropoxycarbonyl)oxy]meth-oxy]phosphinyl]methoxy]propyl]adenine fumarate
Chemical formula	$C_{19}H_{30}N_5O_{10}P.C_4H_4O_4$
Molecular weight	635.5 g/mol
Physical state	White to off-white, crystalline powder
Melting point	115-118 °C
Water solubility	13.4 mg/mL
Hydrophobicity (Log P)	1.2
Ionization constant (pKa)	3.75
Water solubility	13.4 mg/mL at 25 °C
Hygroscopicity	Non-hygroscopic

1.8.2 Clinical pharmacology

1.8.2.1 Mechanism of action

TDF is an acyclic nucleotide phosphonate diester analog of adenosine monophosphate. It requires initial diester hydrolysis (by esterases) for conversion to TNF. Subsequently, this active form is taken up in cells where it undergoes phosphorylation by cellular nucleotide kinases which converts it to its diphosphate form. This form of TNF competes with the natural deoxyadenosine triphosphate for the active binding site on the HIV-induced reverse transcriptase. Once the diphosphate form gets incorporated into the viral DNA it causes chain termination which stops the process of the generation of complimentary DNA from the viral RNA template. Therefore, inhibition of this step prevents the proliferation of HIV (Fung, Stone, & Piacenti, 2002).

1.8.2.2 Activity of tenofovir

The *in vitro* activity of TDF and TNF were studied in MT-2 and PBMC cells (Robbins, Srinivas, Kim, Bischofberger, & Fridland, 1998; Srinivas & Fridland, 1998). In these studies, it was observed that both TDF and TNF had the ability to prevent the propagation of HIV. However, there was a 36-90 fold decrease in the 50% effective concentration for TDF, this could be attributed to the significantly higher uptake of TDF into the cells when compared to TNF.

1.8.3 ADME of tenofovir (when administered as the diester prodrug – TDF)

1.8.3.1 Absorption

The clinical pharmacokinetic studies, when performed for an oral dose of 300 mg, indicated rapid absorption with a C_{max} of 208 µg/L which was achieved by 2.3 h after administration. The AUC for this dose was observed to be 2730 µg.h/L and dose dependent increase in the C_{max} and AUC values were observed for a dose range of 75-600 mg in HIV patients. The oral bioavailability of TDF was observed to be around 25% in humans in fasted state (Kearney, Flaherty, & Shah, 2004).

1.8.3.2 Distribution

The protein binding studies indicated that TNF has a very low binding of 1% and 7.2% in human plasma and serum respectively. The tissue distribution of TNF was observed to be very high with a volume of distribution of 813 mL/kg in humans.

1.8.3.3 Metabolism and elimination

Metabolic studies of TDF and TNF in rat hepatocytes indicated that both the prodrug and its active form are not metabolized by cytochrome P450 (CYP-450) enzymes but, TDF was observed to be metabolized by liver esterases (apart from intestinal esterases). It was also

observed that TDF caused the induction of CYP1A and CYP2B metabolic enzymes. Hence, it was observed that TNF is majorly eliminated via renal excretion in the unchanged form with an elimination half-life of 17 h (Fung et al., 2002).

1.8.4 Adverse effects

Most commonly reported side effects of TNF include asthenia, headache, diarrhea, flatulence and nausea. However, there have been a few reports suggesting that TNF can cause acute nephrotoxicity. Further, preclinical studies in rats and dogs showed that TNF decreases the bone mineral content and density. A few mutagenic potential studies have shown that TDF can cause DNA damage (Foggia et al., 2008).

1.8.5 Dosage and administration

The recommended dose of TDF is one immediate release tablet having a dose of 300 mg. The frequency of dosing is once daily to be taken orally on an empty stomach (Foggia et al., 2008). A few generic manufacturers make combination formulations consisting of TDF either with emtricitabine or with lamivudine, in these products also the dosage of TDF is 300 mg.

1.9 Problem definition and objectives

TNF is the only NtRI that has demonstrated efficacy as a part of HAART in the treatment of both naïve and experienced patients (Gallant et al., 2004; Nelson et al., 2007). The preclinical studies for TNF have shown that it has very low oral bioavailability (2% in mice, 17.1% in dogs, 5.3% in monkeys) (Kearney et al., 2004) because of the presence of free hydroxyl groups in its chemical structure which makes it highly ionic (thereby having low permeability). Therefore, a prodrug form of TNF was developed by esterifying the two hydroxyl groups with isopropyloxycarbonyloxymethyl moieties to form phosphodiester linkages (Arimilli et al., 1997). The resultant prodrug, TDF, has higher lipophilicity (Log P value of 1.2) as compared to TNF (Log P of –1.6) (Choi, Bui, & Ho, 2008; Yuan, Dahl, & Oliyai, 2001), which was

intended to be cleaved by the plasma esterases thereby releasing the active form (TNF) in blood plasma. However, it has been reported that TDF, when administered through the oral route, is susceptible to the intestinal esterase enzymes converting the prodrug (a phosphodiester) to its monoester form (TMF) whose structure is shown in fig. 1.5c. This conversion exposes the ionic moieties present in its structure leading to a reduction in its lipophilic characteristics and hence, the ability to permeate into the intestinal membrane because of which the oral bioavailability of TDF was reported to be 25% in humans (Naesens et al., 1998; Shaw et al., 1997).

Hence, different strategies have been used to increase the oral absorption of TDF. Kamboj et al. (2014) have designed niosomes for oral delivery of TDF and observed a 1.6 fold increase in the oral bioavailability of TDF when compared to free drug. Pokharkar et al. (2015) used the formulation approach by developing polymer-lipid hybrid nanoparticles of TDF for nasal delivery and observed a 33% increase in the flux of TDF in sheep nasal mucosa when compared to TDF gel. Whereas, Van Gelder et al. (2000, 2002) used the pharmacokinetic approach by studying the effect of ester rich fruit juices (FJs) – strawberry juice and banana juice, discrete esters and ester mixtures on the oral absorption of TDF. It was observed that strawberry juice and ester mixture containing 0.02% propylparaben, 0.02% octyl acetate and 0.01% ethyl caprylate could increase the uptake of TDF in Caco-2 cell lines and enhance the intestinal absorption of TDF in the rat. Some research groups have reported the use of polymeric and lipid based nanoparticles (NPs) for pre-exposure prophylaxis (Destache et al., 2016; Ramanathan, Jiang, Read, Golan-Paz, & Woodrow, 2016; Zhang, Sturgis, & Youan, 2011). Further, a few groups have also worked on the active form (i.e. TNF) by designing lipid based delivery systems to increase its oral absorption (Freeling, Koehn, Shu, Sun, & Ho, 2015; Zidan, Spinks, Habib, & Khan, 2013).

It can be observed that only three published works, two with pharmacokinetic approach (by Van Gelder et al. (2000, 2002)) and one with formation approach (by Kamboj et al. (2014)) are

available in the current literature that worked with the aim of enhancing the intestinal absorption of TDF. Hence, there is a need to explore alternative and novel methods that can increase the oral bioavailability of TDF and also understand the mechanism involved in the increased oral absorption of TDF.

The purpose of this work was to explore the possible pharmacokinetic and novel formulation approaches that can be used to increase the oral bioavailability of TDF. Therefore, the objectives of the current research work were envisaged as follows:

1. Develop and validate analytical methods for the quantitation of TDF, TMF and TNF and bioanalytical method for the quantitation of TNF.
2. Evaluate the effect of ester rich fruit juices and pharmaceutical excipients containing ester bonds on the oral absorption of TDF.
3. Employ the concepts of design of experiments (DoE) in the design, preparation and optimization of polymeric nanocarriers for TDF.
4. Perform physical characterization, determine the *in vitro* release kinetics and carry out the in vitro luminal fluid metabolic studies for the optimized nanocarrier formulation.
5. Carry out, *ex vivo* everted gut sac and *in vivo* pharmacokinetic studies for the selected nanocarrier formulations in suitable animal models.

References

Akhtar, F., Rizvi, M. M. A., & Kar, S. K. (2012). Oral delivery of curcumin bound to chitosan nanoparticles cured Plasmodium yoelii infected mice. *Biotechnology Advances*, *30*(1), 310–320.

Anderson, R. G. W. (1998). The caveolae membrane system. *Annual Review of Biochemistry*, *67*(1), 199–225.

Arimilli, M. N., Kim, C. U., Dougherty, J., Mulato, A., Oliyai, R., Shaw, J. P., … Bischofberger, N. (1997). Synthesis, in vitro biological evaluation and oral bioavailability of 9-[2-(phosphonomethoxy)propyl]adenine (PMPA) prodrugs. *Antiviral Chemistry & Chemotherapy*, *8*(6), 557–564.

Barasa, S. S. (2011). True story about HIV: theory of viral sequestration and reserve infection. *HIV/AIDS (Auckland, N.Z.)*, *3*, 125–33.

Brodsky, F. M. (1988). Living with clathrin: its role in intracellular membrane traffic. *Science (New York, N.Y.)*, *242*(4884), 1396–402.

Choi, S.U., Bui, T., & Ho, R. J. Y. (2008). pH-Dependent Interactions of Indinavir and Lipids in Nanoparticles and Their Ability to Entrap a Solute. *Journal of Pharmaceutical Sciences*, *97*(2), 931–943.

Crow, J. A., Bittles, V., Borazjani, A., Potter, P. M., & Ross, M. K. (2012). Covalent inhibition of recombinant human carboxylesterase 1 and 2 and monoacylglycerol lipase by the carbamates JZL184 and URB597. *Biochemical Pharmacology*, *84*(9), 1215–22.

Destache, C. J., Mandal, S., Yuan, Z., Kang, G., Date, A. A., Lu, W., … Li, Q. (2016). Topical Tenofovir Disoproxil Fumarate Nanoparticles Prevent HIV-1 Vaginal

Transmission in a Humanized Mouse Model. *Antimicrobial Agents and Chemotherapy*, *60*(6), 3633–3639.

Dudhani, A. R., & Kosaraju, S. L. (2010). Bioadhesive chitosan nanoparticles: Preparation and characterization. *Carbohydrate Polymers*, *81*(2), 243–251.

Esté, J. A., & Cihlar, T. (2010). Current status and challenges of antiretroviral research and therapy. *Antiviral Research*, *85*(1), 25–33.

Foggia, M., Nappa, S., Bonadies, G., Cotugno, M., Di Filippo, G., Borrelli, F., … Borgia, G. (2008). Tenofovir disoproxil fumarate in the clinical practice: An overview. *Anti-Infective Agents in Medicinal Chemistry*, *7*, 285–295.

Freed, E. O. (1998). HIV-1 Gag Proteins: Diverse Functions in the Virus Life Cycle. *Virology*, *251*(1), 1–15.

Freeling, J. P., Koehn, J., Shu, C., Sun, J., & Ho, R. J. Y. (2015). Anti-HIV Drug-Combination Nanoparticles Enhance Plasma Drug Exposure Duration as Well as Triple-Drug Combination Levels in Cells Within Lymph Nodes and Blood in Primates. *AIDS Research and Human Retroviruses*, *31*(1), 107–114.

Fung, H. B., Stone, E. A., & Piacenti, F. J. (2002). Tenofovir disoproxil fumarate: a nucleotide reverse transcriptase inhibitor for the treatment of HIV infection. *Clinical Therapeutics*, *24*(10), 1515–48.

Gallant, J. E., Staszewski, S., Pozniak, A. L., DeJesus, E., Suleiman, J. M. A. H., Miller, M. D., … 903 Study Group. (2004). Efficacy and Safety of Tenofovir DF vs Stavudine in Combination Therapy in Antiretroviral-Naive Patients: A 3-Year Randomized Trial. *JAMA*, *292*(2), 191-201.

Gavhane, Y. N., & Yadav, A. V. (2012). Loss of orally administered drugs in GI tract. *Saudi Pharmaceutical Journal*, *20*(4), 331–344.

Global AIDS Update 2016 | UNAIDS. (2016). Available at: http://www.unaids.org/en/resources/documents/2016/Global-AIDS-update-2016.

Hillaireau, H., & Couvreur, P. (2009). Nanocarriers' entry into the cell: relevance to drug delivery. *Cellular and Molecular Life Sciences : CMLS*, *66*(17), 2873–96.

Hilleman, M. R. (1995). Overview: practical insights from comparative immunology and pathogenesis of AIDS, hepatitis B, and measles for developing an HIV vaccine. *Vaccine*, *13*(18), 1733–40.

Hogg, R. S., O'Shaughnessy, M. V, Gataric, N., Yip, B., Craib, K., Schechter, M. T., & Montaner, J. S. (1997). Decline in deaths from AIDS due to new antiretrovirals. *The Lancet*, *349*(9061), 1294.

Imai, T., & Ohura, K. (2010). The role of intestinal carboxylesterase in the oral absorption of prodrugs. *Current Drug Metabolism*, *11*(9), 793–805.

Jayaraman, S., & Shah, K. (2008). Comparative studies on inhibitors of HIV protease: a target for drug design. *In Silico Biology*, *8*(5–6), 427–47.

Kamboj, S., Saini, V., & Bala, S. (2014). Formulation and Characterization of Drug Loaded Nonionic Surfactant Vesicles (Niosomes) for Oral Bioavailability Enhancement. *The Scientific World Journal*, *2014*, 1–8.

Kearney, B. P., Flaherty, J. F., & Shah, J. (2004). Tenofovir disoproxil fumarate: clinical pharmacology and pharmacokinetics. *Clinical Pharmacokinetics*, *43*(9), 595–612.

Kumari, G., & Singh, R. K. (2012). Highly Active Antiretroviral Therapy for treatment of HIV/AIDS patients: Current status and future prospects and the Indian scenario. *HIV & AIDS Review*, *11*(1), 5–14.

Lee, Y. H., & Sinko, P. J. (1999). Preface. *Advanced Drug Delivery Reviews*, *39*(1), 1–3.

Li, P., Callery, P. S., Gan, L. S., & Balani, S. K. (2007). Esterase inhibition attribute of grapefruit juice leading to a new drug interaction. *Drug Metabolism and Disposition*, *35*(7), 1023–1031.

Li, P., Callery, P. S., Gan, L.-S., & Balani, S. K. (2007a). Esterase inhibition by grapefruit juice flavonoids leading to a new drug interaction. *Drug Metabolism and Disposition: The Biological Fate of Chemicals*, *35*(7), 1203–8.

Masaki, K., Hashimoto, M., & Imai, T. (2007). Intestinal first-pass metabolism via carboxylesterase in rat jejunum and ileum. *Drug Metabolism and Disposition: The Biological Fate of Chemicals*, *35*(7), 1089–95.

McColl, D. J., & Chen, X. (2010). Strand transfer inhibitors of HIV-1 integrase: bringing IN a new era of antiretroviral therapy. *Antiviral Research*, *85*(1), 101–18.

Miller, V., & Hodder, S. (2014). Beneficial impact of antiretroviral therapy on non-AIDS mortality. *AIDS*, *28*(2), 273–274.

Mittal, G., Sahana, D. K., Bhardwaj, V., & Ravi Kumar, M. N. V. (2007). Estradiol loaded PLGA nanoparticles for oral administration: effect of polymer molecular weight and copolymer composition on release behavior in vitro and in vivo. *Journal of Controlled Release*, *119*(1), 77–85.

Modi, J., Joshi, G., & Sawant, K. (2013). Chitosan based mucoadhesive nanoparticles of

ketoconazole for bioavailability enhancement: formulation, optimization, *in vitro* and *ex vivo* evaluation. *Drug Development and Industrial Pharmacy*, *39*(4), 540–547.

Montaner, J. S. G., Lima, V. D., Harrigan, P. R., Lourenço, L., Yip, B., Nosyk, B., … Kendall, P. (2014). Expansion of HAART Coverage Is Associated with Sustained Decreases in HIV/AIDS Morbidity, Mortality and HIV Transmission: The "HIV Treatment as Prevention" Experience in a Canadian Setting. *PLoS ONE*, *9*(2), e87872.

Naesens, L., Bischofberger, N., Augustijns, P., Annaert, P., Van den Mooter, G., Arimilli, M. N., … De Clercq, E. (1998). Antiretroviral efficacy and pharmacokinetics of oral bis(isopropyloxycarbonyloxymethyl)-9-(2-phosphonylmethoxypropyl)adenine in mice. *Antimicrobial Agents and Chemotherapy*, *42*(7), 1568–73.

Nelson, M. R., Katlama, C., Montaner, J. S., Cooper, D. A., Gazzard, B., Clotet, B., … Rooney, J. F. (2007). The safety of tenofovir disoproxil fumarate for the treatment of HIV infection in adults: the first 4 years. *AIDS*, *21*(10), 1273–1281.

Phillips, K. D. (1996). Protease inhibitors: a new weapon and a new strategy against HIV. *The Journal of the Association of Nurses in AIDS Care : JANAC*, *7*(5), 57–71.

Pierson, T., McArthur, J., & Siliciano, R. F. (2000). Reservoirs for HIV-1: Mechanisms for Viral Persistence in the Presence of Antiviral Immune Responses and Antiretroviral Therapy. *Annual Review of Immunology*, *18*(1), 665–708.

Plapied, L., Duhem, N., des Rieux, A., & Préat, V. (2011). Fate of polymeric nanocarriers for oral drug delivery. *Current Opinion in Colloid & Interface Science*, *16*(3), 228–237.

Pokharkar, V. B., Jolly, M. R., & Kumbhar, D. D. (2015). Engineering of a hybrid polymer–lipid nanocarrier for the nasal delivery of tenofovir disoproxil fumarate: Physicochemical,

molecular, microstructural, and stability evaluation. *European Journal of Pharmaceutical Sciences*, *71*, 99–111.

Ramanathan, R., Jiang, Y., Read, B., Golan-Paz, S., & Woodrow, K. A. (2016). Biophysical characterization of small molecule antiviral-loaded nanolipogels for HIV-1 chemoprophylaxis and topical mucosal application. *Acta Biomaterialia*, *36*, 122–131.

Rambaut, A., Posada, D., Crandall, K. A., & Holmes, E. C. (2004). The causes and consequences of HIV evolution. *Nature Reviews Genetics*, *5*(1), 52–61.

Ravi, P. R., Vats, R., Balija, J., Adapa, S. P. N., & Aditya, N. (2014). Modified pullulan nanoparticles for oral delivery of lopinavir: Formulation and pharmacokinetic evaluation. *Carbohydrate Polymers*, *110*, 320–328.

Ravi, P. R., Vats, R., Dalal, V., Gadekar, N., & N, A. (2015). Design, optimization and evaluation of poly- ε -caprolactone (PCL) based polymeric nanoparticles for oral delivery of lopinavir. *Drug Development and Industrial Pharmacy*, *41*(1), 131–140.

Ravi, P. R., Vats, R., Dalal, V., & Murthy, A. N. (2014). A hybrid design to optimize preparation of lopinavir loaded solid lipid nanoparticles and comparative pharmacokinetic evaluation with marketed lopinavir/ritonavir coformulation. *Journal of Pharmacy and Pharmacology*, *66*(7), 912–926.

Robbins, B. L., Srinivas, R. V, Kim, C., Bischofberger, N., & Fridland, A. (1998). Anti-human immunodeficiency virus activity and cellular metabolism of a potential prodrug of the acyclic nucleoside phosphonate 9-R-(2-phosphonomethoxypropyl)adenine (PMPA), Bis(isopropyloxymethylcarbonyl)PMPA. *Antimicrobial Agents and Chemotherapy*, *42*(3), 612–7.

Satoh, T., & Hosokawa, M. (2006). Structure, function and regulation of carboxylesterases. *Chemico-Biological Interactions*, *162*(3), 195–211.

Shaw, J. P., Sueoko, C. M., Oliyai, R., Lee, W. A., Arimilli, M. N., Kim, C. U., & Cundy, K. C. (1997). Metabolism and pharmacokinetics of novel oral prodrugs of 9-[(R)-2-(phosphonomethoxy)propyl]adenine (PMPA) in dogs. *Pharmaceutical Research*, *14*(12), 1824–9.

Snoeck, V., Goddeeris, B., & Cox, E. (2005). The role of enterocytes in the intestinal barrier function and antigen uptake. *Microbes and Infection*, *7*(7–8), 997–1004.

Srinivas, R. V, & Fridland, A. (1998). Antiviral activities of 9-R-2-phosphonomethoxypropyl adenine (PMPA) and bis(isopropyloxymethylcarbonyl)PMPA against various drug-resistant human immunodeficiency virus strains. *Antimicrobial Agents and Chemotherapy*, *42*(6), 1484–7.

Taketani, M., Shii, M., Ohura, K., Ninomiya, S., & Imai, T. (2007). Carboxylesterase in the liver and small intestine of experimental animals and human. *Life Sciences*, *81*(11), 924–932.

Temesgen, Z., Warnke, D., & Kasten, M. J. (2006). Current status of antiretroviral therapy. *Expert Opinion on Pharmacotherapy*, *7*(12), 1541–1554.

Van Gelder, J., Deferme, S., Annaert, P., Naesens, L., De Clercq, E., Van den Mooter, G., … Augustijns, P. (2000). Increased absorption of the antiviral ester prodrug tenofovir disoproxil in rat ileum by inhibiting its intestinal metabolism. *Drug Metabolism and Disposition: The Biological Fate of Chemicals*, *28*(12), 1394–6.

Van Gelder, J., Deferme, S., Naesens, L., De Clercq, E., Van Den Mooter, G., Kinget, R., & Augustijns, P. (2002). Intestinal absorption enhancement of the ester prodrug tenofovir disoproxil fumarate through modulation of the biochemical barrier by defined ester mixtures. *Drug Metabolism and Disposition*, *30*(8), 924–930.

Vyas, T. K., Shah, L., & Amiji, M. M. (2006). Nanoparticulate drug carriers for delivery of HIV/AIDS therapy to viral reservoir sites. *Expert Opinion on Drug Delivery*, *3*(5), 613–28.

Wadkins, R. M., Hyatt, J. L., Yoon, K. J. P., Morton, C. L., Lee, R. E., Damodaran, K., … Potter, P. M. (2004). Discovery of novel selective inhibitors of human intestinal carboxylesterase for the amelioration of irinotecan-induced diarrhea: synthesis, quantitative structure-activity relationship analysis, and biological activity. *Molecular Pharmacology*, *65*(6), 1336–43.

Wheelock, C. E., Severson, T. F., & Hammock, B. D. (2001). Synthesis of New Carboxylesterase Inhibitors and Evaluation of Potency and Water Solubility. *Chemical Research in Toxicology*, *14*(12), 1563–1572.

Wong, H. L., Chattopadhyay, N., Wu, X. Y., & Bendayan, R. (2010). Nanotechnology applications for improved delivery of antiretroviral drugs to the brain. *Advanced Drug Delivery Reviews*, *62*(4–5), 503–17.

Yang, Y., Aloysius, H., Inoyama, D., Chen, Y., & Hu, L. (2011). Enzyme-mediated hydrolytic activation of prodrugs. *Acta Pharmaceutica Sinica B*, *1*(3), 143–159.

Young, B. M., Hyatt, J. L., Bouck, D. C., Chen, T., Hanumesh, P., Price, J., … Webb, T. R. (2010). Structure-activity relationships of substituted 1-pyridyl-2-phenyl-1,2-ethanediones: potent, selective carboxylesterase inhibitors. *Journal of Medicinal*

Chemistry, *53*(24), 8709–15.

Yuan, L. C., Dahl, T. C., & Oliyai, R. (2001). Degradation kinetics of oxycarbonyloxymethyl prodrugs of phosphonates in solution. *Pharmaceutical Research*, *18*(2), 234–237.

Zhang, T., Sturgis, T. F., & Youan, B.-B. C. (2011). pH-responsive nanoparticles releasing tenofovir intended for the prevention of HIV transmission. *European Journal of Pharmaceutics and Biopharmaceutics*, *79*(3), 526–536.

Zidan, A. S., Spinks, C. B., Habib, M. J., & Khan, M. A. (2013). Formulation and transport properties of tenofovir loaded liposomes through Caco-2 cell model. *Journal of Liposome Research*, *2104*(4), 1–9.

Chapter 2

Analytical Method Development and Validation

2.1 Introduction

The aim of our research work was to use the pharmacokinetic and nanocarrier formulation approach for enhancing the oral bioavailability of TDF. For this purpose, development of suitable analytical techniques for the quantitation of TDF is indispensable. However, TDF being a phosphodiester, gets metabolized to its monoester form (TMF) in the presence of gut wall esterases (Kearney, Flaherty, & Shah, 2004) and after entering the systemic circulation it gets metabolized to its active form (TNF). Hence, there is a need to develop aqueous analytical methods for the quantitation of TMF and TNF (in addition to TDF) in aqueous samples and also in *in vitro* or *ex vivo* metabolic studies. There have been a few published works that focused on improving the systemic uptake of TDF by using different novel techniques so as to improve the management of HIV/AIDS (Pokharkar, Jolly, & Kumbhar, 2015; Van Gelder et al., 2000) therefore, understanding the pharmacokinetic profile of TDF is an important aspect of such studies. Further, rat models have been widely used for pre-clinical evaluation of such approaches but TDF is reported to get rapidly converted to its active form (Geboers et al., 2015), this phenomenon which was also observed in-house. Hence, an analytical method that estimates TNF (instead of TDF) in rat plasma is needed which is simple, reproducible and cost effective.

From the literature, it is evident that there are a few works that have estimated TDF (Anandakumar, Abirami, Murugan, & Ashok, 2013; Ashenafi et al., 2010; Bhavsar, Patel, & Patel, 2012) in aqueous samples and TNF in biological matrices however, there is no published analytical work that has developed a method for the estimation of TMF. Table 2.1 compares the current analytical technique with existing liquid chromatographic methods for the estimation of TNF in different biological matrices. Analytical methods were developed using high performance liquid chromatography (HPLC) with ultraviolet (UV) detector (Bezy, Morin, Couerbe, Leleu, & Agrofoglio, 2005; Rezk, Crutchley, & Kashuba, 2005; Sentenac, Fernandez,

Thuillier, Lechat, & Aymard, 2003), fluorescence detector (Jullien, Tréluyer, Pons, & Rey, 2003; Sparidans, Crommentuyn, Schellens, & Beijnen, 2003), mass spectrophotometer (Bennetto-Hood, Long, & Acosta, 2007; Takahashi et al., 2007) and tandem mass (MS-MS) spectrophotometer (Delahunty, Bushman, & Fletcher, 2006; Delahunty, Bushman, Robbins, & Fletcher, 2009; El Barkil, Gagnieu, & Guitton, 2007; Gomes, Vaidya, Pudage, Joshi, & Parekh, 2008; Jung, Rezk, Bridges, Corbett, & Kashuba, 2007; Nirogi et al., 2009). Almost all the reported methods were meant for the analysis of TNF in human plasma; only one study by V. Bezy et al. (2005) was reported for the analysis of TNF in rat plasma. However, in this particular study, the tailing factor of TNF was very high (1.7) and the suitability of the method for a pharmacokinetic study was not reported. Further, the drug-free plasma was spiked with pentostatin (an anti-metabolite) before addition of analytes and then the resultant plasma samples were processed by solid-phase extraction. However, in a pharmacokinetic study, the analyte is administered to rats and only after blood collection pentostatin can be added. This change in the sequence of addition might cause a significant variation in recovery. Additionally, our literature survey showed only two published works (Bezy et al., 2005; Walters, Jacobs, Tomaszewski, & Graves, 1999) used such a procedure of processing plasma samples, and none of these published works addressed this particular aspect nor did they report any data to show that such a method can be used for a pharmacokinetic study. Thus, there is a need for an analytical technique that is more pragmatic for the quantitation of TNF in rat plasma.

The objective of the proposed work was to develop analytical methods that are simple, cost-effective, reproducible, accurate and also applicable for routine lab analysis. Protein precipitation was used as an extraction technique for the estimation of TNF, and a simple isocratic mobile phase was used. Necessary validation studies were performed and most importantly, pharmacokinetic application of the bioanalytical method is exhibited.

Table 2.1: Bioanalytical methods reported for TNF using liquid chromatography as a separation technique

Species	Matrix (Inj. Vol)	Analytes	CC Range ng/mL	Sample Prep.	Further Pretreatment	Elution Type	Detection (ionization/ λ (nm))	Run Time (min)	Remarks	Ref.
Rat	Plasma (50µL)	TNF	250-4000	PP	ETD, Reconst. With pH 4 AA buffer	Isocratic	UV (260)	22	PK application of the method is reported	CM
Rat	Plasma (20µL)	TNF, many ARTs	30-10000	SPE	ETD, Reconst. With Water	Gradient	UV (260) & MS/MS (ESI-QqQ)	15	Plasma preprocesssed, PK application not shown	Bezy (2005)
Human	Plasma (80µL)	TNF, EMT	10-10000	SPE	ETD, Reconst. With MP	Gradient	UV (259)	16	PK application of the method is reported	Rezk (2005)
Human	Plasma (Not Sp.)	TNF	10-4000	SPE	ETD, Reconst. With Na_2HPO_4 pH 7 buffer	Gradient	UV (259)	10	PK application of the method is reported	Sentenac (2003)
Human	Plasma (80µL)	TNF	5-1000	PP with MeOH	ETD, Reconst. With derivatization agent	Isocratic	Fluori (Ext. 236 Emm. 420)	20	PK application of the method is reported	Jullien (2003)
Human	Plasma (50µL)	TNF	20-1000	PP with 20% TCA	Addition of 50µL derivatization agent	Gradient	Fluori (Ext. 254 Emm. 425)	20	PK application of the method is reported	Sparidans (2003)
Human	Plasma (5µL)	TNF	19-1567	PP with 2mL ACN	ETD, Reconst. with MP	Gradient	MS (ESI-Q)	12	PK application of the method is reported	Takahashi (2007)
Human	Plasma (Not Sp.)	TNF	1-750	SPE	ETD, Reconst. with water	Isocratic	MS (ESI-Q)	10	PK application of the method is reported	Bennetto-Hood (2007)
Human	Plasma (2µL)	TNF	10-1000	SPE	ETD, Reconst. with water	Isocratic	UV(260)-MS (ESI-Q)	6	PK application of the method is reported	Barkil (2007)
Human	Plasma (10µL)	TNF, EMT	10-1500	PP with TFA	Addn. of NH_4OH for neutralization	Isocratic	MS/MS (ESI-QqQ)	12	PK application of the method is reported	Delahunty (2006 & 2009)
Human	Plasma (20µL)	TNF, ARTs	30-10000	SPE	ETD, Reconst. with water	Gradient	MS/MS (ESI-QqQ)	20	PK application of the method is reported	Jung (2007)
Human	Plasma (20µL)	TNF, EFV, EMT	20-2000	SPE	ETD, Reconst. with MP	Gradient	MS/MS (TIS-QqQ)	4	PK application of the method is reported	Nirogi (2009)
Human	Plasma (3µL)	TNF, EMT	10-600	SPE	ETD, Reconst. with 1% acetic acid in 10 mM AA buffer	Isocratic	MS/MS (ESI-QqQ)	2	PK application of the method is reported	Gomes (2008)

λ-wavelength; AA-Ammonium Acetate; ACN-Acetonitrile; ARTs-Antiretrovirals; CC-Calibration Curve; CM-Current Method; EFV-Efavirenz; EMT-Emtricitabine; ESI-Electrospray Ionization; ETD-Evaporated to dryness; Fluori-Spectrofluorometer; Inj. Vol-Injection Volume; MeOH-Methanol; MP-Mobile Phase; MS-Mass Spectrophotometer; MS/MS-Tandem MS; Na_2HPO_4-Disodium orthophosphate; Not Sp.-Not Specified; PK-Pharmacokinetic; TNF-Tenofovir; PP-Protein Precipitation; Prep.-Preparation; Q-Single Quadruple; QqQ-Triple Quadruple; Reconst.-Reconstituted; Ref.-Reference; SPE-Solid Phase Extraction; TCA-Trichloroacetic Acid; TFA-Trifluoroacetic Acid; TIS-TurboIonspray.

2.2 Materials

2.2.1 Reagents and animals

Tenofovir monohydrate and monoester for tenofovir (TMF) were obtained as a gift sample from Gilead sciences, Inc., CA, USA. TDF was obtained from Strides Arcolab Limited, KA, India. HPLC grade acetonitrile, methanol were purchased from HiMedia Laboratories, Mumbai, India; ammonium acetate and perchloric acid (HPLC Grade) were purchased from SD Fine-Chem Limited, Mumbai, India; sodium citrate, sodium hydroxide, glacial acetic acid (GAA) and ammonium hydroxide (HPLC Grade) were purchased from SRL Chemicals Ltd., Mumbai, India; trifluroacetic acid (HPLC Grade) was purchased from Sigma-Aldrich, Mumbai, India**.** Milli–Q water purification system (Millipore®, MA, USA) was used for obtaining high quality HPLC grade water. Male Wistar rats were procured from Sainath agencies, Hyderabad, India.

2.2.2 Instruments

The HPLC system consisted of two solvent delivery LC–20AD pumps, an SIL–20AC HT auto-injector and an SPD–M20A photodiode array-UV detector (Shimadzu, Tokyo, Japan). Data collection and integration were accomplished using LC Solutions, 1.25 version software. Plasma processing was done using Eppendorf Research® Micropipettes (Eppendorf India Ltd., Chennai, India. pH meter (Model Eutech pH 2700, Eutech Instruments, Mumbai, India) was used to measure and adjust the pH of buffer solutions. Vortex mixer (Model VX-200, Labnet International Inc., NJ, USA), sonicator (Model SONICA® 2200 MH, Soltec, Italy), refrigerated centrifuge (Model C-24 BL, Remi, Mumbai, India) and deep freezer (Model BFS-345-S, Celfrost Innovations Pvt. Ltd., Mumbai, India) were used for preparation and processing of samples in method development and validation. Membrane filters of 0.22 µm (Millipore®, MA, USA) were used for filtration of the aqueous phase of mobile phase system.

2.3 Method I: Analytical method development of tenofovir disoproxil fumarate in HPLC

2.3.1 Instrument

The HPLC system used for the analytical method development of TDF was the same as described in section 2.2.2.

2.3.2 Mobile Phase Optimization

The mobile phase composition, pH and other chromatographic conditions were optimized by evaluating the impact of changing these parameters on the peak shape, tailing factor and retention time.

2.3.3 Chromatographic Conditions

Chromatographic separation was performed on a Spincotech C18G enabled column (250 × 4.6 mm, 5 µm). The mobile phase consisted of 10 mM ammonium acetate buffer (pH 4.0 ± 0.1, pH adjusted with GAA) and methanol in the ratio of 50:50 *v/v*. The buffer was pre-filtered through 0.22 µm Millipore filtration membrane. Isocratic conditions were employed at a flow rate of 1 mL/min and TDF was monitored at a wavelength of 260 nm. The HPLC system was stabilized for 1 h at 1 mL/min flow rate, through baseline monitoring prior to actual analysis. An injection volume of 50 µL was set for the optimized method.

2.3.4 Sample preparation

A primary stock solution of TDF having a concentration of 1 mg/mL was prepared in 10 mM ammonium acetate buffer (pH 4.0). From this primary stock solution, working stock solution having a concentration of 200 μg/mL of TDF was prepared. Appropriate dilutions of this working stock solution were made with 10 mM ammonium acetate buffer (pH 4.0) to get different concentrations of aqueous standards of TDF.

2.3.5 Method validation

2.3.5.1 Selectivity

The selectivity of the developed method was determined by spiking TDF with the excipients used for the preparation of nanocarrier formulation. These samples were then vortexed for 5 min and centrifuged (Remi, Mumbai, India) at 7800 × g for 15 minutes. A clear supernatant was obtained which was diluted appropriately and analyzed in HPLC. Further, placebo samples (free of TDF) were prepared and processed in a similar way and injected into HPLC system to check for the interference at the retention time of TDF.

2.3.5.2 Linearity and range

The linearity plot was constructed for TDF in the range of 250 to 4000 ng/mL with six concentrations (250, 500, 750, 1000, 2000 and 4000 ng/mL). The equation of the calibration curve was developed by least-square regression for the peak area and concentration of TDF. The coefficient of regression (R^2), slope and intercept values were determined and statistically evaluated. Validation was performed at three concentration levels (lower quality control (LQC) = 350, middle quality control (MQC) = 1500 and higher quality control (HQC) = 3000 ng/mL) of TDF. Further, the calibration curve was used to predict the concentration of quality control samples.

2.3.5.3 Accuracy and precision

The accuracy and precision were assessed by determining the variations in the intra-day and inter-day samples. For this study, the three quality control standards i.e. LQC, MQC and HQC were used and the accuracy and precision were expressed in terms of percent bias (%bias) and percentage of relative standard deviation (%RSD) of the assay results respectively. For the intra-day repeatability, the samples were assessed by using five replicates of the quality control

standards two times in a day. The inter-day repeatability was determined by preparing similar quality control standards and analyzing them for three consecutive days.

2.3.5.4 Sensitivity

The sensitivity of this analytical method was evaluated by determining the standard deviation of the intercepts (σ) and mean of the slopes (s) of the calibration curves (n = 18). These values were used to calculate the limit of detection (LOD) and limit of quantitation (LOQ) by using the following equations:

$$LOD = \frac{3.3\sigma}{S}; LOQ = \frac{10\sigma}{S}$$

2.3.5.5 Stability studies

The solution stability of TDF was carried out at bench top and refrigerated conditions. A stock solution of 200 µg/mL of TDF was prepared in methanol. The solution was further diluted to get the TDF concentration of 2000 ng/mL and analyzed at pre-determined time intervals (0, 12 and 24 h). For evaluating the long-term stability, the stock solution was stored at –20 °C and analyzed after every 10 days for 30 days.

2.3.6 Results and discussion

2.3.6.1 Method development

To determine the effect of mobile phase pH on the peak properties of TDF, the analysis was performed at various pH conditions of the mobile phase (pH 3, 5.5, and 7.0), it was observed that there was no significant deviation of the retention time for TDF from 8.9 min at the pH range tested. The peak shape was found to be good across the pH range. However, Yuan et al. (2001) observed that storing TDF in basic or near basic pH conditions leads to rapid

degradation (which was also observed in-house). Hence, slightly acidic conditions were maintained because of which a pH of 4.5 was selected for the mobile phase for further analysis.

Methanol and acetonitrile were used to evaluate the effect of the type of organic phase on the peak properties of TDF. Even, though there was no impact on the peak shape and tailing factor of TDF, it was observed that a better control on the retention time of TDF was observed with the use of methanol. Hence, methanol was selected as the organic phase component of the mobile phase.

The effect of the mobile phase composition was evaluated and it was observed that changes in the methanol composition had a significant impact on the quality of chromatogram. A longer retention time of more than 15.0 min and a broad peak of TDF was obtained with low methanol (25%) composition in the mobile phase. Additionally, the peak tailing of TDF was more than 1.5. To reduce the peak tailing and total elution time of TDF, the organic phase component of the mobile phase was increased up to 50%. Higher amounts of methanol significantly reduced the elution time of TDF to 8.9 with tailing factor less than 1.5.

Based on these results, the final optimum chromatographic conditions for analysis of TDF were: mobile phase consisting 10 mM ammonium acetate buffer (pH 4.0) and methanol in the ratio 50:50 *v/v*, flow rate of 1 mL/min, Spincotech C18G enabled column (250 × 4.6 mm, 5 µm) and an operating temperature of 40 ºC.

2.3.6.2 Method validation

Selectivity

There was no interference of the excipients with which TDF was spiked in the vicinity of the retention time of TDF. This indicated that the developed method was selective towards the estimation of TDF in the presence of the selected formulation excipients (fig. 2.1).

Linearity and range

The least square regression analysis showed a linear response for chosen concentration range of 250–4000 ng/mL with a regression coefficient (R^2) value of 0.9996. The equation of the best-fit line was $y = 57.78x - 276.92$, where 'y' is the peak area of TDF and 'x' is the concentration of TDF in ng/mL. The variation of the tested concentrations was evaluated by determining the %RSD values which were observed to be low (< 5%). The peak areas at individual concentration points are presented in table 2.2.

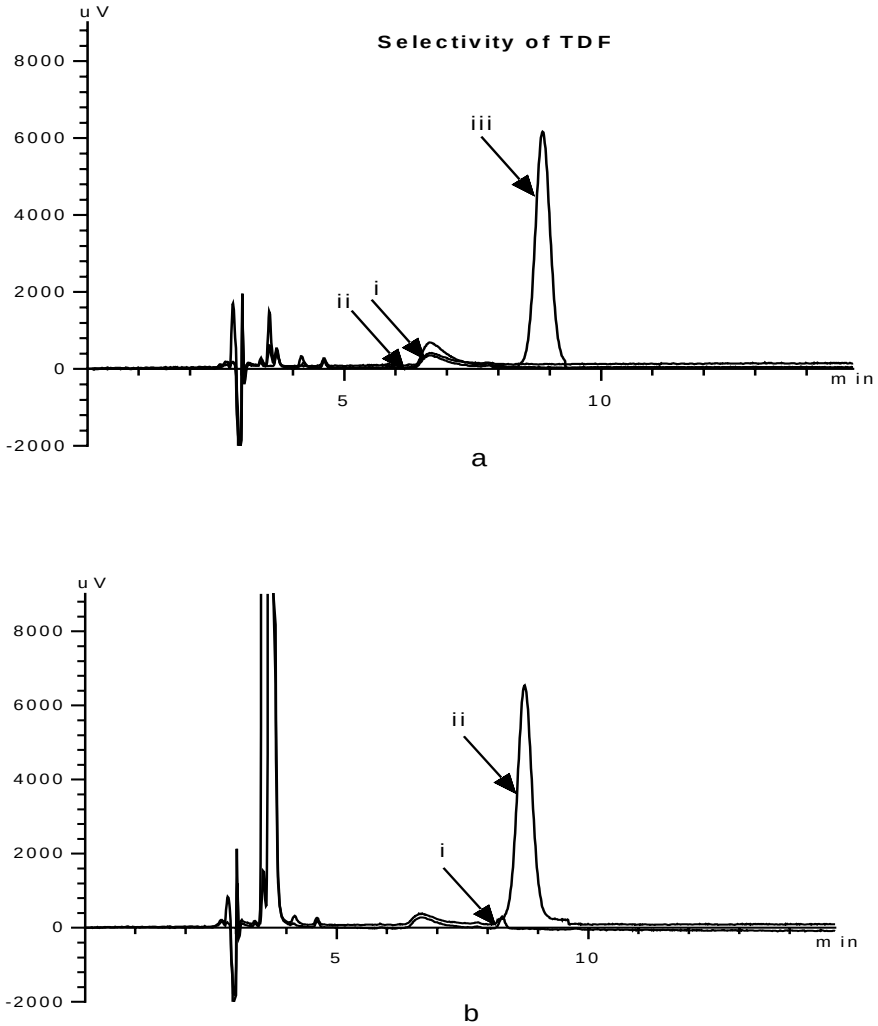

Fig. 2.1: Overlaid chromatograms of (a) (i) chitosan (ii) sodium tripolyphosphate and (iii) a physical mixture of chitosan, sodium tripolyphosphate and TDF (10 µg/mL) (b) (i) PLGA (ii) a physical mixture of PLGA and TDF (10 µg/mL).

Table 2.2: Linearity and range of TDF in HPLC (*n* = 5).

Nominal concentration (ng/mL)	Average area ± SD[b]	RSD[c] (%)	Predicted concentration[a] (ng/mL)	Bias[d] (%)
250	14009 ± 76.9	0.55	250.64	0.25
500	28784 ± 77.2	0.24	509.85	1.97
750	42628 ± 123.1	0.29	752.73	0.36
1000	57421 ± 463.1	0.81	1012.24	1.22
2000	116347 ± 3610.5	3.10	2046.03	2.30
4000	228076 ± 1487.6	0.65	4006.19	0.15

[a]Predicted concentration of TDF was calculated from least-square linear regression equation.
[b]Standard deviation.
[c]Percentage relative standard deviation.
[d]Accuracy is given in relative error percent = [100 × (predicted concentration – nominal concentration)/nominal concentration)].

Accuracy and precision

The %bias of all the three quality control samples were in the range of -4.70% to 3.73%, this shows the accuracy of the developed method for the estimation of TDF (table 2.3).

The precision was carried out by evaluating the variation of the intra-day and inter-day samples at all the three quality control standards. The %RSD was determined for these samples which were in the range of 1.72% to 3.90% and 2.54 to 3.81% for the intra-day and inter-day samples respectively (table 2.3). From this data, it can be concluded that the developed HPLC method precisely estimated TDF.

Table 2.3: Accuracy and precision for the HPLC method of TDF (*n* = 5).

Quality Control Level (Nominal concentration)	Predicted concentration (ng/mL) Mean ± SD	Accuracy Range (%bias	Intra-day repeatability (%RSD) (*n* = 5)			Inter-day repeatability (%RSD) (*n* = 15)
LQC (350 ng/mL)	346.77 ± 13.21	-4.70 – 2.85	3.73 3.04	3.92 2.53	1.72 2.11	3.81
MQC (1500 ng/mL)	1508.69 ± 38.35	-1.98 – 3.14	2.33 3.28	2.50 3.31	2.52 1.89	2.54
HQC (3000 ng/mL)	3006.81 ± 105.12	-3.28 – 3.73	3.87 2.19	3.54 3.18	3.90 2.04	3.50

Sensitivity

The LOD and LOQ values for the HPLC method were calculated as 54.8 and 182.8 ng/mL respectively. For the calibration curve, the LOQ was chosen as 250 ng/mL. Further, Six different samples having the concentration of 250 ng/mL were analyzed that had the percent bias in the range of -4.00% to 3.53% with %RSD of 2.93%. This indicates that the LOQ of the developed method was accurate, precise and sensitive.

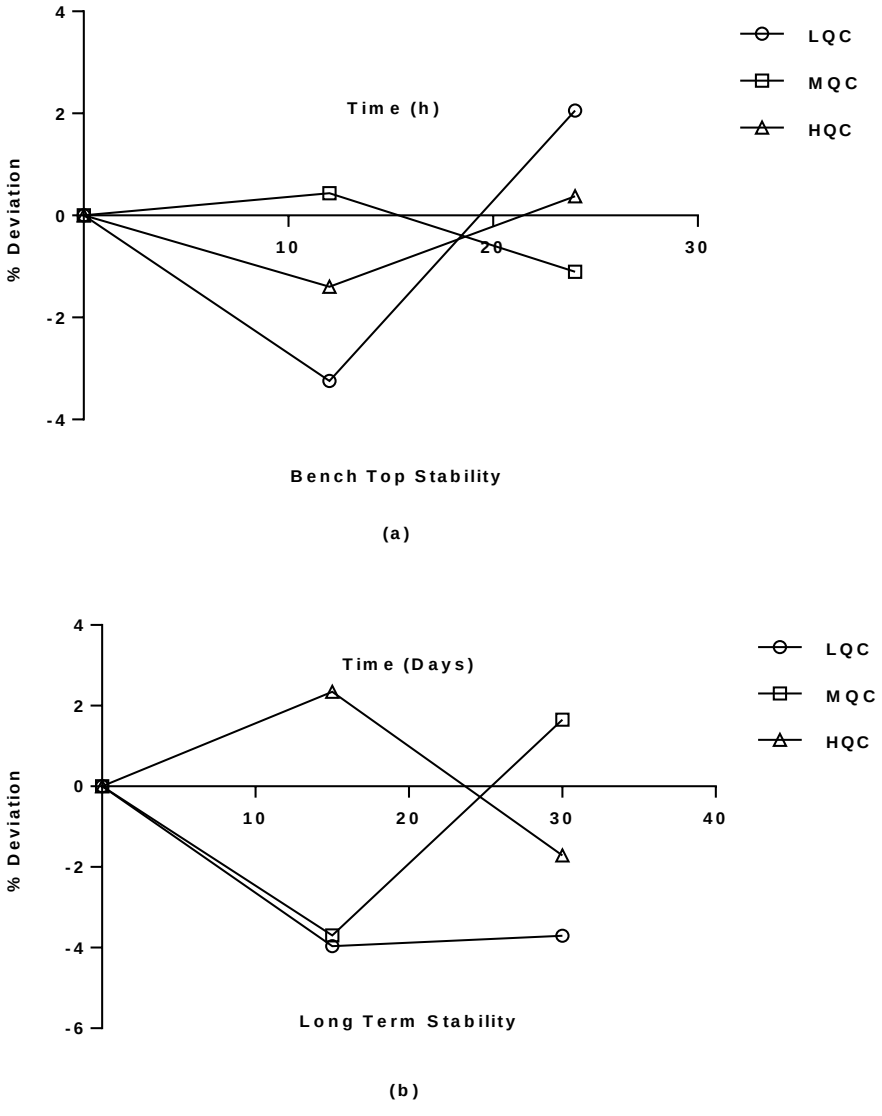

Fig. 2.2: Stability study of TDF (a) bench-top stability and (b) long-term stability.

Stability

While determining the solution stability of TDF, it was observed that the aqueous solution of TDF is stable at bench top conditions for 24 h and also in refrigerated conditions for 30 days (fig. 2.2).

2.4 Method II: Analytical method development of tenofovir in HPLC

2.4.1 Instrument

The HPLC system used for the analytical method development of TNF was the same as described in section 2.2.2.

2.4.2 Chromatographic Conditions

For the estimation of TNF all the chromatographic conditions i.e. column, buffer composition (salt, strength and pH), organic phase composition, wavelength, flow rate and injection volume were kept same as that of TDF. However, the buffer to methanol ratio of the mobile phase was changed from 50:50 to 97:3.

2.4.3 Sample preparation

Standard Stock solution of TNF (2 mg/mL) was prepared by dissolving 10.6 mg of tenofovir monohydrate (molecular weight 305.23 g/mol) in 5 mL of Milli-Q grade water containing 75 µL of 5 M sodium hydroxide solution (Rezk et al., 2005; Sentenac et al., 2003). The working standard and calibration standards solutions of TNF were prepared by making appropriate dilutions of the aliquots of the standard solution with 10 mM ammonium acetate buffer (pH 4.0).

2.4.4 Method validation

2.4.4.1 Selectivity

The selectivity of the developed method was determined by spiking TNF with the excipients used for the preparation of nanocarrier formulation. A similar processing technique as mentioned for TDF in section 2.3.5.1 was followed and analyzed to check for the interference at the retention time of TNF.

2.4.4.2 Linearity and range

The construction of calibration curve and calculation of the coefficient of regression (R^2), slope and intercept for TNF was done for the concentration range of 125 to 4000 ng/mL. An eight point calibration curve was plotted having concentrations of 125, 250, 500, 750, 1000, 1500, 2000 and 4000 ng/mL. Further, three quality control concentrations were chosen to carry out the validation process for TNF which were 200 ng/mL (LQC), 900 ng/mL (MQC) and 3000 ng/mL (HQC).

2.4.4.3 Accuracy and precision

A procedure similar to that described in the estimation of accuracy and precision of TDF mentioned in section 2.3.5.3 was followed in which the intra-day and inter-day variations of the prepared samples of TNF were determined. The samples were prepared for all the quality control standards i.e. LQC, MQC and HQC with each quality control standard having five replicates. The accuracy and precision were evaluated by calculating the %bias and %RSD of the prepared samples respectively. The intra-day repeatability was carried out two times in a day whereas, the inter-day repeatability was determined for three consecutive days.

2.4.4.4 Sensitivity

The sensitivity of this analytical method was determined by calculating the LOD and LOQ values with the help of the following equations:

$$LOD = \frac{3.3\sigma}{S}; LOQ = \frac{10\sigma}{S}$$

Where, 'σ' is the standard deviation of the intercepts and 'S' mean of the slopes of the calibration curves of TNF (n = 18).

2.4.5 Results and discussion

The final chromatographic conditions for analysis of TNF were: mobile phase consisting 10 mM ammonium acetate buffer (pH 4.0) and methanol in the ratio 97:3 *v/v*, flow rate of 1 mL/min, Spincotech C18G enabled column (250 × 4.6 mm, 5 µm) and a column temperature of 40 ºC. The retention was observed to be 19.9 min at which the peak of TNF was sharp with very less tailing factor (< 1.5).

2.4.5.1 Method validation

Selectivity

The selected excipients, when spiked with TNF, did not have any interfering peaks at and around the retention time of TNF. This shows the selective nature of the developed method for the estimation of TNF (fig. 2.3).

Linearity and range

The regression coefficient (R^2) was observed to be 0.9999 which indicates that the selected concentration range of 125–4000 ng/mL had a linear response. The equation of the best-fit line was $y = 127.9x - 8615.7$, where 'x', 'y' are the concentration (ng/mL) and the peak area of TNF respectively. The %RSD and %bias were calculated for these concentrations to evaluate the variation of the observations which seemed to be low (< 5%). The peak area values at individual concentration points are presented in table 2.4.

Accuracy and precision

The %bias of the quality control standards of TNF were in the range of -3.33% to 2.58%, while the %RSD values of the intra-day and inter-day repeatability studies of TNF were in the range

of 0.56% to 4.25% and 2.05% to 2.55% for the samples respectively (table 2.5). This shows that the developed method was both accurate and precise for the estimation of TNF.

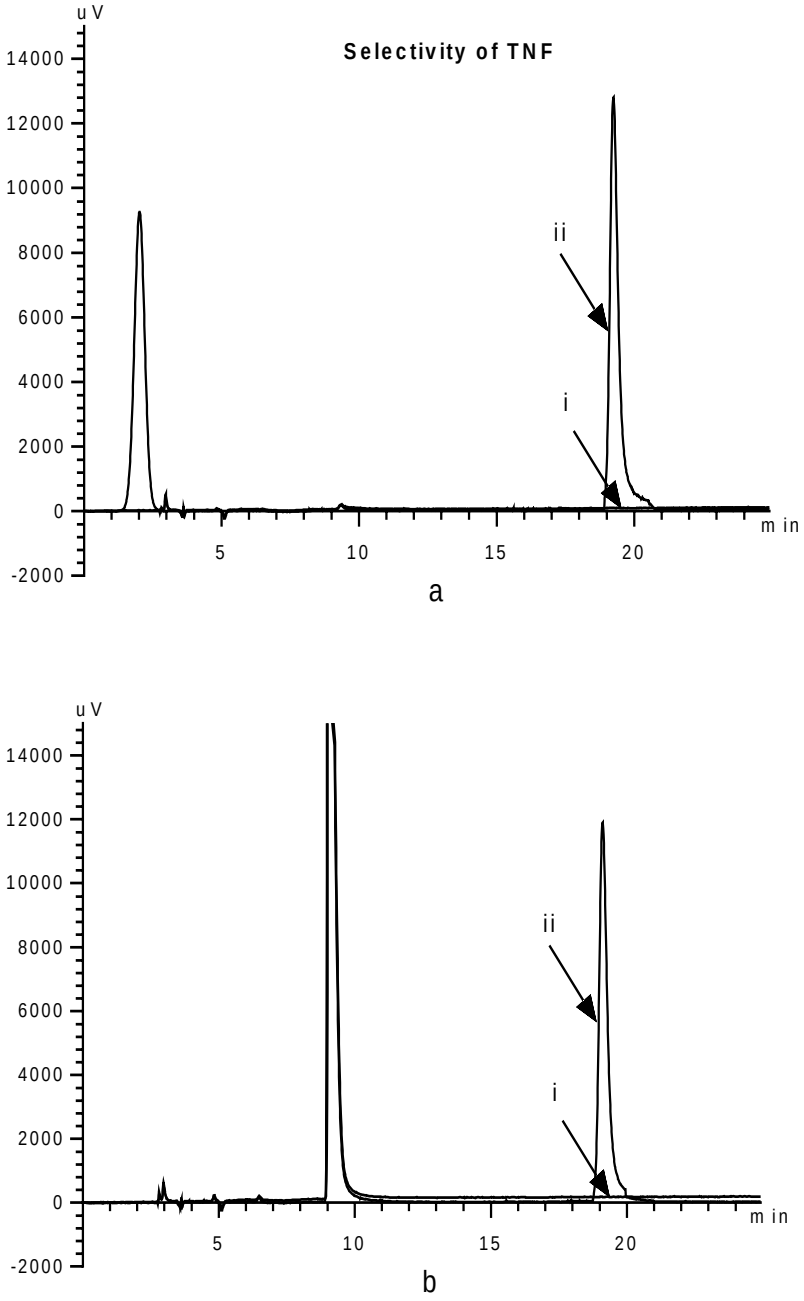

Fig. 2.3: Overlaid chromatograms of (a) (i) chitosan and (ii) a physical mixture of chitosan and TNF (10 µg/mL) (b) (i) PLGA (ii) a physical mixture of PLGA and TNF (10 µg/mL).

Table 2.4: Linearity and range of TNF in HPLC (*n* = 5).

Nominal concentration (ng/mL)	Average area ± SD[b]	RSD[c] (%)	Predicted concentration[a] (ng/mL)	Bias[d] (%)
125	7871 ± 365.68	4.65	128.80	3.04
250	24546 ± 869.82	3.54	259.07	3.64
500	55252 ± 1256.02	2.27	498.96	-0.21
750	86202 ± 1062.16	1.23	740.76	-1.23
1000	118757 ± 2696.54	2.27	995.10	-0.49
1500	183554 ± 3558.46	1.94	1501.33	0.09
2000	246715 ± 4466.23	1.81	1994.77	-0.26
4000	503646 ± 8272.98	1.64	4002.04	0.05

[a]Predicted concentration of TDF was calculated from least-square linear regression equation.
[b]Standard deviation.
[c]Percentage relative standard deviation.
[d]Accuracy is given in relative error percent = [100 × (predicted concentration – nominal concentration)/nominal concentration)].

Table 2.5: Accuracy and precision for the HPLC method of TNF (*n* = 5).

Quality Control Level (Nominal concentration)	Predicted concentration (ng/mL)	Accuracy Range (%bias	Intra-day repeatability (%RSD) (*n* = 5)			Inter-day repeatability (%RSD) (*n* = 15)
	Mean ± SD					
LQC (200 ng/mL)	197.39 ± 4.06	-3.33 – 0.73	3.92 2.86	3.99 3.38	3.35 2.64	2.05
MQC (900 ng/mL)	904.25 ± 18.94	-1.63 – 2.58	3.06 2.37	3.76 3.09	4.25 3.87	2.09
HQC (3000 ng/mL)	2983.86 ± 75.99	-3.07 – 2.00	0.56 1.61	0.71 1.05	1.60 1.42	2.55

Sensitivity

The LOD and LOQ values of the developed method for the estimation of TNF were 18.8 and 62.8 ng/mL respectively. However, 125 ng/mL was chosen as the LOQ for all the practical purposes. Further, accuracy and precision of this LOQ was determined by analyzing its six replicates. The %bias was observed to be in the range of -1.51% to 2.90% with a %RSD of 2.93%. Hence, the LOQ of 125 ng/mL for the developed method was observed to be accurate, precise and sensitive.

2.5 Method III: Analytical method development of tenofovir monoester in HPLC

2.5.1 Instruments

The HPLC system used for the isolation of TMF was the same as described in section 2.2.2. Additionally, for mass analysis LC-MS system (Shimadzu LCMS-2020, Shimadzu Corporation, Kyoto, Japan) was used

2.5.2 Degradation studies

Degradation studies were performed to generate TMF from TDF and develop a suitable analytical technique to isolate TMF from TDF. The protocol for this study was employed from the published work of Yuan et al. (2001). Briefly, a stock solution of TDF (2 mg/mL) was prepared in water and appropriate dilutions were made with pH 8.0 phosphate buffer (USP) from this stock to prepare TDF samples having a concentration of 200 µg/mL (n = 3). These samples were stored at 50 °C for 24 h after which appropriate dilutions were made and analyzed immediately with HPLC. The results were compared with freshly prepared samples from the same stock of TDF (stored at –20 °C) having same concentration of 200 µg/mL (diluted appropriately).

2.5.3 Method development

Trials with different mobile phase compositions were performed to isolate the monoester peak with a reasonable run-time and peak characteristics

2.5.4 Chromatographic conditions

The chromatographic conditions for the estimation of TMF were same as that of TDF, the only difference was in the ratio of buffer and methanol in the mobile phase which was changed from 50:50 to 70:30 *v/v*.

2.5.5 MS analysis

To confirm that the isolated chromatogram obtained from the degradation studies of TDF belonged to TMF, the same samples were analyzed in mass spectrophotometer by making appropriate dilutions in methanol. The obtained spectra was scrutinized to determine the presence of TMF in the degraded samples.

2.5.6 Sample Preparation

A primary stock solution of TMF having a concentration of 2 mg/mL was prepared in 10 mM ammonium acetate buffer (pH 4.0). Working stock solution having a concentration of 200 μg/mL of TMF was then prepared by diluting the aliquot taken from the primary stock. Aqueous standards having different concentrations were prepared by taking required amount of aliquots of the working stock solution and diluting it with 10 mM ammonium acetate buffer (pH 4.0).

2.5.7 Method validation

2.5.7.1 Linearity and range

A five point calibration curve for TMF was constructed for the concentration range of 225 to 4000 ng/mL. Three quality control concentrations were chosen to carry out the validation process for TMF which were 300 ng/mL (LQC), 1000 ng/mL (MQC) and 3000 ng/mL (HQC).

2.5.7.2 Accuracy and precision

The intra-day and inter-day variations were determined for all the quality control standards i.e. LQC, MQC and HQC with each quality control standard having five replicates. The %bias and %RSD were calculated to determine the accuracy and precision of the prepared samples respectively. The intra-day repeatability was carried out two times in a day whereas, the inter-day repeatability was determined for three consecutive days.

2.5.7.3 Sensitivity

The sensitivity of this analytical method for the quantitation of TMF was determined by calculating the LOD and LOQ values with the help of the following equations:

$$LOD = \frac{3.3\sigma}{S}; LOQ = \frac{10\sigma}{S}$$

Where, 'σ' is the standard deviation of the intercepts and 'S' mean of the slopes of the calibration curves of TMF (n = 15).

2.5.8 Results and discussion

2.5.8.1 Degradation studies

The degradation samples were analyzed for TDF and TNF and compared with freshly prepared samples. It was observed that in the degradation samples both the TDF and TNF peaks were not present at detectable levels and in the case of the freshly prepared samples only the TDF peak was present (fig. 2.4). Hence, it can be concluded that there was a definite and complete degradation of the prodrug (i.e. TDF) however it did not convert to its active form (i.e. TNF).

2.5.8.2 Method development

As, TDF and TNF were not present in the degradation samples, these samples were run with varying compositions of buffer and methanol in the mobile phase. The variation of the mobile phase composition ranged from 50:50 to 97:3 of buffer and methanol respectively because the expected product of degradation was TMF whose polarity lies between TDF and TNF. At the buffer and methanol ratio of 70:30 a sharp peak with a retention time of 10.8 min was observed with the same level of response as that of TDF which could most likely correspond to TMF (fig. 2.5). However, further confirmation studies were required.

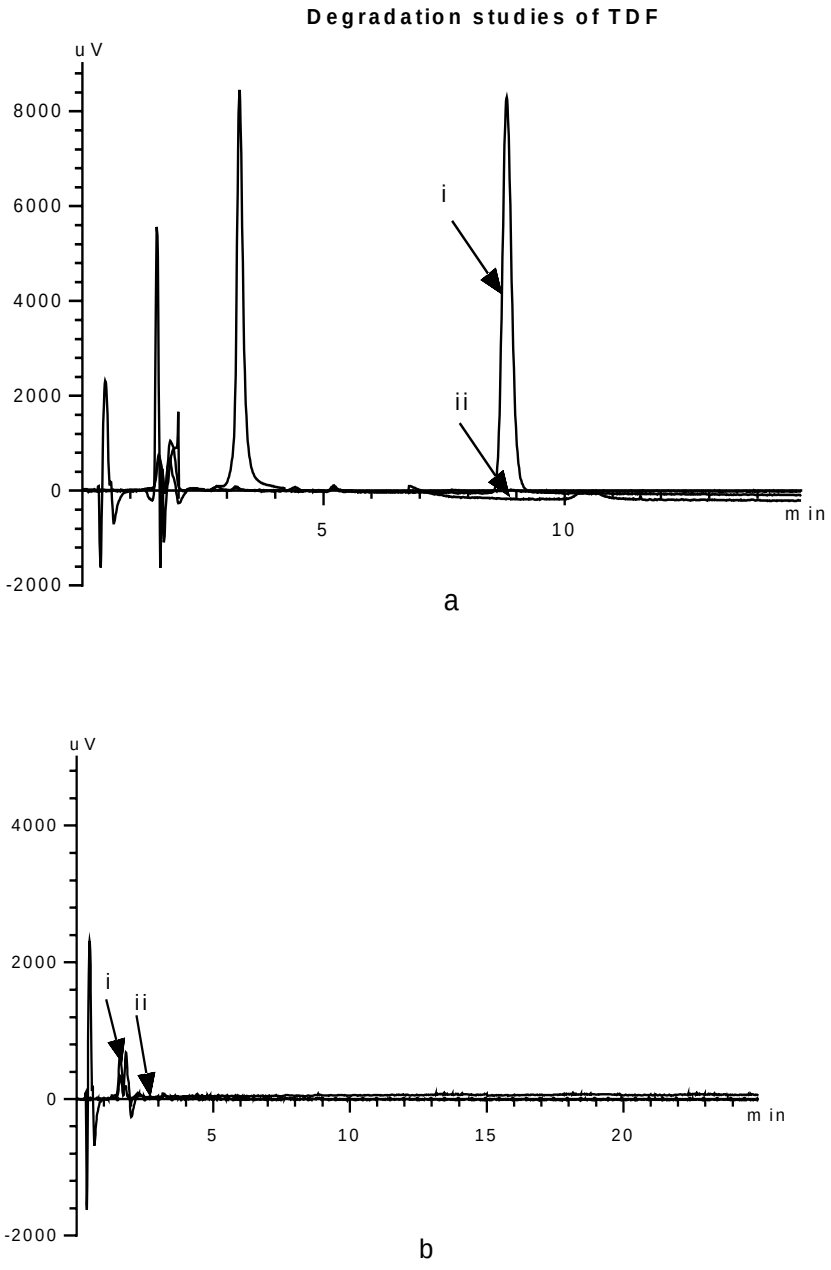

Fig. 2.4: Overlaid chromatograms of (a) (i) Fresh sample of TDF (15 µg/mL) and (ii) Degradation sample of TDF when both were estimated for TDF using the chromatographic conditions of TDF HPLC method (b) (i) Fresh sample of TDF and (ii) Degradation sample of TDF when both were estimated for TNF using the chromatographic conditions of TNF HPLC method.

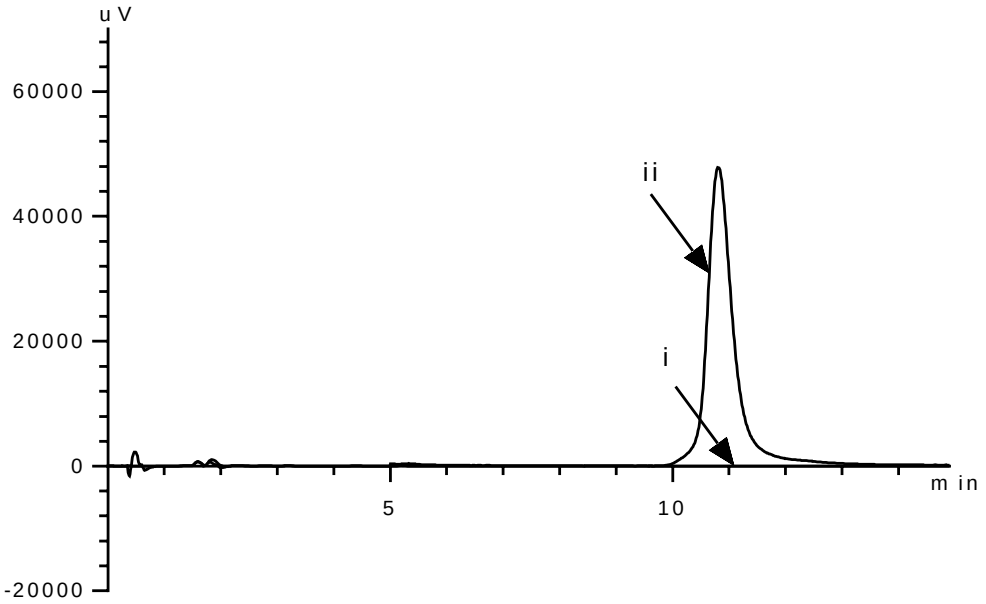

Fig. 2.5: Overlaid chromatograms of (i) Blank (ii) Degradation sample of TDF when estimated for TMF.

2.5.8.3 MS analysis

Fig. 2.6 shows the positive ion mass spectra obtained after mass spectrophotometric analysis of the degradation samples and that of the freshly prepared samples. It can be observed that the freshly prepared samples had a response at a m/z value of 520 which corresponds to the molecular weight of tenofovir disoproxil, however in the case of degraded samples the response at the m/z value of 520 was absent and a response at a m/z value of 404 was observed which corresponds to the molecular weight of TMF. Hence, it can be concluded that the degradant observed and the peak obtained in HPLC at 70:30 of buffer and methanol mobile phase composition correspond to TMF. The calibration curve of TMF was then developed and validated.

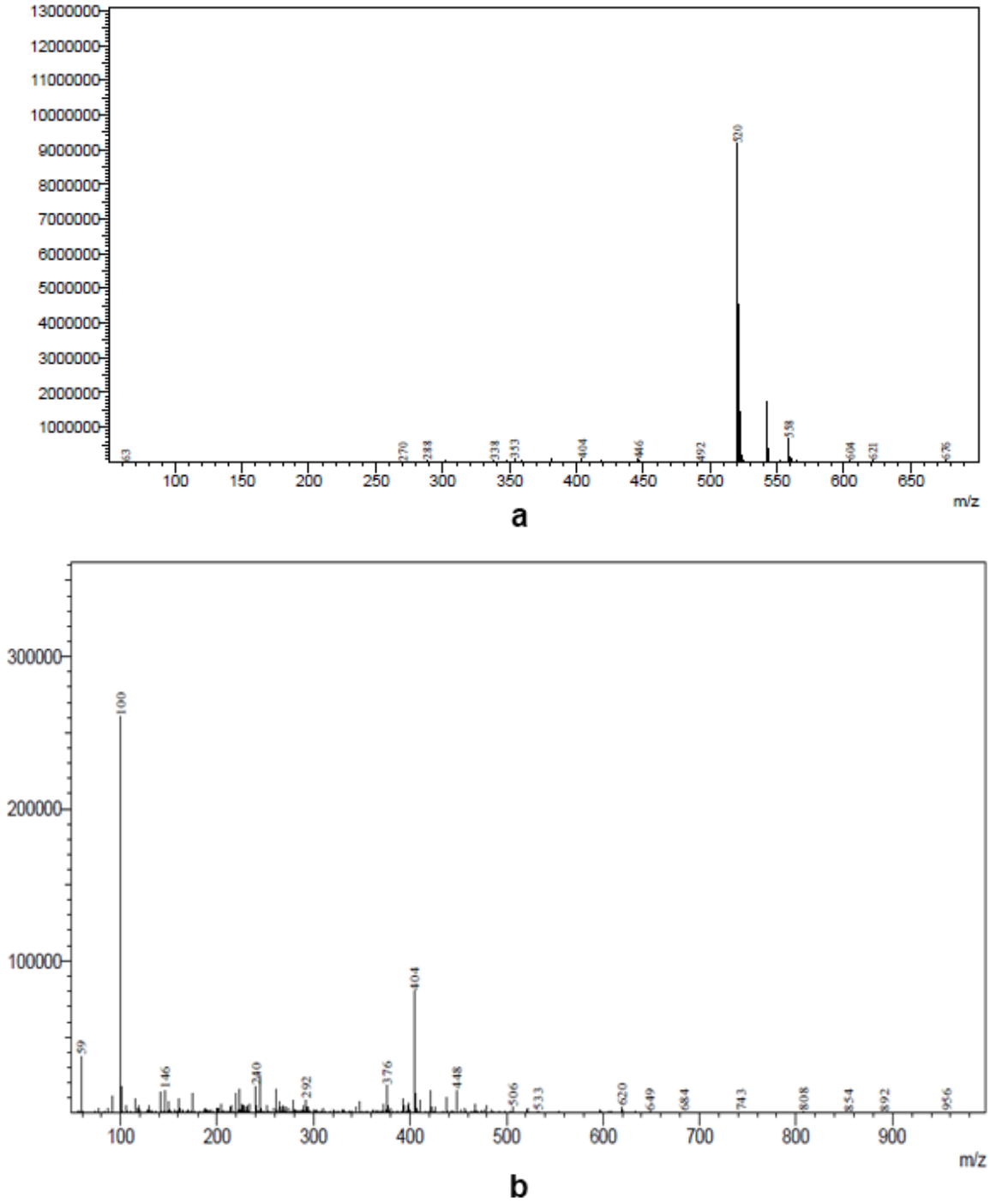

Fig. 2.6: Positive ion mass spectra obtained after mass spectrophotometric analysis of (a) the freshly prepared samples and (b) the degradation samples.

2.5.8.4 Method validation

Linearity and range

For the selected concentration range of 225–4000 ng/mL, a regression coefficient (R^2) of 0.9999 was observed showing a linear response. The equation of the best-fit line was $y =$

$67.862x - 2855.1$, where 'x', 'y' are the concentration (ng/mL) and the peak area of TMF respectively. The peak area, %RSD and %bias values of the individual concentrations in the caliberation range are presented in table 2.6

Table 2.6: Linearity and range of TMF in HPLC (*n* = 5).

Nominal concentration (ng/mL)	Average area ± SD[b]	RSD[c] (%)	Predicted concentration[a] (ng/mL)	Bias[d] (%)
225	13001 ± 163.1	1.25	233.65	3.84
400	24192 ± 295.4	1.22	398.56	-0.36
800	52650 ± 1449.7	2.75	817.91	2.24
1200	76521 ± 713.7	0.93	1169.68	-2.53
4000	268941 ± 4850.5	1.80	4005.14	0.13

[a]Predicted concentration of TDF was calculated from least-square linear regression equation.
[b]Standard deviation.
[c]Percentage relative standard deviation.
[d]Accuracy is given in relative error percent = [100 × (predicted concentration – nominal concentration)/nominal concentration)].

Table 2.7: Accuracy and precision for the HPLC method of TMF (*n* = 5).

Quality Control Level (Nominal concentration)	Predicted concentration (ng/mL)	Accuracy Range (%bias	Intra-day repeatability (%RSD) (*n* = 5)			Inter-day repeatability (%RSD) (*n* = 30)
	Mean ± SD					
LQC (300 ng/mL)	299.86 ± 5.17	-1.77 – 1.68	2.97 2.61	0.93 1.45	1.81 2.38	1.72
MQC (1000 ng/mL)	992.23 ± 8.45	-1.62 – 0.08	2.11 1.94	2.72 3.05	3.89 3.42	0.85
HQC (3000 ng/mL)	2948.24 ± 38.69	-3.02 – -0.44	2.61 2.24	2.90 2.49	1.19 1.88	1.31

Accuracy and precision

The %bias of the quality control standards of TMF were in the range of -3.02% to 1.68%. The %RSD values of the intra-day and inter-day repeatability studies of TMF were in the range of 0.93% to 3.89% and 0.85% to 1.72% for the samples respectively (table 2.7). The low %bias

and %RSD values shows the accuracy and the precision of the developed method for the estimation of TMF.

Sensitivity

The LOD and LOQ values of the developed method for the estimation of TMF were 63.5 and 211.6 ng/mL respectively. However, 225 ng/mL was chosen as the LOQ for all the practical purposes. The accuracy and precision of this LOQ was determined by analyzing its six replicates. The %bias was observed to be in the range of -2.07% to 3.46% with a %RSD of 2.90%. Hence, the LOQ of 225 ng/mL for the developed method was observed to be accurate, precise and sensitive.

2.6 Method IV: Analytical method development of tenofovir in rat plasma using HPLC

2.6.1 Instruments

The HPLC system used for the bioanalytical method development of TNF was the same as described in section 2.2.2.

2.6.2 Mobile phase optimization

The optimization of mobile phase was done based on the level of resolution of the analyte from the plasma components, peak properties (retention time, tailing factor and asymmetric factor), ease of preparation and applicability of the method for *in vivo* studies in rats. To achieve this, the effect of different buffer salts, pH and varying proportions with acetonitrile and methanol with buffer were investigated.

2.6.3 Chromatographic conditions

Chromatographic separation was performed on a Spincotech C18G enabled column (250 × 4.6 mm, 5 µm). The mobile phase consisted of 10 mM ammonium acetate buffer (pH 4.0) and methanol in the ratio of 97:3 *v/v*. Buffer was pre-filtered through 0.22 µm Millipore filtration

membrane. Isocratic conditions were employed at a flow rate of 1 mL/min and TNF was monitored at a wavelength of 260 nm. The HPLC system was stabilized for 1 h at 1 mL/min flow rate, through baseline monitoring prior to actual analysis. An injection volume of 50 µL was set for the optimized method.

2.6.4 Preparation of standard stock and working standard solutions

Standard Stock solution of TNF (2 mg/mL) was prepared by dissolving 10.6 mg of tenofovir monohydrate (molecular weight 305.23 g/mol) in 5 mL of Milli-Q grade water containing 75 µL of 5 M sodium hydroxide solution. The working standard solutions of TNF were prepared by making appropriate dilutions of the aliquots of the standard solution with 10 mM ammonium acetate buffer (pH 4.0).

2.6.5 Blood collection and plasma separation

Blood was collected from the male Wistar rats by puncturing the retro-orbital plexus with the help of rat bleeding capillaries. The collected blood samples were centrifuged at 905 × g rpm for 10 min and the separated plasma was collected and stored at -80 °C. Ethical clearance was taken for the protocol of blood collection and plasma separation and carrying out *in vivo* oral pharmacokinetic studies from the institute's animal ethics committee (approval No.: IAEC–02/01–14).

2.6.6 Preparation of plasma calibration standard, quality control samples and plasma blank

To prepare plasma calibration standards with concentrations of 250, 500, 750, 1000, 1500, 2000, 3000 and 4000 ng/mL; 10 µL of appropriate working standard solution (10X) of TNF was spiked in 90 µL drug-free rat plasma. Similar procedure was followed for preparing plasma low quality control (LQC) 400 ng/mL, medium quality control (MQC) 900 ng/mL and high

quality control (HQC) 2500 ng/mL samples. Plasma blank was prepared by spiking 10 µL of 10 mM ammonium acetate buffer (pH 4.0) in 90 µL of drug-free rat plasma.

2.6.7 Sample pre-treatment

Different protein precipitating agents were explored to check if protein precipitation can be used as a viable technique for extraction of TNF from rat plasma. Other extraction techniques like liquid-liquid extraction (LLE) and salting-out assisted liquid-liquid extraction (SLLE) were also evaluated. In the optimized pre-treatment method, 100 µL of plasma sample was taken in a 1.5 mL eppendroff tube; the plasma proteins were precipitated by adding the following in sequence: 10 µL of trifluoroacetic acid (13 M), 15 µL of 35% *v/v* perchloric acid, and 400 µL of acetonitrile. The samples were vortex-mixed for 30 seconds and then centrifuged at 7800 × g at 4 °C for 15 min. The supernatant was then transferred into a glass tube; acids were neutralized partially with 10 µL of ammonium hydroxide (14.8 M). This neutralized supernatant was evaporated under a gentle stream of nitrogen gas at 40 °C. The dried extracts were then reconstituted with 100 µL of 10 mM ammonium acetate buffer (pH 4.0), centrifuged at 11300 × g at 4 °C for 10 min and the supernatant transferred into sample loading vials. The samples were injected into the HPLC system without further processing.

2.6.8 Method validation

The guidelines of International Conference on Harmonization and United States Pharmacopoeia were employed in validating the analytical method. Linearity, accuracy, precision, specificity, recovery, sensitivity and stability of the method were evaluated. Specificity was determined by comparing six different lots of drug-free plasma samples and TNF spiked plasma samples to check the potential chromatographic interference from plasma matrix at the retention time of drug peak. An eight–point calibration curve was developed in the range of 250 ng/mL to 4000 ng/mL (analyzed in five independent runs). The equation of

the calibration curve was developed by least-square regression for the peak area and concentration of analyte (TNF). The homoscedasticity of variances of the data used in the linear model was checked with the help of Cochran's C test ('t Lam, 2010). For determining the intra-day accuracy and precision, five replicates of each quality control samples of TNF were analyzed twice on the same day. The inter-day accuracy and precision were assessed by analysis of five replicates of quality control samples on three different days. LOD and LOQ were determined from the standard deviation of response and the slope of calibration curve. To determine the recovery of TNF, the peak area of the analyte (TNF) obtained from plasma samples was compared with that of the analytical samples at the same nominal concentration. Recovery studies were performed across all the quality control levels and precision of TNF recovery at each level (n = 5) was determined. The stability studies were done at each of the quality control levels. To evaluate the freeze–thaw stability of TNF in rat plasma at -20 °C, three freeze–thaw cycles were performed for three consecutive days and one set of quality control samples (n = 5) were analyzed after each cycle. Short-term stability of TNF in rat plasma was determined by preparing five sets of samples at each quality control level and storing at room temperature; each set (n = 5) was analyzed every 6^{th} h for a period of 24 h. Long-term stability of TNF in rat plasma was determined by analyzing one set of quality control samples (n = 5) that were frozen at -20 °C on 7^{th}, 14^{th}, 21^{st} and the 28^{th} day after sample preparation. The percentage deviation from the mean concentrations observed at zero time was calculated in all the stability studies. The stability of TNF stock solution was also established by storing it at room temperature for a period of 24 h and comparing the response of 1.5 µg/mL solution prepared from this stock solution (after 24 h storage period) against the same concentration prepared using a fresh stock solution. To show the applicability of the method for estimation of samples well above the linearity range the dilution integrity studies were performed. In this study, plasma samples with concentrations of 10, 20 and 30 µg/mL were

prepared, which were 2.5, 5 and 7.5 times the highest concentration (4000 ng/mL) in the linearity range respectively. These samples were diluted appropriately with drug-free plasma, vortex-mixed for 5 min, and then processed and analyzed as per the procedure described above.

2.6.9 Pharmacokinetic application

To evaluate the suitability of the method for a pharmacokinetic study, single dose intravenous (IV) bolus studies were performed using male Wistar rats weighing 180 to 220 g (n = 5). Prior approval of the protocol was obtained from the Institutional Animal Ethics Committee of BITS-Pilani, Hyderabad campus, Hyderabad, India (Approval No.: IAEC–01/15–13). All animals were housed under controlled environmental conditions (22 ± 1 °C room temperature; 55 ± 10% relative humidity; 12 h light/dark cycle) and were allowed access to food and water *ad libitum*. Aqueous solution of TDF was prepared and administered at 22 mg/kg dose (equivalent to 10 mg/kg of TNF) through tail vein injection. Blood samples were collected by retro-orbital puncture, at pre-dose, 0.083, 0.167, 0.25, 0.5, 1, 2, 3 and 4 h following IV bolus administration of TNF. The collected blood samples were centrifuged at 4 °C for 10 min at 950 × g to separate the plasma. The separated plasma was stored at -20 °C until further analysis. All plasma samples were processed and analyzed. Non-compartmental analysis of the obtained pharmacokinetic data was performed with the help of Phoenix WinNonlin® software (version 7.00, Pharsight Corporation, CA, USA).

2.6.10 Results and discussion

2.6.10.1 Method development

The primary challenge associated with the method development for TNF is its short elution time, even at low organic phase concentration. This leads to an improper resolution of TNF from plasma proteins. Therefore, the optimization process for this method was focused on achieving good resolution of TNF, without compromising on its peak properties.

Effect of solvent

When acetonitrile was used as an organic phase, a drastic reduction in retention time was observed even with slight increase in its proportion with respect to buffer. However, when methanol was used as the organic phase, the change in retention time was less drastic. It was easier to optimize the retention time of TNF with methanol than with acetonitrile, therefore, methanol was selected as an organic phase for the method. In the optimized mobile phase the composition of methanol in the mobile phase was kept minimum (buffer: methanol::97:3 *v/v*).

Effect of buffer on drug peak properties

Variation in buffer pH, strength and salt type did not affect peak tailing factor and asymmetric factor. Further, the variation in buffer strength and salt type had no impact on the retention time. However, the retention time was sensitive to the changes in buffer pH. As, TNF is a weakly acidic drug, an increase in pH bought about a reduction in the retention time. This caused an interference with the plasma proteins. Conversely, decreasing pH increased the retention time, and thereby, the run-time of the method. Good peak properties with an acceptable run-time and resolution were observed at pH 4.

The optimized mobile phase comprised of 10 mM ammonium acetate buffer (pH 4.0) and methanol in the ratio 97:3 *v/v*. This composition provided minimal interference with plasma components and had optimal peak properties: the retention time of TNF was 19.23 ± 0.27 min (for n = 8, 99% confidence interval (CI) 18.42 – 20.04 min) and the tailing factor was 1.09 ± 0.03 (for n = 8, 99% CI 1.00 and 1.18).

2.6.10.2 Method validation

Selectivity

The LLE and SLLE techniques were not able to extract TNF because of its ionic nature. However, protein precipitation was able to efficiently extract TNF. Optimization of this extraction technique was done using different precipitating agents like acetonitrile (Takahashi et al., 2007), methanol (Jullien et al., 2003), trichloroacetic acid (Sparidans et al., 2003), trifluoroacetic acid (Delahunty et al., 2009), and perchloric acid (Schreiber-Deturmeny & Bruguerolle, 1996) individually and also in combination (fig. 2.7). In the optimized pre-treatment method, 10 µL of trifluoroacetic acid (13 M), 15 µL 35% *v/v* perchloric acid, and 400 µL of acetonitrile were added in sequence to 100 µL of plasma samples to precipitate the proteins and the collected supernatant was then partially neutralized with 10 µL of ammonium hydroxide (14.8 M) before evaporation. This extraction technique was found suitable for selective estimation of TNF in rat plasma with little/no interference from endogenous plasma proteins. This is evident from overlaid chromatograms of blank plasma, *in vivo* test sample and plasma calibration standard (fig. 2.8).

Linearity and range

A linear calibration curve was developed for the concentration range of 250 ng/mL to 4000 ng/mL as shown in table 2.8. The %RSD values did not exceed 5.59 for any of the concentrations. After linear regression analysis, the slope (± standard error of the mean) and intercept (± standard error of the mean) for the calibration curve of TNF were 103.7 (± 0.67) and 1404.1 (± 1342) respectively, with a regression coefficient (R^2) value of 0.999. The homogeneity of the highest variance with the variance of the remaining calibration curve points was checked with the help of Cochran's C test. The experimental value of this test (C_{expt}) was 0.3446, whereas, the critical value (C_{crit}) at $\alpha = 0.05$ was 0.4627, as the $C_{expt} < C_{crit}$, the values of the calibration curve are homoscedastic.

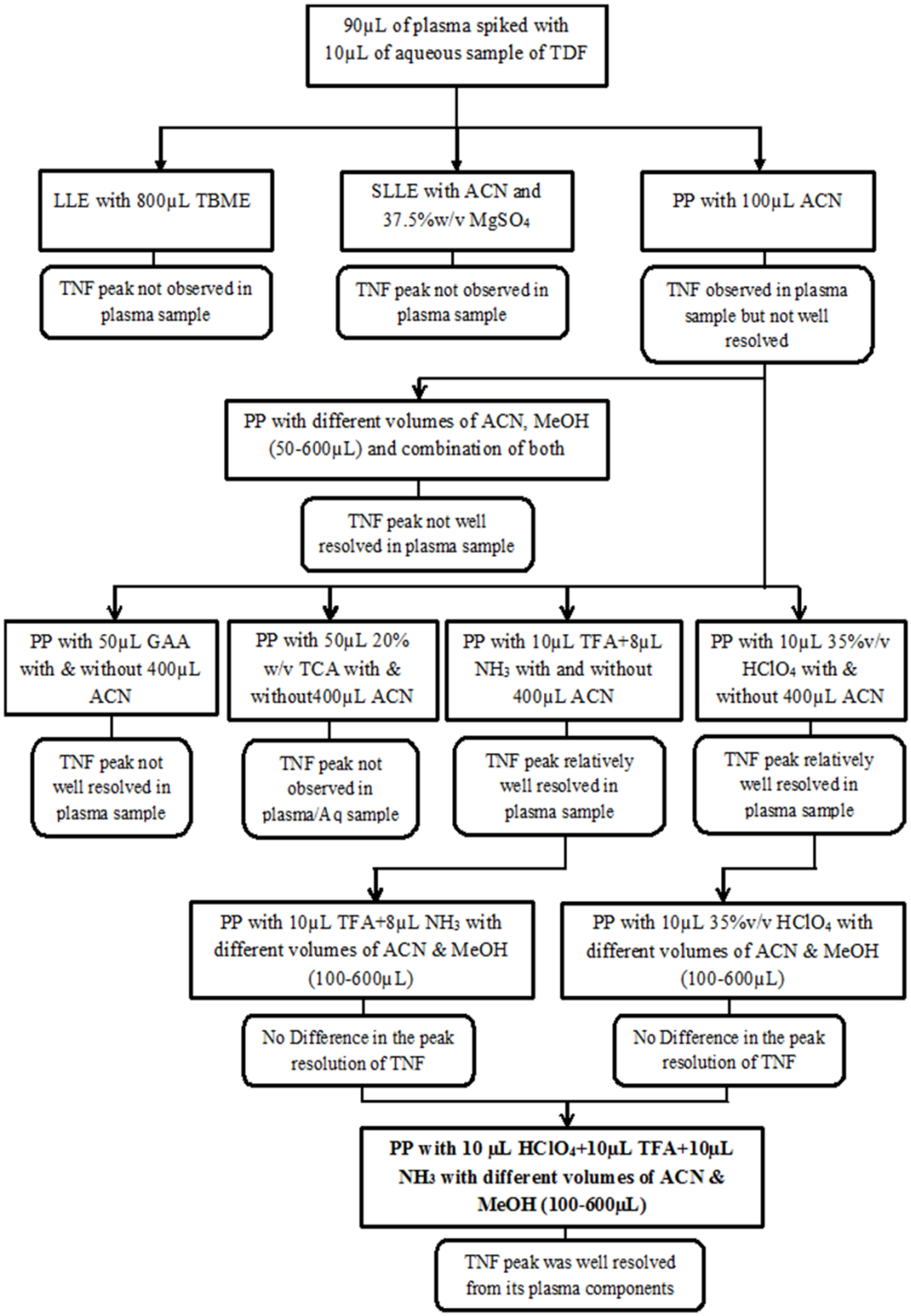

Fig. 2.7: Flow chart depicting the trials involved in optimizing a suitable pre-treatment technique for the plasma samples of TNF.

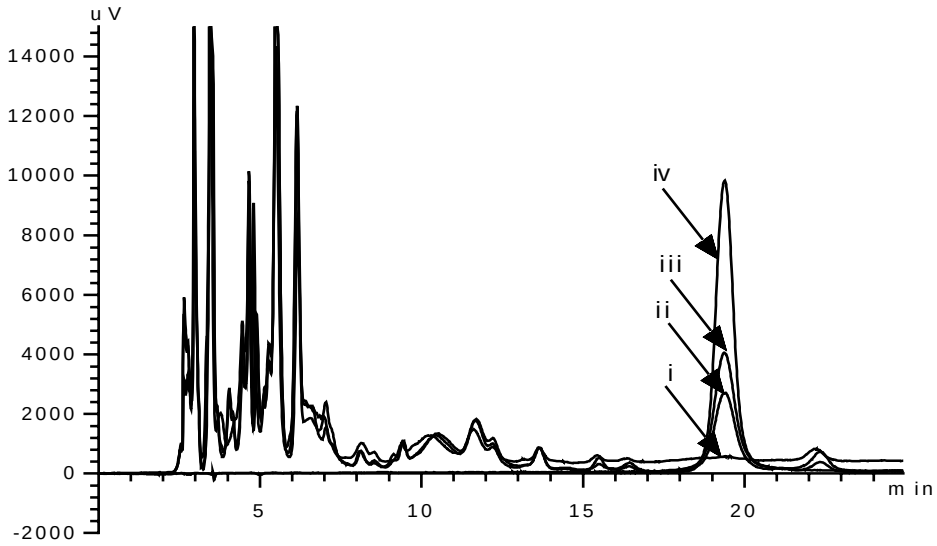

Fig. 2.8: Overlaid chromatograms of (i) blank plasma, (ii) *in vivo* test sample of TNF (iii) plasma calibration standard (1500 ng/mL) of TNF (iv) Aqueous Sample (3000 ng/mL) of TNF.

Table 2.8: Linearity and range of TNF in rat plasma using HPLC (n = 5).

Nominal concentration (ng/mL)	Average area ± SD[b]	RSD[c] (%)	Predicted concentration[a] (ng/mL)	Bias[d] (%)
250	26094 ± 975.03	3.74	238.02	-4.79
500	52124 ± 2661.80	5.11	488.96	-2.21
750	80511 ± 4495.86	5.58	762.62	1.68
1000	102660 ± 3212.14	3.13	976.15	-2.39
1500	158970 ± 8520.11	5.36	1519.00	1.27
2000	212590 ± 4478.97	2.11	2035.91	1.80
3000	312066 ± 6136.41	1.97	2994.91	-0.17
4000	414719 ± 4418.19	1.07	3984.53	-0.39

[a]Predicted concentration of TDF was calculated from least-square linear regression equation.
[b]Standard deviation.
[c]Percentage relative standard deviation.
[d]Accuracy is given in relative error percent = [100 × (predicted concentration – nominal concentration)/nominal concentration)].

Accuracy and precision

All three quality control samples (LQC = 400 ng/mL, MQC = 900 ng/mL and HQC = 2500 ng/mL) showed percent bias ranging from -4.39% to 3.15%, establishing the accuracy of the method for the determination of TNF in rat plasma (table 2.9).

From the results obtained in intermediate repeatability studies, the %RSD values for intra-day and inter-day variation were not more than 4.84% and 4.2**7%** respectively (table 2.8). Lower %RSD values indicate repeatability, reliability and precision of the proposed method.

Table 2.9: Accuracy, precision and recovery for the HPLC method of TNF in rat plasma (*n* = 5).

Quality Control Level (Nominal concentration)	Predicted concentration (ng/mL)		Accuracy range	Intra-day repeatability (%RSD) (*n* = 5)			Inter-day repeatability (%RSD) (*n* = 30)	Recovery
	Mean ± SD	%RSD		Day-1	Day-2	Day-3		Mean (%RSD)
LQC (400 ng/mL)	397.52 ± 15.07	3.79	-4.39 – 3.15	4.18 4.19	2.98 3.54	2.06 3.59	4.27	98.84 (1.92)
MQC (900 ng/mL)	911.90 ± 11.76	1.29	0.02 – 2.63	1.47 2.48	2.18 0.73	1.89 2.02	4.24	97.34 (2.08)
HQC (2500 ng/mL)	2499.30 ± 9.25	0.37	-0.40 – 0.34	4.84 4.34	2.25 1.67	3.32 3.03	3.54	101.07 (1.54)

Sensitivity

The LOD and LOQ values for the HPLC method were calculated as 66.1 and 220.2 ng/mL respectively. The LOQ was chosen as 250 ng/mL for all practical purposes. Further, Six different samples having the concentration of 250 ng/mL were analyzed that had the percent bias in the range of -4.52% to 3.18% with %RSD of 2.65%. This indicates that the LOQ of the developed method was accurate, precise and sensitive and the LOQ was adequate enough to estimate TNF in a pharmacokinetic study performed in rats.

Extraction recovery

Percent recovery of TNF from the spiked rat plasma samples ranged between 97% to 101% (%RSD < 2.1). The high (nearly 100%) mean percent recovery values precluded the use of an internal standard. Low %RSD values (%RSD < 5) established the extraction efficiency for the selected solvents used in combination for precipitation and also affirmed the robustness of the method.

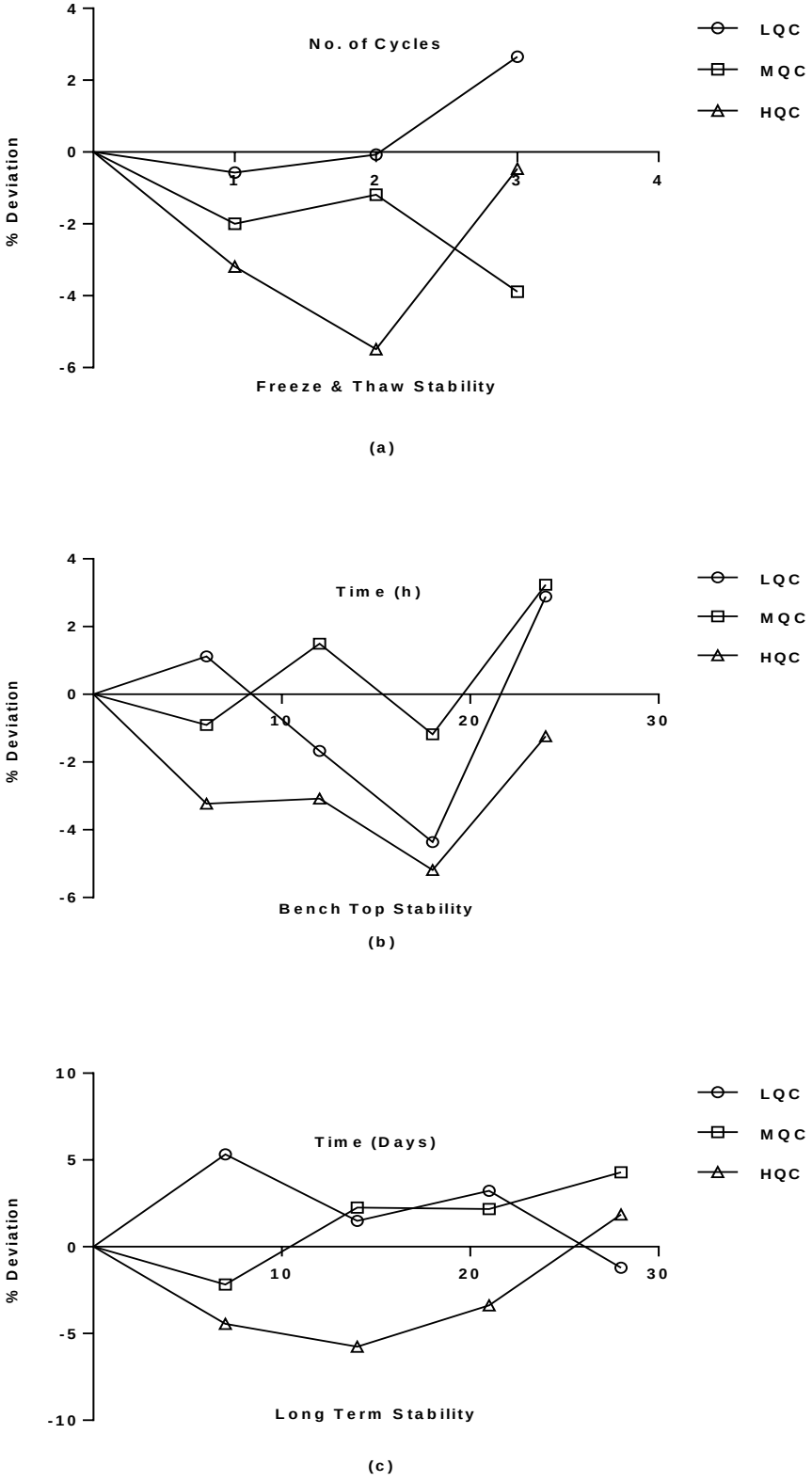

Fig. 2.9: Stability study of TNF in rat plasma (a) freeze-thaw stability, (b) post-preparative stability and (c) long-term stability. Each point represents mean of five independent determinations.

Stability

The degradation studies of TNF in rat plasma were observed under different stress conditions (fig. 2.9): bench top storage at room temperature for 24 h, three freeze-thaw cycles and long-term storage at -20 °C for 28 days. The deviation from the zero time concentration was in the range of -5.19% to 3.24% for bench top stability, -5.49% to 2.65% for freeze-thaw cycles and -5.76% to 5.33% for long-term storage stability studies. The results of this study indicated that storage temperature of -20 °C was adequate to preserve the samples for at least 28 days. At room temperature, the stock solution was stable for a period of 24 h.

Dilution integrity

All the samples (10, 20, 30 µg/mL) had a %bias in the range of -1.18% to 4.67% and the maximum %RSD value observed was 4.89%. This indicates that the method can accurately estimate plasma concentrations that are 7.5 times the higher than the maximum concentration in the linearity range when the appropriate dilutions are made with drug-free plasma.

2.6.10.3 Pharmacokinetic application

In this study, the plasma time course of TNF after administering TDF along the IV route is shown in fig. 2.10. The pharmacokinetic parameters obtained using non-compartmental modeling were: total area under the curve (AUC_{total}) = 12124.85 ± 573.58 h*ng/mL, mean residence time (MRT) = 0.74 ± 0.03 h, concentration at time zero (C_0) = 16392.84 ± 967.65 ng/mL, elimination half-life ($T_{1/2}$) = 0.51 ± 0.03 h, volume of distribution (V_{ss}) = 0.61 ± 0.02 L/kg and total plasma clearance (CL_s) = 0.82 ± 0.02 L/h/kg.

The proposed HPLC method was able to analyze the TNF samples collected till the 3rd hour post IV dosing (approximately equal to 5 times the half-life of TNF in rat). This indicates the suitability of the proposed method in analyzing TNF from pharmacokinetic studies in rats.

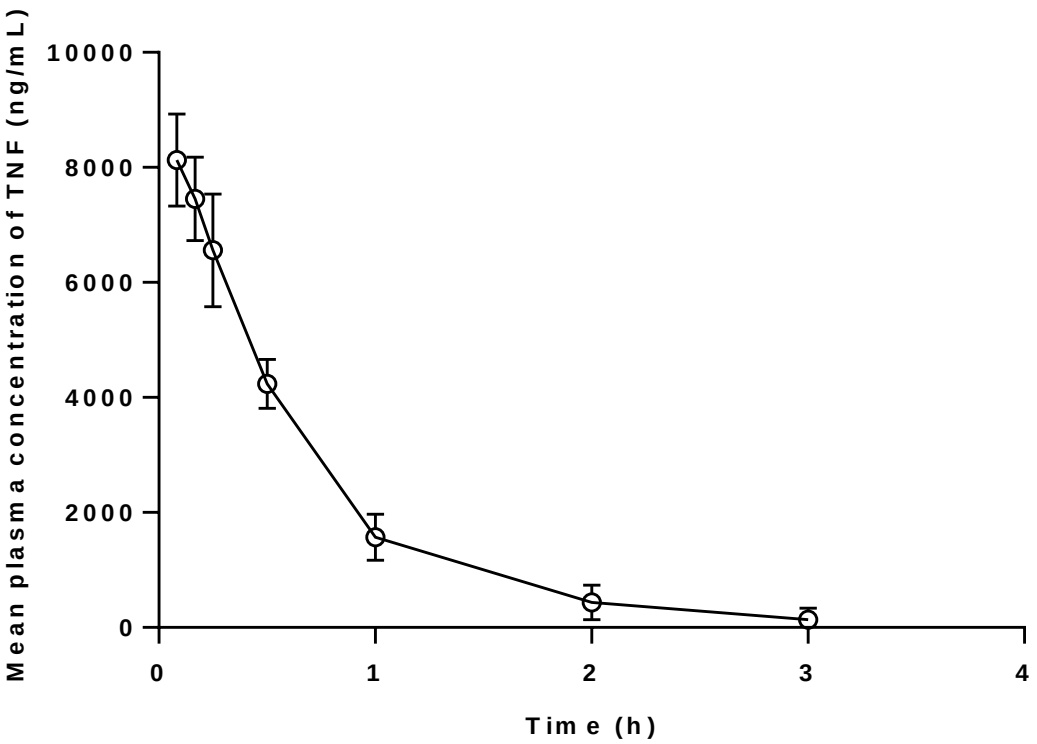

Fig. 2.10: The mean plasma concentration versus time profile of TNF in rats after intravenous bolus administration of the drug (22 mg/kg, *n* = 5).

2.7 Conclusion

Simple, specific, reproducible, precise and cost-effective methods were developed for the estimation of various analytes (i.e. TDF, TMF and TNF). The processing technique was efficient and repeatable, as, nearly complete recovery was obtained throughout the study. Further, the analytes were stable under the processing and storage conditions used for analysis. In the case of the analytical method of TNF the run-time of 25 min could not be reduced further as it would affect the resolution of drug peak from the endogenous plasma components. Nonetheless, our study demonstrates that the developed method could be utilized in analyzing TNF in the samples collected from in vivo pharmacokinetic studies in male Wistar rats.

References

't Lam, R. U. E. (2010). Scrutiny of variance results for outliers: Cochran's test optimized. *Analytica Chimica Acta*, *659*(1–2), 68–84.

Anandakumar, K., Abirami, G., Murugan, S., & Ashok, B. (2013). RP-HPLC method for simultaneous estimation of lamivudine, tenofovir disoproxil fumarate and efavirenz in tablet formulation. *Journal of Analytical Chemistry*, *68*(9), 815–821.

Ashenafi, D., Chintam, V., van Veghel, D., Dragovic, S., Hoogmartens, J., & Adams, E. (2010). Development of a validated liquid chromatographic method for the determination of related substances and assay of tenofovir disoproxil fumarate. *Journal of Separation Science*, *33*(12), 1708–1716.

Bennetto-Hood, C., Long, M. C., & Acosta, E. P. (2007). Development of a sensitive and specific liquid chromatography/mass spectrometry method for the determination of tenofovir in human plasma. *Rapid Communications in Mass Spectrometry : RCM*, *21*(13), 2087–94.

Bezy, V., Morin, P., Couerbe, P., Leleu, G., & Agrofoglio, L. (2005). Simultaneous analysis of several antiretroviral nucleosides in rat-plasma by high-performance liquid chromatography with UV using acetic acid/hydroxylamine buffer Test of this new volatile medium-pH for HPLC-ESI-MS/MS. *Journal of Chromatography. B, Analytical Technologies in the Biomedical and Life Sciences*, *821*(2), 132–43.

Bhavsar, D. S., Patel, B. N., & Patel, C. N. (2012). RP-HPLC method for simultaneous estimation of tenofovir disoproxil fumarate, lamivudine, and efavirenz in combined tablet dosage form. *Pharmaceutical Methods*, *3*(2), 73–78.

Delahunty, T., Bushman, L., & Fletcher, C. V. (2006). Sensitive assay for determining

plasma tenofovir concentrations by LC/MS/MS. *Journal of Chromatography. B, Analytical Technologies in the Biomedical and Life Sciences*, *830*(1), 6–12.

Delahunty, T., Bushman, L., Robbins, B., & Fletcher, C. V. (2009). The simultaneous assay of tenofovir and emtricitabine in plasma using LC/MS/MS and isotopically labeled internal standards. *Journal of Chromatography. B, Analytical Technologies in the Biomedical and Life Sciences*, *877*(20–21), 1907–14.

El Barkil, M., Gagnieu, M.-C., & Guitton, J. (2007). Relevance of a combined UV and single mass spectrometry detection for the determination of tenofovir in human plasma by HPLC in therapeutic drug monitoring. *Journal of Chromatography. B, Analytical Technologies in the Biomedical and Life Sciences*, *854*(1–2), 192–7.

Food and Drug Administration, HHS. (2003). International Conference on Harmonisation; Stability Data Package for Registration Applications in Climatic Zones III and IV; Stability Testing of New Drug Substances and Products; availability. Notice. *Federal Register*, *68*(225), 65717–8.

Geboers, S., Haenen, S., Mols, R., Brouwers, J., Tack, J., Annaert, P., & Augustijns, P. (2015). Intestinal behavior of the ester prodrug tenofovir DF in humans. *International Journal of Pharmaceutics*, *485*(1–2).

Gomes, N. A., Vaidya, V. V, Pudage, A., Joshi, S. S., & Parekh, S. A. (2008). Liquid chromatography-tandem mass spectrometry (LC-MS/MS) method for simultaneous determination of tenofovir and emtricitabine in human plasma and its application to a bioequivalence study. *Journal of Pharmaceutical and Biomedical Analysis*, *48*(3), 918–26.

Jullien, V., Tréluyer, J.-M., Pons, G., & Rey, E. (2003). Determination of tenofovir in human

plasma by high-performance liquid chromatography with spectrofluorimetric detection. *Journal of Chromatography. B, Analytical Technologies in the Biomedical and Life Sciences*, *785*(2), 377–81.

Jung, B. H., Rezk, N. L., Bridges, A. S., Corbett, A. H., & Kashuba, A. D. M. (2007). Simultaneous determination of 17 antiretroviral drugs in human plasma for quantitative analysis with liquid chromatography-tandem mass spectrometry. *Biomedical Chromatography : BMC*, *21*(10), 1095–104.

Kearney, B. P., Flaherty, J. F., & Shah, J. (2004). Tenofovir disoproxil fumarate: clinical pharmacology and pharmacokinetics. *Clinical Pharmacokinetics*, *43*(9), 595–612.

Nirogi, R., Bhyrapuneni, G., Kandikere, V., Mudigonda, K., Komarneni, P., Aleti, R., & Mukkanti, K. (2009). Simultaneous quantification of a non-nucleoside reverse transcriptase inhibitor efavirenz, a nucleoside reverse transcriptase inhibitor emtricitabine and a nucleotide reverse transcriptase inhibitor tenofovir in plasma by liquid chromatography positive io. *Biomedical Chromatography: BMC*, *23*(4), 371–381.

Pokharkar, V. B., Jolly, M. R., & Kumbhar, D. D. (2015). Engineering of a hybrid polymer–lipid nanocarrier for the nasal delivery of tenofovir disoproxil fumarate: Physicochemical, molecular, microstructural, and stability evaluation. *European Journal of Pharmaceutical Sciences*, *71*, 99–111.

Rezk, N. L., Crutchley, R. D., & Kashuba, A. D. M. (2005). Simultaneous quantification of emtricitabine and tenofovir in human plasma using high-performance liquid chromatography after solid phase extraction. *Journal of Chromatography. B, Analytical Technologies in the Biomedical and Life Sciences*, *822*(1–2), 201–8.

Schreiber-Deturmeny, E., & Bruguerolle, B. (1996). Simultaneous high-performance liquid chromatographic determination of caffeine and theophylline for routine drug monitoring

in human plasma. *Journal of Chromatography. B, Biomedical Applications*, *677*(2), 305–12.

Sentenac, S., Fernandez, C., Thuillier, A., Lechat, P., & Aymard, G. (2003). Sensitive determination of tenofovir in human plasma samples using reversed-phase liquid chromatography. *Journal of Chromatography. B, Analytical Technologies in the Biomedical and Life Sciences*, *793*(2), 317–24.

Sparidans, R. W., Crommentuyn, K. M. L., Schellens, J. H. M., & Beijnen, J. H. (2003). Liquid chromatographic assay for the antiviral nucleotide analogue tenofovir in plasma using derivatization with chloroacetaldehyde. *Journal of Chromatography. B, Analytical Technologies in the Biomedical and Life Sciences*, *791*(1–2), 227–33.

Takahashi, M., Kudaka, Y., Okumura, N., Hirano, A., Banno, K., & Kaneda, T. (2007). Determination of plasma tenofovir concentrations using a conventional LC-MS method. *Biological & Pharmaceutical Bulletin*, *30*(9), 1784–6.

Van Gelder, J., Annaert, P., Naesens, L., De Clercq, E., Van den Mooter, G., Kinget, R., & Augustijns, P. (1999). Inhibition of intestinal metabolism of the antiviral ester prodrug bis(POC)-PMPA by nature-identical fruit extracts as a strategy to enhance its oral absorption: an in vitro study. *Pharmaceutical Research*, *16*(7), 1035–40.

Van Gelder, J., Deferme, S., Annaert, P., Naesens, L., De Clercq, E., Van den Mooter, G., … Augustijns, P. (2000). Increased absorption of the antiviral ester prodrug tenofovir disoproxil in rat ileum by inhibiting its intestinal metabolism. *Drug Metabolism and Disposition: The Biological Fate of Chemicals*, *28*(12), 1394–6.

Walters, D. L., Jacobs, D. L., Tomaszewski, J. E., & Graves, S. (1999). Analysis of various nucleosides in plasma using solid phase extraction and high-performance liquid

chromatography with UV detection. *Journal of Pharmaceutical and Biomedical Analysis*, *19*(6), 955–65.

Yuan, L. C., Dahl, T. C., & Oliyai, R. (2001). Degradation kinetics of oxycarbonyloxymethyl prodrugs of phosphonates in solution. *Pharmaceutical Research*, *18*(2), 234–237.

Chapter 3

Pharmacokinetic Interaction of TDF with Pharmaceutical Excipients and Ester Rich Fruit Juices

3.1 Introduction

Different fruit juices (FJs) and pharmaceutical excipients have been explored to study their effect on the oral absorption of drugs that are prone to enzymatic degradation or P-gp efflux in the gut. Among the FJs, grapefruit juice (GFJ) has been reported extensively to increase the oral absorption of drugs like lopinavir (Ravi, Vats, Thakur, Srivani, & Aditya, 2012), amlodipine, nitrendipine, saquinavir etc., by inhibiting intestinal enzymes (cytochrome P450 (CYP) 3A4, CYP1A2, esterases) and efflux proteins (P-gp) (Bailey, Malcolm, Arnold, & Spence, 1998; Kane & Lipsky, 2000; P. Li, Callery, Gan, & Balani, 2007). It is a citrus fruit of Rutaceae family and is known to be rich in furanocoumarins and flavonoids. It has many medicinal properties like anticancer, antioxidant and hypocholesterolemic etc., and is also reported to be beneficial against atherosclerosis (De Castro, Mertens-Talcott, Derendorf, & Butterweck, 2008; Kelebek, 2010; Kiani & Imam, 2007). Orange juice (OJ) has been reported to inhibit P-gp and multi-drug resistant protein 2 (MRP-2) efflux proteins affecting the oral pharmacokinetic profile of vinblastine, atenolol and saquinavir (Honda et al., 2004; Lilja, Raaska, & Neuvonen, 2005; Takanaga et al., 2000). Similar to GFJ it is a citrus fruit whose family name is Rutaceae. The majority of polyphenols present in OJ are in the form of hydroxycinnamic acids and flavonoids, among which flavanones are predominant. Hydroxycinnamic acids occur mainly as esters of ferulic, *p*-coumaric, sinapic and caffeic acids (Gross, Carmon, Lifshitz, & Sklarz, 1975; Klimczak, Małecka, Szlachta, & Gliszczyńska-Świgło, 2007; Titta et al., 2010). Cranberry juice (CBJ) has been reported to increase the oral absorption of nifedipine by inhibiting the gut wall CYP3A enzymes in rats (Mohri & Uesawa, 2001). Its botanical name is Vaccinium macrocarpon and belongs to Ericaceae family. CBJ is reported to be effective in the prevention of urinary tract infections. Additionally, CBJ is also shown to be effective in inhibiting Helicobacter pylori adhesion. It is a rich source of phytochemicals like flavonol glycosides, anthocyanins, proanthocyanidins (condensed

tannins), and organic and phenolic acids. Additionally, quercetin and myricetin are reported to be the major flavonoids present in CBJ (Chen, Zuo, & Deng, 2001; Kontiokari et al., 2001; Seeram, Adams, Hardy, & Heber, 2004). Pomegranate whose botanical name is Punica Granatum belongs to Lythraceae family. It is a rich source of punicalagin, ellagitannins, gallotannins, and flavonoids because of which it is known to have inhibitory effects on atherosclerotic lesions, antihypertensive, chemoprotective (especially against breast cancer), and antioxidant properties (Aviram & Dornfeld, 2001; Aviram & Rosenblat, 2012; Kim et al., 2002). A few studies have reported the interaction of pomegranate juice (PJ) with CYP3A4 and CYP2C9 thereby altering the intestinal absorption of nitrendipine and carbamazepine respectively (Voruganti, Yamsani, Ravula, Gannu, & Yamsani, 2012).

There are many FJs that have not yet been explored for its pharmacokinetic involvement with drugs but nevertheless are rich in polyphenols or ellagitannins (having ester bonds). Black cherry (prunus serotina) is one such fruit that belongs to Rosaceae family. It is reported to constitute ellagitannins, anthocyanins, ursolic acid, uvaol, and polyphenols. It is known to have antioxidant and antihypertensive properties (Luna-Vázquez et al., 2013). Blueberry (Vaccinium corymbosum) belongs to Ericaceae family. It is reported to be rich in anthocyanins, polyphenols and flavonoids. It is known to have antihypertensive and antioxidant properties. It is also known to reduce the progression of Alzheimer's, and reduce the levels of plasma lipids (Krikorian et al., 2010; Shaughnessy, Boswall, Scanlan, Gottschall-Pass, & Sweeney, 2009; Sinelli, Di Egidio, Casiraghi, Spinardi, & Mignani, 2009). Concorde grape juice (CGJ) is a rich source of the antioxidant flavonoids catechin, epicatechin, quercetin, and anthocyanins. It has been reported for its antioxidant properties with the ability to inhibit oxidation of LDL (O'Byrne, Devaraj, Grundy, & Jialal, 2002; Rice-Evans, Miller, & Paganga, 1996).

Additionally, pharmaceutical excipients like cremophor EL (C-EL), tween 20 (T-20), tween 80 (T-80), D-α-Tocopherol polyethylene glycol 1000 (Vit E TPGS), polyethylene glycol-300 and

400, n-dodecyl-β-D-maltopyranoside etc., were reported to inhibit P-gp efflux and improve the oral uptake of drugs like digoxin, ganciclovir which are known to be P-gp substrates (Cornaire et al., 2004; M. Li et al., 2011).

As discussed in the section 1.9 of the 'Chapter 1' it was observed that TDF is a substrate of esterase because of which it is reported to show altered absorption kinetics along the oral route when co-administered with esterase modulators (Tong et al., 2007; Van Gelder et al., 2002). Hence, the aim of this study was to evaluate the pharmacokinetic interaction of TDF with some selected pharmaceutical excipients that have ester bonds in their structure (i.e. C-EL, T-20, T-80 and Vit E TPGS), two FJs belonging to Ericaceae family (i.e. blueberry juice – BBJ and CBJ), three FJs belonging to Rutaceae family (GFJ, OJ and ruby red grapefruit juice – RGFJ), and three FJs belonging to miscellaneous class of families i.e. Rosaceae (black cherry – BCJ), Vitaceae (CGJ) and Lythraceae (PJ). The selected FJs are reported to be rich in ellagitannins, flavonoids and several other polyphenols which may have the potential to interfere with the metabolic process of TDF that can alter the absorption kinetics of TDF. For this purpose, *in vitro* and *ex vivo* studies were conducted for TDF in the presence of each of the pharmaceutical excipients and FJs in male Wistar rats to elucidate the mechanism of interaction during the oral absorption of TDF. Further, single dose oral pharmacokinetic studies were performed by administering TDF in combination with selected FJs/excipients (based on the results of the *in vitro* and *ex vivo* studies).

Ethical clearance was taken for the protocol for blood collection and plasma separation and for carrying out *in vitro* esterase inhibition studies, *ex vivo* everted gut sac studies and *in vivo* oral pharmacokinetic studies from the institute's animal ethics committee (approval No.: IAEC–02/01–14).

3.2 Materials and methods

3.2.1 Materials

Gift samples of TDF and TNF were obtained from Strides Arcolab Limited, KA, India and TNF by Gilead Sciences, Inc., CA, USA respectively. Potassium dihydrogen orthophosphate, sodium hydroxide, sodium citrate, ethyl acetate, ammonium hydroxide and dimethyl sulfoxide (DMSO) of analytical grade were purchased from SRL Chemicals Ltd., Mumbai, India. Methylcellulose (15 cps, Mol Wt.: 14000 Daltons), glacial acetic acid, perchloric acid, tween 80 and tween 20 of analytical grade and ammonium acetate of HPLC grade were purchased from SD Fine-Chem Limited, Mumbai, India. Analytical grade glucose, diethyl ether, Dulbecco's phosphate buffer (pH 7.4 – DPBS) and HPLC grade methanol and acetonitrile were purchased from HiMedia Laboratories, Mumbai, India. Urethane (analytical grade), Trifluoroacetic acid (HPLC grade), D-α-Tocopherol polyethylene glycol 1000 and Cremophor-EL 35 were purchased from Sigma-Aldrich, Mumbai, India. GFJ (white) and RGFJ was purchased from Ocean Spray Cranberries, Inc., MA, USA. BCJ, BBJ, CBJ, CGJ and PJ were procured from Dynamic Health Laboratories, Inc., NY, USA. OJ was procured from Minute Maid, GA, USA. Rats (Male Wistar) were purchased from Sainath Agencies, Hyderabad, India.

3.2.2 *In vitro* esterase inhibition study

The procedure for this study was based on a previously published work (Crauste-Manciet et al., 1997; P. Li et al., 2007). Briefly, male Wistar rats (n = 5) fasted overnight and on the day of the study they were anesthetized by administering urethane (ip-1.25 g/kg). Laparotomy was done on the anesthetized rats and the small intestine was cut and separated from each animal. The intestinal washing was collected by rinsing each of the small intestines with 1 mL of pH 7.0 phosphate buffer and pooling all of the rinse fluid and finally making up the volume to 7 mL with pH adjusted to 7.0. From this intestinal lumenal fluid, 100 µL was added to each of

the three types of incubation chambers. The first incubation chambers contained 100 µL of pH 7.0 phosphate buffer containing 5 µM of TDF. The second type of incubation chambers contained 100 µL of 40% and 80% *v/v* concentration of each FJ separately containing 5 µM of TDF (pH adjusted to 7.0). The third type of incubation chambers contained 100 µL of 0.5% and 1% of each excipient separately containing 5 µM of TDF (pH adjusted to 7.0). Further, corresponding to the treatment groups, incubation chambers without TDF were also prepared, which served as blanks (to check for the interference of the matrices) in the analysis of TDF and TMF for their respective samples. The reaction was terminated after 30 min by adding 200 µL of acetonitrile and the samples were stored at –80 °C until analysis. The study was done in triplicate for each treatment condition.

3.2.3 *Ex vivo* everted gut sac studies

In order to obtain ester rich compounds present in the FJs, each of the FJs was extracted based on the procedure reported previously (Honda et al., 2004; Tian et al., 2002). Briefly, for each FJ, 50 mL of FJ and 100 mL of ethyl acetate were mixed by shaking vigorously in a separating funnel for 10 min and then kept for standing for 30 min. Then the supernatant (ethyl acetate layer) was collected into a round bottom flask and concentrated under low temperature (40 °C) and pressure (250 mbar) in a rotary evaporator (Hei-VAP PRECISION ML/HB/G3, Heidolph, Schwabach, Germany). The residue obtained was reconstituted with 0.5 mL of DMSO and 200 mL of DPBS (containing 25 mM of glucose) was added to it to form 25% diluted FJ extract.

Rats were fasted overnight and on the day of the experiment they were anesthetized (urethane 1.25 g/kg-ip) and dissected. After anesthesia, laparotomy was done and the entire intestine was removed by cutting across the upper end of the duodenum and the lower end of the ileum and stripping the mesentery manually. The intestine was washed carefully with the normal saline (0.9% *w/v* NaCl) using a syringe equipped with a blunt end. Intestinal segments (i.e. jejunal

part of the intestine beginning from the ligament of Treitz) of 7.5 cm length was cut and carefully everted over a glass rod. The everted intestine was then slipped off the glass rod and tied at one end. From the other end, with the help of a blunt syringe, 750 µL of DPBS buffer was added and tied to form a sac. In the study, these everted gut sacs were kept in each of the three types of reservoirs maintained at 37 °C and oxygenated with O_2/CO_2 (95/5%). The first type of reservoir contained 20 mM TDF in 50 mL of DPBS buffer. The second type of reservoir contained 20 mM TDF and 25% *v/v* of each of the diluted FJ extract in 50 mL of DPBS buffer. The third type of reservoir contained 20 mM TDF and 1% *w/v* of each excipient in 50 mL of DPBS buffer. Further, corresponding to the treatment groups, reservoirs without TDF were also prepared (i.e. reservoirs containing only DPBS buffer, DPBS buffer with each of the FJs separately and DPBS buffer with each of the excipient separately) which acted as blank to check for interference during analysis. The samples were collected from both the donor and receiver compartments from all the reservoirs after 60 min of incubation. The samples were immediately stored at –20 °C until analysis. The study was done in triplicate.

3.2.4 Single-dose oral pharmacokinetic study

Male Wistar rats were used in the study. Rats weighing 200–250 g were housed at 22 ± 1 °C, 55 ± 10% RH (relative humidity) with 12 h light dark cycle. The animals were fasted overnight with access to water *ad libitum* and continued fasting till 4 h post dosing of different treatments on the day of study. Thereafter, rat chow diet was provided ad libitum. In the study, rats were divided into six treatment groups with three rats in each group (n = 3). All the treatments were administered through oral route using a gavage. The first treatment group was administered with 100 mg/kg of free TDF (suspended in 0.5% *w/v* methyl cellulose in water) which is equivalent to 45 mg/kg of TNF. The second treatment group was administered with 100 mg/kg of TDF and 1 mg/kg C-EL. The remaining four treatment groups were administered with 100 mg/kg of TDF and 10 mL/kg of each FJ (i.e. BBJ. BCJ, CBJ, CGJ, GFJ, PJ, OJ and RGFJ)

separately. Blood samples were collected at pre-dose, 5, 10, 15, 30, 60, 120, 240 and 360 min post dosing of the treatments. The blood collection was done from the retro-orbital plexus into a microcentrifuge containing 3.5% *w/v* sodium citrate solution. The collected blood samples were centrifuged at 905 × g for 10 min to harvest the plasma. The plasma samples were immediately stored at –80 °C until analysis.

3.2.5 Sample pretreatment and analysis

The samples were pretreated as per the processing technique mentioned previously for the extraction of TNF from plasma samples in the section 2.6.7 of 'Chapter 2'. After the pretreatment process, each sample was analysed for TNF, TMF and TDF.

3.2.6 Data analysis

The experimental results were represented in terms of mean ± standard deviation (SD). Non-compartmental analysis was performed for the data obtained from the pharmacokinetic studies using Phoenix WinNonlin® software (version 7.00, Pharsight Corporation, CA, USA). To evaluate the statistical significance between the experimental groups, analysis of variance (ANOVA) was performed followed by Bonferroni's multiple comparison test using GraphPad prism software (version 5.03, GraphPad Software, Inc., CA, USA). The significance level was set at 5% (P_{crit}), however, we also reported the calculated *P* value (P_{cal}).

3.3 Results and discussion

3.3.1 Results and discussion of free TDF

3.3.1.1 In vitro esterase inhibition study

In this study, we determined the percentage of TDF remaining (%TDF remaining) and the percentage of TMF formed when compared to free TDF (%TMF formed). In the case of free TDF, the %TDF remaining was found to be 5.92 ± 0.68% whereas, the %TMF formed was

observed to be 100 ± 0.72%. These values were used to evaluate the statistical significance of the metabolic protection provided by the excipients and FJs. Further, the rate of metabolism of TDF to TMF in pH 7.0 phosphate buffer was found to be 275 pmol/mL/min. Further, the extensive metabolism of TDF when incubated in the intestinal washings indicates that the esterases present in the mucosal homogenates of the intestinal washings are capable of metabolizing TDF.

3.3.1.2 Ex vivo everted gut sac studies

This study was performed to understand the effect of FJs and pharmaceutical excipients on the permeability of TDF. TDF and its equivalents (TMF and TNF) were estimated both in donor as well as receiver compartments. After 60 min of incubation, only TMF was recovered from receiver compartment while TDF and TNF were not detected. In the donor compartment, TMF and TDF (in some treatment conditions) could be detected while TNF was not detected in all the treatment conditions.

The Permeability flux of TMF was calculated using the equation, $J = (dQ/dt)/A$, where '*J*' is the permeability flux, 'dQ/dt' is the rate of appearance of TMF in the receiver compartment and 'A' is the surface area of the everted gut sac. The %TMF formed in the donor compartment was also calculated for all the treatment conditions.

The flux of TMF for free TDF was observed to be 4.8 ± 0.7 ng/cm^2/min and the %TMF formed was 99.9 ± 6.4%. It can be observed that nearly complete metabolism of TDF was observed in the donor compartment which further shows the ability of the gut wall enzymes to extensively metabolize TDF.

3.3.1.3 Single-dose oral pharmacokinetic study

The plasma time-course of TNF after single dose oral administration of free TDF is shown is fig. 3.1. In this study, the pharmacokinetic analysis was done for TNF as we could quantify

only TNF and did not observe any detectable levels of TDF or TMF in the plasma samples. The maximum plasma concentration (C_{max}) and the mean total area under the curve (AUC_{total}) of TNF when free TDF was administered were observed to be 1467.5 ± 141.2 ng/mL and 4967.9 ± 575.2 h*ng/mL respectively. Whereas, the elimination half-life ($T_{1/2}$) was observed to be 1.8 ± 0.3 h with the time taken for TNF to reach the maximum level of plasma concentration (T_{max}) to be in the range of 1.0–1.5 h. In the study, we could only estimate TNF in the plasma samples because the plasma esterases rapidly metabolized TDF/TMF to TNF (Geboers et al., 2015). This was further confirmed by our group when both TDF and TMF were spiked individually into blank rat plasma and analysed immediately (after processing) we could only estimate TNF while TDF and TMF were not detected. The $AUC_{0\text{-}6h}$ and AUC_{total} of all the treatment groups showed no statistical difference indicating that the duration of the study was appropriate.

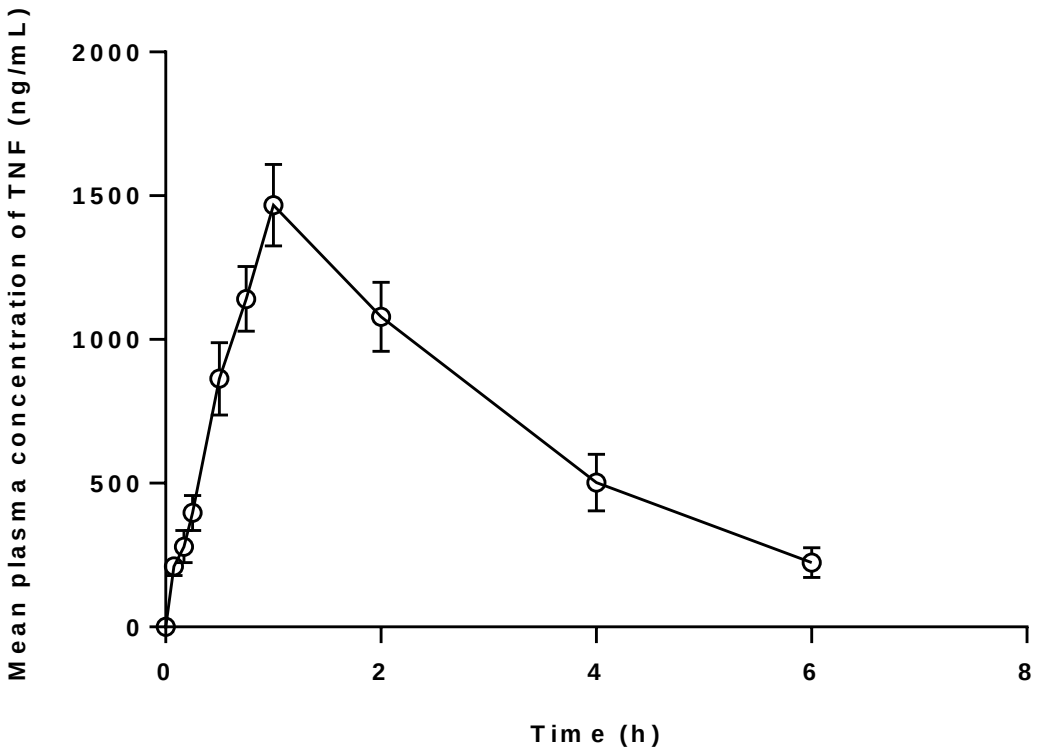

Fig. 3.1: Plasma time course of TNF obtained following oral administration of free TDF (100 mg/kg). Each data point is represented as mean ± SD (*n* = 5).

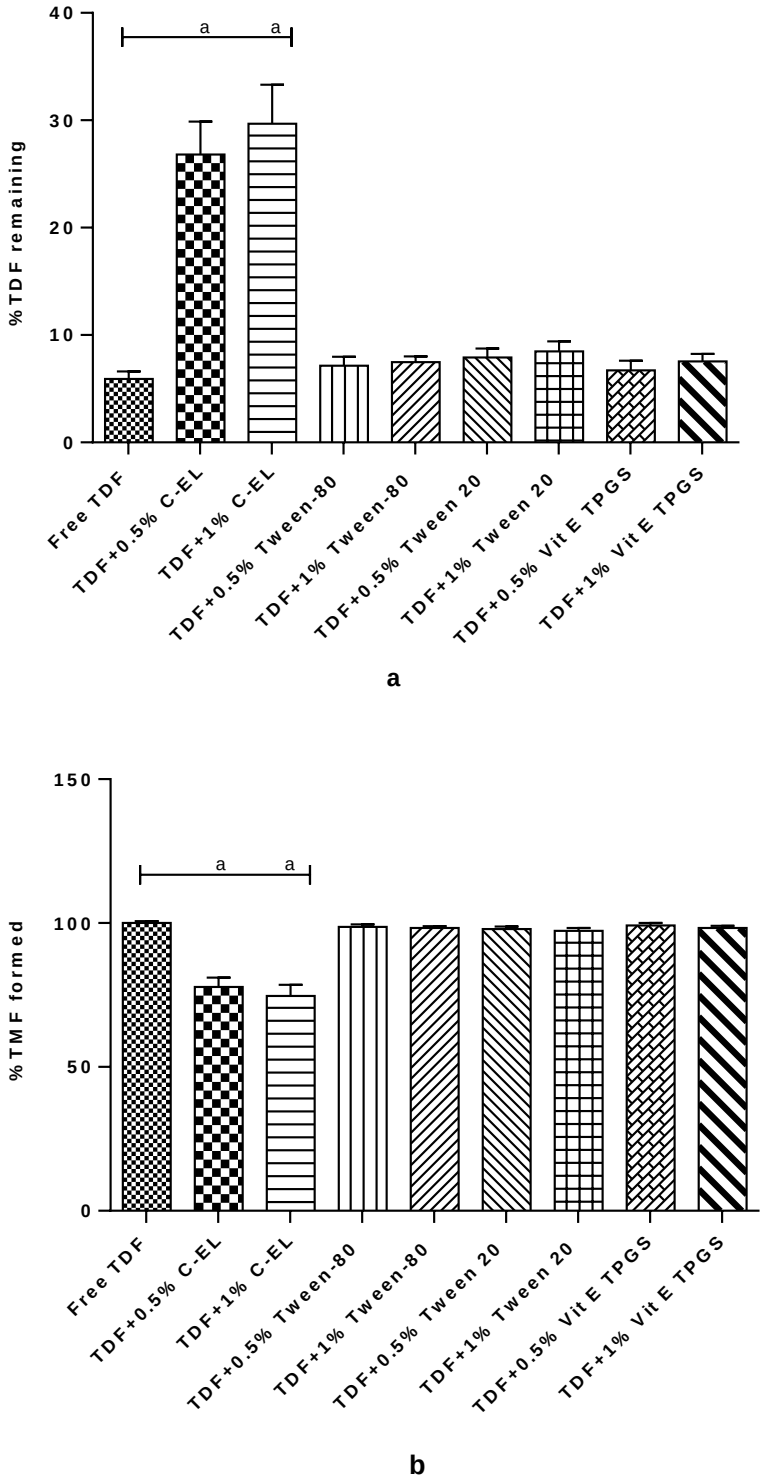

Fig. 3.2: a) %TDF remaining in the intestinal washing after 30 min of incubation in the presence of each of the pharmaceutical excipients at 0.5% and 1.0% *w/v* concentration. b) %TMF formed (when compared to free TDF) in the intestinal washing after 30 min of incubation in the presence of each of the pharmaceutical excipients at 0.5% and 1.0% *w/v* concentration. The values represented are mean ± SD (n = 3). [a]Statistical significance observed at $P_{crit} < 0.001$.

3.3.2 Results and discussion of pharmaceutical excipients

3.3.2.1 In vitro esterase inhibition study

The %TDF remaining and %TMF formed when TDF was incubated with the excipients is shown in fig. 3.2. For C-EL, %TDF remaining was observed to be 26.8 ± 3.1% and 29.6 ± 3.6% at 0.5% and 1% *w/v* concentrations respectively. Whereas, the %TMF formed was found to be 77.7 ± 3.2% and 74.7 ± 3.8% at 0.5% and 1% *w/v* concentrations respectively. These values when compared to free TDF were found to be statistically significant ($P_{cal} < 0.001$) indicating that C-EL could provide a considerable level of metabolic protection for TDF from esterases. However, the inhibition level did not seem to be concentration dependent at the chosen concentrations. Additionally, none of the remaining excipients had any impact on the metabolism of TDF. The probable reason for this phenomenon could be because C-EL apart from having ester bonds in its structure could fit well into the esterase enzyme pocket thereby causing a competitive inhibition of esterase enzymes in metabolizing TDF while the remaining excipients could not.

3.3.2.2 Ex vivo everted gut sac studies

The intestinal flux of TMF in the presence of pharmaceutical excipients C-EL, T-20, T-80 and Vit E TPGS were observed to be 5.74 ± 0.378, 5.82 ± 0.15, 4.46 ± 0.51 and 4.66 ± 0.47 ng/cm^2/min respectively. Whereas, the %TMF formed for the same was found to be 52.80 ± 3.00%, 97.81 ± 8.19%, 99.10 ± 8.55% and 97.73 ± 6.69%.

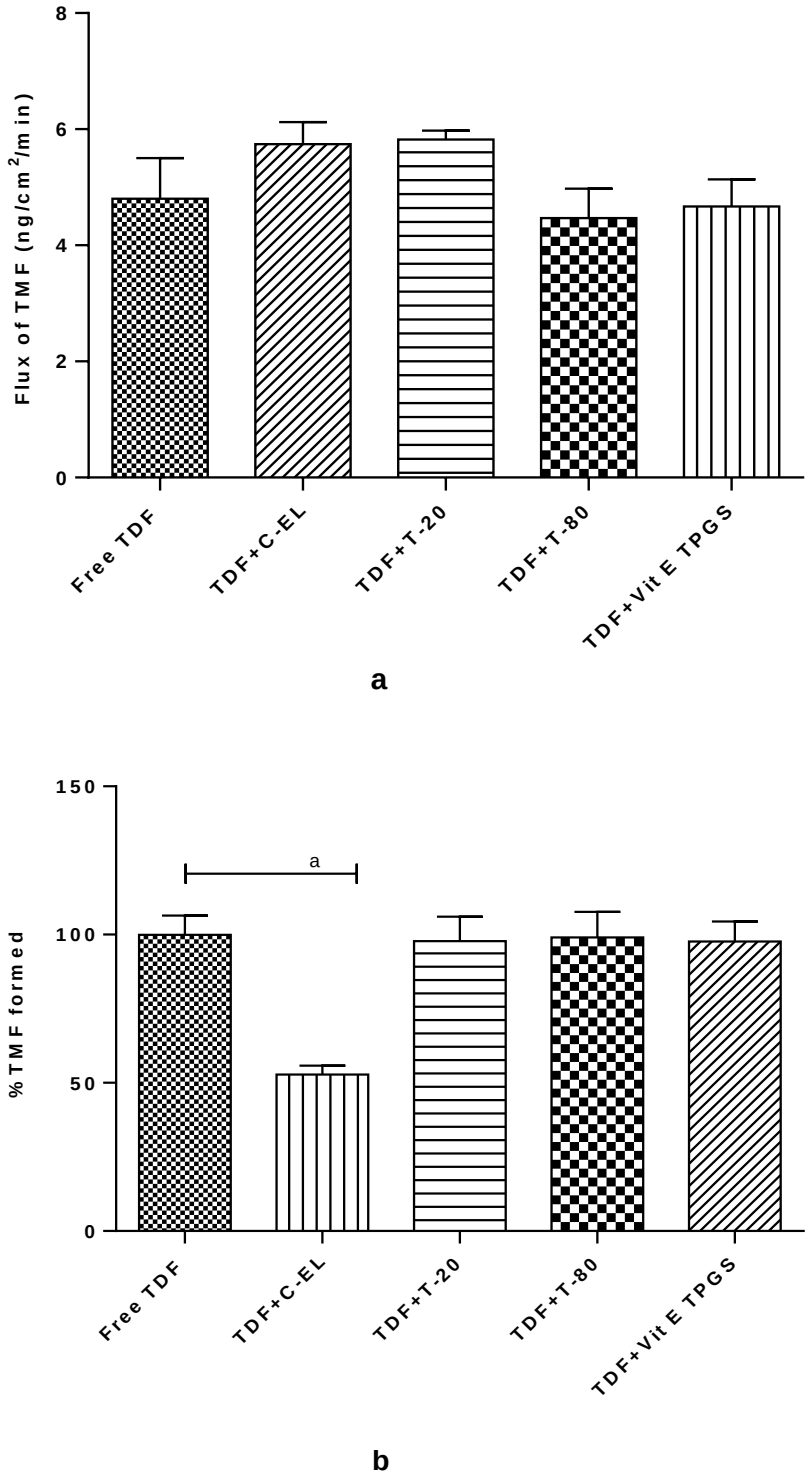

Fig. 3.3: a) The *J* of TMF across the everted gut sac from the donor compartment (lumenal side) to the receiver compartment (serosal side) in the presence of each of the pharmaceutical excipients. b) %TMF formed in the donor compartment in free TDF and in the presence of each of the pharmaceutical excipients. The values represented are mean ± SD (n = 5). [a]Statistical significance observed at $P_{crit} < 0.001$.

The comparison of flux and %TMF formed in different treatment conditions are shown in fig. 3.3. It was observed except C-EL, all the remaining excipients did not have any impact on the metabolism of TDF as there was no significant change in the %TMF formed. The metabolic protection provided by C-EL was observed to statistically significant at $P_{cal} < 0.001$. These observations correlated well with the *in vitro* studies. However, in the donor compartment, we could detect TMF and TDF which indicates that even though C-EL could provide metabolic protection in the donor compartment, when TDF is traversing the gut wall it is getting metabolized to TMF which C-EL is unable to prevent. Further, the comparison of flux values apparently indicated that there was no significant change in the flux of TMF when TDF was incubated with each of the excipients. Even C-EL which could provide metabolic protection in the donor compartment did not have any significant effect on the flux of TMF. To further confirm this observation oral pharmacokinetic studies were performed by co-administering TDF with C-EL.

3.3.2.3 Single-dose oral pharmacokinetic study

The pharmacokinetic profile of TNF when TDF was co-administered with C-EL is shown in fig. 3.4. The C_{max} and AUC_{total} of TNF were observed to be 1645.1 ± 185.2 ng/mL and 5589.6 ± 281.9 h*ng/mL respectively. Whereas, $T_{1/2}$ was 1.9 ± 0.31 h and T_{max} was in the range of 0.75-1.5 h.

Statistical analysis of the pharmacokinetic parameters obtained for free TDF and TDF co-administered with C-EL indicated that there was no significant difference between the C_{max} ($P_{cal} \geq 0.1267$) and AUC_{total} ($P_{cal} \geq 0.0619$) of the two treatment conditions. These results were apparently similar to the observations made in the everted gut sac study which further reaffirms that C-EL was incapable of enhancing the oral absorption of TDF along the oral route. This could be attributed to the inability of C-EL to prevent the metabolism of TDF occurring within

the gut wall as in the everted gut sac studies it was observed that only TMF could be detected in the receiver compartment.

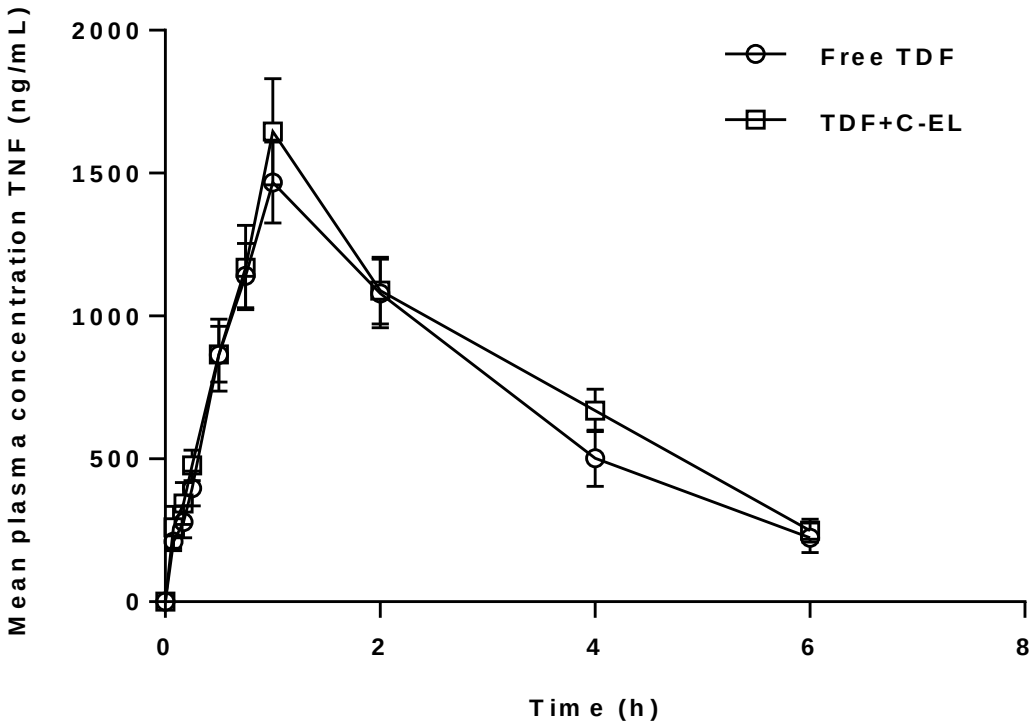

Fig. 3.4: Plasma time course of TNF obtained following oral administration of free TDF (100 mg/kg) and TDF (100 mg/kg) with C-EL (1 mg/kg). Each data point is represented as mean ± SD (n = 5).

3.3.3 Results and discussion of FJs belonging to Ericaceae family

3.3.3.1 In vitro esterase inhibition study

The %TDF remaining after incubation for 30 min in the presence of BBJ was 24.26 ± 3.2% and 27.60 ± 3.4% at 40% and 80% *v/v* concentration levels respectively. %TMF formed in the presence of BBJ was observed to be 80.18 ± 3.5% and 76.57 ± 3.7% at 40% and 80% *v/v* concentration levels respectively. In the presence of CBJ the %TDF remaining was found to be 46.2 ± 3.4% and 52.2 ± 2.4% at 40% and 80% *v/v* concentration levels respectively. The %TMF formed when CBJ was present was observed to be 57.1 ± 3.6% and 50.8 ± 2.6% at 40% and 80% *v/v* concentration levels respectively.

Fig. 3.5 compares the level of metabolic protection provided by these FJs. It can be observed that both the FJs were able to provide a significantly higher level of metabolic protection. However, the level metabolic protection provided by CBJ was higher than BBJ at both the concentration levels. Further, the metabolic protection provided by CBJ was observed to be concentration dependent whereas, for BBJ this phenomenon was not observed for the selected concentration range.

3.3.3.2 Ex vivo everted gut sac studies

After 60 min of incubation, the mean *J* value of TMF in the presence of BBJ and CBJ were 4.2 ± 0.38 and 6.5 ± 0.26 ng/cm^2/min respectively. The %TMF formed in the presence of BBJ and CBJ in the donor compartment was observed to be 49.8 ± 5.63% and 41.7 ± 4.96% respectively. The results of this study indicate that both BBJ and CBJ provided a significant level of metabolic protection for TDF (P_{cal} < 0.001) but, only CBJ could increase the intestinal absorption of TDF. Even though CBJ provided a similar level of metabolic protection as that of BBJ, its presence increased the *J* of TMF while BBJ had no effect. This indicates the possibility that some of the components of the FJs that increased the *J* of TMF have the ability to permeate the gut wall and inhibit the esterase enzymes present within the gut wall. This phenomenon may be more critical than the quantum of esterase inhibition provided by FJs in enhancing the absorption of TMF because TDF being more lipophilic than TMF, has better permeability through the gut wall membranes. To further confirm the observations from this study oral single-dose pharmacokinetic studies were performed in rats.

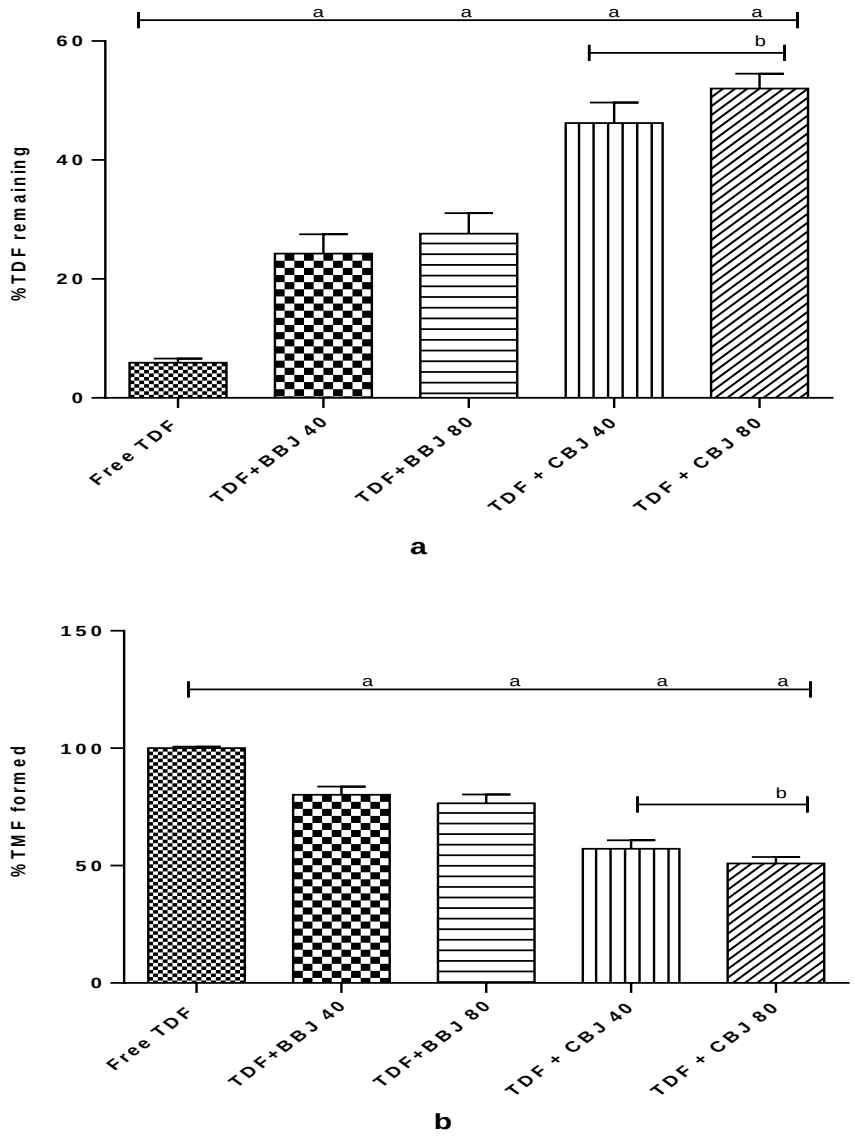

Fig. 3.5: a) %TDF remaining in the intestinal washing after 30 min of incubation in the presence of FJs belonging to Ericaceae family (i.e. BBJ and CBJ) at 40% and 80% *v/v* concentration. b) %TMF formed (when compared to free TDF) in the intestinal washing after 30 min of incubation in the presence of FJs belonging to Ericaceae family (i.e. BBJ and CBJ) at 40% and 80% *v/v* concentration. The values represented are mean ± SD (n = 3). [a]Statistical significance observed at $P_{crit} < 0.001$; [b]Statistical significance observed at $P_{crit} < 0.01$.

3.3.3.3 Single-dose oral pharmacokinetic study

The pharmacokinetic profile of TNF when TDF was co-administered with BBJ and CBJ separately are shown in fig. 3.6. The C_{max} and AUC_{total} of TNF when TDF was co-administered with BBJ were observed as 1495.4 ± 164.3 ng/mL and 5227.1 ± 302.39 h*ng/mL respectively. Whereas, $T_{1/2}$ was 2.2 ± 0.46 h and T_{max} was in the range of 0.5-0.75 h. In the case of CBJ, the

C_{max} and AUC_{total} of TNF were observed to be 2018.3 ± 198.3 ng/mL and 6181.4 ± 477.8 h*ng/mL. The $T_{1/2}$ was found to be 1.6 ± 0.2 h and T_{max} was in the range of 0.5-0.75 h.

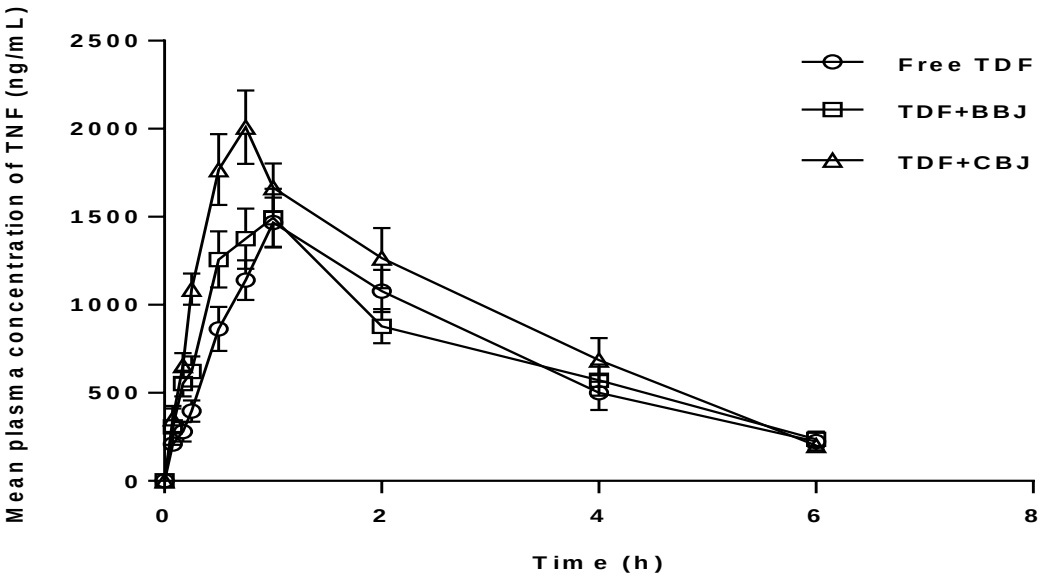

Fig. 3.6: Plasma time course of TNF obtained following oral administration of free TDF (100 mg/kg) and TDF (100 mg/kg) with FJs belonging to Ericaceae family (i.e. BBJ and CBJ – 10 mL/kg). Each data point is represented as mean ± SD (n = 5).

The AUC_{total} and C_{max} values of TNF when TDF was co-administered with BBJ (P_{cal} > 0.999) were not affected significantly when compared to administering free TDF. However, in the case of CBJ, there was a 24% and 38% increase in the C_{max} ($P_{cal} \leq 0.007$) and AUC_{total} ($P_{cal} \leq 0.03$) values respectively. Additionally, there was no significant difference between the $T_{1/2}$ of TNF in the presence and absence of CBJ which indicates that the altered pharmacokinetic profile of TNF is due to the changes in the absorption kinetics of TNF. Hence, these observations apparently imply that the presence of CBJ provided a significant enhancement of the absorption of TDF which correlated well with the observations made in the *ex vivo* studies despite BBJ and CBJ providing the same level of metabolic protection. Even though CBJ is reported to alter the absorption kinetics of warfarin and nifedipine by inhibiting CYP2C9 and CYP3A (Mohri & Uesawa, 2001), there has been no reported work that evaluated the esterase inhibition property of CBJ. Hence, the active components present in CBJ that are responsible for the inhibition of this metabolic process of TDF needs to be identified.

3.3.4 Results and discussion of FJs belonging to Rutaceae family

3.3.4.1 In vitro esterase inhibition study

Table 3.1 compares the %TDF remaining and the %TMF formed when TDF is incubated with GFJ, OJ and RGFJ separately. It can be observed that there was a significant level of metabolic protection of TDF. GFJ could provide the highest level of metabolic protection as there was a significant increase in the %TDF remaining and a significant decrease in the %TMF formed when compared to OJ and RGFJ at both the concentration levels. Additionally, for the tested concentrations both GFJ ($P_{cal} \leq 0.02$) and RGFJ ($P_{cal} \leq 0.002$) provided a concentration dependent metabolic protection for TDF whereas, the metabolic protection provided by OJ was not concentration dependent.

Table 3.1: %TDF remaining and %TMF formed (when compared to free TDF) in the intestinal washing after 30 min of incubation in the presence FJs belonging to Rutaceae family (at 40% and 80% *v/v* concentration).

Treatment group	Concentration	%TDF Remaining	%TMF Formed
Free TDF	5 µM	5.92 ± 0.68	100.00 ± 0.72
TDF + GFJ[d]	40% *w/v*	76.19 ± 2.79[a]	25.31 ± 2.96[a]
	80% *w/v*[c]	83.37 ± 2.98[a]	17.67 ± 3.17[a]
TDF + OJ	40% *w/v*	42.92 ± 3.71[a]	60.67 ± 3.94[a]
	80% *w/v*	47.76 ± 4.43[a]	55.52 ± 4.71[a]
TDF + RGFJ	40% *w/v*	50.93 ± 6.71[a]	51.47 ± 7.21[a]
	80% *w/v*[b]	62.54 ± 3.84[a]	38.98 ± 4.14[a]

The values represented are mean ± SD (n = 3). [a]Statistical significance observed at $P_{crit} < 0.001$ when compared to free TDF; [b]Statistical significance observed at $P_{crit} < 0.01$ when compared to the corresponding FJ at 40% *v/v* concentration; [c]Statistical significance observed at $P_{crit} < 0.01$ when compared to the corresponding FJ at 40% *v/v* concentration; [d]Statistical significance observed at $P_{crit} < 0.001$ when compared to remaining FJs.

3.3.4.2 Ex vivo everted gut sac studies

After 60 min of incubation, the mean J value of TMF in the presence of GFJ, OJ and RGFJ were 10.6 ± 0.8, 5.00 ± 0.4 and 8.4 ± 0.7 ng/cm^2/min respectively. The %TMF formed in the presence of GFJ, OJ and RGFJ in the donor compartment was observed to be 12.6 ± 1.4%, 36.5 ± 2.4% and 20.2 ± 1.3% respectively.

The results of this study indicate that all the FJs belonging to Rutaceae family provided a significant level of metabolic protection for TDF ($P_{cal} < 0.001$) however, GFJ ($P_{cal} < 0.001$) and RGFJ ($P_{cal} \leq 0.014$) could increase the absorption of TDF across the intestinal sac while OJ could not increase the absorption of TDF. The metabolic protection provided by GFJ was found to be the highest when compared to OJ ($P_{cal} < 0.001$) and RGFJ ($P_{cal} < 0.0244$). Also, when the flux values of TMF in the presence of GFJ and RGFJ were analyzed GFJ was able to provide a significantly higher increase in the flux of TMF when compared to RGFJ ($P_{cal} \geq 0.0312$) observed. To further confirm these observations we performed single-dose oral pharmacokinetic studies by individually co-administering TDF with each of the FJs belonging to Rutaceae family in rats.

3.3.4.3 Single-dose oral pharmacokinetic study

The pharmacokinetic profile of TNF when TDF was co-administered with GFJ, OJ and RGFJ separately are shown in fig. 3.7. Further, the pharmacokinetic parameters obtained after the non-compartmental analysis of the pharmacokinetic profiles is shown in table 3.2.

The AUC_{total} and C_{max} values of TNF when TDF was co-administered with OJ ($P_{cal} > 0.999$) were not affected significantly when compared to administering free TDF. However, in the case of GFJ and RGFJ there was a 150% ($P_{cal} < 0.001$) and 36% ($P_{cal} \leq 0.006$) increase in the C_{max} and 97% ($P_{cal} < 0.001$) and 40% ($P_{cal} \leq 0.002$) in the AUC_{total} values respectively. Additionally, there was no significant difference between the $T_{1/2}$ of TNF in the presence and absence of GFJ and RGFJ which indicates that the altered pharmacokinetic profile of TNF is only due to the changes in the absorption kinetics of TNF. Hence, these observations apparently indicate a significant enhancement of the absorption of TDF when co-administered with GFJ and RGFJ.

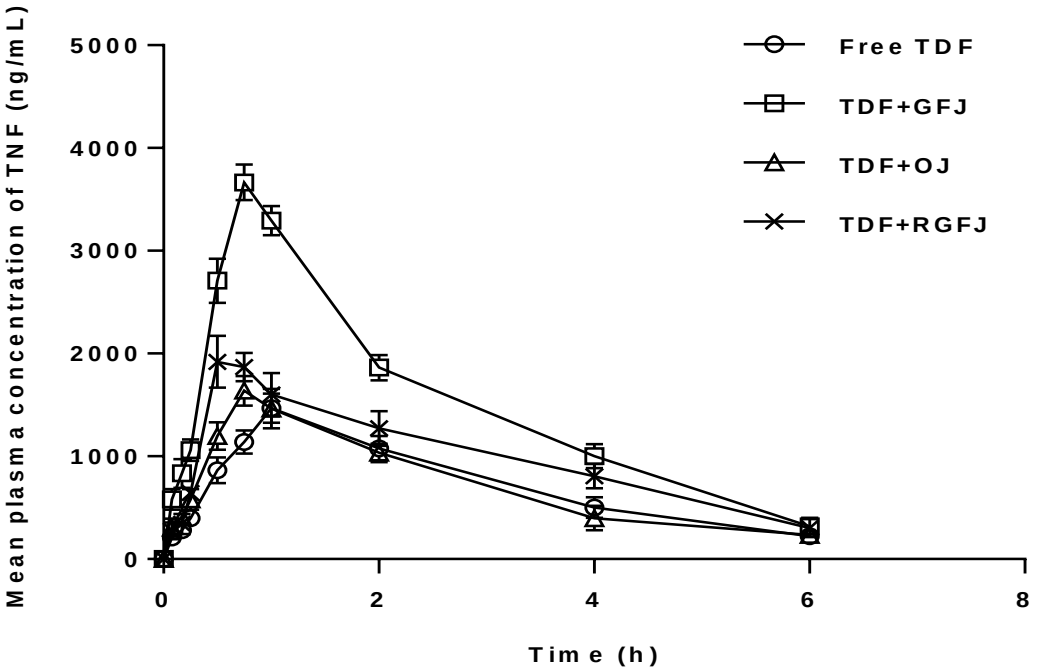

Fig. 3.7: Plasma time course of TNF obtained following oral administration of free TDF (100 mg/kg) and TDF (100 mg/kg) with FJs belonging to Rutaceae family (i.e. GFJ, OJ and RGFJ – 10 mL/kg). Each data point is represented as mean ± SD (*n* = 5).

The quantum of metabolic inhibition and increase in flux provided by GFJ in the everted gut sac studies was highest and so was the increase in the AUC_{total} and C_{max} values of TNF. Further, this increase in the intestinal absorption of TDF in the presence of GFJ and RGFJ further affirms the possibility of ester containing compounds in GFJ and RGFJ to penetrate the gut wall and prevent the metabolic process of TDF within the gut wall leading to an increase in the oral absorption. GFJ has been studied for its esterase inhibition previously but for other drugs (lovastatin and enalapril). Further, it was also reported that naringenin and kaempferol, which are extensively present in GFJ, inhibited the esterase metabolism and increased the oral absorption of lovastatin and enalapril (P. Li et al., 2007). However, the type of GFJ (white, red, pink, ruby red, star ruby etc.,) used was not mentioned as each type has slightly different components and that too at different concentration levels (Fukuda, Guo, Ohashi, Yoshikawa, & Yamazoe, 2000; Imai & Ohura, 2010). Interestingly, Ho et al. (2000) and Ross et al. (2000) have reported that the total flavonoid content including kaempferol and naringenin are reported

to be present at significantly lower levels in RGFJ when compared to the white variety of the grapefruit juice which could explain the better absorption enhancement capability of white variety of the GFJ observed in our study when compared to RGFJ. However, further studies are required to confirm this observation.

Table 3.2: Pharmacokinetic parameters of TNF obtained following oral administration of free TDF (100 mg/kg) and TDF (100 mg/kg) with each FJ belonging to Rutaceae family (i.e. GFJ, OJ and RGFJ – 10 mL/kg) separately.

Treatment group	Pharmacokinetic parameters			
	$T_{1/2}$ (h)	T_{max} (h)	C_{max} (ng/mL)	AUC_{total} (h*ng/mL)
Free TDF	1.81 ± 0.30	1.00–1.50	1467.53 ± 101.20	4967.98 ± 275.25
TDF+GFJ	1.56 ± 0.15[#]	0.5-0.75	3666.53 ± 172.33[a]	9798.14 ± 435.82[a]
TDF+OJ	1.85 ± 0.21[#]	0.50–1.00	1663.70 ± 136.57[#]	5002.11 ± 123.32[#]
TDF+RGFJ	2.15 ± 0.65[#]	0.75-1.50	1997.57 ± 198.71[b]	6934.23 ± 583.43[b]

The values represented are mean ± SD (n = 3). [a]Statistical significance observed at $P_{crit} < 0.001$ when compared to free TDF; [b]statistical significance observed at $P_{crit} < 0.01$ when compared to free TDF; [#]no statistical significance observed at $P_{crit} > 0.05$ when compared to free TDF.

3.3.5 Results and discussion of FJs belonging to miscellaneous class of families

3.3.5.1 In vitro esterase inhibition study

The %TDF remaining and the %TMF formed when TDF was incubated with BCJ, CGJ and PJ separately is shown in table 3.3. A significant level of the inhibition of the metabolic conversion of TDF to its monoester form was observed with PJ providing the highest level of metabolic protection as the %TDF remaining was significantly increased and consequently %TMF formed was significantly decreased at both the concentration levels. Additionally, for the tested concentrations only PJ ($P_{cal} \leq 0.012$) showed a concentration dependent metabolic protection of TDF.

3.3.5.2 Ex vivo everted gut sac studies

The mean J value of TMF after incubating TDF with BCJ, CGJ and PJ were 4.6 ± 0.5, 5.00 ± 0.4 and 8.67 ± 0.49 ng/cm^2/min respectively. The %TMF formed in the donor compartment in

the presence of BCJ, CGJ and PJ was observed to be 42.1 ± 4.6%, 35.1 ± 2.2% and 9.3 ± 1.1% respectively.

The results of this study indicate that all the FJs used in this study provided a significant level of metabolic protection for TDF (P_{cal} < 0.001). Further, the metabolic protection provided PJ was found to be the highest when compared to BCJ (P_{cal} < 0.001) and CGJ (P_{cal} < 0.0244). Additionally, PJ (P_{cal} < 0.001) was the only FJ that could significantly increase the intestinal flux of TMF. To evaluate the validity of these observations we performed single-dose oral pharmacokinetic studies by individually co-administering TDF with each of the FJs in rats.

Table 3.3: %TDF remaining and %TMF formed (when compared to TDF) in the intestinal washing after 30 min of incubation in the presence FJs belonging to the miscellaneous class of families (at 40% and 80% *v/v* concentration).

Treatment group	Concentration	%TDF Remaining	%TMF Formed
Free TDF	5 µM	5.92 ± 0.68	100.00 ± 0.72
TDF + BCJ	40% *w/v*	32.43 ± 4.88[a]	71.38 ± 5.25[a]
	80% *w/v*	35.44 ± 4.97[a]	68.14 ± 5.35[a]
TDF + CGJ	40% *w/v*	38.16 ± 4.45[a]	65.72 ± 4.73[a]
	80% *w/v*	43.46 ± 1.95[a]	60.09 ± 2.07[a]
TDF + PJ[c]	40% *w/v*	70.31 ± 2.61[a]	30.61 ± 2.81[a]
	80% *w/v*[b]	80.51 ± 6.51[a]	19.65 ± 7.01[a]

The values represented are mean ± SD (n = 3). [a]Statistical significance observed at P_{crit} < 0.001 when compared to free TDF; [b]Statistical significance observed at P_{crit} < 0.05 when compared to the corresponding FJ at 40% *v/v* concentration; [d]Statistical significance observed at P_{crit} < 0.001 when compared to remaining FJs.

3.3.5.3 Single-dose oral pharmacokinetic study

The plasma time course of TNF when TDF was co-administered with BCJ, CGJ and PJ separately are shown in fig. 3.8. Further, the pharmacokinetic parameters obtained after the non-compartmental analysis of the data obtained after performing the pharmacokinetic study is shown in table 3.4.

The AUC_{total} and C_{max} values of TNF when TDF was co-administered with BCJ (P_{cal} > 0.999) and CGJ (P_{cal} > 0.999) were not affected significantly when compared to free TDF. However,

in the case of PJ, there was a 100% ($P_{cal} < 0.001$) and 99% ($P_{cal} \leq 0.001$) increase in the C_{max} and AUC_{total} values respectively. Further, there was no significant change in $T_{1/2}$ of FJs indicating that the overall disposition characteristics of TNF were unaffected.

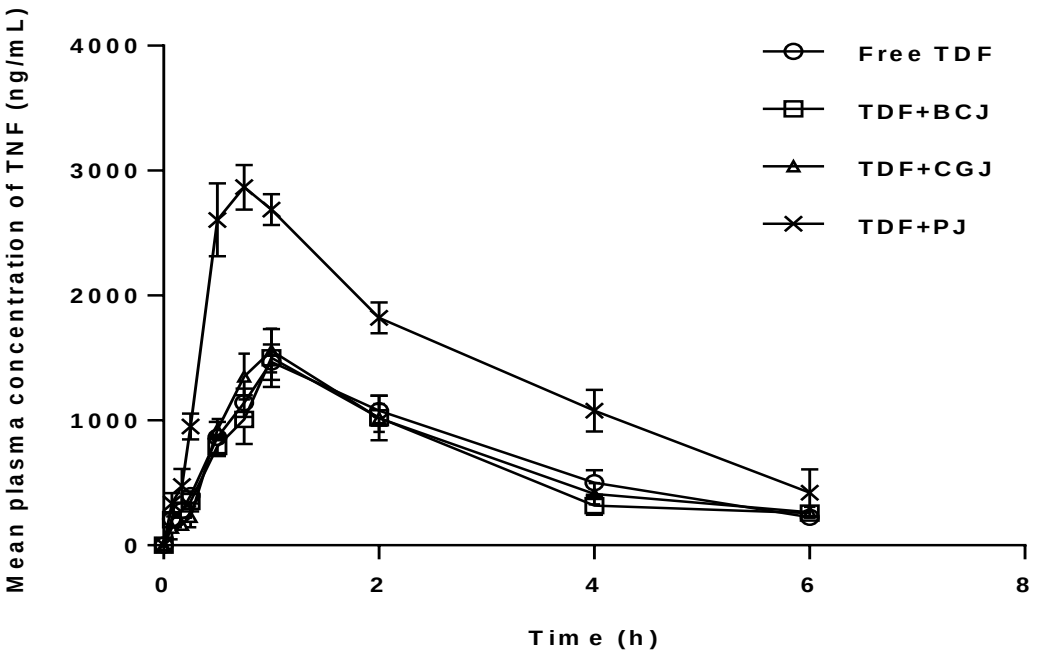

Fig. 3.8: Plasma time course of TNF obtained following oral administration of free TDF (100 mg/kg) and TDF (100 mg/kg) with FJs belonging to the miscellaneous class of families (i.e. BCJ, CGJ and PJ – 10 mL/kg). Each data point is represented as mean ± SD (n = 5).

Therefore, we can infer that the changes in the oral pharmacokinetics of TDF in the presence of PJ was due to its interaction during the absorption process. Hence, these observations apparently indicate a significant enhancement of the absorption of TDF when co-administered with PJ. This could be attributed to the prevention of the metabolic conversion of TDF to TMF. It has been reported that these juices contain compounds which have numerous ester linkages (like polyphenols, ellagitannins etc.,) which may competitively inhibit the metabolism of TDF by esterases in the lumen and gut wall. This results in a higher proportion of TDF being available for permeation, as compared to when TDF is administered alone. TDF being more lipophilic than TMF has better permeability and intestinal absorption resulting in the higher systemic availability of TNF. Further, the permeability flux of TMF showed that PJ showed a

considerable increase in the transport of TMF across the intestine. As, the presence of TMF in the receiver compartment indicates that TDF gets metabolized within the gut wall, therefore, the increase in the oral absorption in the pharmacokinetic studies and the flux of TMF in the *ex vivo* everted gut sac studies could be due to the ability of PJ to permeate into the intestinal membrane and inhibit the enzymes present within the gut wall (though not completely) apart from preventing the metabolism by esterase enzymes present in the epithelial cells lining the intestine. This ability of PJ to permeate the gut wall and provide metabolic protection for TDF could be attributed to the differences in the nature and concentration of the compounds containing ester linkages present in PJ as compared to BCJ and CGJ. PJ has been extensively reported to cause inhibition of CYP3A and CYP2C9 (Hidaka et al., 2005; Nagata et al., 2007; Voruganti et al., 2012) and apparently, no one has reported on its gut wall esterase inhibition capacity. Hence, there is a need to identify the components of PJ that are responsible for preventing the metabolism of TDF by esterases. Based on the results obtained, we could say that not all FJs rich in chemical constituents having ester like structures can affect the oral absorption of TDF, however, those components that can penetrate the gut wall and provide metabolic protection in the gut wall have the capacity to increase the oral absorption of TDF.

Table 3.4: Pharmacokinetic parameters of TNF obtained following oral administration of free TDF (100 mg/kg) and TDF (100 mg/kg) with each FJ belonging to miscellaneous families (i.e. BCJ, CGJ and PJ – 10 mL/kg) separately.

Treatment group	Pharmacokinetic parameters			
	$T_{1/2}$ (h)	T_{max} (h)	C_{max} (ng/mL)	AUC_{total} (h*ng/mL)
Free TDF	1.81 ± 0.30	1.00–1.50	1467.53 ± 101.20	4967.98 ± 275.25
TDF+BCJ	2.09 ± 0.39[#]	1.00-1.50	1500.25 ± 231.18[#]	4711.63 ± 314.17[#]
TDF+CGJ	2.07 ± 0.28[#]	0.75–1.00	1559.12 ± 175.78[#]	5034.53 ± 398.24[#]
TDF+PJ	1.95 ± 0.49[#]	0.75-1.50	2935.24 ± 134.71[a]	9877.62 ± 1441.22[a]

The values represented are mean ± SD (n = 3). [a]Statistical significance observed at $P_{crit} < 0.001$ when compared to free TDF; [#]no statistical significance observed at $P_{crit} > 0.05$ when compared to free TDF.

3.4 Conclusion

In this study, we evaluated the role of esterase inhibition by ester rich FJs and excipients on the oral absorption process of TDF in male Wistar rats. *In vitro* esterase inhibition and *ex vivo* everted gut sac studies showed that all FJs and C-EL (among the excipients) could significantly prevent the metabolism of TDF. Further, the everted gut sac studies also indicated that only CBJ, GFJ, PJ and RGFJ could increase the *J* of TMF even though all the FJs prevented the esterase metabolism of TDF. The Single dose oral pharmacokinetic studies in rats also showed that CBJ, GFJ, PJ and RGFJ could increase the oral absorption of TDF. Hence, these observations suggest that the ability of the components of CBJ, GFJ, PJ and RGFJ to prevent the metabolic process of TDF especially within the gut wall plays a crucial role in increasing the intestinal absorption of TDF. However, this study warrants further investigation on the active components of the four FJs that have the potential in increasing the oral absorption of TDF and a thorough clinical investigation is necessary to extrapolate the results observed in this study to humans.

Further, we have explored the ability of the nanocarrier formulation approaches in enhancing the oral absorption of TDF by using a polymer of natural origin (i.e. chitosan) and a synthetic polymer (i.e. PLGA). To prepare and optimize these nanocarrier systems we used design of experiments approach and the optimized nanocarrier system was extensively characterized.

References

Aviram, M., & Dornfeld, L. (2001). Pomegranate juice consumption inhibits serum angiotensin converting enzyme activity and reduces systolic blood pressure. *Atherosclerosis*, *158*(1), 195–198.

Aviram, M., & Rosenblat, M. (2012). Pomegranate protection against cardiovascular diseases. *Evidence-Based Complementary and Alternative Medicine*, *2012*.

Bailey, D. G., Malcolm, J., Arnold, O., & Spence, J. D. (1998). Grapefruit juice-drug interactions. *British Journal of Clinical Pharmacology*, *46*(2), 101–10.

Chen, H., Zuo, Y., & Deng, Y. (2001). Separation and determination of flavonoids and other phenolic compounds in cranberry juice by high-performance liquid chromatography. *Journal of Chromatography. A*, *913*(1–2), 387–95.

Cornaire, G., Woodley, J., Hermann, P., Cloarec, A., Arellano, C., & Houin, G. (2004). Impact of excipients on the absorption of P-glycoprotein substrates in vitro and in vivo. *International Journal of Pharmaceutics*, *278*(1), 119–131.

Crauste-Manciet, S., Huneau, J. F., Decroix, M. O., Tomé, D., Farinotti, R., & Chaumeil, J. C. (1997). Cefpodoxime proxetil esterase activity in rabbit small intestine: A role in the partial cefpodoxime absorption. *International Journal of Pharmaceutics*, *149*(2), 241–249.

De Castro, W. V., Mertens-Talcott, S., Derendorf, H., & Butterweck, V. (2008). Effect of grapefruit juice, naringin, naringenin, and bergamottin on the intestinal carrier-mediated transport of talinolol in rats. *Journal of Agricultural and Food Chemistry*, *56*(12), 4840–4845.

Fukuda, K., Guo, L., Ohashi, N., Yoshikawa, M., & Yamazoe, Y. (2000). Amounts and

variation in grapefruit juice of the main components causing grapefruit-drug interaction. *Journal of Chromatography B: Biomedical Sciences and Applications*, *741*(2), 195–203.

Geboers, S., Haenen, S., Mols, R., Brouwers, J., Tack, J., Annaert, P., & Augustijns, P. (2015). Intestinal behavior of the ester prodrug tenofovir DF in humans. *International Journal of Pharmaceutics*, *485*(1–2).

Gross, J., Carmon, M., Lifshitz, A., & Sklarz, B. (1975). Structural elucidation of some orange juice carotenoids. *Phytochemistry*, *14*(1), 249–252.

Hidaka, M., Okumura, M., Fujita, K. I., Ogikubo, T., Yamasaki, K., Iwakiri, T., … Arimori, K. (2005). Effects of pomegranate juice on human cytochrome P450 3A (CYP3A) and carbamazepine pharmacokinetics in rats. *Drug Metabolism and Disposition*, *33*(5), 644–648.

Ho, P. C., Saville, D. J., Coville, P. F., & Wanwimolruk, S. (2000). Content of CYP3A4 inhibitors, naringin, naringenin and bergapten in grapefruit and grapefruit juice products. *Pharmaceutica Acta Helvetiae*, *74*(4), 379–85.

Honda, Y., Ushigome, F., Koyabu, N., Morimoto, S., Shoyama, Y., Uchiumi, T., … Sawada, Y. (2004). Effects of grapefruit juice and orange juice components on P-glycoprotein- and MRP2-mediated drug efflux. *British Journal of Pharmacology*, *143*(7), 856–64.

Imai, T., & Ohura, K. (2010). The role of intestinal carboxylesterase in the oral absorption of prodrugs. *Current Drug Metabolism*, *11*(9), 793–805.

Kane, G. C., & Lipsky, J. J. (2000). Drug-grapefruit juice interactions. *Mayo Clinic Proceedings. Mayo Clinic*, *75*(9), 933–942.

Kelebek, H. (2010). Sugars, organic acids, phenolic compositions and antioxidant activity of Grapefruit (Citrus paradisi) cultivars grown in Turkey. *Industrial Crops and Products*,

32(3), 269–274.

Kiani, J., & Imam, S. Z. (2007). Medicinal importance of grapefruit juice and its interaction with various drugs. *Nutrition Journal*, *6*, 33.

Kim, N. D., Mehta, R., Yu, W., Neeman, I., Livney, T., Amichay, A., … Lansky, E. (2002). Chemopreventive and adjuvant therapeutic potential of pomegranate (Punica granatum) for human breast cancer. *Breast Cancer Research and Treatment*, *71*(3), 203–17.

Klimczak, I., Małecka, M., Szlachta, M., & Gliszczyńska-Świgło, A. (2007). Effect of storage on the content of polyphenols, vitamin C and the antioxidant activity of orange juices. *Journal of Food Composition and Analysis*, *20*(3), 313–322.

Kontiokari, T., Sundqvist, K., Nuutinen, M., Pokka, T., Koskela, M., & Uhari, M. (2001). Randomised trial of cranberry-lingonberry juice and Lactobacillus GG drink for the prevention of urinary tract infections in women. *BMJ (Clinical Research Ed.)*, *322*(7302), 1571.

Krikorian, R., Shidler, M. D., Nash, T. a, Kalt, W., Vinqvist-tymchuk, M. R., Shukitt-hale, B., & James, A. (2010). Blueberry Supplementation Improves Memory in Older Adults. *J Agric Food Chem*, *58*(7), 3996–4000.

Li, M., Si, L., Pan, H., Rabba, A. K., Yan, F., Qiu, J., & Li, G. (2011). Excipients enhance intestinal absorption of ganciclovir by P-gp inhibition: Assessed in vitro by everted gut sac and in situ by improved intestinal perfusion. *International Journal of Pharmaceutics*, *403*(1–2), 37–45.

Li, P., Callery, P. S., Gan, L.-S., & Balani, S. K. (2007). Esterase inhibition by grapefruit juice flavonoids leading to a new drug interaction. *Drug Metabolism and Disposition: The Biological Fate of Chemicals*, *35*(7), 1203–8.

Lilja, J. J., Raaska, K., & Neuvonen, P. J. (2005). Effects of orange juice on the pharmacokinetics of atenolol. *European Journal of Clinical Pharmacology*, *61*(5–6), 337–340.

Luna-Vázquez, F. J., Ibarra-Alvarado, C., Rojas-Molina, A., Rojas-Molina, J. I., Yahia, E. M., Rivera-Pastrana, D. M., … Zavala-Sánchez, M. Á. (2013). Nutraceutical value of black cherry prunus serotina ehrh. Fruits: Antioxidant and antihypertensive properties. *Molecules*, *18*(12), 14597–14612.

Mohri, K., & Uesawa, Y. (2001). Effects of furanocoumarin derivatives in grapefruit juice on nifedipine pharmacokinetics in rats. *Pharmaceutical Research*, *18*(2), 177–182.

Nagata, M., Hidaka, M., Sekiya, H., Kawano, Y., Yamasaki, K., Okumura, M., & Arimori, K. (2007). Effects of pomegranate juice on human cytochrome P450 2C9 and tolbutamide pharmacokinetics in rats. *Drug Metabolism and Disposition*, *35*(2), 302–305.

O'Byrne, D. J., Devaraj, S., Grundy, S. M., & Jialal, I. (2002). Comparison of the antioxidant effects of Concord grape juice flavonoids alpha-tocopherol on markers of oxidative stress in healthy adults. *The American Journal of Clinical Nutrition*, *76*(6), 1367–74.

Ravi, P. R., Vats, R., Thakur, R., Srivani, S., & Aditya, N. (2012). Effect of grapefruit juice and ritonavir on pharmacokinetics of lopinavir in wistar rats. *Phytotherapy Research*, *26*(10), 1490–1495.

Rice-Evans, C. A., Miller, N. J., & Paganga, G. (1996). Structure-antioxidant activity relationships of flavonoids and phenolic acids. *Free Radical Biology & Medicine*, *20*(7), 933–56.

Ross, S. A., Ziska, D. S., Zhao, K., & ElSohly, M. A. (2000). Variance of common flavonoids by brand of grapefruit juice. *Fitoterapia*, *71*(2), 154–61.

Seeram, N. P., Adams, L. S., Hardy, M. L., & Heber, D. (2004). Total cranberry extract versus its phytochemical constituents: antiproliferative and synergistic effects against human tumor cell lines. *Journal of Agricultural and Food Chemistry*, *52*(9), 2512–7.

Shaughnessy, K. S., Boswall, I. A., Scanlan, A. P., Gottschall-Pass, K. T., & Sweeney, M. I. (2009). Diets containing blueberry extract lower blood pressure in spontaneously hypertensive stroke-prone rats. *Nutrition Research*, *29*(2), 130–138.

Sinelli, N., Di Egidio, V., Casiraghi, E., Spinardi, A., & Mignani, I. (2009). Evaluation of quality and nutraceutical content in blueberries (Vaccinium corymbosum) by near and mid infrared spectroscopy. *Acta Horticulturae*, *810*, 807–816.

Takanaga, H., Ohnishi, A., Yamada, S., Matsuo, H., Morimoto, S., Shoyama, Y., … Sawada, Y. (2000). Polymethoxylated flavones in orange juice are inhibitors of P- glycoprotein but not cytochrome P450 3A4. *Journal of Pharmacology and Experimental Therapeutics*, *293*(1), 230–236.

Tian, R., Koyabu, N., Takanaga, H., Matsuo, H., Ohtani, H., & Sawada, Y. (2002). Effects of grapefruit juice and orange juice on the intestinal efflux of P-glycoprotein substrates. *Pharmaceutical Research*, *19*(6), 802–809.

Titta, L., Trinei, M., Stendardo, M., Berniakovich, I., Petroni, K., Tonelli, C., … Giorgio, M. (2010). Blood orange juice inhibits fat accumulation in mice. *International Journal of Obesity (2005)*, *34*(3), 578–88.

Tong, L., Phan, T. K., Robinson, K. L., Babusis, D., Strab, R., Bhoopathy, S., … Ray, A. S. (2007). Effects of human immunodeficiency virus protease inhibitors on the intestinal absorption of tenofovir disoproxil fumarate in vitro. *Antimicrobial Agents and Chemotherapy*, *51*(10), 3498–3504.

Van Gelder, J., Deferme, S., Naesens, L., De Clercq, E., Van Den Mooter, G., Kinget, R., & Augustijns, P. (2002). Intestinal absorption enhancement of the ester prodrug tenofovir disoproxil fumarate through modulation of the biochemical barrier by defined ester mixtures. *Drug Metabolism and Disposition*, *30*(8), 924–930.

Voruganti, S., Yamsani, S. K., Ravula, S. K., Gannu, R., & Yamsani, M. R. (2012). Effect of pomegranate juice on intestinal transport and pharmacokinetics of nitrendipine in rats. *Phytotherapy Research*, *26*(8), 1240–1245.

Chapter 4

Design and evaluation of TDF loaded CS NPs

4.1 Introduction

The biodegradable polymeric nanoparticles (NPs) used to prepare nanoparticles can be broadly classified as a) polymers of natural origin (chitosan, Pullulan acetate) and b) synthetic polymers (poly(lactic-co-glycolic acid), Poly-ε-caprolactone). There have been several published reports that have demonstrated the use of biodegradable natural polymers for designing nanocarrier formulation of drugs and macromolecules for improving their oral bioavailability. These nanocarrier formulations were reported to load drugs with diverse physicochemical properties (Akhtar, Rizvi, & Kar, 2012; Cohen-Sela, Chorny, Koroukhov, Danenberg, & Golomb, 2009; Dudhani & Kosaraju, 2010) and improve the therapeutic outcomes by addressing the problems of the loaded drugs (like low aqueous solubility, poor permeability, susceptibility to gut wall and/or hepatic first pass metabolism, P-gp efflux and rapid elimination) (Ravi, Vats, Thakur, Srivani, & Aditya, 2012; Ravi, Vats, Dalal, Gadekar, & N, 2015; Wang & Zhang, 2012).

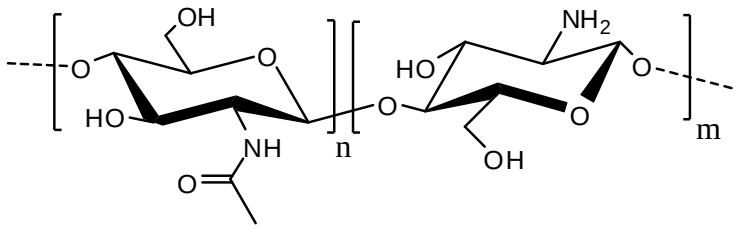

Fig. 4.1: Structure of CS.

After cellulose, chitin is the most abundant polysaccharide, it is extensively present in the exoskeleton of invertebrates. Chitin is a homopolymer having β-(1,4)-linked N-acetyl-glucosamine units. Chitosan (CS) is a biodegradable cationic polymer (fig. 4.1), it is a linear amino polysaccharide formed by alkaline deacetylation of chitin. The degree of deacetylation dictates the physicochemical properties of CS (Shukla & Tiwari, 2012). Apart from the non-toxic and biodegradable nature of CS, it has the ability to increase the residence through mucoadhesion and enhance the permeability of various xenobiotics. CS is reported to interpenetrate the mucin glycoproteins lining the epithelial cells due to the electrostatic

interactions (between negatively charged CS and positively charged mucus glycoprotein) and it is also reported to be taken up by active endocytic pathways. Further, crosslinking of CS leads to the formation of permanent covalent network which has rate controlling property, enhanced mechanical strength and makes its physicochemical properties immune to changes in pH and temperature (Harish Prashanth KV, 2006; Huang, Zhang, Liu, & Li, 2012). The chemical crosslinking of CS has been reported with low molecular weight counterions (sodium tripolyphosphate), hydrophobic counterions (alginate) and high molecular weight counterions (lauryl sulphate).Chitosan-based nanoparticles (CS NPs) have been used for improving the oral bioavailability of several drugs including doxorubicin, albendazole, ketoconazole etc., (Feng et al., 2013; Liu et al., 2013; Modi, Joshi, & Sawant, 2013). Different methods have been used for the crosslinking of CS, some of them are as follows:

- Ionotropic gelation: This is the most commonly employed method of crosslinking in which the selected crosslinker is added to the CS solution under stirring (Sinha et al., 2004).
- Wet phase inversion: Mi et al. (1999) followed this method by adding the CS solution in glacial acetic acid through a nozzle dropwise into the solution containing the counterion.
- Emulsification crosslinking: In this method, the CS solution (dispersed phase) was added to an immiscible solvent (continuous phase) forming a w/o emulsion. The solution containing the counterion was added at different time intervals leading to ionotropic gelation (Sinha et al., 2004).
- Thermal crosslinking: Orienti et al. (1996) prepared indomethacin loaded CS microspheres. This was achieved by adding the CS solution to citric acid which was cooled to 0 °C. This mixture was then added to corn oil followed by heating to 120 °C which lead to the crosslinking of CS and citric acid.

The objective of our work was to design and optimize TDF loaded CS NPs for improving the oral bioavailability of TDF. A hybrid statistical design was prepared with the help of design of experiments. This design was used for the formulation optimization process and to study the effect of various formulation and process factors on the critical quality attributes like particle size and entrapment efficiency of the NPs. Different characterization studies were performed to evaluate the shape, size, zeta potential, entrapment efficiency, physical stability and cytotoxicity of the NPs. Pharmacokinetic studies were conducted to determine *in vivo* efficacy of the optimized formulations in male Wistar rats. Further, mucoadhesion and everted gut sac studies were conducted to understand the mechanisms involved in the oral uptake of TDF loaded CS NPs.

4.2 Materials and methods

4.2.1 Materials

The prodrug TDF was provided by Strides Arcolab Limited, Bengaluru, India and its active form TNF was provided by Gilead Sciences, Inc., CA, USA as a gift samples. CS (molecular weight: 190-310 kDa, 75–85% degree of deacetylation), sodium tripolyphosphate (STPP), mannitol, urethane (analytical grade), chlorpromazine, trifluoroacetic acid (HPLC grade), mucin from porcine stomach and Dulbecco's phosphate-buffered saline (DPBS) were obtained from Sigma-Aldrich, Mumbai, India. HPLC grade methanol, acetonitrile and ammonium acetate and analytical grade dimethyl sulphoxide (DMSO), diethyl ether, potassium dihydrogen orthophosphate, nystatin were supplied by SD Fine-Chem Limited, Mumbai, India. Analytical grade glacial acetic acid (GAA), perchloric acid, liquid ammonia, methyl cellulose, sodium hydroxide, sodium citrate and sodium chloride were bought from SRL Chemicals Ltd., Mumbai, India. Rats (Male Wistar) were purchased from Sainath Agencies, Hyderabad, India.

Table 4.1: Experimental design generated by Design Expert software in BBD and the observed responses after running the design for TDF loaded CS NPs.

Run	Critical factors			Observed response	
	Amount of CS (mg, X_1)	Amount of STPP (mg, X_2)	Duration of ultrasonication (min, X_3)	PS (nm, Y_1)	EE% (%, Y_2)
1	70	10	3	168	23
2	100	40	1.75	240	50
3	70	25	1.75	164	50
4	100	25	0.5	260	47
5	100	25	3	212	42
6	70	25	1.75	160	49
7	70	25	1.75	155	48
8	70	25	1.75	162	48
9	100	10	1.75	226	28
10	70	10	0.5	199	29
11	40	25	3	149	31
12	40	10	1.75	141	20
13	70	40	3	211	42
14	40	40	1.75	182	30
15	70	25	1.75	159	49
16	70	40	0.5	220	42
17	40	25	0.5	166	35

4.2.2 Experimental design for optimization of TDF loaded CS NPs

The design of experiments (DoE) was used to optimize the TDF loaded CS NPs. Out of the various quality attributes, we have identified particle size (PS) and entrapment efficiency (EE%) as the critical quality attributes (referred to as 'responses' in DoE) for the optimization process. PS and EE% of the drug loaded NPs have a significant effect on the absorption properties and also on the *in vivo* time course of the drug. Several formulation and process factors (referred to as 'factors' in DoE) can affect the PS and EE% of TDF loaded CS NPs. As the number of factors to be studied was very high, we have followed a hybrid statistical design for the optimization process. First, a low-resolution Plackett-Burman Design (PBD, a type of screening design) was employed to screen various formulation and process related factors affecting the responses. The factors selected for the screening design were as follows: amount of CS (40 and 100 mg), amount of STPP (10 and 40 mg), pH of STPP (4.5 and 6.5),

rate of addition of STPP (2 and 5 mL/min), homogenization speed (5000 and 20000 rpm), duration of homogenization (2 and 10 min), amplitude of ultrasonication (40% and 75%) and duration of ultrasonication (0.5 and 3 min). These factors were tested at two different levels [maximum (+1) and minimum (-1)] with three centre points to study their effect on the responses, PS and EE%.

Three critical factors (amount of CS – X_1, amount of STPP – X_2 and duration of ultrasonication – X_3) affecting the responses, PS (Y_1) and EE% (Y_2), were selected based on the results obtained from PBD. Then a high-resolution Box-Behnken Design (BBD) was used to examine the individual and interaction effects of the selected critical factors on the responses and to optimize the preparation of TDF loaded CS NPs. BBD is a subtype of response surface design that can be used to construct second-order polynomial equation with minimum trials for the optimization of the responses. The BBD comprised of 3 factors and 17 runs evaluated at 3 levels with 5 centre points (to check for reproducibility) as shown in table 4.1. The second order polynomial equation generated from BBD is of the following form:

$$Y = b_0 + b_1X_1 + b_2X_2 + b_3X_3 + b_{11}X_1^2 + b_{22}X_2^2 + b_{33}X_3^2 + b_{12}X_1X_2 + b_{13}X_1X_3 + b_{23}X_2X_3$$

Where '*Y*' is the response, b_i's and b_{ii}'s (i = 1, 2 and 3) are coefficients of individual linear and quadratic effects respectively and b_{ij}'s (i, j = 1, 2 and 3; $i < j$) are coefficients of the effect of the interaction between i^{th} and j^{th} parameter and b_0 is the intercept value. The optimized formulation was obtained with the help of desirability function based on the criteria for response mentioned in table 4.2. The design of experiments, statistical analysis and optimization of the formulation was done with the help of the Design Expert software (version 10.0.3.1, Stat-Ease Inc., MN, USA).

Table 4.2: Values of the critical factors set for BBD at different levels and the criteria set for responses of TDF loaded CS NPs.

Factor	**Levels used**		
	–1	0	+1
Independent factors			
***X₁* – Amount of chitosan (mg)**	40	70	100
***X₂* – Amount of STPP (mg)**	10	25	40
***X₃* – Duration of ultrasonication (min)**	0.5	1.75	3
Dependent factors		**Constraints**	
***Y₁* – PS (nm)**		Minimize	
***Y₂* – EE% (%)**		Maximize	

4.2.3 Preparation of TDF loaded CS NPs

The ionic gelation method used in this study for the preparation of TDF loaded CS NPs (represented schematically in fig. 4.2) is based on the work published by Calvo et al. (1997). Briefly, CS (quantity as per the experimental design) was dissolved in 15 mL of 1% *v/v* of GAA solution. To this, a solution containing 20 mg of TDF dissolved in 5 mL of 1% *v/v* GAA was added. Subsequently, 20 mL of STPP aqueous solution (quantity of STPP and pH was varied as per the experimental design) was added at a specific rate as per the experimental design to the above mixture under homogenization (Polytron PT, 3100D, Kinemetica, Lucerne, Switzerland). The speed and duration of homogenization was varied as per the experimental design. The formed complex was ultrasonicated with the help of probe sonicator (Vibra cell, Sonics, Connecticut, USA). The duration and amplitude of ultrasonication were varied as per the experimental design. A dispersion of TDF loaded NPs was obtained which was washed and centrifuged three times to remove the free drug. The washed TDF loaded CS NPs were re-suspended in deionized water and stored at –80 °C for 24 h. TDF loaded CS NPs were freeze–dried in a lyophilizer (Coolsafe 110-4, Scanvac, Lynge, Denmark) with 5% *w/v* of mannitol as a cryoprotectant. The lyophilized powder was stored in sealed glass vial at 2–4 °C until further use. The blank CS NPs were also prepared by following a similar procedure without incorporating TDF.

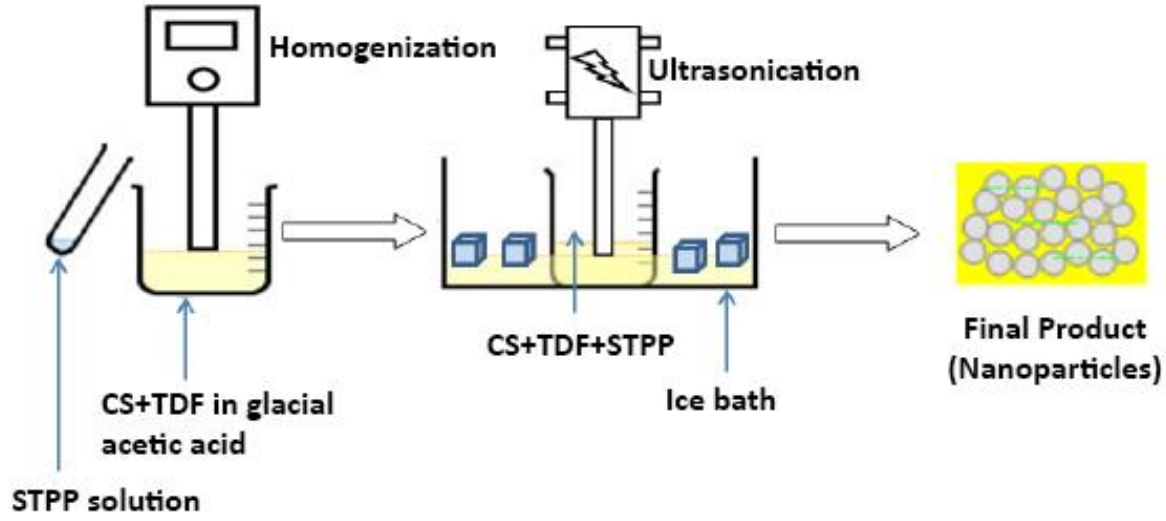

Fig. 4.2: Schematic representation of the preparation method for TDF loaded CS NPs.

4.2.4 Characterization studies

4.2.4.1 Measurement of particle size and zeta potential

The particles size, polydispersity index (PDI) and the zeta potential were measured with the help of zetasizer (Nano ZS, Malvern Instruments Ltd., Worcestershire, UK). The intensity of the scattered light was measured at 173° (backscattering angle). The instrument was set for 10 min in serial mode and the sample measurement time was 30 ms and the temperature was set to 25 °C.

4.2.4.2 Determination of entrapment efficiency

The EE% was determined using ultrafiltration technique based on the work reported by Ravi et al. (2014). Briefly, 0.5 mL of freshly prepared TDF loaded CS NPs dispersion was transferred to micro-filters (Amicon Ultra, Millipore, MA, USA; molecular weight cut-off (MWCO): 10 kDa). These filters were centrifuged at 7500 × g to separate the unentrapped (free) drug from the entrapped drug. The unentrapped drug diffused through the micro-filter membrane into the filtrate while the drug entrapped in the NPs remained within the micro-filter along with the NPs. The amount of TDF present in the filtrate was analysed using a validated HPLC method and the EE% was calculated based on the following equation:

$$EE\% = \frac{(W_{\text{total TDF}} - W_{\text{free TDF}})}{W_{\text{total TDF}}} \times 100$$

Where, $W_{\text{total TDF}}$ is the amount of TDF added during the preparation of the NPs; $W_{\text{free TDF}}$ is the amount of TDF determined in the filtrate.

To study the adsorption (non-specific binding) of TDF towards the micro-filter membranes, TDF solution (1 µg/mL) prepared in phosphate buffer saline (pH of 5.2) was filtered through micro-filters. High recovery (more than 99%) of TDF in the filtrate confirmed minimal adsorption of TDF to the micro-filter membranes.

4.2.4.3 Surface Morphological Analysis

The morphology of the TDF loaded CS NPs was analysed with the help of scanning electron microscope (Carl Zeiss MERLIN Compact, Oberkochen, Germany). 100 µL of TDF loaded CS NPs was placed on an aluminum stub and dried under vacuum and then sputtered with gold (Q 150T ES, Quorum Technologies, Laughton, UK). The coated samples were placed in vacuum and the images were captured at an acceleration voltage of 3 kV.

4.2.4.4 Differential scanning calorimetry

Thermal analysis of TDF loaded CS NPs was carried out using differential scanning calorimeter (DSC 60, Shimadzu Corporation, Kyoto, Japan). The samples were accurately weighed, transferred into aluminum pans and crimp sealed. The sealed pans were placed in the DSC furnace chamber and equilibrated at 30 °C. Dry nitrogen gas was purged into the furnace chamber at a flow rate of 20 mL/min to provide inert environment. The thermograms were obtained by subjecting the samples to heating run over a temperature range of 30–400 °C at a heating rate of 10 °C/min.

4.2.4.5 Powder X-ray diffraction studies

The powder X-ray diffraction (pXRD) study was carried out to characterize the physical state of the samples with Rigaku, Ultima IV diffractometer (Texas, USA). The samples were illuminated with a Ni-filtered Cu-K_α radiation (λ = 1.54 Å) at a voltage of 40 kV and a current of 40 mA. The analysis was performed for a 2θ range of 10-70° at a scanning rate of 1 degree/min.

4.2.5 Stability studies of TDF loaded CS NPs

The stability of TDF loaded CS NPs was evaluated as per the international council of harmonization (ICH) guidelines, Q1A (R2) (Food and Drug Administration, HHS, 2003). The study was carried out at accelerated conditions in which the optimized freeze dried TDF loaded CS NPs kept in sealed glass vials (n = 3) were stored at 25 ± 2 ℃ with a relative humidity (RH) of 60 ± 5% for 3 months in environmental test chamber (Remi, Mumbai, India). The corresponding control samples were stored at 2-8 °C. Samples were collected at a monthly interval and evaluated for PS, zeta potential, PDI and EE%.

4.2.6 *In vitro* dissolution studies

The *in vitro* drug release studies (n = 6) of free TDF and TDF loaded CS NPs were conducted using dialysis bag method (MWCO: 12–14 kDa; pore size: 2.4 nm). In this study, 1 mg of free TDF or TDF loaded CS NPs (equivalent to 1 mg of TDF) were taken in the dialysis bag and sealed. The sealed dialysis bag was then submerged in a beaker containing 50 mL of phosphate buffer (pH of 5.2) maintained at 37 °C under uniform stirring at 100 rpm using a magnetic bead. pH of 5.2 was selected because significant levels TDF was degraded to its monoester form (TMF) at higher pH (i.e. above 6.8 – data no shown). Samples of 1 mL were collected at predetermined time intervals using syringe fitted with filter unit (hydrophilic PVDF membrane of 33 mm diameter having a pore size of 0.1 µm; Medical Millex – VV syringe filter unit, Millipore, MA, USA) for analysis. The NPs that got pulled into the syringe

filter during sampling were returned back to dissolution media by 'backwashing' same volume of fresh media (1 mL of pH 5.2 phosphate buffer) through the syringe. The samples were then analysed by a validated HPLC method. The data was fit into various kinetic models (Barzegar-Jalali et al., 2008) to determine the model that best describes the drug release profile from the NPs. Regression analysis was used to determine the best fit model. Using the best fit model, the time taken for 50% drug release ($T_{50\%}$) was calculated. The models used to fit the data are as follows:

Zero order model: $F = K_o \times t$,
First order model: $\ln(1 - F) = -K_f \times t$,
Higuchi model: $F = K_H \times \sqrt{t}$,
Reciprocal powered time model: $(1/F - 1) = m/t^b$ and
Korsmeyer–Peppas model: $\frac{M_t}{M_\infty} = K \times t^n$,

Where, 'F' is fraction of drug released up to time t; 'K_o', 'K_f', 'K_H', 'm' and 'b' are model parameters. 'M_t' is the amount of drug released at time t, 'M_∞' is the maximum amount of drug released, 'K' is release rate constant and 'n' is the exponent of drug release.

4.2.7 Cytotoxicity studies

The cytotoxicity studies of TDF loaded CS NPs were performed in RAW 264.7 cell lines (mouse monocyte-macrophages) with the help of MTT (3-(4,5-Dimethylthiazol-2-yl)-2,5-diphenyltetrazolium bromide) assay. Briefly, microtiter plates containing 10000 cells/well were incubated for 24 h at 37 °C with 5% CO_2 and 95% O_2 and 100% RH. Appropriate aliquots of samples (free TDF/TDF loaded CS NPs/Blank CS NPs/Triton X-100) were added to the microtiter plates to achieve the desired concentration (0.1, 1 and 10 µM) and were allowed to incubate for 24 h. The wells were then spiked with 10 µL of 10 mg/mL of MTT and incubated for 2 h at 37 °C to allow the formation of formazan crystals. The microtiter plates were then centrifuged and the media was removed after which 200 µL DMSO was

added to dissolve the bound formazan crystals. The optical density of the dissolved formazan crystals was measured with the help of microplate reader (Spectramax M2e, Molecular Devices, CA, USA) at a wavelength of 560 nm. The cell viability was evaluated by comparing the absorbance of the treated cells with the untreated ones which acted as a control. The study was done in pentaplicates (n = 5).

4.2.8 *In vitro* stability in rat intestinal mucosal homogenates

The mucosal homogenates of rat intestine were collected based on a previously published work (Crauste-Manciet, Decroix, Farinotti, & Chaumeil, 1997; Li, Callery, Gan, & Balani, 2007). Briefly, laparotomy was performed on male Wistar rats (n = 5) that were fasted overnight and the small intestine was cut and separated. The rats were then sacrificed by cervical dislocation. The mucosal homogenates were collected by washing the small intestines with 1 mL of pH 7.0 phosphate buffer and the intestinal washings were pooled and finally made up the volume to 7 mL with pH adjusted to 7.0. Further, 100 µL of this intestinal washing was added to each of the three incubation chambers which were as follows: 1) The first incubation chamber contained 100 µL of 5 µM of TDF. 2) The second incubation chamber contained 100 µL of TDF loaded CS NPs (equivalent to 5 µM of TDF). 3) The third incubation chamber contained 100 µL of a physical mixture of TDF and CS. Further, corresponding to the treatment groups, incubation chambers without TDF were also prepared by adding 100 µL of intestinal washings to 100 µL of pH 7.0 buffer and to 100 µL of Blank CS NPs. These served as blanks in the analysis of TDF and TMF for their respective samples (to check for the interference of the matrices in HPLC analysis). The reaction was terminated after 30 min by adding 200 µL of acetonitrile and the samples were stored at –20 °C until analysis. The study was done in triplicate (n = 3) for each treatment condition.

4.2.9 Mucoadhesion studies

4.2.9.1 In vitro mucoadhesion studies

This study was based on the work published by Yin et al. (2006). Briefly, 1 mL of 100 µg/mL porcine stomach mucin was incubated with a 1 mL suspension of NPs for 30 min. After the incubation period, the samples were centrifuged at 8000 × g. The supernatant containing unbound mucin was removed and analysed with UV spectrophotometer (V-650, Tokyo, Japan) at a wavelength of 258 nm. The percentage (%) of binding efficiency of the NPs to porcine mucin was calculated with the following formula:

$$\%Binding\ efficiency\ of\ NPs = \frac{(C_0 - C_s) \times 100}{C_0}$$

Where, C_0 is the initial concentration of porcine mucin and C_s is the concentration of unbound mucin after incubating with NPs.

4.2.9.2 Ex vivo mucoadhesion studies

The mucoadhesion studies of TDF loaded CS NPs were performed based on the work previously reported by Dünnhaupt et al. (2011). Briefly, male Wistar rats that were fasted overnight were dissected and the jejunum was separated. The separated jejunum was cleaned and 2.5 cm segments were cut and tied at one end. Then the segments were filled with DPBS buffer containing either free TDF or TDF loaded CS NPs (equivalent to 1 mg/mL of TDF) and then tied at the other end to form sacs. These sacs were incubated in Petri plates containing DPBS buffer for 2 h at 37 °C, afterwards the intestinal sacs were untied and rinsed to remove any unbound drug or NPs. Then the jejunal segments were cut open and the mucosal layer was carefully scraped off from the internal surface of the intestine. The collected mucosal layer was suspended in acetonitrile and stored at – 80 °C and on the day of analysis the samples were processed suitably analysed using a validated HPLC method. The study was done in triplicate (n = 3).

4.2.10 *Ex vivo* everted gut sac studies

Male Wistar rats were fasted overnight and on the day of the experiment were anaesthetized (urethane at 1.2 g/kg dose through intraperitoneal route) and laparoscopy was performed to isolate the intestine. The jejunal part of the intestine was isolated, washed with 0.9% *w/v* of NaCl and divided into segments of each having a length of 7.0 – 8.0 cm. Each segment was then gently everted with the help of a glass rod and tied at one end to fill 750 µL of DPBS buffer. After filling the buffer the other end of the segment was also tied to form a sac. The everted sacs were kept in reservoirs containing either free TDF or TDF loaded CS NPs (equivalent to 20 mM of TDF) prepared in DPBS buffer maintained at 37 °C and oxygenated with 95%/5% of CO_2/O_2.

To discern the uptake mechanism, everted gut sacs were incubated at 4 °C and also in the presence of specific endocytic pathway inhibitors – chlorpromazine (10 mg/mL) or nystatin (25 mg/mL) at 37 °C. After 60 min of incubation time, samples were collected from both donor and receiver side of the sac and stored at – 80 °C until analysis. The samples were analysed using a validated HPLC method. The study was done in triplicate (n = 3).

4.2.11 *In vivo* single-dose pharmacokinetic studies

The single-dose pharmacokinetic studies were performed on male Wistar rats. The rats were housed at 22 ± 1 °C and 50 ± 10% RH. The protocol for this study was approved by the institutional animal ethics committee (IAEC) (Protocol Approval number: IAEC No.: IAEC–02/01–14). Prior to the day of the experiment, the rats were kept in special cages to prevent coprophagia and were fasted overnight with free access to water till 4 h post dosing on the day of the experiment.

In the study, rats were divided into three treatment groups with six animals in each group (n = 6). The first treatment group received free TDF solution (TDF dissolved in water at a dose of

22 mg/kg, equivalent to 10 mg/kg of TNF) through intravenous (IV) route via the tail vein. The second treatment group received a suspension of free TDF (TDF at a dose of 100 mg/kg, equivalent to 45 mg/kg of TNF) through the oral route. Free TDF suspension was prepared by dispersing TDF homogenously in 0.5% *w/v* methylcellulose (molecular weight: 14000 Da; viscosity: 15 cps) in water. The third treatment group received TDF loaded CS NPs (equivalent to 100 mg/kg of TDF) through the oral route. In second and third treatment groups, formulations were administered through oral route with the help of an oral feeding gavage.

Blood (150 µL) was collected in microcentrifuge tubes containing anticoagulant (3.8% *w/v* sodium citrate) at predose, 0.08, 0.17, 0.25, 1, 2, 3, 4 h for the first treatment group and at predose, 0.25, 0.5, 0.75, 1, 1.25, 1.5, 2, 4, 6, 8, and 12 h for the second and third treatment groups. Plasma was collected by centrifuging the blood samples at 905 × g for 10 min and stored at –80 °C until analysis. The samples were processed suitably and analysed using a validated HPLC method.

4.2.12 Data analysis

The results obtained from all the studies were represented in terms of mean ± standard deviation (SD). To evaluate the statistical significance between the experimental groups, analysis of variance (ANOVA) was performed followed by Bonferroni's multiple comparison test using GraphPad prism software (version 6.01, GraphPad Software, Inc., CA, USA). The significance level was set at 5% (P_{crit}), however, we also reported the calculated *P* value (P_{cal}) as and when required. Non-compartmental analysis was performed for the data obtained from the pharmacokinetic studies using Phoenix WinNonlin® software (version 7.0, Pharsight Corporation, CA, USA).

4.3 Results and discussion

4.3.1 Screening of factors using Plackett-Burman Design

The main effects of eight different formulation and process related factors on the PS and EE% of TDF loaded CS NPs were determined with the help of low-resolution PBD. Out of the eight factors tested in this study, we observed that three factors namely, amount of CS, amount of STPP and duration of ultrasonication had statistically significant impact on the PS and EE%. Hence, these three factors were considered as critical factors and the rest five were taken as non-critical factors. The statistical analysis of the model generated from PBD revealed a significant *F* value for both PS (250.7; $P_{cal} < 0.0001$) and EE% (29.4; $P_{cal} < 0.0001$) for the model with a statistically insignificant lack of fit ($P_{crit} > 0.05$). In addition, there was a close agreement between predicted and adjusted R^2 values thereby validating the regression model obtained in the PBD.

4.3.2 Optimization of TDF loaded CS NPs using Box-Behnken design

In the optimization studies the levels of five non-critical factors, identified from PBD, were maintained constant as follows: a) the rate of addition of STPP was set to 3.5 mL/min; b) pH of STPP was set to 5.5; c) the homogenization speed was set to 12500 rpm; d) the duration of homogenization was set to 6 min; e) the amplitude for ultrasonication was set to 40%. A high-resolution BBD comprising of 17 runs was used to study the main and interaction effects of the three critical factors by varying them at three different levels (+1, 0 and -1). Five centre points were also included in the study design to check for reproducibility. Table 4.3 summarizes the statistical analysis of the results obtained from the experimental trials conducted based on BBD for the effect of the three critical factors on both the responses (i.e. PS and EE%).

4.3.2.1 Effect of critical factors on particle size

The least square second order polynomial equation showing the relationship between the critical factors and PS (response, Y_1) is as follows:

$$PS\ (Y_1) = 160 + 37.5X_1 + 14.88X_2 - 13.13X_3 + 17.25X_1^2 + 20.0X_2^2 + 19.5X_3^2 + 6.75X_1X_2 + 7.75X_1X_3 + 5.5X_2X_3$$

Where, X_1 = amount of CS, X_2 = amount of STPP and X_3 = duration of ultrasonication. As shown in Table 4.3, except for the 'X_2X_3' interaction term, rest all terms had statistically significant ($P_{crit} < 0.05$) effect on the PS. The quadratic model had an F value of 98.04 ($P_{cal} < 0.0001$) with an R^2 of 0.9921. Further, the lack of fit with F value of 3.26 ($P_{cal} = 0.14$) indicated that it was not significant when compared to pure error. From the diagnostic plots (data not shown), the difference between predicted and adjusted R^2 was less than 0.2 indicating a reasonable agreement between these values. The distribution of residuals seemed to be random around zero and there was no apparent effect of the sequence of the trial on the distribution of residuals. These indicators show the statistical validity of the model.

In the experimental trials conducted, the maximum PS was observed for the 4th run with a PS of 260 nm and minimum PS was observed for the 12th run with a PS of 141 nm (table 4.1).

The effect of the amount of CS and the amount of STPP on PS of TDF loaded CS NPs, for a given duration of ultrasonication is shown in fig. 4.3a and 4.4a. PS increased significantly with increase in the amount of CS. This can be attributed to the increased viscosity of the dispersion medium with the increase in the amount of CS which leads to decreased cavitation of the ultrasonic waves emitted from the probe sonicator and also reduced the shear capacity of the homogenizer (Derakhshandeh & Fathi, 2012). PS of TDF loaded CS NPs also increased with increase in the amount of STPP. With the increase in the amount of STPP, the number of phosphate ions of STPP available to bind the amide groups of CS will increase which leads to an increase in the rigidity of the complex formed between STPP and CS. At

constant energy output, as the rigidity of complex formed increases size reduction will not be effective and therefore PS of TDF loaded CS NPs increases (Modi et al., 2013). The amount of CS and amount of STPP had a positive interaction effect (X_1X_2) on the PS of TDF loaded CS NPs.

Table 4.3: Results of statistical analysis (ANOVA–Partial sum of squares) of particle size and entrapment efficiency for TDF loaded CS NPs.

Source	PS (Y_1)				EE% (Y_2)			
	Sum of Squares	df	F Value	P_{cal}	Sum of Squares	df	F Value	P_{cal}
Model	20010.78	9	98.04	< 0.0001*	1686.95	9	186.10	< 0.0001*
X_1	11250.00	1	496.06	< 0.0001*	325.12	1	322.81	< 0.0001*
X_2	1770.12	1	78.05	< 0.0001*	512.00	1	508.36	< 0.0001*
X_3	1378.12	1	60.76	0.00011*	28.12	1	27.92	0.0011*
X_1X_2	182.25	1	8.03	0.0252*	36.00	1	35.74	0.0005*
X_1X_3	240.25	1	10.59	0.0139*	0.25	1	0.2482	0.6336#
X_2X_3	121.00	1	5.33	0.0542#	9.00	1	8.93	0.0202*
X_1^2	1252.89	1	55.24	0.0002*	152.84	1	151.76	< 0.0001*
X_2^2	1684.21	1	74.26	< 0.0001*	488.84	1	485.37	< 0.0001*
X_3^2	1601.05	1	70.59	< 0.0001*	68.21	1	67.72	< 0.0001*
Residual	158.75	7			7.05	7		
Lack of Fit	112.75	3	3.26	0.14#	4.25	3	2.02	0.2531#
Pure Error	46.00	4			2.8	4		
Total	20169.53	16			1694	16		

*significant at $\alpha < 0.05$; #not significant at $\alpha > 0.05$

Fig. 4.3b and fig. 4.4b shows the effect of the amount of CS and duration of ultrasonication on PS of TDF loaded CS NPs, at a fixed amount of STPP. In the figure, it can be observed that at any given amount of CS, an increase in the duration of ultrasonication decreased the PS. This is because, as the duration of ultrasonication is increasing the total energy provided by the probe sonicator for the size reduction of the particles increases and therefore PS decreases (Ravi, Aditya, Kathuria, Malekar, & Vats, 2014; Ravi, Vats, et al., 2014). Further, a positive interaction effect albeit to a lesser effect was observed between these two factors (X_1X_3) on PS (P_{cal} = 0.0139). However, the interaction effects (X_2X_3) between the amount of

STPP and duration of ultrasonication on PS of TDF loaded CS NPs were not significant (P_{cal} = 0.0542).

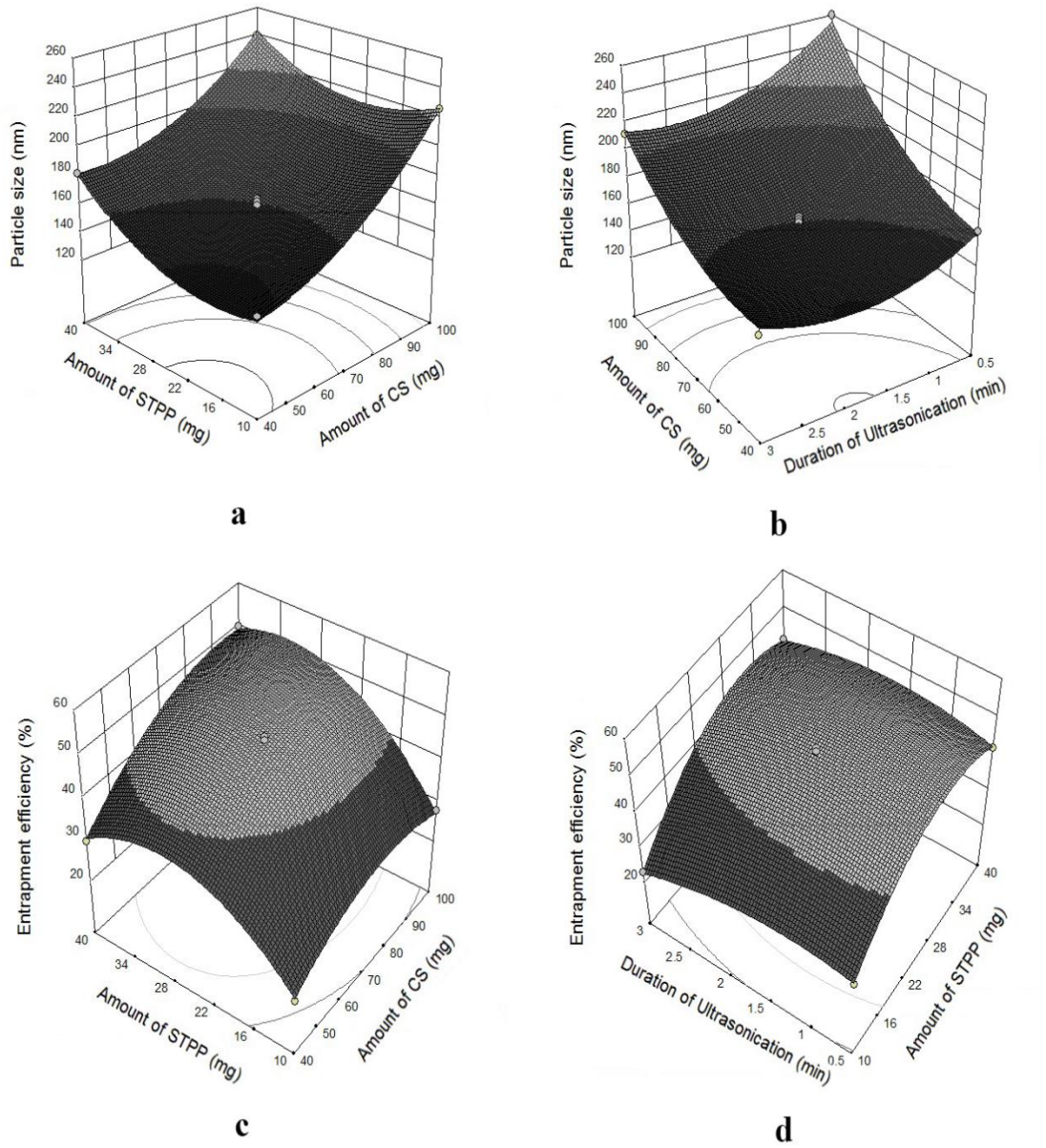

Fig. 4.3: Response surface plot of showing the effect of (a) amount of STPP and amount of CS on particle size; (b) amount of CS and duration of ultrasonication on particle size; (c) amount of STPP and amount of CS on entrapment efficiency; (d) amount of STPP and duration of ultrasonication on entrapment efficiency.

4.3.2.2 Effect of critical factors on entrapment efficiency

The least square second order polynomial equation showing the relationship between the critical factors and EE% (response, Y_2) is as follows:

$$EE\ (Y_2) = 48.8 + 6.375X_1 + 8.00X_2 - 1.875X_3 - 6.025X_1^2 - 10.775X_2^2 - 4.025X_3^2 + 3.00X_1X_2 - 0.25X_1X_3 + 1.5X_2X_3$$

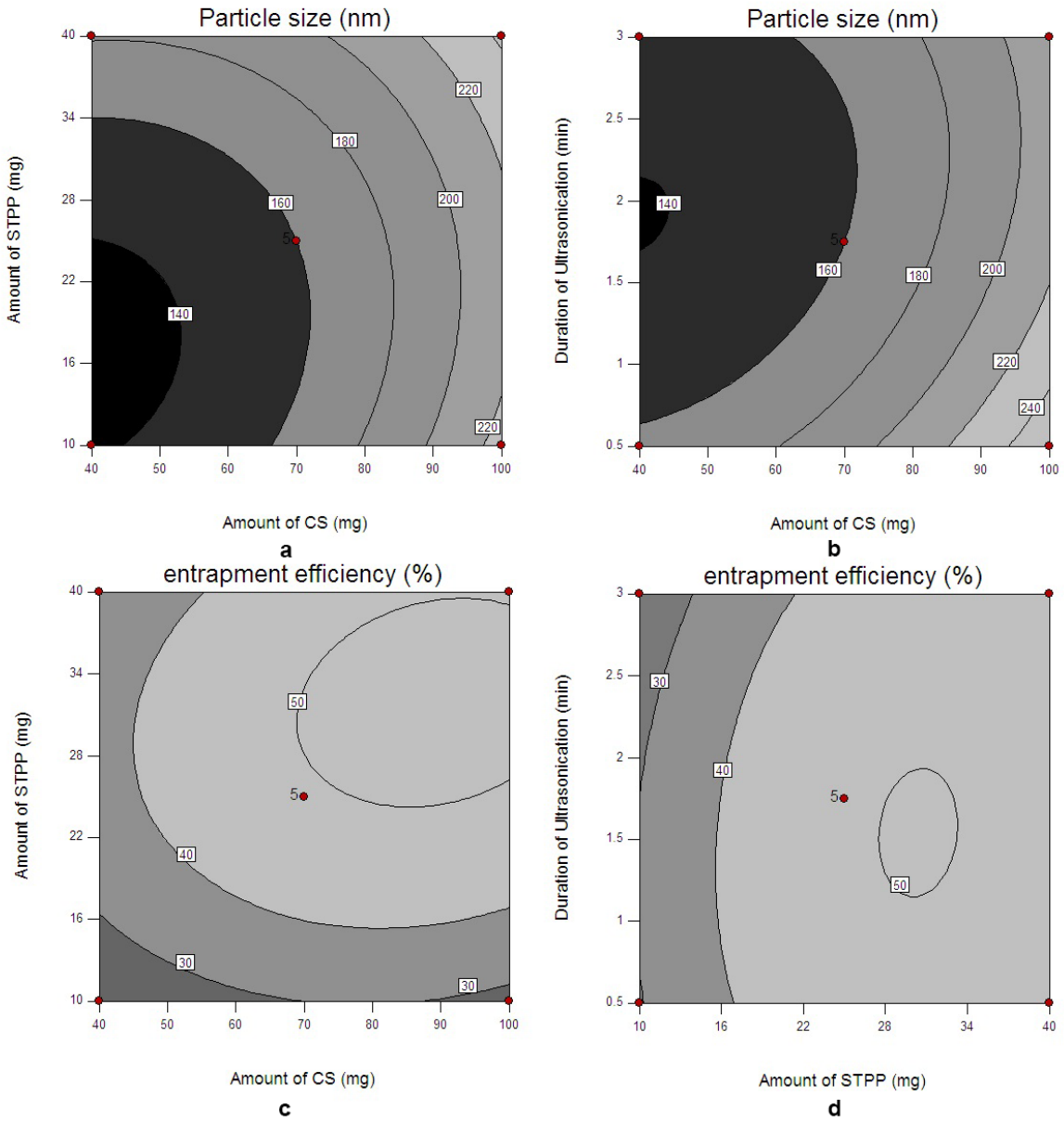

Fig. 4.4: Contour plot of showing the effect of (a) amount of STPP and amount of CS on particle size; (b) amount of CS and duration of ultrasonication on particle size; (c) amount of STPP and amount of CS on entrapment efficiency; (d) amount of STPP and duration of ultrasonication on entrapment efficiency.

Similar to PS, the quadratic model for EE% was found to be statistically significant. The *F* value of the model was statistically significant (186.11, $P_{cal} < 0.0001$) and R^2 was observed to be high (0.9958). Further, the lack of fit value of 2.02 ($P_{cal} = 0.25$) apparently indicated that model fit was significant. The difference between predicted and adjusted R^2 values was less

than 0.2 indicating a reasonable agreement between these values. The distribution of residuals seemed to be random around zero and there was no apparent effect of the sequence of the trial on the distribution of residuals. All the model terms (except 'X_1X_3') of the polynomial equation were found to be significant. In the trials conducted the maximum EE% was 50% observed for the 2nd and 3rd runs and minimum EE% was 23% observed for the 1st run (table 4.1). The observations from these trials indicated that the selected factors had a significant impact on EE%.

For a given duration of ultrasonication, an increase in the CS amount increased the EE% (fig. 4.3c and 4.4c), this is because a higher amount of CS was available for ionic crosslinking with STPP thereby increasing the possibility of entrapping TDF in the formed complex. Further, an increase in STPP amount also increased EE% of TDF which is attributed to an increase in the STPP ions available for ionic gelation by crosslinking with the amino groups of CS. Additionally, a synergistic effect on EE% was observed when both the CS and STPP levels are varied, indicating the existence of a positive interaction effect (X_1X_2) between the two factors and EE%.

For a given amount of CS, it was observed that there was a slight decrease in the EE% of TDF when the duration of ultrasonication was increased (fig. 4.3d and 4.4d). As, an increase in duration of ultrasonication leads to a decrease in PS which in turn leads to a decrease in the length of diffusional pathways for TDF (Budhian, Siegel, & Winey, 2007; Song et al., 2008). Additionally, a marginal positive interaction effect was observed between the amount of STPP and duration of ultrasonication (X_1X_3) on EE%.

4.3.2.3 Optimization and validation

Desirability function value for the optimized formulation was found to be 0.91. To obtain the optimized formulations, the criteria set for the responses were to minimize PS and maximize

EE%. However, the upper limit for PS and lower limit for EE% were provided into the software based on the maximum PS and minimum EE% values obtained in the experimental runs of BBD. The experimental conditions for the optimized formulation predicted by the software based on the quadratic model were: amount of CS - 67 mg; amount of STPP - 27 mg and duration of ultrasonication - 2 min. In order to check the validity of the model for the optimized formulation, verification runs (n = 6) were carried out. Formulations were prepared based on the experimental conditions predicted by the model and the PS and EE% of the formulations were determined. Further, Wilcoxon signed rank test was performed to evaluate the statistical difference between the observed and predicted values at $\alpha = 0.05$. However, there was no significant difference between the observed and predicted values for both the responses i.e. PS (P_{cal} = 0.4375) and EE% (P_{cal} = 0.7813) indicating the validity of the statistical model. The optimized formulation had a PS of 156 ± 5 nm and an EE% of 48.2 ± 1.0%.

4.3.3 Characterization studies

The scanning electron microscope images are shown in fig. 4.5 which apparently indicated that the TDF loaded CS NPs have a smooth spherical surface. The PS and PDI of the optimized TDF loaded CS NPs were found to be 156 ± 5 nm and 0.16 ± 0.06 (n = 6). The lower PDI values indicate the formation of stable NPs with a narrow PS distribution. The zeta potential was found to be 32.33 ± 1.1 mV for the optimised formulation. The positive zeta potential is mainly attributed to the amino groups of CS present on the surface of the NPs (Ing, Zin, Sarwar, & Katas, 2012). The EE% of the drug was found to be 48.2 ± 1.0%.

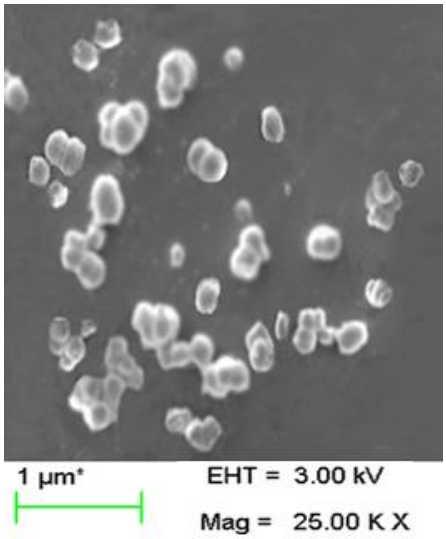

Fig. 4.5: Scanning electron micrograph of the optimized TDF loaded CS NPs.

Fig. 4.6 shows the DSC thermograms of pure TDF, CS, physical mixture of TDF and CS in the ratio of 1:1, blank CS NPs and TDF loaded CS NPs. A sharp endothermic peak was observed at 117 °C for pure TDF. The pure CS gave a characteristic broad endothermic peak at 71 °C which is attributed to the loss of water molecules and an exothermic peak at 310 °C which is due to the decomposition of amine units present in its structure (Bhumkar & Pokharkar, 2006). Further, there was no observable shift in the characteristic peak positions of CS and TDF in their physical mixture. In blank CS NPs and TDF loaded CS NPs, a sharp endothermic peak was observed at 162 °C corresponding to mannitol that was added as a cryoprotectant during the lyophilisation of NPs. Apparently, the absence of endothermic peak of TDF at 117 °C in TDF loaded CS NPs could indicate that it is present in amorphous form in the nanoparticle matrix. In blank CS NPs, there was a shift in the exothermic peak of CS to 285 °C which could be due to the ionic interaction between CS and STPP.

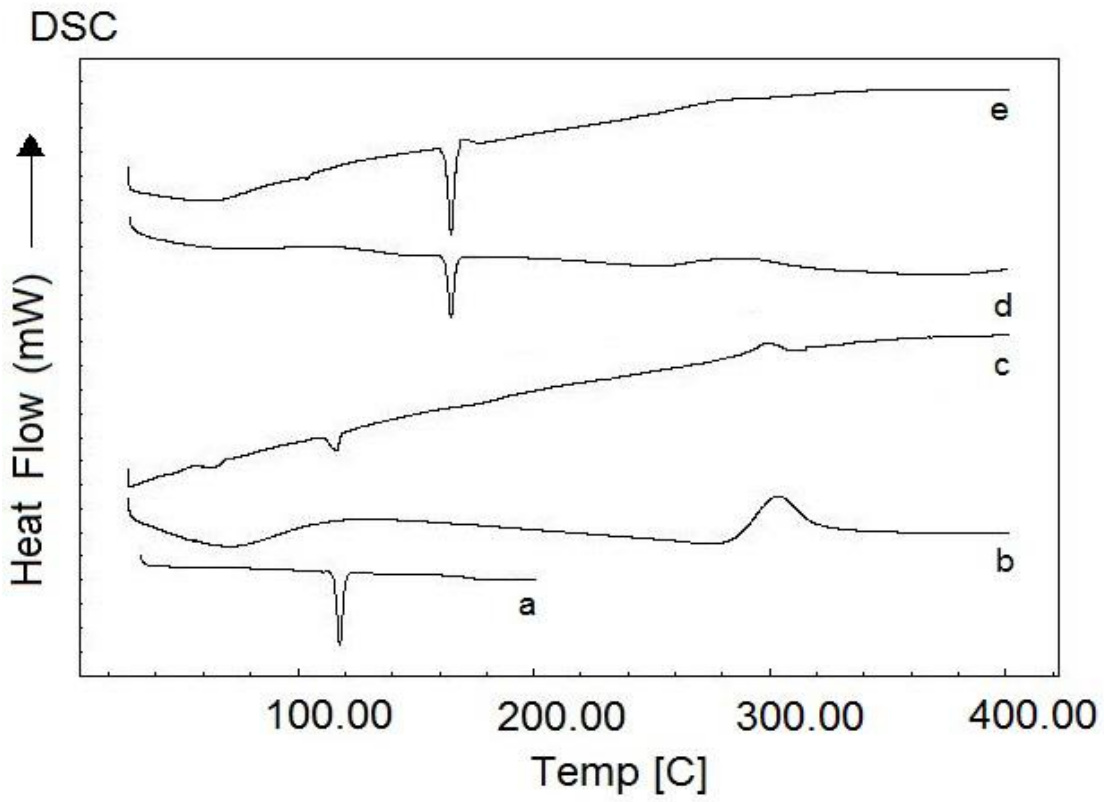

Fig. 4.6: Overlay of differential scanning calorimetric thermograms of (a) bulk tenofovir disoproxil fumarate (TDF); (b) bulk chitosan; (c) physical mixture of tenofovir disoproxil fumarate and chitosan (PM); (d) Blank CS NPs; (e) optimized TDF loaded CS NPs.

The pXRD graphs of pure TDF, CS, physical mixture of TDF and CS in the ratio of 1:1, blank CS NPs and TDF loaded CS NPs are shown in fig. 4.7. The pXRD graphs reaffirm the observations of DSC studies that TDF is present in the amorphous state in nanoparticle matrix. The prominent crystalline peaks of TDF between 2θ values of 20°–30° seen in pure TDF graph were also present in the physical mixture of TDF and CS. However, in the case of TDF loaded CS NPs, there was a significant reduction in the intensity of TDF's characteristic peaks especially at 25.1°, 22° and 20°. This indicates that major amount of TDF is present in amorphous form in the NPs. Further, the characteristic CS peak at 20° was absent in blank CS NPs which could be due to the change in the arrangement of the molecules of the crystal lattice of CS because of the ionic gelation of CS with STPP (Shah, Pal, Kaushik, & Devi, 2009).

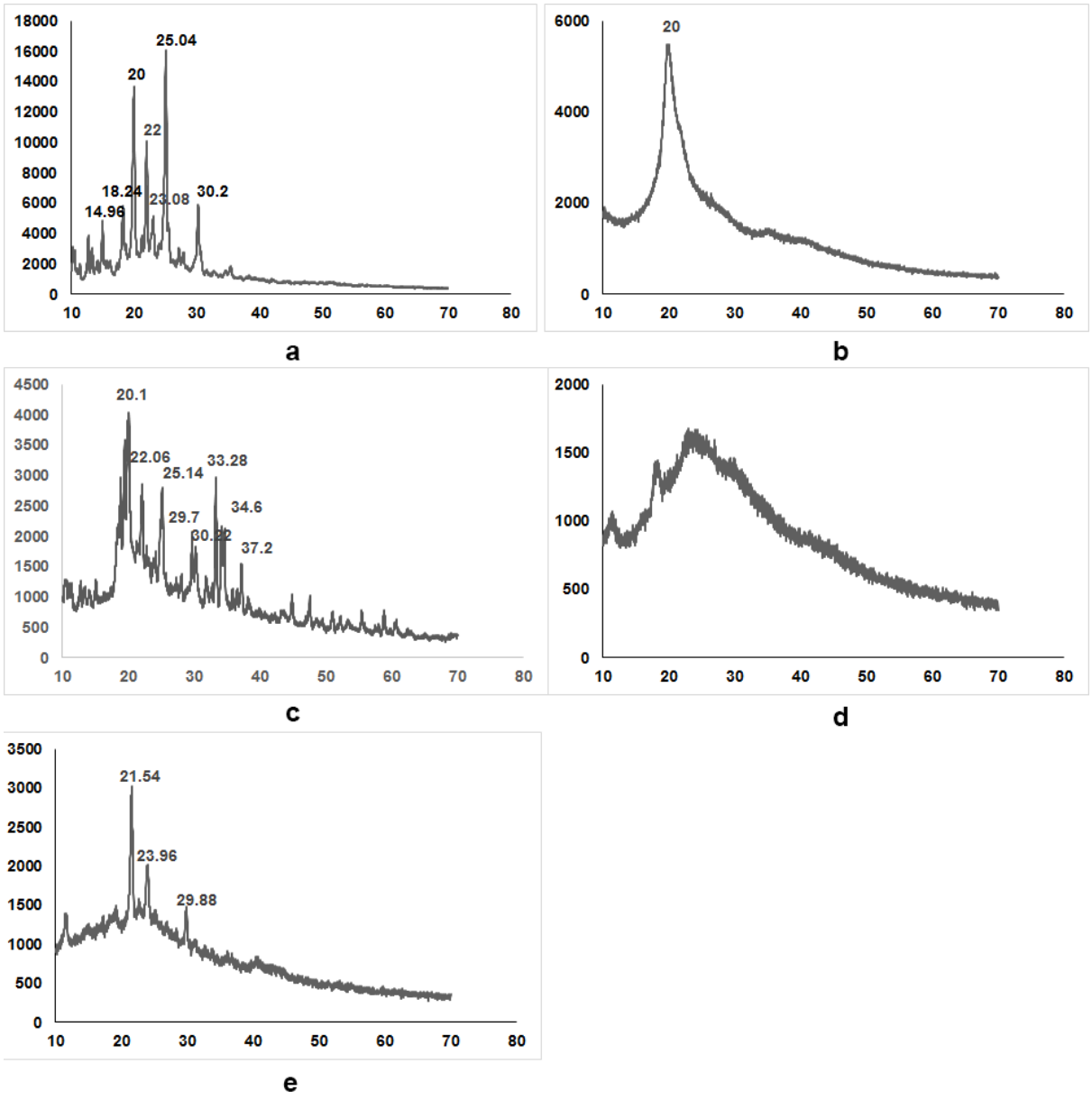

Fig. 4.7: X-ray diffractograms of (a) bulk tenofovir disoproxil fumarate; (b) bulk chitosan; (c) physical mixture of bulk tenofovir disoproxil fumarate, bulk chitosan and sodium tripolyphosphate; (d) Blank CS NPs; (e) optimized TDF loaded CS NPs.

4.3.4 Stability studies of TDF loaded CS NPs

The stability of the freeze dried TDF loaded CS NPs with 5% mannitol was evaluated by estimating the PS, PDI, EE% and zeta potential of the NPs during the three month study period. The statistical analysis of the results shown in fig. 4.8 indicated that there was no significant change in all the factors of the samples that were stored at accelerated conditions (i.e. 25 ± 2 °C with an RH of 60 ± 5%) over a period of three months. Similarly, there was no

significant change in the control samples (2-8 °C) during this time period. Hence, this study demonstrates the physical and chemical stability of the designed TDF loaded CS NPs.

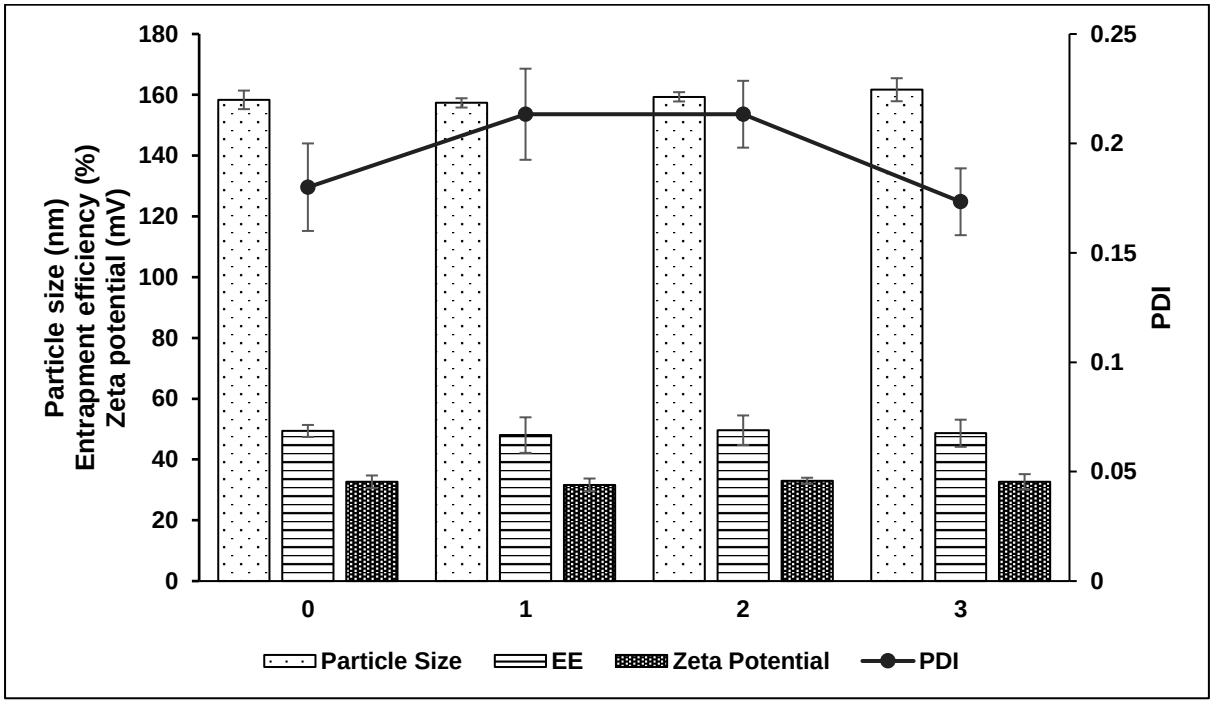

Fig. 4.8: Stability data of freeze dried TDF loaded CS NPs determined in terms of particle size (nm), entrapment efficiency (%) and zeta potential (mV) of the NPs at 25 ± 2 °C and 60 ± 5% for 3 months. The values are expressed in terms of mean ± SD of three independent observations (n = 3).

4.3.5 *In vitro* dissolution studies

The *in vitro* release studies were performed to evaluate the mechanism of drug release from TDF loaded CS NPs. The release profiles of free TDF and TDF loaded CS NPs are shown in fig. 4.9. As evident from the release profiles, the free TDF was completely dissolved within 4 h. On the other hand, TDF loaded CS NPs had a biphasic release pattern with 30% drug release in the first 3 h followed by a slow and sustained release with 60% drug release at 48 h. The initial burst release is due to the dissolution of TDF adhered on the surface of the NPs. The slow and sustained drug release is attributed to the rate control provided by the matrix formed due to the cross-linking between CS and STPP through which TDF needs to diffuse.

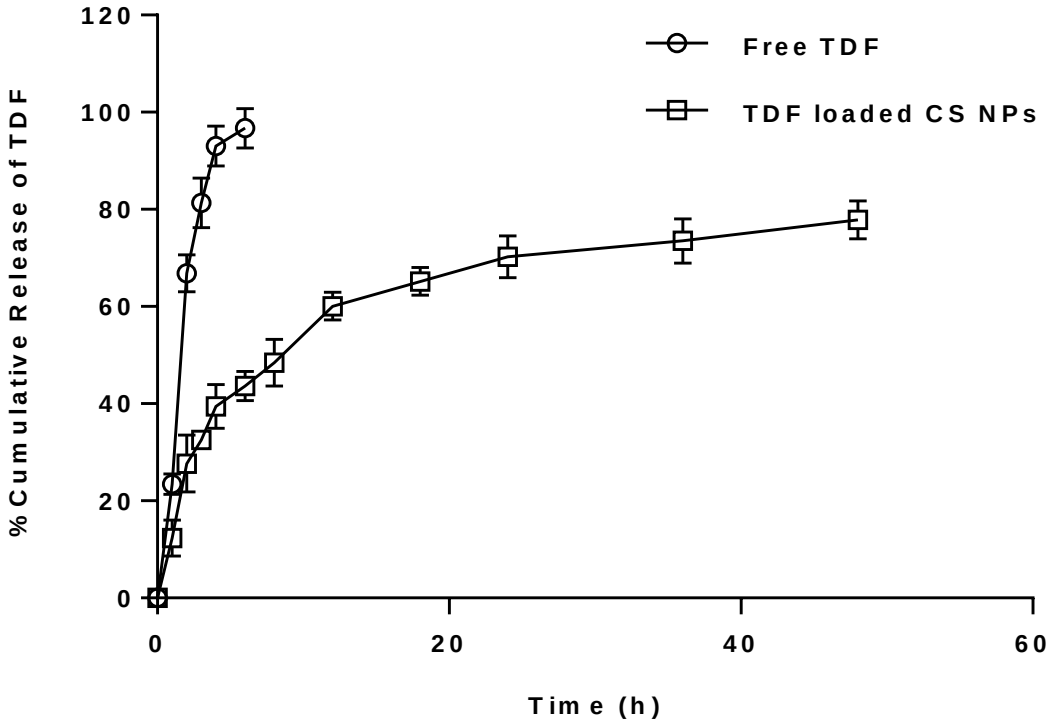

Fig. 4.9: *In vitro* release profile of free TDF and TDF loaded CS NPs in phosphate buffer solution (pH 5.2). Each data point is a mean ± SD of five independent observations (n = 5).

The release profile of TDF from the NPs was fit to different release kinetics models and it was observed that the reciprocal powered time model (R^2 = 0.9799) was the best fit when compared to zero order kinetics model (R^2 = 0.7008), first order kinetics model (R^2 = 0.8586), Higuchi kinetics model (R^2 = 0.9071) and Hixon-Crowell model (R^2 = 0.9146). This indicates that the drug release from the CS NPs is dependent on the diffusion of the drug through the matrix and dissolution process of the matrix system. Based on the reciprocal powered time model, the time take for 50% drug release ($T_{50\%}$) was found to be 8.3 h.

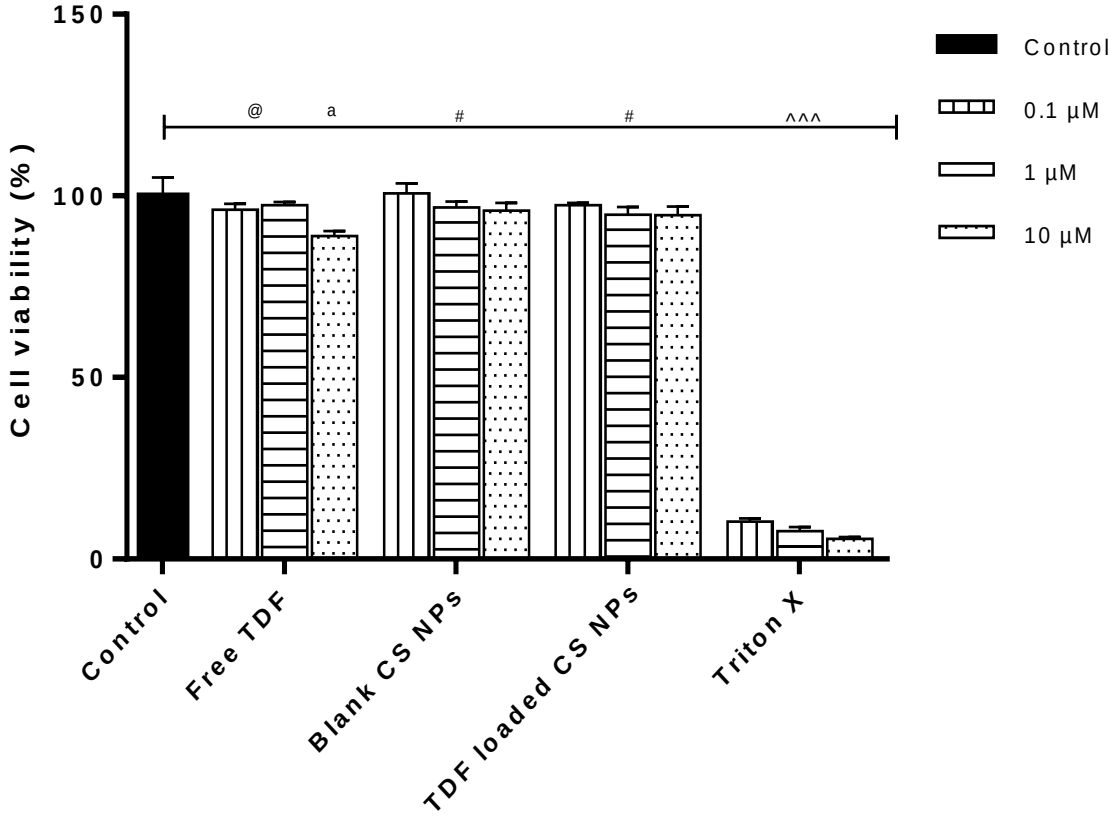

Fig. 4.10: Cell viability (%) of RAW 264.7 cells in the presence of (a) free TDF (b) Blank CS NPs (c) TDF loaded CS NPs (d) triton X – 100 (Triton X) at 0.1, 1 and 10 µM concentrations. [a]Statistical significance observed for 10 µM concentration of free TDF at P_{crit} < 0.001 when compared to control; [^^^]Statistical significance observed for all the concentrations of triton X-100 at P_{crit} < 0.001 when compared to control; [#]No statistical significance observed for all the concentrations at P_{crit} > 0.05 when compared to control; [@]No statistical significance observed for 0.1 and 1 µM concentrations of free TDF at P_{crit} > 0.05 when compared to control.

4.3.5 Cytotoxicity studies

This study was done to determine the viability of RAW 264.7 cells in the presence of free TDF, blank CS NPs and TDF loaded CS NPs at three different concentrations (0.1, 1 and 10 µM) with triton X-100 as a positive control. The results of this study are presented in fig. 4.10. In the case of free TDF, there was no significant effect (P_{crit} > 0.05) on the cell viability at 0.1 µM (96.1 ± 1.64%) and 1 µM of TDF (96.8 ± 1.46%) as compared to control (98.5 ± 1.46%). However, a slight decrease in the viability of the cells was observed at 10 µM concentration (88.9 ± 1.35%) when compared to control (P_{crit} < 0.05). Further, in the case of

blank CS NPs and TDF loaded CS NPs the mean values for cell viability were 100.7 ± 2.72% and 97.4 ± 0.62% at 0.1 µM, 96.9 ± 1.56% and 94.8 ± 2.12% at 1 µM, and 95.9 ± 2.12% and 94.7 ± 2.42% at 10 µM concentrations respectively. Statistical analysis of this data indicated that there was no significant decrease in the cell viability in the presence of both blank CS NPs and TDF loaded CS NPs at all the concentrations when compared to the control (P_{Crit} > 0.05). Therefore, we can say that both blank CS NPs and TDF loaded CS NPs are not cytotoxic.

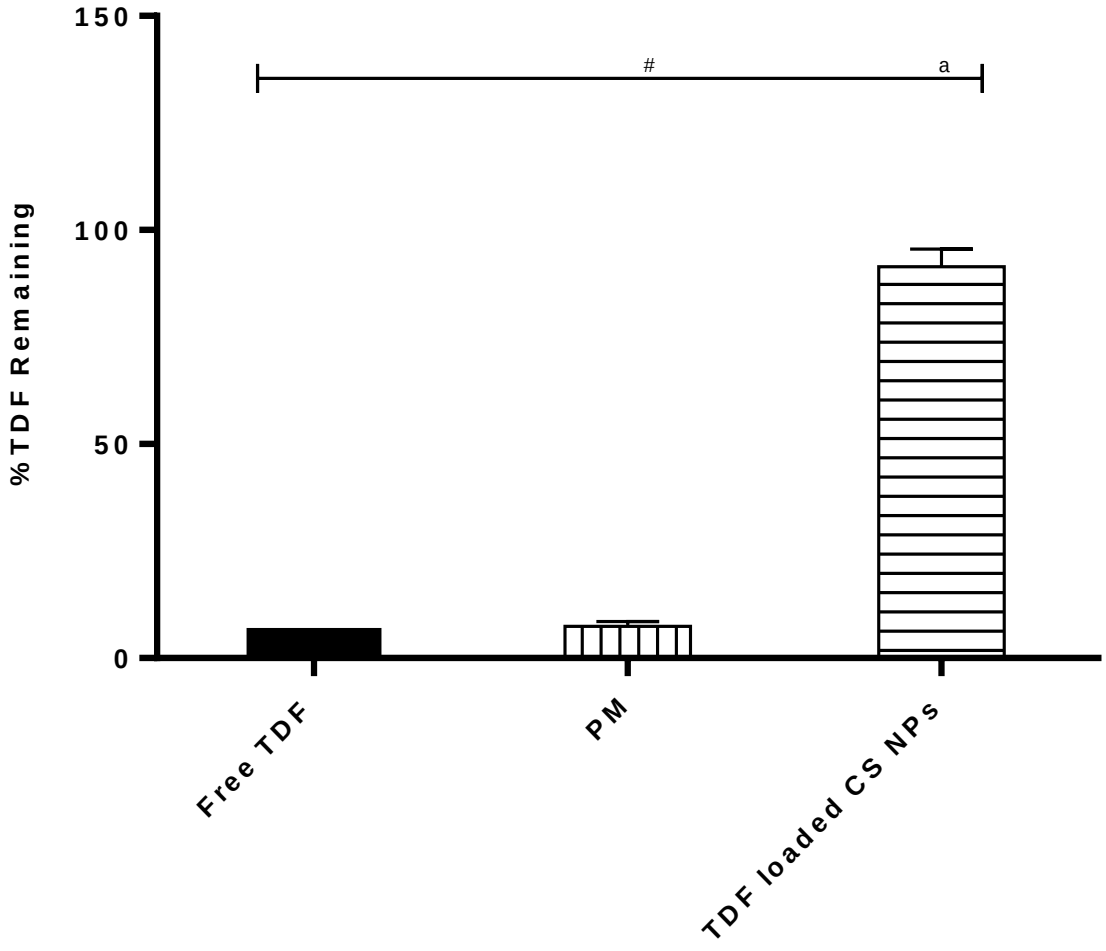

Fig. 4.11: Metabolic stability of TDF in the rat intestinal mucosal washings determined by calculating %TDF remaining after an incubation period of 30 min for (a) free TDF (b) physical mixture of TDF, CS and STPP (PM); (c) TDF loaded CS NPs. Each value is a representation of mean ± SD of five independent observations (n = 5). [a]Statistical significance observed at P_{crit} < 0.001 when compared to free TDF; [#]No statistical significance observed at P_{crit} > 0.05 when compared to free TDF.

4.3.6 *In vitro* stability in mucosal homogenates

The results obtained from the *in vitro* stability studies in mucosal homogenates are presented in fig. 4.11. From the figure, it is evident that %TDF remaining to be metabolized for TDF loaded CS NPs (91.3 ± 1.8%) was significantly higher (P_{cal} < 0.001) when compared to free TDF (6.6 ± 0.3%) and physical mixture (6.5 ± 0.5%). The results indicate that CS NPs provided significant metabolic protection to TDF when exposed to esterase enzymes present in the mucosal cells of the intestinal washings. Further, there was no significant difference (P_{crit} > 0.05) in the %TDF remaining in the physical mixture when compared to free TDF indicating that the excipients (CS/STPP) used in the preparation of TDF loaded CS NPs inherently cannot prevent the metabolism of TDF by esterase enzymes.

4.3.7 Mucoadhesion studies

The %binding efficiency was evaluated from *in vitro* mucoadhesion studies with NPs and porcine mucin. The study indicated that the designed NPs had a binding efficiency of 43.32 ± 4.2%. The mucoadhesive property of the designed NPs was also evaluated by incubating the TDF loaded CS NPs in the intestinal sacs *ex vivo* and compared with the free TDF. After 2 h of the samples (TDF loaded CS NPs or free TDF), the percentage of TNF equivalents (i.e. TDF and TMF) recovered from the mucosal layer was determined and it was observed that in the case of free drug the average recovery was observed to be 8.8 ± 1.3% of TDF. Whereas, the samples containing TDF loaded CS NPs the average recovery was significantly increased to 36.2 ± 3.3% (P_{cal} < 0.001).

This increase in the %binding efficiency (*in vitro*) and recovery (*ex vivo*) indicates the mucoadhesive property of the designed NPs and could be in part attributed to the high positive zeta potential of the NPs which helps in adhering to the negatively charged mucus layer of the gastrointestinal tract (Russo et al., 2016; Sogias, Williams, & Khutoryanskiy,

2008). Further, the mucoadhesive nature of the NPs decreases its mobility in the intestinal lumen and prolongs the residence in the gastrointestinal tract thereby, allowing the energy-dependent active uptake pathways to act and increase the chances of uptake of NPs across gut wall (Modi et al., 2013; Yin et al., 2009).

4.3.8 *Ex vivo* everted gut sac studies

In the everted gut sac studies with free TDF, when the samples collected from receiver chamber were analysed, only TMF was detected. However, in the case of TDF loaded CS NPs both TDF and TMF were detected (with TDF present in a higher proportion) in the samples collected from receiver chamber. Hence, the permeability flux was determined for both TDF and TMF and represented as TNF equivalents.

The permeability flux (*J*) values were calculated using the following equation:

$$J = \frac{(dQ/dt)}{A}$$

Where, $'dQ/dt'$ is the amount of TDF traversed into the receiver chamber per unit time and 'A' is the area of the intestinal sac exposed to the drug media.

Fig. 4.12 shows the *J* values obtained for free TDF and TDF loaded CS NPs in various test conditions. The *J* values of TNF equivalents across the everted intestinal sac for free TDF and TDF loaded CS NPs at 37 °C were 0.116 ± 0.013 and 0.536 ± 0.022 pmol/cm^2/min respectively. The results showed a 3.6 fold increase in the uptake of TNF equivalents from the NPs when compared to free TDF at 37 ^{o}C. This demonstrates that TDF loaded CS NPs can efficiently cross the intestinal barriers compared to free TDF.

Further, to evaluate the role of active endocytic uptake in the absorption of free TDF and TDF loaded CS NPs, the *J* values were determined at 4 °C where most of the energy-dependent uptake mechanisms are inactive. At 4 °C the flux of TNF equivalents from free

TDF and TDF loaded CS NPs were 0.204 ± 0.009 pmol/cm^2/min and 0.267 ± 0.019 pmol/cm^2/min respectively. There was a significant decrease (P_{cal} < 0.001) in the *J* values for TDF loaded CS NPs at 4 °C when compared to 37 °C, indicating that the role of active endocytic uptake process in the absorption of TDF loaded CS NPs. However, the *J* values increased significantly (P_{Crit} < 0.05) for free TDF at 4 °C compared to 37 °C. This could be due to the decrease in esterase enzyme activity at 4 °C compared to 37 °C because of which the metabolism of TDF decreased thereby increasing the overall flux of TNF equivalents. In the study conducted at 4 °C, TDF was detected in the samples collected from receiver chamber. Decreased enzyme activity coupled with higher permeability characteristics of TDF as compared to TMF were responsible for the increase in *J* values at 4 °C when compared to 37 °C. Further, to know the type of active endocytic (clathrin or caveolae) process involved in the uptake of NPs, we have determined the *J* values of TDF loaded CS NPs in the presence of chlorpromazine and nystatin. Chlorpromazine and nystatin are reported to inhibit the clathrin and caveolae-mediated endocytosis respectively (Platel et al., 2016; Tariq et al., 2015). The *J* value of TDF loaded CS NPs in the presence of chlorpromazine at 37 °C (0.292 ± 0.031 pmol/cm^2/min) decreased significantly (P_{cal} < 0.001) as compared to TDF loaded CS NPs at 37 °C without the presence of chlorpromazine. This shows the preponderant role of clathrin-mediated endocytic uptake in the absorption of NPs. However, nystatin had no significant effect (P_{Crit} > 0.05) on the permeability flux of TDF loaded CS NPs. At 37 °C, *J* value of TDF loaded CS NPs in the presence of nystatin was found to be and 0.497 ± 0.05 pmol/cm^2/min. This shows that apparently, caveolae-mediated endocytic process does not have a significant role in the absorption of NPs. Similar observations were made by other research groups (Harush-Frenkel, Debotton, Benita, & Altschuler, 2007; Ma & Lim, 2003; Montaner et al., 2014) where they have reported the importance of clathrin-mediated endocytic process in the absorption of CS NPs loaded with other drugs.

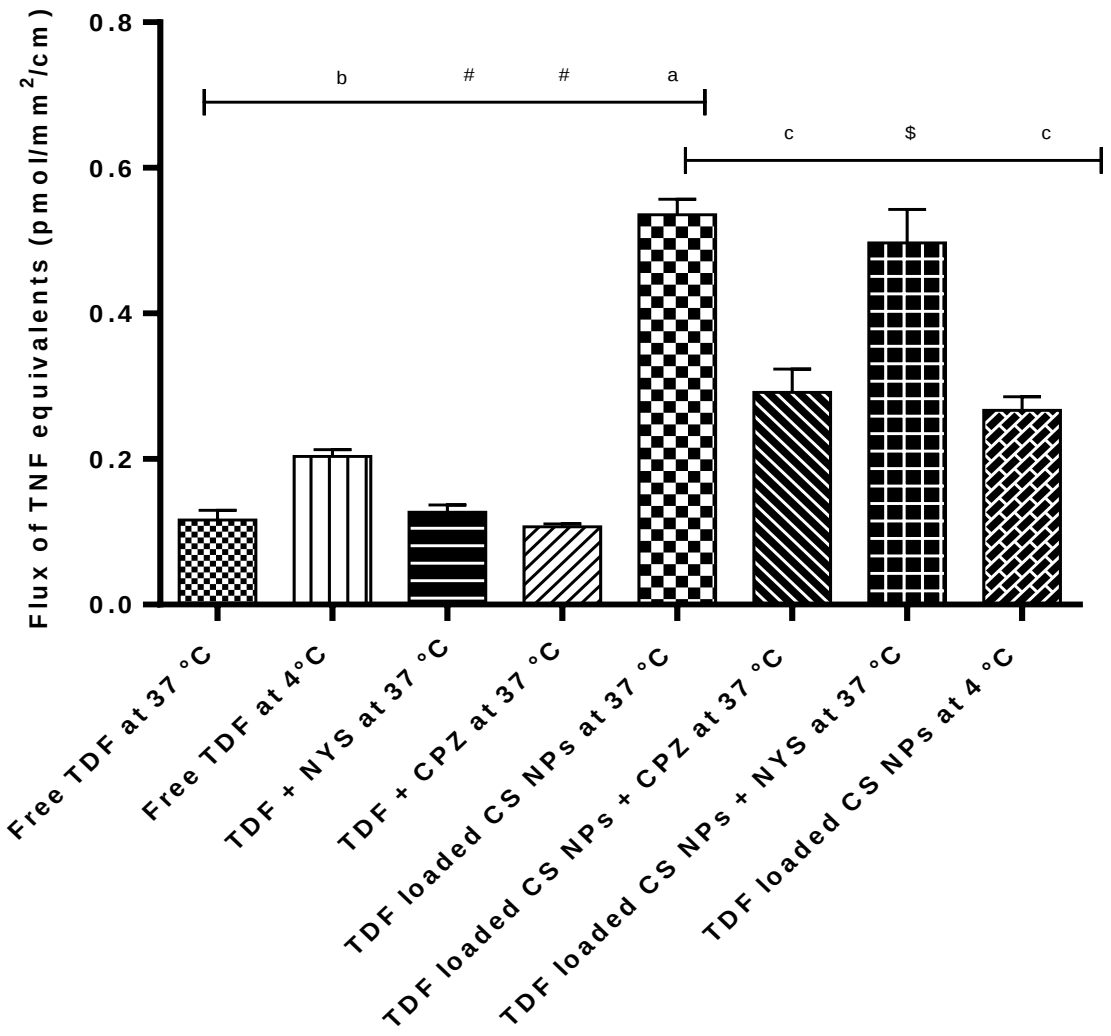

Fig. 4.12: Flux of TNF equivalents across the everted sacs of rat intestine for free TDF and TDF loaded CS NPs incubated at (a) 37 °C, (b) 4 °C, (c) in the presence of chlorpromazine (CPZ) and (d) in the presence of nystatin (NYS). [a]Statistical significance observed at P_{crit} < 0.001 when compared to free TDF at 37 °C; [b]Statistical significance observed at P_{crit} < 0.05 when compared to free TDF at 37 °C; [#]No statistical significance observed at P_{crit} > 0.05 when compared to free TDF at 37 °C; [c]Statistical significance observed at P_{crit} < 0.001 when compared to TDF loaded CS NPs at 37 °C; [$]No statistical significance observed at P_{crit} > 0.05 when compared to TDF loaded CS NPs at 37 °C.

4.3.9 *In vivo* single dose pharmacokinetic studies

To evaluate the effectiveness of CS NPs in enhancing the oral bioavailability of TDF we performed *in vivo* pharmacokinetic studies for the optimized TDF loaded CS NPs and free TDF in male Wistar rats. The plasma time course and relevant pharmacokinetic parameters of

TNF obtained following oral and IV administration of free TDF and oral administration of TDF loaded CS NPs are shown in fig. 4.13 and table 4.4 respectively.

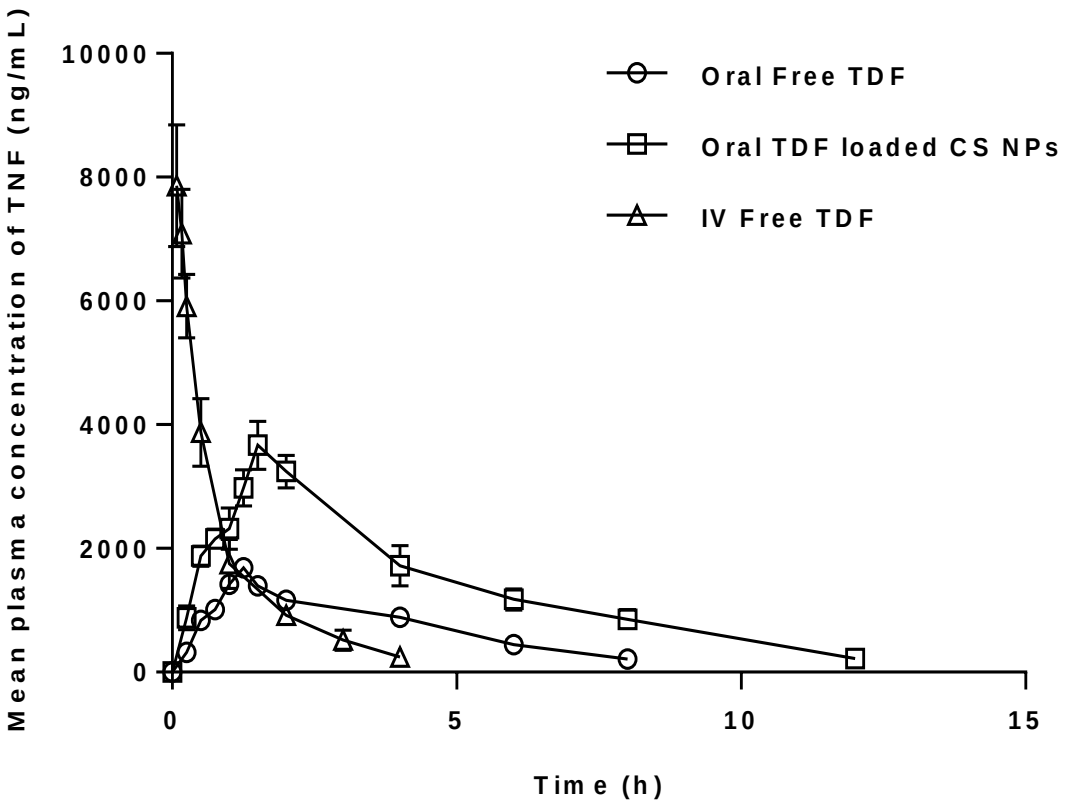

Fig. 4.13: Oral pharmacokinetic profile of free TDF and TDF loaded CS NPs and IV pharmacokinetic profile of free TDF in rats. Each value is a mean ± SD of five independent observations (n = 5).

In all the pharmacokinetic studies conducted, only TNF was detected in the plasma samples while both TDF and TMF were not detected. This could be attributed to the rapid metabolism of TDF to its active form (TNF) when exposed to plasma esterases which was also confirmed by Geboers et al. (2015) and Shailender et al. (2016). Further, when we externally spiked TDF into blank plasma and analysed the sample immediately in HPLC (after suitable pretreatment), we could only detect TNF but did not observe the presence of TDF or TMF peaks.

Table 4.4. Pharmacokinetic parameters of TNF obtained following oral and IV administration of free TDF (22 mg/kg – IV and 100 mg/kg – oral) and oral administration of TDF loaded CS NPs (equivalent to 100 mg/kg of TDF).

Parameters	Treatment group		
	Free TDF, IV	**Free TDF, Oral**	**TDF loaded CS NPs, Oral**
T_{max} (h)	---	1.00-1.50	1.25–2.00
C_{max} (ng/mL)	7862.61 ± 979.6	1687.53 ± 119.4	3712.72 ± 333.4[a]
AUC_{total} (h*ng/mL)	6240.13 ± 353.6	4020.93 ± 56.9	16786.57 ± 1252.8[a]
F_{abs}	---	0.14	0.59[a]
F_{rel}	---	---	4.17
MRT (h)	1.13 ± 0.06	3.11 ± 0.18	4.47 ± 0.23[a]

The values represented are mean ± SD (n = 5). [a]Statistical significance observed at P_{crit} < 0.001 when compared to oral free TDF.

From the oral pharmacokinetic studies (table 4.4 and fig. 4.13), it is evident that plasma time course of TDF improved significantly (in terms of total area under the curve (AUC_{total}), maximum plasma concentration (C_{max}) and mean residence time (MRT) with $P_{cal} < 0.001$) for TDF loaded CS NPs compared to free TDF. TDF loaded CS NPs showed a 380% increase in AUC_{total}, 220% increase in C_{max} and 143% increase in MRT as compared to free TDF administered through the oral route. Further, the absolute bioavailability (F_{abs}) of free TDF was observed to be 14% and that of TDF loaded CS NPs was 59% with a relative bioavailability (F_{rel}) of 417%. The increase in the oral absorption characteristics (AUC_{total} and C_{max}) of TDF loaded CS NPs could be due to higher permeability characteristics and metabolic protection of TDF by the CS NPs from intestinal esterase enzymes. This argument is further supported from the results obtained for TDF loaded CS NPs from *ex vivo* everted gut sac studies and *in vitro* stability studies in mucosal homogenates.

A Wilcoxon signed rank test between the T_{max} values of free TDF and TDF loaded CS NPs indicated that there was no statistical difference between these two groups ($P_{crit} \geq 0.05$). This implies that there was no difference mean absorption time of TDF and TDF loaded CS NPs. However, it was observed that there was a significant increase in the MRT value of TDF loaded CS NPs. Hence, this increase in the oral MRT (which is a summation of mean

absorption time (oral) and MRT (IV)) shows the ability of the NPs to provide a sustained release of TDF in the systemic circulation. Hence, the ability of CS to provide a rate controlling effect *in vivo* confirms the premise under which TDF loaded CS NPs were prepared.

4.4 Conclusion

CS NPs showed promising results in entrapping and enhancing the oral bioavailability of TDF. The DoE was able to determine the critical factors involved in the preparation of TDF loaded CS NPs. The optimized NPs were stable, biocompatible and was able to provide metabolic protection for TDF against the intestinal esterases. Further, a significant increase in the oral absorption of TDF loaded CS NPs was observed in which clathrin-mediated active uptake pathway played a crucial role. Additionally, the mucoadhesion studies indicated that the ability of the NPs to adhere to the mucosal layer may have played a key role in increasing the active uptake of the TDF loaded CS NPs. Therefore, the TDF loaded CS NPs can reduce the dose of TDF and may be beneficial in the treatment of HIV/AIDS. Finally, the designed CS NPs could provide a consistent pharmacokinetic profile with enhanced absorption and can be used for designing carrier systems for drugs that are susceptible to intestinal degradation.

References

Akhtar, F., Rizvi, M. M. A., & Kar, S. K. (2012). Oral delivery of curcumin bound to chitosan nanoparticles cured Plasmodium yoelii infected mice. *Biotechnology Advances*, *30*(1), 310–320.

Barzegar-Jalali, M., Adibkia, K., Valizadeh, H., Shadbad, M. R. S., Nokhodchi, A., Omidi, Y., … Hasan, M. (2008). Kinetic analysis of drug release from nanoparticles. *Journal of Pharmacy & Pharmaceutical Sciences*, *11*(1), 167–77.

Bhumkar, D. R., & Pokharkar, V. B. (2006). Studies on effect of pH on cross-linking of chitosan with sodium tripolyphosphate: A technical note. *AAPS PharmSciTech*, *7*(2), E138–E143.

Budhian, A., Siegel, S. J., & Winey, K. I. (2007). Haloperidol-loaded PLGA nanoparticles: Systematic study of particle size and drug content. *International Journal of Pharmaceutics*, *336*(2), 367–375.

Calvo, P., Remunan-Lopez, C., Vila-Jato, J. L., & Alonso, M. J. (1997). Novel hydrophilic chitosan-polyethylene oxide nanoparticles as protein carriers. *Journal of Applied Polymer Science*, *63*(1), 125–132.

Cohen-Sela, E., Chorny, M., Koroukhov, N., Danenberg, H. D., & Golomb, G. (2009). A new double emulsion solvent diffusion technique for encapsulating hydrophilic molecules in PLGA nanoparticles. *Journal of Controlled Release*, *133*(2), 90–95.

Crauste-Manciet, Decroix, Farinotti, & Chaumeil. (1997). Cefpodoxime-proxetil hydrolysis and food effects in the intestinal lumen before absorption: in vitro comparison of rabbit and human material. *International Journal of Pharmaceutics*, *157*(2), 153–161.

Derakhshandeh, K., & Fathi, S. (2012). Role of chitosan nanoparticles in the oral absorption

of Gemcitabine. *International Journal of Pharmaceutics*, *437*(1–2), 172–177.

Dudhani, A. R., & Kosaraju, S. L. (2010). Bioadhesive chitosan nanoparticles: Preparation and characterization. *Carbohydrate Polymers*, *81*(2), 243–251.

Dünnhaupt, S., Barthelmes, J., Hombach, J., Sakloetsakun, D., Arkhipova, V., & Bernkop-Schnürch, A. (2011). Distribution of thiolated mucoadhesive nanoparticles on intestinal mucosa. *International Journal of Pharmaceutics*, *408*(1–2), 191–199.

Feng, C., Wang, Z., Jiang, C., Kong, M., Zhou, X., Li, Y., … Chen, X. (2013). Chitosan/o-carboxymethyl chitosan nanoparticles for efficient and safe oral anticancer drug delivery: in vitro and in vivo evaluation. *International Journal of Pharmaceutics*, *457*(1), 158–67.

Food and Drug Administration, HHS. (2003). International Conference on Harmonisation; Stability Data Package for Registration Applications in Climatic Zones III and IV; Stability Testing of New Drug Substances and Products; availability. Notice. *Federal Register*, *68*(225), 65717–8.

Geboers, S., Haenen, S., Mols, R., Brouwers, J., Tack, J., Annaert, P., & Augustijns, P. (2015). Intestinal behavior of the ester prodrug tenofovir DF in humans. *International Journal of Pharmaceutics*, *485*(1–2), 131–7.

Harish Prashanth KV, Thranathan R. N. (2006). Crosslinked chitosan—preparation and characterization. *Carbohydrate Research*, *341*(1), 169-73.

Harush-Frenkel, O., Debotton, N., Benita, S., & Altschuler, Y. (2007). Targeting of nanoparticles to the clathrin-mediated endocytic pathway. *Biochemical and Biophysical Research Communications*, *353*(1), 26–32.

Huang, W., Zhang, H., Liu, W., & Li, C. (2012). Survey of antioxidant capacity and phenolic composition of blueberry, blackberry, and strawberry in Nanjing. *Journal of Zhejiang University. Science. B*, *13*(2), 94–102.

Ing, L. Y., Zin, N. M., Sarwar, A., & Katas, H. (2012). Antifungal Activity of Chitosan Nanoparticles and Correlation with Their Physical Properties. *International Journal of Biomaterials*, *2012*, 1–9.

Li, P., Callery, P. S., Gan, L. S., & Balani, S. K. (2007). Esterase inhibition attribute of grapefruit juice leading to a new drug interaction. *Drug Metabolism and Disposition*, *35*(7), 1023–1031.

Liu, Y., Wang, X., Ren, W., Chen, Y., Yu, Y., Zhang, J., … Zhang, X. (2013). Novel albendazole-chitosan nanoparticles for intestinal absorption enhancement and hepatic targeting improvement in rats. *Journal of Biomedical Materials Research. Part B, Applied Biomaterials*, *101*(6), 998–1005.

Ma, Z., & Lim, L.-Y. (2003). Uptake of chitosan and associated insulin in Caco-2 cell monolayers: a comparison between chitosan molecules and chitosan nanoparticles. *Pharmaceutical Research*, *20*(11), 1812–9.

Mi, F. L., Shyu, S. S., Chen, C. T., & Schoung, J. Y. (1999). Porous chitosan microsphere for controlling the antigen release of Newcastle disease vaccine: preparation of antigen-adsorbed microsphere and in vitro release. *Biomaterials*, *20*(17), 1603–12.

Modi, J., Joshi, G., & Sawant, K. (2013). Chitosan based mucoadhesive nanoparticles of ketoconazole for bioavailability enhancement: formulation, optimization, *in vitro* and *ex vivo* evaluation. *Drug Development and Industrial Pharmacy*, *39*(4), 540–547.

Montaner, J. S. G., Lima, V. D., Harrigan, P. R., Lourenço, L., Yip, B., Nosyk, B., …

Kendall, P. (2014). Expansion of HAART Coverage Is Associated with Sustained Decreases in HIV/AIDS Morbidity, Mortality and HIV Transmission: The "HIV Treatment as Prevention" Experience in a Canadian Setting. *PLoS ONE*, *9*(2), e87872.

Orienti, I., Aiedeh, K., Gianasi, E., Bertasi, V., & Zecchi, V. (1996). Indomethacin loaded chitosan microspheres. Correlation between the erosion process and release kinetics. *Journal of Microencapsulation*, *13*(4), 463–72.

Platel, A., Carpentier, R., Becart, E., Mordacq, G., Betbeder, D., & Nesslany, F. (2016). Influence of the surface charge of PLGA nanoparticles on their *in vitro* genotoxicity, cytotoxicity, ROS production and endocytosis. *Journal of Applied Toxicology*, *36*(3), 434–444.

Ravi, P. R., Aditya, N., Kathuria, H., Malekar, S., & Vats, R. (2014). Lipid nanoparticles for oral delivery of raloxifene: Optimization, stability, in vivo evaluation and uptake mechanism. *European Journal of Pharmaceutics and Biopharmaceutics*, *87*(1), 114–124.

Ravi, P. R., Vats, R., Dalal, V., Gadekar, N., & N, A. (2015). Design, optimization and evaluation of poly- ε -caprolactone (PCL) based polymeric nanoparticles for oral delivery of lopinavir. *Drug Development and Industrial Pharmacy*, *41*(1), 131–140.

Ravi, P. R., Vats, R., Dalal, V., & Murthy, A. N. (2014). A hybrid design to optimize preparation of lopinavir loaded solid lipid nanoparticles and comparative pharmacokinetic evaluation with marketed lopinavir/ritonavir coformulation. *Journal of Pharmacy and Pharmacology*, *66*(7), 912–926.

Ravi, P. R., Vats, R., Thakur, R., Srivani, S., & Aditya, N. (2012). Effect of grapefruit juice and ritonavir on pharmacokinetics of lopinavir in wistar rats. *Phytotherapy Research*,

26(10), 1490–1495.

Russo, E., Selmin, F., Baldassari, S., Gennari, C. G. M., Caviglioli, G., Cilurzo, F., … Parodi, B. (2016). A focus on mucoadhesive polymers and their application in buccal dosage forms. *Journal of Drug Delivery Science and Technology*, *32*, 113–125.

Shah, S., Pal, A., Kaushik, V. K., & Devi, S. (2009). Preparation and characterization of venlafaxine hydrochloride-loaded chitosan nanoparticles and *in vitro* release of drug. *Journal of Applied Polymer Science*, *112*(5), 2876–2887.

Shailender, J., Ravi, P. R., Saha, P., & Myneni, S. (2016). Oral pharmacokinetic interaction of ester rich fruit juices and pharmaceutical excipients with tenofovir disoproxil fumarate in male Wistar rats. *Xenobiotica*. DOI: 10.1556/AChrom.27.2015.4.2.

Shukla, R. K., & Tiwari, A. (2012). Carbohydrate polymers: Applications and recent advances in delivering drugs to the colon. *Carbohydrate Polymers*, *88*(2), 399–416.

Sinha, V. ., Singla, A. ., Wadhawan, S., Kaushik, R., Kumria, R., Bansal, K., & Dhawan, S. (2004). Chitosan microspheres as a potential carrier for drugs. *International Journal of Pharmaceutics*, *274*(1–2), 1–33.

Sogias, I. A., Williams, A. C., & Khutoryanskiy, V. V. (2008). Why is Chitosan Mucoadhesive? *Biomacromolecules*, *9*(7), 1837–1842.

Song, X., Zhao, Y., Wu, W., Bi, Y., Cai, Z., Chen, Q., … Hou, S. (2008). PLGA nanoparticles simultaneously loaded with vincristine sulfate and verapamil hydrochloride: systematic study of particle size and drug entrapment efficiency. *International Journal of Pharmaceutics*, *350*(1–2), 320–9.

Tariq, M., Alam, M. A., Singh, A. T., Iqbal, Z., Panda, A. K., & Talegaonkar, S. (2015). Biodegradable polymeric nanoparticles for oral delivery of epirubicin: In vitro, ex vivo,

and in vivo investigations. *Colloids and Surfaces B: Biointerfaces*, *128*, 448–456.

Wang, X.-Q., & Zhang, Q. (2012). pH-sensitive polymeric nanoparticles to improve oral bioavailability of peptide/protein drugs and poorly water-soluble drugs. *European Journal of Pharmaceutics and Biopharmaceutics*, *82*(2), 219–229.

Yin, Y., Chen, D., Qiao, M., Lu, Z., & Hu, H. (2006). Preparation and evaluation of lectin-conjugated PLGA nanoparticles for oral delivery of thymopentin. *Journal of Controlled Release*, *116*(3), 337–345.

Yin, L., Ding, J., He, C., Cui, L., Tang, C., & Yin, C. (2009). Drug permeability and mucoadhesion properties of thiolated trimethyl chitosan nanoparticles in oral insulin delivery. *Biomaterials*, *30*(29), 5691–5700.

Chapter 5

Design and evaluation TDF loaded PLGA NPs

5.1 Introduction

There have been numerous polymers used in the design of NPs, among them poly(lactic-co-glycolic acid) (PLGA) is one of the most extensively used polymers because of its biocompatible and biodegradable properties along with having versatile degradation kinetics (Ghasemian et al., 2013; Mittal, Sahana, Bhardwaj, & Ravi Kumar, 2007). It is a copolymer of poly(lactic acid) and poly(glycolic acid) because of which it is available in different molecular weights and copolymer compositions. This can be very useful in obtaining desired permeability and release properties (Cohen-Sela, Chorny, Koroukhov, Danenberg, & Golomb, 2009; Mittal et al., 2007). PLGA is synthesized by hydrolysis of lactide and glycolide in the presence of stannous octoate which acts as a catalyst, the reaction needs to be conducted under high vacuum at temperature ranging between 160 –190 °C (fig. 5.1). PLGA is amorphous in nature with a glass transition temperature ranging between 45–55 °C. Further, the glass transition temperature is reported to decrease with decreasing lactide concentration (Kapoor et al., 2015). PLGA is reported to undergo hydrolytic degradation where the ester linkages present along the entire backbone of the polymer are cleaved. This degradation leads to the formation of water soluble fragments which are further hydrolysed to its monomer units (lactic and glycolic acid) (Danhier et al., 2012).

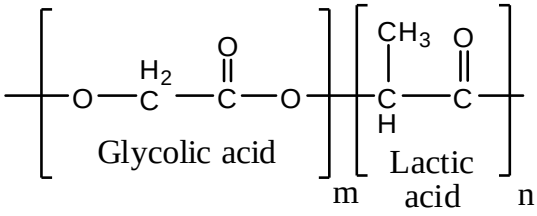

Fig. 5.1: Structure of PLGA.

PLGA has also been used especially in the form of nanoparticles to enhance the oral bioavailability of various drugs (Joshi, Kumar, & Sawant, 2014; Mittal et al., 2007; Singh & Pai, 2014; Tariq et al., 2015). There have been different active uptake mechanisms reported for the oral absorption of NPs, among them clathrin mediated endocytosis is said to be the

predominant uptake pathway for PLGA NPs (Plapied, Duhem, des Rieux, & Préat, 2011; Sahay, Alakhova, & Kabanov, 2010) although, a few works have also reported the involvement of caveolae mediated uptake of PLGA NPs (Platel et al., 2016; Tariq et al., 2015). Different techniques have been developed for preparing PLGA based NPs, some of the commonly reported methods (Astete & Sabliov, 2006; Sadat Tabatabaei Mirakabad et al., 2014; Sah & Sah, 2015) are as follows:

- W/O emulsion and phase separation: In this method the aqueous solution of drug is emulsified in an organic solvent (dichloromethane) in which PLGA is dissolved. To this emulsion an antisolvent of PLGA (silicone oil) is added which leads to the phase separation of PLGA. PLGA coacervates around the aqueous phase leading to the entrapment of the drug. This technique is primarily used for the encapsulation of hydrophilic drugs.
- O/W emulsion and solvent evaporation: PLGA and drug are dissolved in an organic phase having low boiling point and emulsified in an aqueous phase containing a suitable stabilizer (polyvinyl alcohol). The emulsified organic phase is evaporated under continuous stirring usually at room temperature which leads to phase separation of PLGA NPs and the entrapment of drug within the NPs.
- O/O emulsion and solvent evaporation: In this method drug and PLGA are dissolved in an organic solvent having lower boiling points which is emulsified in a non-aqueous antisolvent (silicone oil). The dispersed phase is evaporated by stirring overnight and the formed NPs are separated by centrifugation.
- O/W emulsion and reverse salting out: Drug and PLGA are dissolved in a water miscible organic solvent. This solution is emulsified in aqueous medium saturated with electrolyte. After emulsifying the organic solution, the aqueous solution is reverse

salted out by adding electrolyte free aqueous media under stirring. This leads to the coacervation of PLGA which entraps the drug and forms NPs.

- Multiple emulsion techniques:
    - W/O/W emulsion and solvent evaporation/extraction: In this method the drug dissolved in water and emulsified in an organic solvent containing PLGA. This primary emulsion is then emulsified in an aqueous solution containing a suitable stabilizer leading to the formation of a secondary emulsion. The organic solution is removed which causes PLGA to coacervate around the internal aqueous phase and encapsulate the drug.
    - W/O/O emulsion and solvent evaporation/extraction: In this method, similar to the previous technique, a primary W/O emulsion is prepared. This is then added to an oil phase which is miscible with the organic phase of the primary emulsion but is an antisolvent to PLGA and drug.
- Nanoprecipitation: PLGA and drug are dissolved in a water miscible organic solvent. This solution is added to an aqueous solvent containing a stabilizer under mild stirring. As, the organic phase diffuses into the aqueous phase leading to the aggregation of PLGA to form NPs.

In this study, we have designed TDF loaded PLGA NPs with the purpose of enhancing the oral absorption of TDF. In order to obtain NPs with least particle size and with maximum possible entrapment efficiency (EE%) of TDF, it is necessary to have a comprehensive understanding of the impact of different critical formulation and process factors on the particle size and EE% of the NPs. This was achieved by performing extensive experimental trials in which different process and formulation factors were varied, these experimental trials were designed with the help of design expert software. The optimization studies were done in two stages. The first stage was a low-resolution factorial design which helped in identifying the various critical

factors involved in the preparation of the NPs. Further, in the second stage, the interactions between these critical factors and the kind of relationship they hold (with the responses) was evaluated by employing a response surface methodology. The optimized NPs were characterized for shape, size, surface charge, EE%, stability and cytotoxicity. This was followed by the evaluation of the absorption enhancement capability of the designed NPs along the oral route (*in vivo*). Additionally, *ex vivo* everted gut sac studies were also performed to evaluate the probable mechanisms of uptake of the designed NPs.

5.2 Material and methods

5.2.1 Materials

TNF and its prodrug form (TDF) were provided as gift samples by Gilead Sciences, Inc. (CA, USA) and Strides Arcolab Limited (Bengaluru, India) respectively. Male Wistar rats were purchased from Sainath Agencies, Hyderabad, India. PLGA (Lactide:Glycolide::50:50; molecular weight: 30,000-60,000 Daltons), Poly(vinyl alcohol) (PVA; molecular weight: 31,000-60,000), urethane (analytical grade), chlorpromazine, trifluoroacetic acid (HPLC grade) and Dulbecco's phosphate-buffered saline (DPBS) were obtained from Sigma-Aldrich, Mumbai, India. Analytical grade polysorbate-80, dichloromethane (DCM), diethyl ether, mannitol, potassium dihydrogen orthophosphate, nystatin and HPLC grade methanol, acetonitrile and ammonium acetate were supplied by SD Fine-Chem Limited, Mumbai, India. Analytical grade dimethyl sulfoxide (DMSO), glacial acetic acid, perchloric acid, liquid ammonia, methyl cellulose (molecular weight: 14000 Daltons), sodium hydroxide, sodium citrate and sodium chloride were procured from SRL Chemicals Ltd., Mumbai, India.

Table 5.1: Experimental trials generated and the values of the responses obtained in Box-Behnken design for TDF loaded PLGA NPs.

Run	Critical factors			Response	
	Polymer amount (mg, X_1)	Concentration of stabilizer (%, X_2)	Ultrasonication time (min, X_3)	PS (nm, Y_1)	EE% (%, Y_2)
1	160	4	1	279	61
2	120	4	3	219	57
3	120	4	3	217	55
4	120	2	5	231	35
5	120	4	3	220	54
6	120	6	1	273	53
7	120	2	1	261	28
8	120	4	3	215	60
9	80	2	3	220	15
10	80	4	1	234	32
11	160	4	5	264	55
12	160	2	3	271	47
13	160	6	3	283	64
14	120	6	5	267	56
15	80	6	3	251	47
16	80	4	5	212	44
17	120	4	3	222	57

5.2.2 Experimental design

The critical factors that impact the preparation of TDF loaded PLGA NPs were determined by evaluating the individual effects of the formulation and process related factors involved in the preparation of these NPs on their PS and EE%. This was performed with the help of a low-resolution Plackett-Burman Design (PBD). A two level design was employed with ten numeric factors and one categoric factor for the screening and identification of critical factors. The various factors studied were as follows: Polymer amount (75 and 200 mg), volume of co-

solvent (0.3 and 1 mL), volume of DCM (5 and 15 mL), volume of stabilizer solution (60 and 160 mL), concentration of stabilizer (1% and 5% *w/v*), type of stabilizer (polysorbate-80 and PVA), homogenization speed (5000 and 20000 rpm), duration of homogenization (5 and 15 min), amplitude of ultrasonication (40% and 70%), ultrasonication time (1 and 5 min) and temperature of stabilizer solution (25 and 40 °C).

This was followed by employing a high-resolution Box-Behnken Design (BBD) to the critical factors that were identified from the initial screening design (PBD). BBD is a type of response surface methodology which comprised of 17 runs evaluated at 3 levels with 5 centre points (to check for reproducibility) as described in table 5.1. It evaluates the interaction effects of the critical factors (polymer amount – X_1, concentration of stabilizer – X_2 and ultrasonication time – X_3) on the responses (PS – Y_1 and EE% – Y_2) by constructing second order polynomial equation which was of the following form:

$$Y_i = b_0 + b_1X_1 + b_2X_2 + b_3X_3 + b_{11}X_1^2 + b_{22}X_2^2 + b_{33}X_3^2 + b_{12}X_1X_2 + b_{13}X_1X_3 + b_{23}X_2X_3$$

Where, Y_i is the response, b_i's and b_{ii}'s (i = 1, 2 and 3) are coefficients of individual linear and quadratic effects respectively and b_{ij}'s (i, j = 1, 2 and 3; i < j) are coefficients of the effect of the interaction between i^{th} and j^{th} parameter and b_0 is the intercept value.

Table 5.2: Range of critical factors (i.e. minimum and maximum values) and the criteria set for responses in Box-Behnken design for TDF loaded PLGA NPs.

Factor	**Levels used**		
	–1	0	+1
Independent factors			
X_1 – Polymer amount (mg)	80	120	160
X_2 – Concentration of stabilizer (%)	2	4	6
X_3 – Ultrasonication time (min)	1	3	5
Dependent factors		**Constraints**	
Y_1 – PS (nm)		Minimize	
Y_2 – EE% (%)		Maximize	

Finally, the desirability function was used by deciding the 'goals' of the responses (table 5.2) to obtain the optimized formulation. The above optimization process was performed with the help of Design Expert software (version: 10.0.3.1, Stat-Ease Inc., MN, USA).

5.2.3 Preparation of TDF loaded PLGA NPs

The preparation of TDF loaded PLGA NPs (represented schematically in fig. 5.2) was based on the procedure published by Cheow et al. (2010) which involved the emulsification of an immiscible phase in an aqueous phase followed by solvent evaporation of the immiscible phase. Briefly, PLGA (amount varied as per the experimental design) was dissolved in a specified quantity of DCM (as per the experimental design). Further, 30 mg of TDF was dissolved in methanol (volume varied as per the experimental design). Subsequently, the drug solution was added to the polymer solution under stirring. This mixture of drug and polymer solution was then emulsified in a specific volume of aqueous phase (as per the experimental design) under homogenization (rpm varied as per the experimental design) using a high-speed homogenizer (Polytron PT 3100D, Kinemetica, Lucerne, Switzerland). The aqueous phase contained a variable amount of stabilizer (as per the experimental design). The formed emulsion was ultrasonicated with the help of probe sonicator at a specified amplitude and duration. A dispersion containing TDF loaded PLGA NPs was obtained which was washed and centrifuged to remove the free drug. The washed TDF loaded PLGA NPs were re-suspended in water and stored at –80 °C for 48 h. This was followed by freeze–drying the NPs in a lyophilizer (Coolsafe 110-4, Scanvac, Lynge, Denmark) for which 3% *w/v* of mannitol was used as a cryoprotectant. The lyophilized powder was stored in air tight glass vials until further use. Additionally, PLGA NPs without incorporating TDF were also prepared by following a similar procedure which acted as blank PLGA NPs.

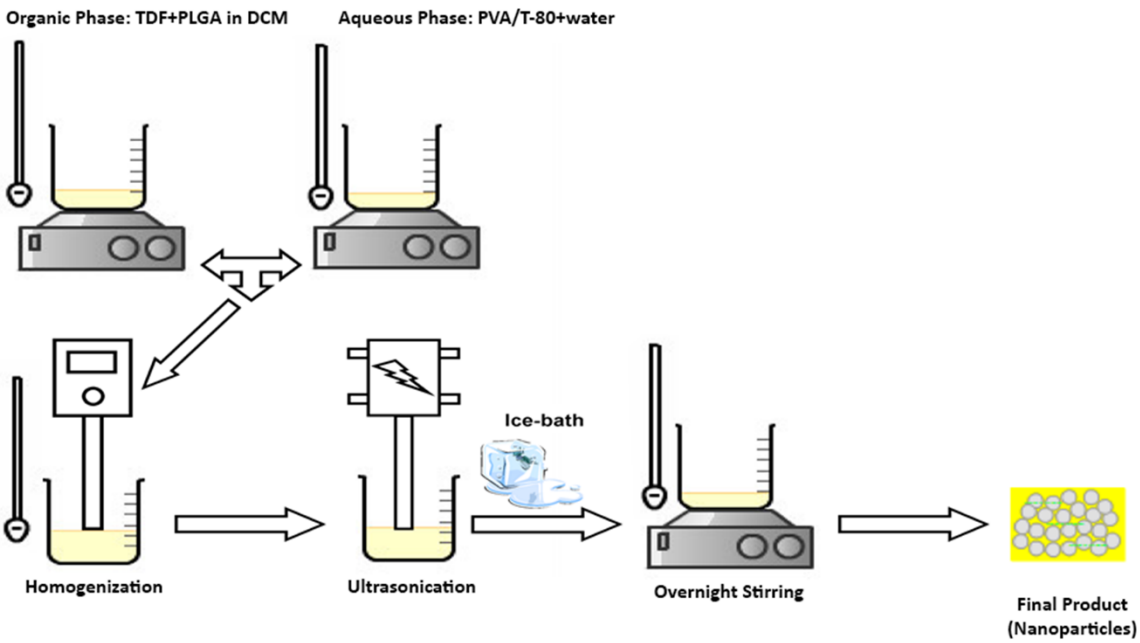

Fig. 5.2: Schematic representation of the preparation method for TDF loaded PLGA NPs.

5.2.4 Characterization studies

5.2.4.1 PS and zeta potential

Zetasizer nano ZS (Malvern Instruments Ltd., Worcestershire, UK) was used to measure the PS, polydispersity index (PDI) and zeta potential of the NPs. The backscattering angle was set to 173° and the samples were analysed at a temperature of 25 °C.

5.2.4.2 Entrapment efficiency (EE%)

The EE% was determined based on the previously reported work (Yue et al., 2009). Briefly, 500 µL of freshly prepared TDF loaded PLGA NPs dispersion was transferred into microfilters (Amicon Ultra, Millipore, MA, USA; molecular weight cut-off (MWCO), 10 KDa). These filters were centrifuged at 7500 × g which led to the diffusion of unentrapped TDF into the filtrate while the TDF entrapped in the NPs was present in the microfilter. This filtrate was analyzed by HPLC and EE% was determined using the following equation:

$$EE\% = \frac{W_{total\,TDF} - W_{free\,TDF}}{W_{total\,TDF}} \times 100$$

5.2.4.3 Scanning electron microscopy (SEM) analysis

The morphology of the TDF loaded PLGA NPs was determined with the help of SEM (Carl Zeiss MERLIN Compact, Oberkochen, Germany). 100 µL of TDF loaded PLGA NPs was placed on an aluminum stub and dried under vacuum. The dried sample was sputtered with gold (Q 150T ES, Quorum Technologies, Laughton, UK) which was then placed in vacuum and imaged at an acceleration voltage of 3 kV.

5.2.4.4 Differential scanning calorimetry (DSC)

Differential scanning calorimetry (DSC 60; Shimadzu Corporation, Kyoto, Japan) was used to perform the calorimetric analysis of various samples. Briefly, a defined amount of each sample was transferred into aluminum pans and crimp sealed. The instrument was equilibrated at 30 °C and the thermograms were obtained in an inert environment over a temperature range of 30 °C to 400 °C at a heating rate of 10 °C/min.

5.2.4.5 Powder X-ray diffraction (pXRD) studies

The pXRD study was carried with Rigaku, Ultima IV diffractometer (Texas, USA). The samples were illuminated with a Ni-filtered Cu-K_α radiation (λ = 1.54 Å) at a voltage of 40 kV and a 2θ range of 10-70° at the rate of 1 degree/min.

5.2.5 Stability of TDF loaded PLGA NPs

The guidelines of the international council of harmonization (ICH) Q1A (R2) were followed to evaluate the stability of TDF loaded PLGA NPs (Food and Drug Administration, HHS, 2003). The freeze-dried samples of the optimized TDF loaded PLGA NPs were transferred into glass vials (n = 3) which were sealed and stored at accelerated conditions i.e. at a temperature

of 25 ± 2 °C and a relative humidity (RH) of 60 ± 5% for 3 months in RH chambers (Remi, Mumbai, India). The corresponding control samples were stored at 2-8 °C. Samples were collected at a monthly interval and characterized for PS, zeta potential, PDI and EE%.

5.2.6 In vitro drug release and kinetics

The dialysis bag method as reported by Singh et al. (2007) was followed to evaluate the *in vitro* release profile of free TDF and its NPs. Free TDF and TDF loaded PLGA NPs (equivalent to 1 mg of TDF) was taken in a dialysis bag (MWCO: 12–14 kDa; pore size: 2.4 nm), which was then sealed and transferred into a beaker containing 50 mL of phosphate buffer solution (pH of 5.2). A uniform temperature of 37 °C was maintained with a stirring speed of 100 rpm. A 1 mL sample was withdrawn at defined time intervals from the dissolution media with a syringe fit to a filtration unit (PVDF membrane of 33 mm diameter having a pore size of 0.1 µm) which was analysed with HPLC. The dissolution media was replenished by backwashing the filter with 1 mL of pH 5.2 buffer. The data obtained after the sample analysis were fit into different mathematical models derived for drug release (Barzegar-Jalali et al., 2008) and the model that best describes the release profile of TDF based on the regression coefficient (R^2) values was identified. The time taken for 50% of drug release ($T_{50\%}$) was calculated using the best-fit model. The equations of the models used to fit the drug release data are shown in table 5.3.

Table 5.3: Equations and values of the model parameters and regression for different release kinetic models used to fit the *in vitro* release data of TDF loaded PLGA NPs.

Model	Equation	Model parameters	Regression (R^2)
Zero order	$F = K_0t$	$K_0 = 1.53$	0.7707
First order	$\ln (1 - F) = -K_ft$	$K_f = 0.2339$	0.9114
Higuchi	$F = K_H\sqrt{t}$	$K_H = 0.1243$	0.9440
Reciprocal powered time	$1/F - 1 = m/t^b$	b = 0.9362; m = 8.48	0.9942
Korsmeyer-Peppas	$M_t/M_\infty = Kt^n$	n = 0.1175; K = 0.21	0.9569

'F' is the fraction of drug released up to time 't'; 'K_0', 'K_f', 'K_H', 'm' and 'b' are model parameters. 'Mt' is amount of drug released at time 't', 'M_∞' is the amount of drug released at infinite time, 'K' is the release kinetics constant and 'n' is the exponent of release.

5.2.7 Cytotoxicity studies

MTT (3-(4,5-Dimethylthiazol-2-yl)-2,5-diphenyltetrazolium bromide) dye was used to evaluate the cytotoxicity of TDF loaded PLGA NPs in RAW 264.7 cell lines (mouse monocyte-macrophages). Briefly, microtitre plates containing 10,000 cells/well were incubated for 24 h at 37 °C with 5% CO_2 and 95% O_2 and 100% RH. All the treatment groups were prepared at three different concentration levels i.e. 0.1, 1 and 10 µM by adding appropriate aliquots of samples to each the microtitre plates. A set of wells to which no sample was added acted as control whereas, the group of wells to which triton X-100 was added acted as a positive control. The treated and untreated wells were incubated for 24 h and then spiked with 10 µL of 10 mg/mL of MTT and incubated for 2 h at 37 °C which allowed the formation of the formazan crystals. After the formation of the formazan crystals, the media was removed and the bound formazan crystals were dissolved in 200 µL of DMSO and the absorbance was measured at a wavelength of 560 nm in a microplate reader (Spectramax M2e, Molecular Devices, CA, USA). The cell viability was determined by comparing the absorbance of the treated cells with the control. The study was done in pentaplicates (n = 5).

5.2.8 Stability of TDF in mucosal homogenates of rats

The intestinal washings containing mucosal homogenates of the rat were collected based on the works of Crauste-Manciet et al. (1997) and Li et al. (2007). Briefly, male Wistar rats (n = 5) were fasted overnight and on the day of the experiment, the rats were anesthetized and then dissected to separate the small intestine. The rats were then sacrificed by cervical dislocation. The small intestine was washed with 1 mL of pH 7.0 phosphate buffer and these intestinal washings were pooled and the volume was made up to 7 mL. 100 µL of this intestinal washing was spiked with 100 µL of either 5 µM TDF solution or TDF loaded PLGA NPs or a physical mixture of TDF and PLGA (50:50 equivalent to 5 µM of TDF). Additionally, to check for the interference of the matrices during the analysis, control samples were prepared for each of the treatment groups. All the samples were estimated for TDF and TMF. The reaction was

terminated after 30 min by adding 200 µL of acetonitrile and the samples were stored at –20 °C until analysis. This study was performed with six replicates (n = 5) for each treatment condition.

5.2.9 Everted gut sac studies in rats

Male Wistar rats were fasted overnight and on the day of the experiment, the rats were anesthetized (1.2 g/kg of urethane I.P.) after which laparoscopy was performed to isolate the intestine. The jejunal part of the intestine was isolated, washed with 0.9% *w/v* of NaCl and divided into segments of each having a length of 7.0 – 8.0 cm. Each segment was then gently everted with the help of a glass rod, tied at one end, filled with 750 µL of DPBS buffer through the other end and tied to form a sac. This everted sac was kept in a reservoir containing DPBS buffer maintained at 37 °C and oxygenated with 95%/5% of CO_2/O_2.

The reservoirs contained either 20 mM of free TDF or TDF loaded PLGA NPs (equivalent to 20 mM of TDF). Everted gut sac studies were conducted at 4 °C and also in the presence of specific endocytic inhibitors i.e. either with chlorpromazine (10 µg/mL) or nystatin (25 µg/mL) so as to discern the mechanism of uptake of free TDF and TDF loaded PLGA NPs. The blanks for the corresponding samples were also prepared to check for interference in the HPLC analysis. The incubation time was set to 60 min after which the contents were collected from both outside the everted gut sac (donor compartment) and within the everted gut sac (receiver compartment) and stored at –20 °C until analysis. The samples were analysed with a validated HPLC method. The study was done in triplicates for each treatment condition (n = 3).

5.2.10 In vivo pharmacokinetic studies

The single-dose pharmacokinetic studies were performed on male Wistar rats. The rats were housed at 22 ± 1 °C and 50 ± 10% RH. The protocol for this study was approved by the institutional animal ethics committee (IAEC) of BITS-Pilani, Hyderabad campus (IAEC No.:

IAEC–02/01–14). Prior to the day of the experiment, the rats were kept for fasting overnight with free access to water till 4 h post dosing on the day of the experiment.

For each pharmacokinetic study, five rats were used (n = 5). For the intravenous (IV) pharmacokinetics of free TDF, the rats were administered with 22 mg/kg of TDF (equivalent to 10 mg/kg of TNF) solution through the tail vein and the blood samples were collected at predose, 0.08, 0.17, 0.25, 1, 2, 3, 4 h. For the oral pharmacokinetics of free TDF, the rats were administered with 100 mg/kg of TDF (suspended homogeneously in an aqueous solution 0.5% *w/v* methyl cellulose) with an oral feeding gavage. The blood samples were collected at predose, 0.25, 0.5, 0.75, 1, 1.25, 1.5, 2, 4, 6 and 8 h. Further, TDF loaded PLGA NPs equivalent to 100 mg/kg of TDF was administered orally to rats and the blood samples were collected at predose, 0.25, 0.5, 1, 1.5, 2, 4, 6, 8, 10, 12 and 18 h. Plasma was harvested from the collected blood samples by centrifuging the samples at 905 × g for 10 min and then stored at –80 °C until analysis. The plasma samples were processed suitably and analysed with validated HPLC method.

5.2.11 Sample pretreatment and analysis

The samples obtained from *in vitro* stability in mucosal homogenates, *ex vivo* everted gut studies and *in vivo* pharmacokinetic studies were processed as per the previously published protocol (P.R. Ravi, Joseph, Avula, & Anthireddy, 2015). Briefly, to a 100 µL sample, 10 µL of trifluoroacetic acid (13 M), 15 µL of 35% *v/v* perchloric acid and 400 µL of acetonitrile and vortexed it for 30 s. The vortexed samples were centrifuged at 7800 × g at 4 °C for 15 min. The supernatant was collected and the acids present were neutralized partially with 10 µL of ammonium hydroxide (14.8 M). The partially neutralized samples were evaporated under a gentle stream of nitrogen gas at 40 °C and the dried residue was reconstituted with 100 µL of pH 4 ammonium acetate buffer and analyzed using HPLC with a PDA detector.

The analytical method used for analysis was developed and validated in-house in which a Spincotech C18G enabled column (250 × 4.6 mm, 5 µm, Spinco Biotech Pvt Ltd, TN, India) was used. The mobile phase used comprised of 10 mM ammonium acetate buffer (pH 4.0 ± 0.1) and methanol in the ratio of 97:3 *v/v* for the estimation of TNF, 70:30 *v/v* for the estimation of TMF and 50:50 *v/v* for the estimation of TDF. The flow rate was 1 mL/min, the injection volume was set to 50 µL and the samples were monitored at a wavelength of 260 nm.

5.2.12 Data analysis

The data obtained from the experimental studies were represented in terms of mean ± standard deviation (SD). The statistical significance between the experimental groups was determined with the help of analysis of variance (ANOVA) followed by Bonferroni's multiple comparison test using GraphPad prism software (version 6.01, GraphPad Software, Inc., CA, USA). The significance level was set at 5% (P_{crit}), and the calculated *P* value (P_{cal}) was also determined. The pharmacokinetic data was analyzed with the non-compartmental model by using Phoenix WinNonlin® software (version 7.00, Pharsight Corporation, CA, USA).

5.3 Results and discussion

5.3.1 Evaluation of individual effects with PBD

Individual effects of different formulation and process related factors on the PS and EE% of TDF loaded PLGA NPs were tested with the help of low-resolution PBD. Among the factors tested, we found that polymer amount, concentration of stabilizer and the ultrasonication time had a significant impact on the PS. Whereas, polymer amount, concentration of stabilizer, the ultrasonication time and type of stabilizer used had a significant impact on the EE%. Further, there was a close agreement between predicted and adjusted R^2 values. The *F* values for PS (of 36.5; $P_{cal} < 0.0001$) and EE% (20.6; $P_{cal} < 0.0001$) were found to be statistically significant for

the model. Hence, the results obtained from ANOVA shows that the model was statistically valid for the given data.

In the experimental trials involving the type of stabilizer – polysorbate 80 and PVA were used. It was observed that the EE% was higher with PVA when compared to polysorbate 80. This could be attributed to the higher saturation solubility of TDF in polysorbate-80 (33.61mg/mL at 1% *w/v* concentration) when compared to PVA (19.45 mg/mL at 1% *w/v* concentration). The higher saturation solubility leads to a higher partition of the drug to the aqueous phase from the internal phase leading to a decrease in the EE%.

Table 5.4: ANOVA–partial sum of squares analysis of the responses in Box-Behnken design for TDF loaded PLGA NPs.

Source	**PS (Y_1)**				**EE% (Y_2)**			
	Sum of Squares	df	F Value	P_{cal}	Sum of Squares	df	F Value	P_{cal}
Model	10645.29	9	145.38	< 0.0001*	2850.60	9	64.35	< 0.0001*
X_1	4050.00	1	497.80	< 0.0001*	990.12	1	201.18	< 0.0001*
X_2	1035.12	1	127.23	< 0.0001*	1128.1	1	229.22	< 0.0001*
X_3	666.12	1	81.87	< 0.0001*	32.00	1	6.50	0.0381*
X_1X_2	90.25	1	11.09	0.0125*	56.25	1	11.42	0.0117*
X_1X_3	12.25	1	1.50	0.2594#	81.00	1	16.45	0.0048*
X_2X_3	144.00	1	17.69	0.0040*	4.00	1	0.81	0.3972#
X_1^2	761.69	1	93.62	< 0.0001*	73.39	1	14.91	0.0061*
X_2^2	2465.85	1	303.08	< 0.0001*	354.44	1	72.02	< 0.0001*
X_3^2	972.80	1	119.57	< 0.0001*	82.44	1	16.75	0.0046*
Residual	56.95	7			34.45	7		
Lack of fit	27.75	3	1.267	0.3982#	13.25	3	0.83	0.5412#
Pure error	29.20	4			21.20	4		
Total	10702.2	16			2885.1	16		

*significant at $\alpha < 0.05$; #not significant at $\alpha \geq 0.05$

In the optimization of process using BBD, the non-critical factors were set to constant values which were as follows: the volume of co-solvent – 500 µL; volume of DCM – 10 mL; volume of stabilizer solution – 60 mL; homogenization speed – 10000 rpm; duration of homogenization – 5 min; the amplitude during ultrasonication – 40%; and the temperature of the stabilizer

solution was 25 °C during evaporation. PVA was used as a stabilizer for the formed dispersion of TDF loaded PLGA NPs.

5.3.2 Box-Behnken design

5.3.2.1 Effect of critical factors on PS

The least square second order polynomial equation depicting the relationship between the selected critical factors taken up for the optimization process and PS is as follows:

$$PS\ (Y_1) = 218.60 + 22.50X_1 + 11.38X_2 - 9.13X_3 - 4.75X_1X_2 + 1.75X_1X_3 + 6.00X_2X_3 + 13.45X_1^2 + 24.20X_2^2 + 15.20X_3^2$$

The *F* value (145.38) for the quadratic model was found to be statistically significant (P_{cal} < 0.0001) and the R^2 value was 0.9947 (showing a good correlation for the data). The *F* value (1.27) for the lack of fit was found to be statistically insignificant (P_{cal} = 0.3982). All the terms except for X_1X_3 interaction term had a significant effect on PS. The distribution of residuals seemed to be random around zero and there was no apparent effect of the sequence of the trial on the distribution of residuals. These indicators show the statistical validity of the model (table 5.4). In the experimental trials, maximum PS was observed in the 13th trial with a PS of 283 nm and minimum PS was observed in the 16th trial with a PS of 212 nm.

For a given ultrasonication time, the PS increased linearly with increase in the polymer amount (fig. 5.3a). The increase in the PS is attributed to the increased viscosity of the organic solvent with increasing polymer amount. Emulsions with higher viscosities decrease the cavitation of the ultrasonic waves and also reduces the shear capacity of the homogenizer, thereby preventing the decrease in PS (Murakami, Kobayashi, Takeuchi, & Kawashima, 1999; Quintanar-Guerrero, Fessi, Allémann, & Doelker, 1996). However, the concentration of stabilizer in the aqueous phase did not have a linear impact on the PS (fig. 5.3a and 5.4a). There was a decrease in the PS with an increase in stabilizer concentration up to 4% *w/v* and as the

concentration was increased from 4% to 8% *w/v* the PS increased. The initial decrease in PS is attributed to the decreased interfacial tension between the immiscible organic and aqueous phases which reduces the globule size thereby decreasing the PS of the NPs. But, at higher stabilizer concentration (i.e. 4-8% *w/v*) the hydrophobic interactions of the stabilizer molecules (adhered on the surface of the NPs) with organic phase might increase to a critical level that causes agglomeration of the formed NPs (Feng & Huang, 2001). Further, a slightly negative interaction effect between the polymer amount and stabilizer concentration (X_1X_2) was observed.

For a given polymer amount, the ultrasonication time had an inverse relationship with PS which could be attributed to the higher amount energy supplied to the system leading to a reduction of PS of the PLGA NPs (Mainardes & Evangelista, 2005). A positive interaction effect between the stabilizer concentration and ultrasonication time (X_2X_3) was observed (fig. 5.3b and 5.4b).

5.3.2.2 Effect of critical factors on EE%

The least square second order polynomial equation for the coded values showing the relationship between the selected factors for BBD and EE% is as follows:

$$EE\%\ (Y_2) = 56.60 + 10.75X_1 + 11.88X_2 + 1.63X_3 + 3.75X_1X_2 + 3.75X_1X_3 - 1.00X_2X_3 - 3.80X_1^2 - 9.55X_2^2 - 4.05X_3^2$$

The quadratic model for EE% was found to be statistically significant (table 5.4), as the *F* value was 64.35 which was significant at $P_{cal} < 0.0001$ and R^2 was higher (0.9880 indicating good correlation). Additionally, the *F* value (0.83) of lack of fit was not significant ($P_{cal} = 0.5412$). The difference of predicted R^2 and adjusted R^2 was less than 0.2 indicating a good agreement between these values. The distribution of residuals were random around zero and there was no apparent effect of the sequence of the trial on the distribution of residuals. In the trials conducted the highest EE% was 64% for the 13th experimental trial and the lowest EE% was

15% for the 9th run. The observations from the responses of the experimental trials indicated that except for X_2X_3 interaction term changes in the levels of the remaining factors had a significant impact on the EE%.

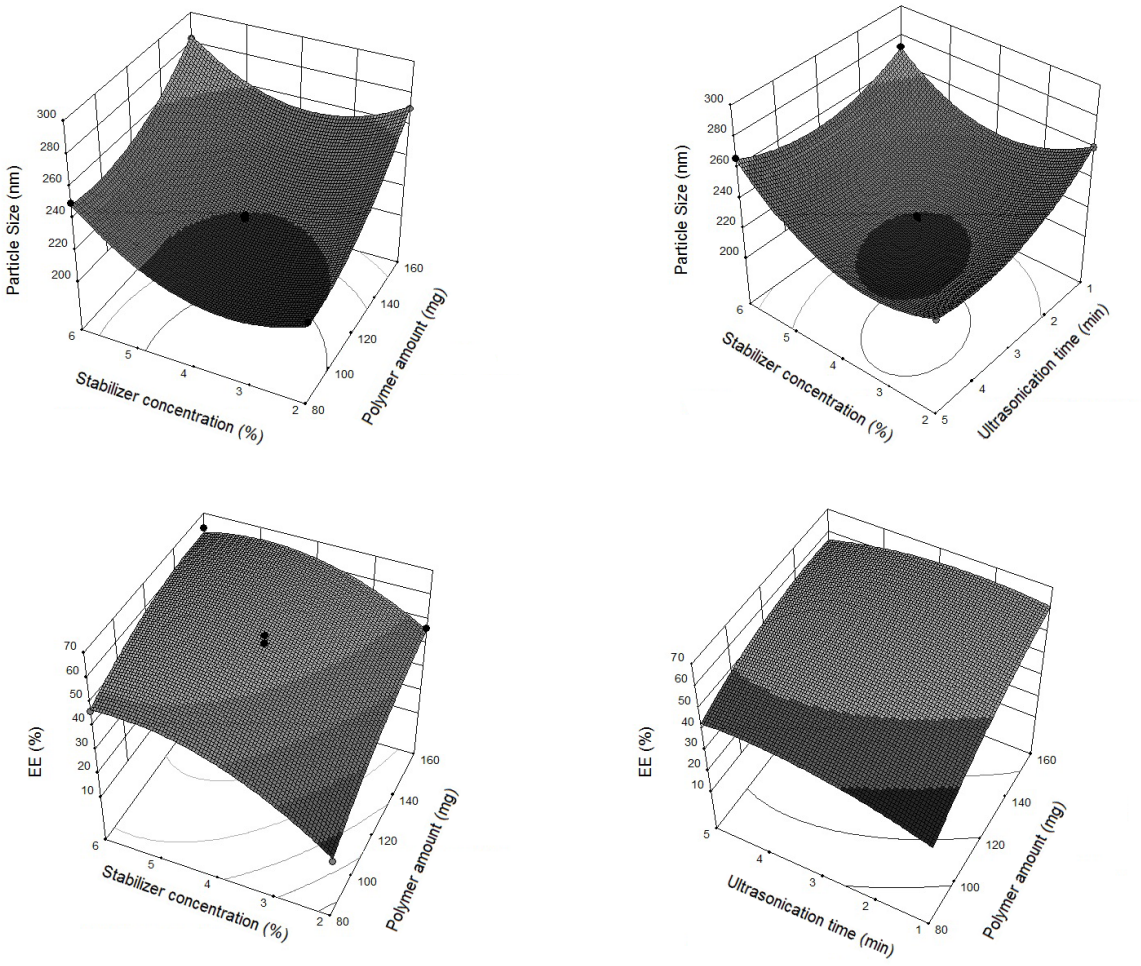

Fig. 5.3: Response surface plot depicting the interaction effect between (a) polymer amount and stabilizer concentration on particle size; (b) stabilizer concentration and ultrasonication time on particle size; (c) polymer amount and stabilizer concentration on EE%; (d) polymer amount and ultrasonication time on EE%.

For a given ultrasonication time, an increase in the polymer amount increased the EE% (fig. 5.3c and 5.4c), this is because, the chances of the entrapment of TDF in the polymer matrix increases. Further, an increase in the stabilizer concentration increased the EE% of TDF. PVA is a stearic stabilizer and a polymer, therefore, as the PVA concentration increases the viscosity increases. This slows down the diffusion of TDF from the internal phase to the external phase leading to a higher entrapment of TDF in the polymeric matrix (Punna Rao Ravi, Aditya,

Kathuria, Malekar, & Vats, 2014). An additional contributing factor could be that an increasing concentration of PVA did not increase the solubility of TDF thus preventing an excess diffusion of TDF into the aqueous phase that could happen when the solubility is increased. There was a positive interaction effect observed between these two factors (X_1X_2).

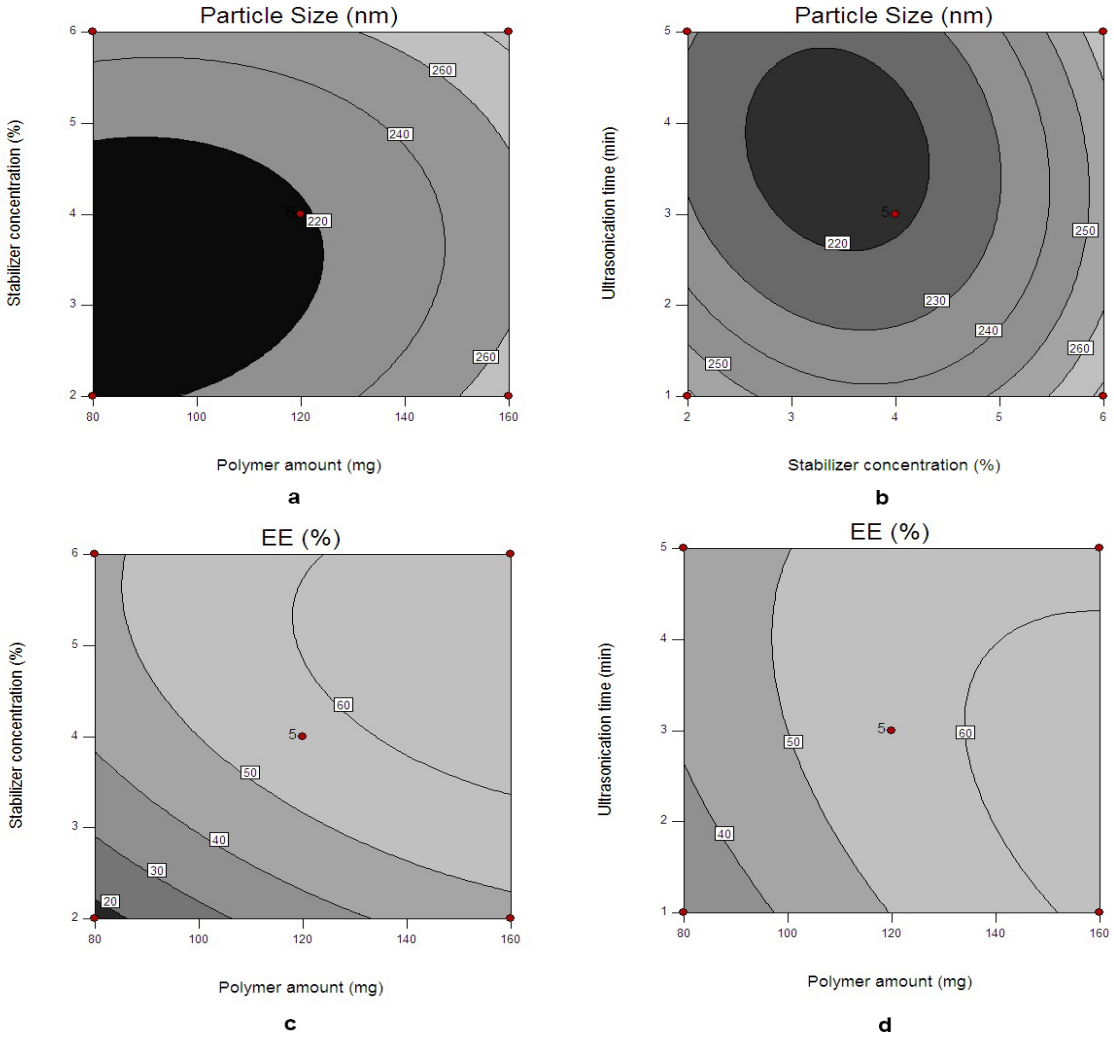

Fig. 5.4: Contour plot depicting the interaction effect between (a) polymer amount and stabilizer concentration on particle size; (b) stabilizer concentration and ultrasonication time on particle size; (c) polymer amount and stabilizer concentration on EE%; (d) polymer amount and stabilizer concentration on EE%.

For a given stabilizer concentration, the ultrasonication time had a mildly positive impact on the EE%. This phenomenon is attributed to the increased surface area because of the formation of particles with relatively smaller size at higher ultrasonication times. Further, a slight positive

interaction effect was seen between the ultrasonication time and polymer amount (X_1X_3) on the EE% (fig. 5.3d and 5.4d).

5.3.2.3 Determination of optimized formulation and its validation

Desirability function value for the optimized formulation was high (0.902). The criteria set for the responses for obtaining the optimized formulation was to minimize PS and maximize EE%, but, the upper and lower limits were set as the maximum and minimum values observed during the experimental trials. The optimal conditions of the critical experimental factors generated based on the developed quadratic model by the software were as follows: polymer amount – 117 mg; stabilizer concentration – 4.3% w/v; ultrasonication time – 3.5 min. In order to check the validity of the model for the optimized formulation, verification runs (n = 6) were carried out. Wilcoxon signed rank test was performed to evaluate the statistical difference between the observed and predicted values at α = 0.05. However, there was no significant difference observed for both the responses i.e. PS (P_{cal} = 0.3125) and EE% (P_{cal} = 0.4375) indicating the validity of the statistical model. The optimized formulation had a PS of 218 ± 3.85 nm and an EE% of 57.3 ± 1.6%.

5.3.3 Characterization studies

The optimized TDF loaded PLGA NPs had a PS and PDI of 218 ± 3.85 nm and 0.23 ± 0.02 respectively (n = 6). The lower PDI values indicate the formation of stable NPs with a narrow PS distribution. The zeta potential of the optimized NP formulation was –4.8 ± 1.2 mV. The EE% of TDF in the optimized PLGA NPs was 57.3 ± 1.6%. The SEM image of the TDF loaded PLGA NPs is shown in fig. 5.5, the NPs were nearly spherical in shape with a smooth surface.

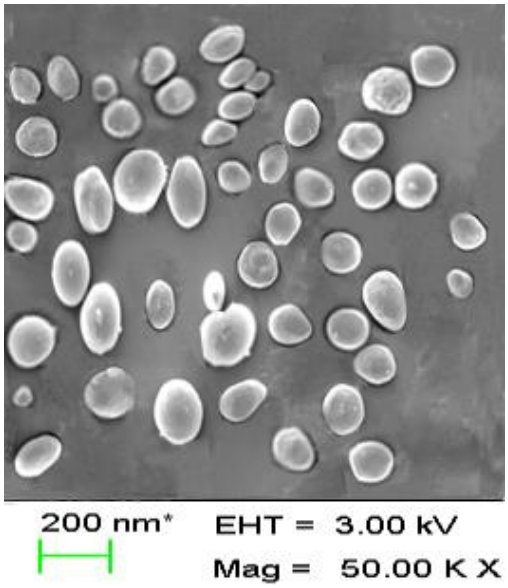

Fig. 5.5: SEM image of TDF loaded PLGA NPs.

The DSC thermograms of free TDF, bulk PLGA, physical mixture of TDF and PLGA in the ratio of 1:1, blank PLGA NPs and TDF loaded PLGA NPs are depicted in fig. 5.6. A sharp endothermic peak at 117 °C was observed for TDF corresponds to the melting point for free TDF. The bulk PLGA had an endothermic peak at 60 °C which is a relaxation peak attributed to the glass transition of PLGA and no other endothermic peak was observed due to the amorphous nature of PLGA (Dillen, Vandervoort, Van den Mooter, Verheyden, & Ludwig, 2004). In the DSC thermograms of the physical mixture of TDF and PLGA, there was no observable shift of the characteristic peak positions of PLGA and TDF. In blank PLGA NPs and TDF loaded PLGA NPs, a sharp endothermic peak was observed at 163 °C corresponding to the presence of mannitol which added as a cryoprotectant during freeze drying of NPs. The absence of endothermic peak of TDF in the TDF loaded PLGA NPs could indicate the entrapment of TDF in the amorphous state within the matrix of PLGA NPs.

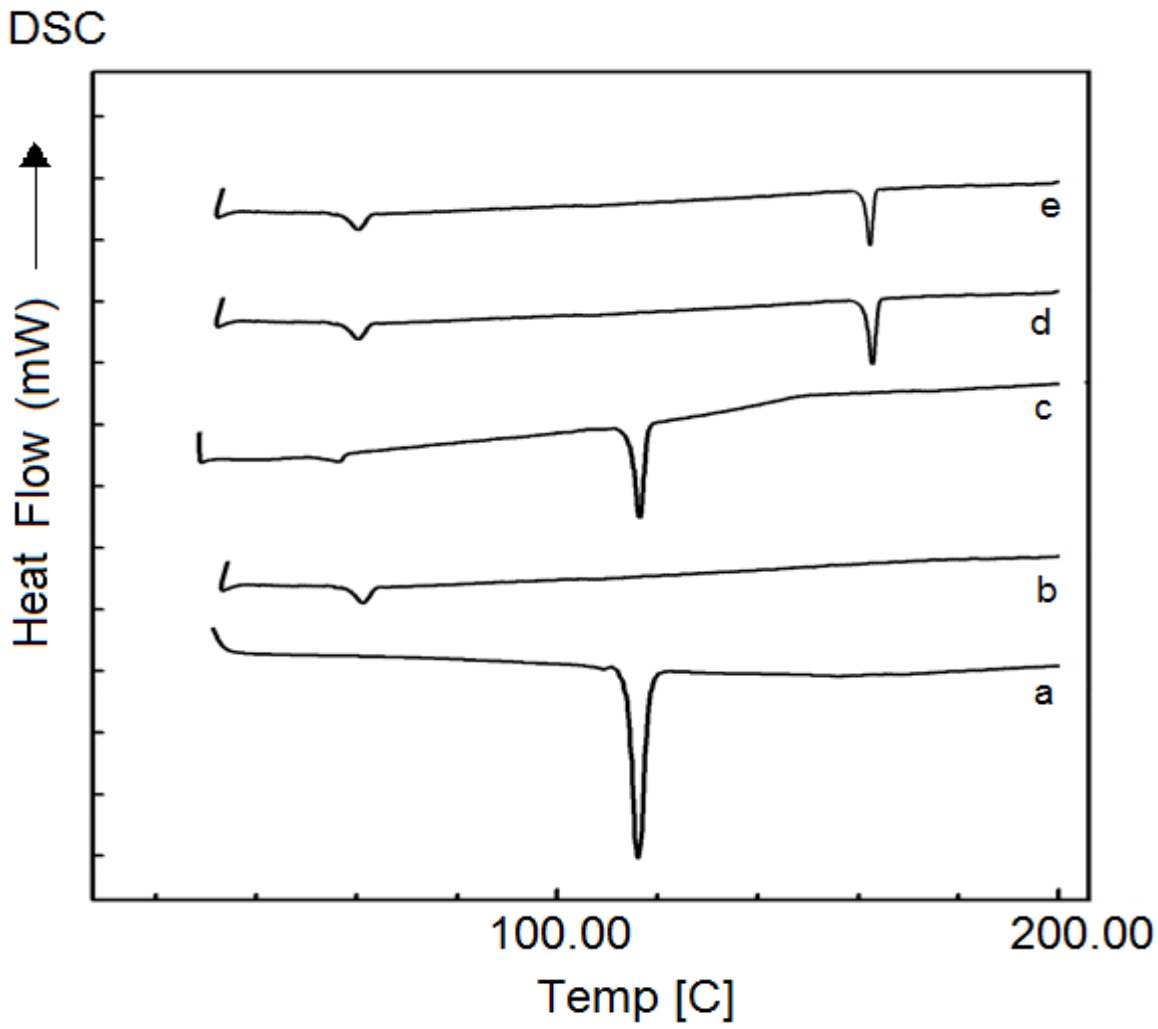

Fig. 5.6: DSC thermograms of (a) free TDF; (b) bulk PLGA 50:50; (c) physical mixture of TDF and PLGA 50:50 (PM); (d) blank PLGA NPs; (e) optimized TDF loaded PLGA NPs.

The pXRD graphs of free TDF, PLGA, physical mixture of TDF and PLGA in the ratio of 1:1, blank PLGA NPs and TDF loaded PLGA NPs are shown in fig. 5.7. The characteristic crystalline peaks of TDF at 2θ values of 18°, 20°, 22°, 25° and 30° were also present in the physical mixture of TDF and PLGA. Further, the low intensity seen in the PLGA diffractogram shows the amorphous nature of PLGA. A similar observation was made in the case of blank PLGA and TDF loaded PLGA NPs. As, the characteristic peaks of TDF were absent in TDF loaded PLGA NPs which indicates the possibility of the entrapment of TDF in amorphous form within PLGA NPs.

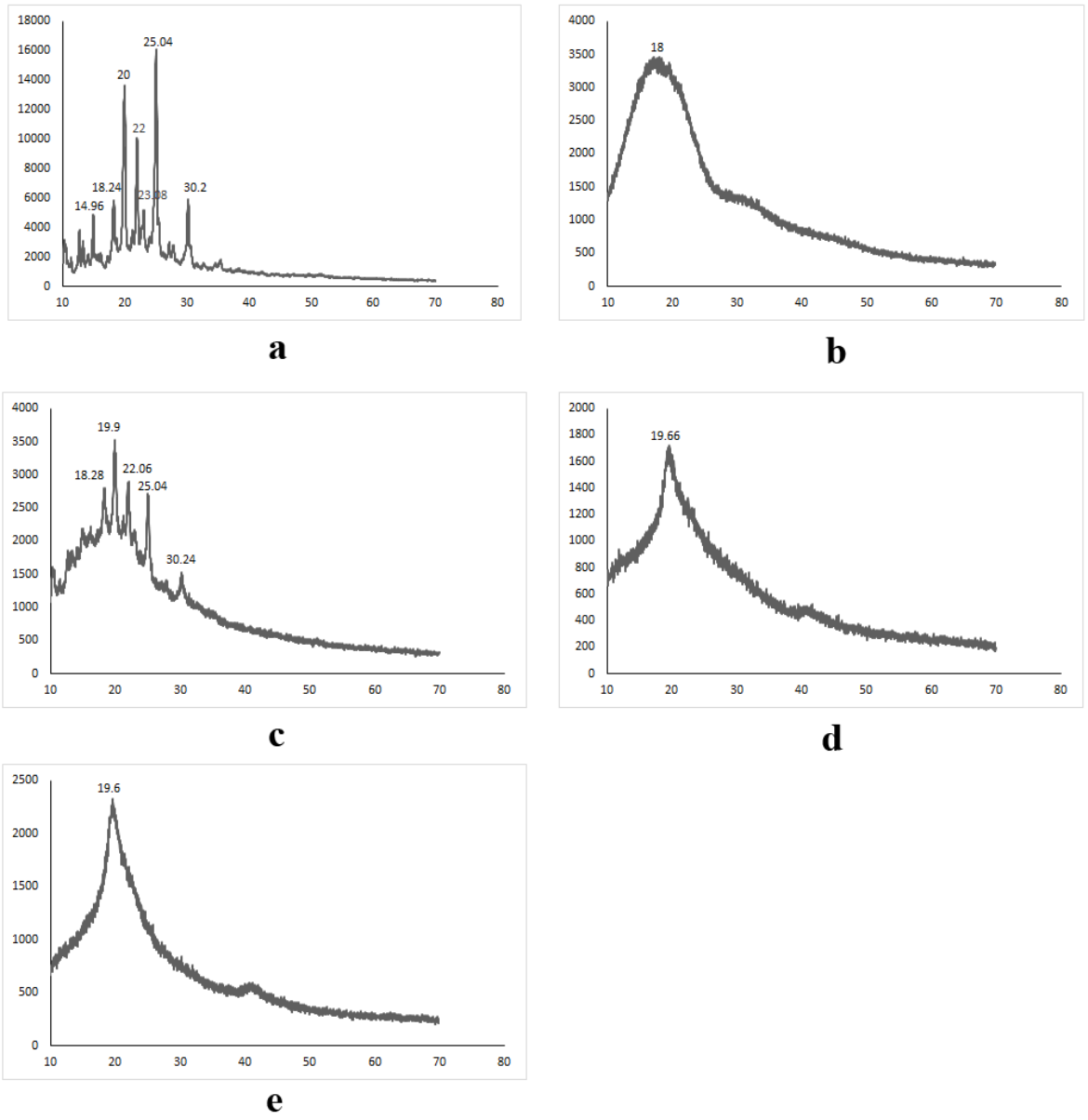

Fig. 5.7: X-ray diffractograms of (a) free TDF; (b) bulk PLGA 50:50; (c) physical mixture of TDF and PLGA 50:50; (d) blank PLGA NPs; (e) optimized TDF loaded PLGA NPs.

5.3.4 Stability of TDF loaded PLGA NPs

The results obtained from the stability studies of the freeze-dried TDF loaded PLGA NPs with 3% mannitol are shown in fig. 5.8. There was no significant change in the factors estimated (PS, EE%, zeta potential and PDI) for the NPs over three months period in accelerated conditions. A similar observation was also made for the control samples that were stored at 2-8 °C during this time period (data not shown). Therefore, these results show the stability of the designed TDF loaded PLGA NPs.

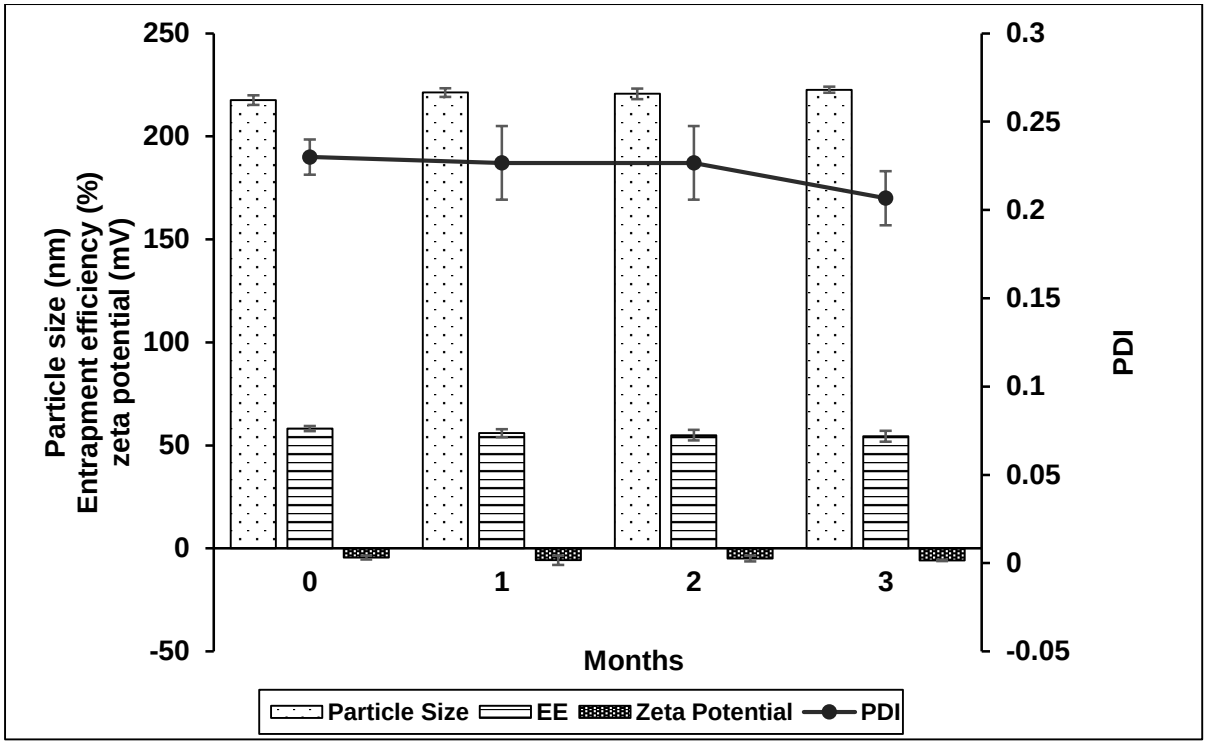

Fig. 5.8: Stability data of freeze dried TDF loaded PLGA NPs assessed by evaluating particle size (nm), EE%, zeta potential (mV) and PDI of the NPs when stored at 25 ± 2 °C and 60 ± 5% for a duration 3 months. The values are expressed in terms of mean ± SD (*n* = 3).

5.3.5 In vitro drug release and kinetics

The release kinetics of TDF loaded PLGA NPs were determined with the help of the *in vitro* release studies using the dialysis bag method. Fig. 5.9 shows the *in vitro* release profile of TDF loaded PLGA NPs and free TDF.

The release data of TDF loaded PLGA NPs was fit to different release kinetic models and the correlation coefficient and release rate constant were determined (table 5.3). It was observed that the reciprocal powered time model (R^2 = 0.9942) was the best fit for the release kinetics of TDF released from PLGA NPs. The time taken for 50% of drug release ($T_{50\%}$) determined based on this model was found to be 9.8 h. The release profile of TDF loaded PLGA NPs showed an initial burst release of 30% within 5 h which was followed by a slow and sustained release up to 48 h. Whereas, the free TDF underwent complete dissolution within 4 h.

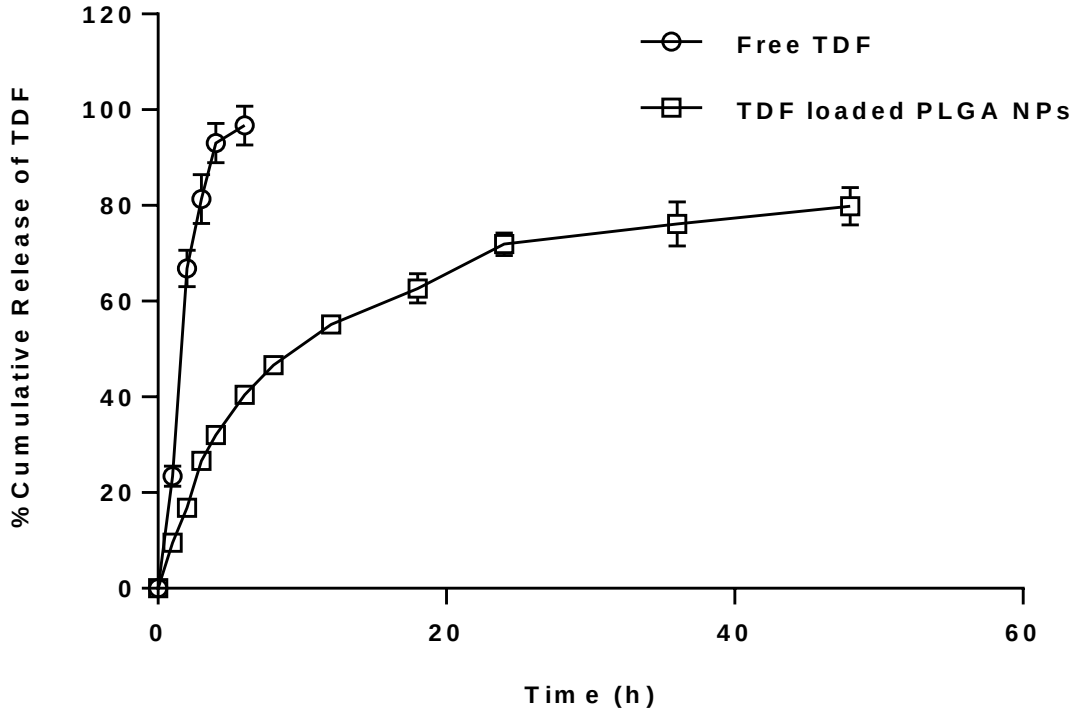

Fig. 5.9: *In vitro* release profile of free TDF and TDF loaded PLGA NPs in phosphate buffer solution (pH 5.2). Each data point is a mean ± SD (*n* = 5).

5.3.6 Cytotoxicity studies

The results of the cytotoxicity studies of the designed NPs was evaluated in terms of cell viability as shown in fig. 5.10. The study showed that for free TDF there was no significant change in the cell viability values at 0.1 µM (97.4 ± 0.90%) and 1 µM of TDF (96.1 ± 1.62%) however, a decrease in the viability of the cells was observed at 10 µM concentration (88.93 ± 1.35%). The mean values for cell viability of blank and drug loaded PLGA NPs were 98.8 ± 1.11% and 97.2 ± 1.65% at 0.1 µM, 96.4 ± 0.83% and 94.6 ± 0.85% at 1 µM, and 95.0 ± 1.53 and 94.6 ± 0.85 at 10 µM concentrations respectively. There was no significant difference in the cell viability of blank NPs at all the three concentration levels when compared to control. Additionally, even in the case of TDF loaded PLGA NPs there was no significant difference in the cell viability at 0.1 and 1 µM concentrations, however, there was a slight decrease in the

viability of the cell at 10 µM concentration. This shows the non-cytotoxic nature of the designed NPs as toxicity was present at high concentrations of drug loaded NPs.

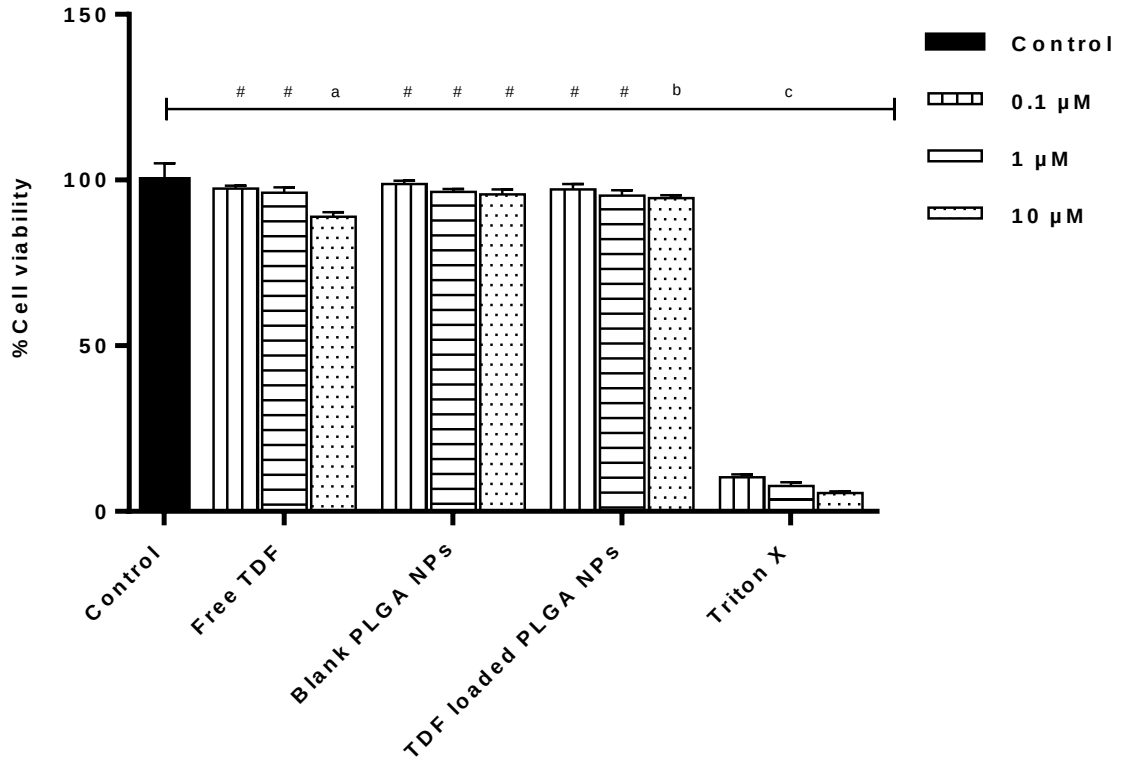

Fig. 5.10: Cell viability (%) of RAW 264.7 cells in the presence of (a) free TDF (b) Blank PLGA NPs (c) TDF PLGA NPs (d) triton X – 100 (Triton X) at 0.1, 1 and 10 µM concentrations. [a]Statistical significance observed at $P_{crit} < 0.001$ when compared to control; [b]Statistical significance observed at $P_{crit} < 0.05$ when compared to control; [c]Statistical significance observed for all the concentrations of triton X-100 at $P_{crit} < 0.05$ when compared to control; [#]No statistical significance observed at $P_{crit} > 0.05$ when compared to control. The values are expressed in terms of mean ± SD ($n = 5$).

5.3.7 Stability of TDF in mucosal homogenates of rats

In this study, we evaluated the percentage of the fraction of TMF formed for each sample when compared to the TMF formed in the case of free TDF and represented it as %TMF formed. The %TMF formed in TDF loaded PLGA NPs was significantly lower ($P_{cal} < 0.001$) when compared to free TDF and physical mixture of TDF and PLGA as shown in fig. 5.11. Further, there was no significant difference ($P_{cal} > 0.999$) in the %TMF formed between free TDF and physical mixture of TDF and PLGA.

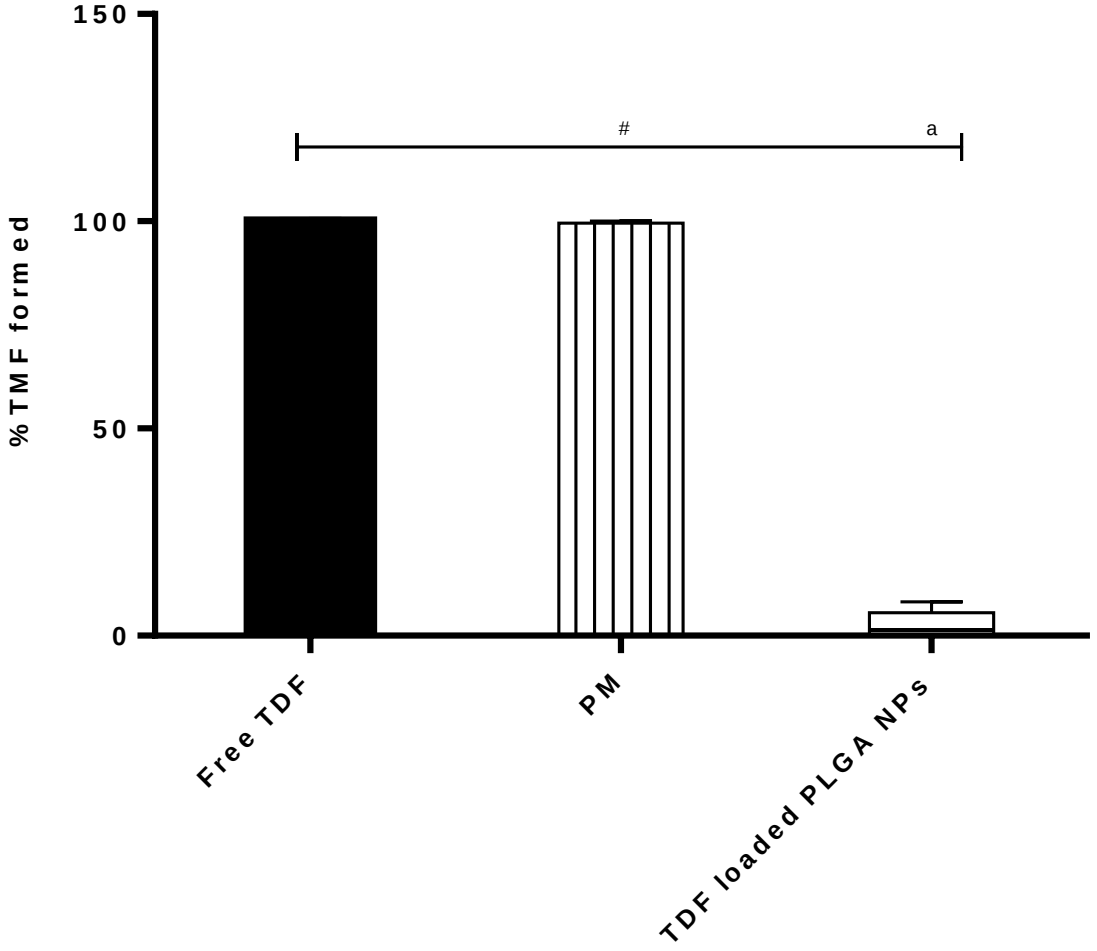

Fig. 5.11: Metabolic stability of TDF in the rat intestinal mucosal washings determined by calculating %TMF formed after an incubation period of 30 min for (a) free TDF (b) physical mixture of TDF and PLGA 50:50 (PM); (c) TDF loaded PLGA NPs. [a]Statistical significance observed at $P_{crit} < 0.001$ when compared to free TDF; [#]No statistical significance observed at $P_{crit} > 0.05$ when compared to free TDF. The values are expressed in terms of mean ± SD (n = 5).

These results indicate a significant level of metabolic protection of TDF by the PLGA NPs when exposed to the esterases present in the mucosal cells of the intestinal washings. However, the presence of PLGA in the physical mixture of TDF and PLGA did not prevent the esterase metabolism of TDF. Hence, the metabolic protection is due to the entrapment of TDF in the PLGA NPs thereby preventing the exposure of TDF to the metabolic enzymes and not due to the presence of PLGA.

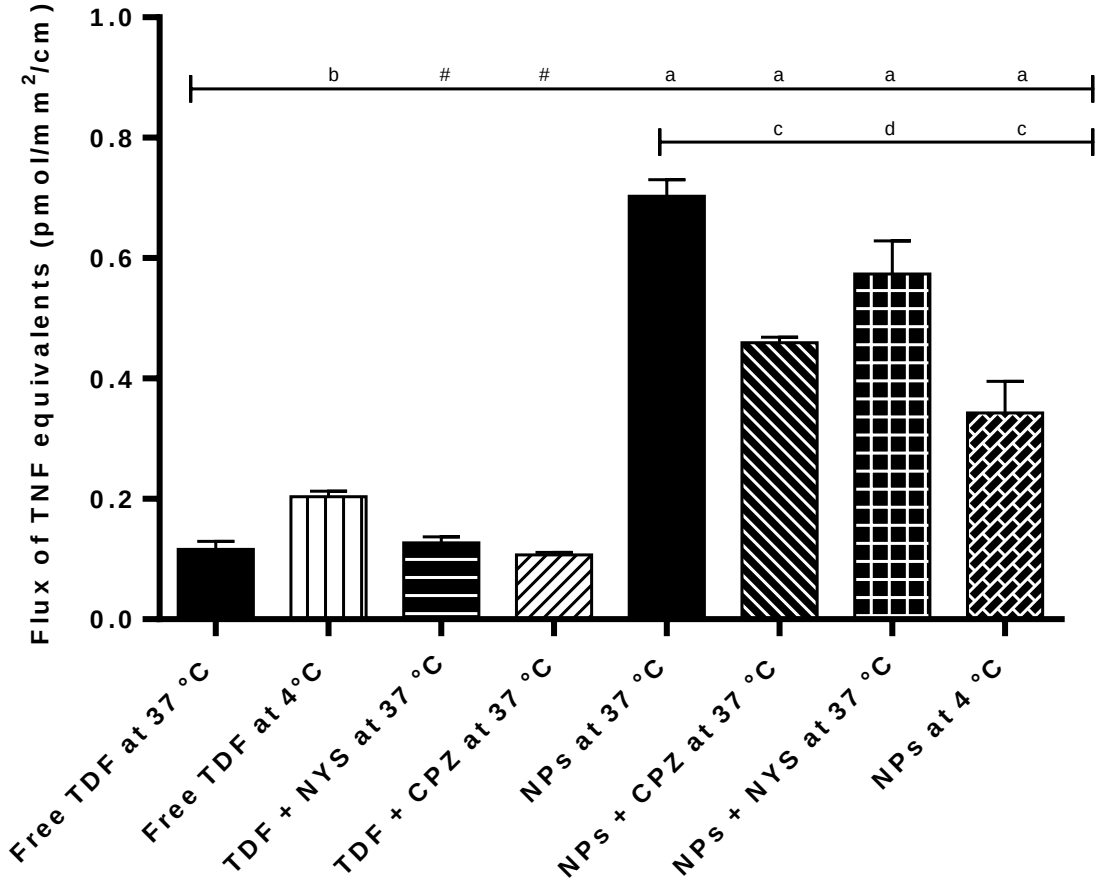

Fig. 5.12: Intestinal flux of TNF equivalents for free TDF and TDF loaded PLGA NPs incubated at 37 °C and 4 °C and with chlorpromazine (CPZ) and nystatin (NYS). [a]Statistical significance observed at $P_{crit} < 0.001$ when compared to TDF at 37 °C; [b]Statistical significance observed at $P_{crit} < 0.05$ when compared to TDF at 37 °C; [c]Statistical significance observed at $P_{crit} < 0.001$ when compared to NPs at 37 °C; [d]Statistical significance observed at $P_{crit} < 0.01$ when compared to NPs at 37 °C; [#]No statistical significance observed at $P_{crit} > 0.05$ when compared to TDF at 37 °C. The values are expressed in terms of mean ± SD ($n = 3$).

5.3.8 Everted gut sac studies in rats

In this study, both TDF and TMF were present in some of the receiver compartments. Hence, the transport of precursors of TNF were collectively represented in terms of flux (J) of TNF equivalents with the help of the following equation:

$$J = \frac{(dQ/dt)}{A}$$

Where, ‘dQ/dt’ is the amount of drug traversed into the receiver chamber per unit time and ‘A’ is the area of the intestinal sac exposed to the drug media.

The PLGA NPs increased (P_{cal} < 0.001) the *J* (0.70 ± 0.03 pmol/cm/min) of TNF equivalents across the everted intestinal sac by 5 fold when compared to free TDF (0.116 ± 0.013 pmol/cm/min) as shown in fig. 5.12. The role of active transport in the uptake of TNF equivalents across the intestine was evaluated by incubating the free TDF and TDF loaded PLGA NPs at 4 °C. The results showed a significant decrease (P_{cal} < 0.001) in the uptake of PLGA NPs (0.34 ± 0.05 pmol/cm/min) at 4 °C. However, there was a significant increase (P_{cal} = 0.024) in the *J* of TNF equivalents from free TDF (0.204 ± 0.009 pmol/cm/min) at 4 °C. This increased absorption of TNF equivalents for free TDF at 4 °C could be attributed to the decrease in the esterase activity at lower temperatures which explains the decreased conversion of TDF to TMF and TDF having better absorption characteristics could increase the *J* of TNF equivalents across the gut wall. Therefore, we can conclude that the intestinal transport of free TDF is predominantly via passive diffusion. However, in the case of TDF loaded PLGA NPs, active uptake played a prominent role because of which there was a significant decrease in the *J* at 4 °C (when the energy-dependent uptake mechanisms become dormant) when compared to its *J* at 37 °C. The major active transport pathways involved in the uptake of NPs include clathrin and caveolae-mediated pathways. Their role in the uptake of TDF loaded PLGA NPs were evaluated by incubating the NPs with chlorpromazine (CPZ) and nystatin (NYS) which specifically inhibit the clathrin and caveolae-mediated pathways respectively (Platel et al., 2016; Tariq et al., 2015). The results showed that there was a significant decrease in the uptake of TNF equivalents in the presence of both CPZ (0.46 ± 0.09 pmol/cm/min; P_{cal} < 0.001) and NYS (0.57 ± 0.05 pmol/cm/min; P_{cal} = 0.007), however, the extent of decrease in the uptake of TNF equivalents was higher when the NPs were incubated with CPZ indicating that the uptake of PLGA NPs is predominantly via clathrin-mediated pathway. The observations from

our work correlated well with previously published works that evaluated the active uptake mechanisms involved in the transport of PLGA NPs. Further, the role of Peyer's patches in the uptake of the designed NPs cannot be ruled out, as it has been well documented that PLGA NPs has affinity towards getting taken up into Peyer's patches via M cells (Ermak, Dougherty, Bhagat, Kabok, & Pappo, 1995; Hariharan et al., 2006; Shakweh, Besnard, Nicolas, & Fattal, 2005).

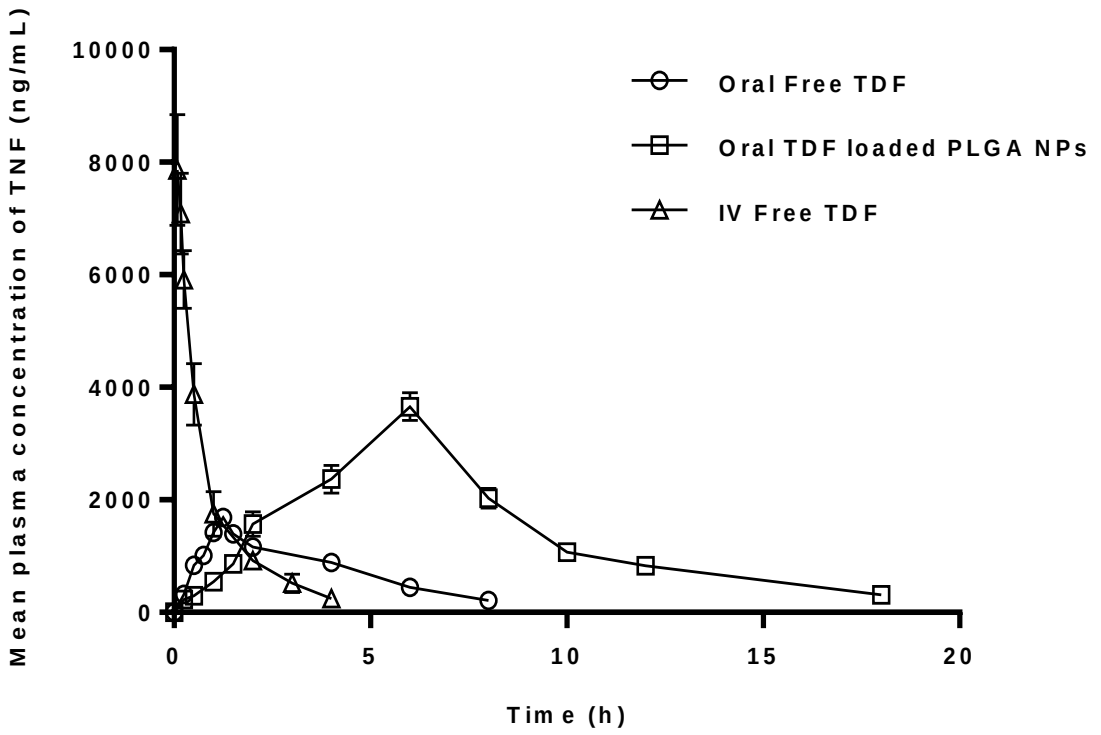

Fig. 5.13: Pharmacokinetic profile of free TDF (IV and oral) and TDF loaded PLGA NPs (oral). Each value is represented as mean ± SD (n = 5).

5.3.9 In vivo pharmacokinetic studies

For evaluating the effectiveness of PLGA NPs in increasing the systemic uptake of TNF as compared to free TDF *in vivo* oral pharmacokinetic studies were carried out for the optimized TDF loaded PLGA NPs and free TDF. Table 5.5 shows the pharmacokinetic parameters of TNF and fig. 5.13 shows the plasma time course of TNF obtained following oral and IV administration of free TDF and oral administration of TDF loaded PLGA NPs.

Table 5.5. Pharmacokinetic parameters (mean ± SD) of TNF after non-compartmental analysis for free TDF (22 mg/kg – IV and 100 mg/kg – oral) and TDF-PLGA NPs (equivalent to 100 mg/kg of TDF – oral).

PK Parameter	Treatment group		
	Free TDF, IV	Free TDF, oral	TDF loaded PLGA NPs, oral
Tmax (h)	---	1.00-1.50	4.00–6.00
C_0 (ng/mL)	7862.61 ± 979.6	---	---
C_{max} (ng/mL)	---	1687.53 ± 119.4	3657.41 ± 246.9[b]
AUC_{total} (h*ng/mL)	6240.13 ± 353.6	4020.93 ± 56.9	27318.89 ± 972.3[a]
MRT (h)	1.13 ± 0.06	3.11 ± 0.18	8.29 ± 0.18[a]
F_{abs}	---	0.14	0.97[a]
F_{rel}	---	---	6.79

The values represented are mean ± SD (n = 5). [a]Statistical significance observed at $P_{crit} < 0.001$ when compared to oral free TDF; [b]Statistical significance observed at $P_{crit} < 0.01$ when compared to oral free TDF.

The non-compartmental analysis of the pharmacokinetic profiles of TDF loaded PLGA NPs and free TDF showed a significant increase in the total area under the curve of the rat plasma profile of TNF (AUC_{total}) and maximum plasma concentration of TNF (C_{max}) of TDF loaded PLGA NPs ($P_{cal} < 0.001$) with a 5.8 fold and 1.2 fold increase in the AUC_{total} and C_{max} values respectively when compared to free TDF. The absolute oral bioavailability (F_{abs}) of free TDF was 0.14 and that of TDF loaded PLGA NPs to be 0.97 with a relative oral bioavailability (F_{rel}) of 6.79 (when compared to oral free TDF). Further, there was a 1.7 fold increase in the mean residence time (MRT) of TDF loaded PLGA NPs when compared to free TDF.

The oral pharmacokinetic studies show the poor oral absorption of TDF in the free form which is predominantly due to its extensive metabolic conversion to its monoester form by intestinal esterases that has relatively poor intestinal absorption characteristics. However, there was a substantial enhancement in the systemic uptake of TDF loaded PLGA NPs which is attributed to the ability of the NPs to provide metabolic protection for TDF and also to the better permeability characteristics of the designed NPs. Further, energy dependent internalization mechanisms were also be involved. Additionally, the significant increase ($P_{cal} < 0.001$) in the MRT of the NPs which apparently can be attributed to an increase in the mean absorption of

time and also an increase in the systemic residence of the PLGA NPs. Hence, the results of this study shows the efficiency of the designed TDF loaded PLGA NPs in improving the oral pharmacokinetic properties of TNF along the oral route.

5.4 Conclusion

The present study suggests that the TDF loaded PLGA NPs could be prepared with the help of emulsification (of the immiscible solvent in the aqueous phase) followed by solvent evaporation (of the immiscible phase) technique. The critical factors were identified with the help of a low-resolution factorial design (PBD). Further, NPs with minimum PS and maximum possible EE% could be achieved by understanding the interactive effects of the critical factors with the help of response surface methodology (by using BBD). Apart from providing control release of TDF *in vitro*, the optimized NPs were found to be stable, non-cytotoxic and were able to provide metabolic protection of TDF in the intestine. The *in vivo* pharmacokinetic studies showed the ability of the NPs to enhance the oral absorption of TDF with a higher residence time in rats. The *ex vivo* everted gut sac studies indicated clathrin-mediated endocytosis played a major role in the uptake of TDF. However, the role other active uptake mechanisms cannot be ruled out. Hence, this study shows the ability of the designed NPs to circumvent the low and erratic oral absorption of TDF thereby, providing better therapeutic action for the patients.

References

Astete, C. E., & Sabliov, C. M. (2006). Synthesis and characterization of PLGA nanoparticles. *Journal of Biomaterials Science. Polymer Edition*, *17*(3), 247–89.

Barzegar-Jalali, M., Adibkia, K., Valizadeh, H., Shadbad, M. R. S., Nokhodchi, A., Omidi, Y., … Hasan, M. (2008). Kinetic analysis of drug release from nanoparticles. *Journal of Pharmacy & Pharmaceutical Sciences*, *11*(1), 167–77.

Cohen-Sela, E., Chorny, M., Koroukhov, N., Danenberg, H. D., & Golomb, G. (2009). A new double emulsion solvent diffusion technique for encapsulating hydrophilic molecules in PLGA nanoparticles. *Journal of Controlled Release*, *133*(2), 90–95.

Cheow, W. S., & Hadinoto, K. (2010). Enhancing encapsulation efficiency of highly water-soluble antibiotic in poly(lactic-co-glycolic acid) nanoparticles: Modifications of standard nanoparticle preparation methods. *Colloids and Surfaces A: Physicochemical and Engineering Aspects*, *370*(1), 79–86.

Crauste-Manciet, S., Huneau, J. F., Decroix, M. O., Tomé, D., Farinotti, R., & Chaumeil, J. C. (1997). Cefpodoxime proxetil esterase activity in rabbit small intestine: A role in the partial cefpodoxime absorption. *International Journal of Pharmaceutics*, *149*(2), 241–249.

Danhier, F., Ansorena, E., Silva, J. M., Coco, R., Le Breton, A., & Préat, V. (2012). PLGA-based nanoparticles: An overview of biomedical applications. *Journal of Controlled Release*, *161*(2), 505–522.

Dillen, K., Vandervoort, J., Van den Mooter, G., Verheyden, L., & Ludwig, A. (2004). Factorial design, physicochemical characterisation and activity of ciprofloxacin-PLGA nanoparticles. *International Journal of Pharmaceutics*, *275*(1–2), 171–87.

Ermak, T. H., Dougherty, E. P., Bhagat, H. R., Kabok, Z., & Pappo, J. (1995). Uptake and transport of copolymer biodegradable microspheres by rabbit Peyer's patch M cells. *Cell and Tissue Research*, *279*(2), 433–6.

Feng, S., & Huang, G. (2001). Effects of emulsifiers on the controlled release of paclitaxel (Taxol) from nanospheres of biodegradable polymers. *Journal of Controlled Release*, *71*(1), 53–69.

Food and Drug Administration, HHS. (2003). International Conference on Harmonisation; Stability Data Package for Registration Applications in Climatic Zones III and IV; Stability Testing of New Drug Substances and Products; availability. Notice. *Federal Register*, *68*(225), 65717–8.

Ghasemian, E., Vatanara, A., Rouholamini Najafabadi, A., Rouini, M. R., Gilani, K., & Darabi, M. (2013). Preparation, characterization and optimization of sildenafil citrate loaded PLGA nanoparticles by statistical factorial design. *Daru : Journal of Faculty of Pharmacy, Tehran University of Medical Sciences*, *21*(1), 68.

Hariharan, S., Bhardwaj, V., Bala, I., Sitterberg, J., Bakowsky, U., & Ravi Kumar, M. N. V. (2006). Design of estradiol loaded PLGA nanoparticulate formulations: a potential oral delivery system for hormone therapy. *Pharmaceutical Research*, *23*(1), 184–95.

Joshi, G., Kumar, A., & Sawant, K. (2014). Enhanced bioavailability and intestinal uptake of Gemcitabine HCl loaded PLGA nanoparticles after oral delivery. *European Journal of Pharmaceutical Sciences*, *60*, 80–9.

Kapoor, D. N., Bhatia, A., Kaur, R., Sharma, R., Kaur, G., & Dhawan, S. (2015). PLGA: a unique polymer for drug delivery. *Therapeutic Delivery*, *6*(1), 41–58.

Li, P., Callery, P. S., Gan, L. S., & Balani, S. K. (2007). Esterase inhibition attribute of grapefruit juice leading to a new drug interaction. *Drug Metabolism and Disposition*, *35*(7), 1023–1031.

Mainardes, R. M., & Evangelista, R. C. (2005). PLGA nanoparticles containing praziquantel: effect of formulation variables on size distribution. *International Journal of Pharmaceutics*, *290*(1–2), 137–44.

Mittal, G., Sahana, D. K., Bhardwaj, V., & Ravi Kumar, M. N. V. (2007). Estradiol loaded PLGA nanoparticles for oral administration: effect of polymer molecular weight and copolymer composition on release behavior in vitro and in vivo. *Journal of Controlled Release*, *119*(1), 77–85.

Murakami, H., Kobayashi, M., Takeuchi, H., & Kawashima, Y. (1999). Preparation of poly(DL-lactide-co-glycolide) nanoparticles by modified spontaneous emulsification solvent diffusion method. *International Journal of Pharmaceutics*, *187*(2), 143–52.

Plapied, L., Duhem, N., des Rieux, A., & Préat, V. (2011). Fate of polymeric nanocarriers for oral drug delivery. *Current Opinion in Colloid & Interface Science*, *16*(3), 228–237.

Platel, A., Carpentier, R., Becart, E., Mordacq, G., Betbeder, D., & Nesslany, F. (2016). Influence of the surface charge of PLGA nanoparticles on their *in vitro* genotoxicity, cytotoxicity, ROS production and endocytosis. *Journal of Applied Toxicology*, *36*(3), 434–444.

Quintanar-Guerrero, D., Fessi, H., Allémann, E., & Doelker, E. (1996). Influence of stabilizing agents and preparative variables on the formation of poly(d,l-lactic acid) nanoparticles by an emulsification-diffusion technique. *International Journal of Pharmaceutics*, *143*(2), 133–141.

Ravi, P. R., Aditya, N., Kathuria, H., Malekar, S., & Vats, R. (2014). Lipid nanoparticles for oral delivery of raloxifene: Optimization, stability, in vivo evaluation and uptake mechanism. *European Journal of Pharmaceutics and Biopharmaceutics*, *87*(1), 114–124.

Ravi, P. R., Joseph, S., Avula, U. S. R., & Anthireddy, S. (2015). A Simple Liquid Chromatographic Method for the Determination of Tenofovir in Rat Plasma and Its Application to Pharmacokinetic Studies. *Acta Chromatographica*, *27*(4), 597–612.

Sadat Tabatabaei Mirakabad, F., Nejati-Koshki, K., Akbarzadeh, A., Yamchi, M. R., Milani, M., Zarghami, N., … Joo, S. W. (2014). PLGA-based nanoparticles as cancer drug delivery systems. *Asian Pacific Journal of Cancer Prevention : APJCP*, *15*(2), 517–35.

Sah, E., & Sah, H. (2015). Recent Trends in Preparation of Poly(lactide- *co* -glycolide) Nanoparticles by Mixing Polymeric Organic Solution with Antisolvent. *Journal of Nanomaterials*, *2015*, 1–22.

Sahay, G., Alakhova, D. Y., & Kabanov, A. V. (2010). Endocytosis of nanomedicines. *Journal of Controlled Release*, *145*(3), 182–95.

Shakweh, M., Besnard, M., Nicolas, V., & Fattal, E. (2005). Poly (lactide-co-glycolide) particles of different physicochemical properties and their uptake by peyer's patches in mice. *European Journal of Pharmaceutics and Biopharmaceutics*, *61*(1–2), 1–13.

Singh, S., & Muthu, M. S. (2007). Preparation and characterization of nanoparticles containing an atypical antipsychotic agent. *Nanomedicine*, *2*(2), 233–240.

Singh, G., & Pai, R. S. (2014). Optimized PLGA nanoparticle platform for orally dosed trans-resveratrol with enhanced bioavailability potential. *Expert Opinion on Drug Delivery*, *11*(5), 647–59.

Tariq, M., Alam, M. A., Singh, A. T., Iqbal, Z., Panda, A. K., & Talegaonkar, S. (2015). Biodegradable polymeric nanoparticles for oral delivery of epirubicin: In vitro, ex vivo, and in vivo investigations. *Colloids and Surfaces B: Biointerfaces*, *128*, 448–456.

Yue, P.-F., Lu, X.-Y., Zhang, Z.-Z., Yuan, H.-L., Zhu, W.-F., Zheng, Q., & Yang, M. (2009). The Study on the Entrapment Efficiency and In Vitro Release of Puerarin Submicron Emulsion. *AAPS PharmSciTech*, *10*(2), 376–383.

Chapter 6

Conclusions

6.1 Conclusions

TDF having diester linkages in its structure is susceptible to esterases which decreases its oral absorption. There are many ingredients rich in ellagitannins and polyphenols that have many ester based structures. We attempted to evaluate the impact of such food ingredients on the oral pharmacokinetics of TDF as the structures present in such foods may competitively inhibit the esterases and prevent the metabolism of TDF. This constituted the pharmacokinetic approach for enhancing the oral bioavailability of TDF.

Nanotechnology has become an integral part of drug delivery research. Nanotechnology based products have overcome several diverse limitations of existing drugs and hence expanded the therapeutic horizon of such molecules. By designing a suitable nanocarrier system, the delivery system can reach and maintain therapeutically beneficial drug levels and access body sites that are inaccessible with conventional formulations. In the current work, we attempted to design and optimize two polymeric nanocarrier systems for TDF to enhance its oral bioavailability, one nanocarrier system contained a polymer from a natural source and the other contained a synthetic polymer. This constituted the nanocarrier formulation approach for enhancing the oral bioavailability of TDF.

Development of robust analytical techniques is essential for food-drug interaction studies and formulation development. Therefore, analytical methods for the estimation of TDF, TMF and TNF were developed and extensively validated. The methods were found to be selective towards the analyte of interest and were successfully employed in the analysis of samples originating from different studies that were conducted. Methods to quantify the drug in the body fluids are essential pre-requisite for *in vivo* studies. Therefore, a bioanalytical method for analysis of TNF in plasma was developed and validated using HPLC. The bioanalytical method was successfully employed for quantifying TNF in biological samples originating from

pharmacokinetic studies conducted in rats. The method was found to be adequately sensitive and selective towards the drug.

The interaction studies of TDF with the pharmaceutical excipients shows that only C-EL could provide a significant metabolic protection of TDF from esterase metabolism but, none of the excipients could significantly alter the oral pharmacokinetic properties of TDF. The interaction study of TDF with FJs rich in ester based structures indicated that the FJs could inhibit the conversion of TDF to TMF by esterases. However, among the FJs tested CBJ, GFJ, PJ and RGFJ could consistently alter the oral absorption of TDF in the studies conducted. These observations suggest that the ability of the components of these FJs to prevent the metabolic process of TDF especially within the gut wall plays a crucial role in increasing the intestinal absorption of TDF. As more amount of the drug was present in the diester form, which has better permeability characteristics. These observations correlated well in all the studies i.e. *in vitro* esterase inhibition, *ex vivo* everted gut sac and *in vivo* oral pharmacokinetic studies. GFJ and PJ had the most impact on the oral absorption of TDF with a 150% and 99% increase in the AUC_{total} values.

NPs for TDF were prepared using CS and crosslinking it with STPP. CS is biodegradable and can load drugs having diverse physicochemical properties, hence was chosen as a Polymeric carrier for TDF during the design of NPs. To optimize the manufacturing conditions, a hybrid-design approach was used. This design comprised of a low-resolution screening design (Plackett–Burman design) and a higher resolution Box-Behnken design which is a part of response surface methodology. This unique approach helped in selection and optimization of few important factors from many possible factors that could affect the properties of the NPs. The optimized formulations were subjected to *in vitro, ex vivo* and *in vivo* evaluation. From the characterization results, it was found that TDF loaded CS NPs were spherical in shape with a PS of 156 ± 5 nm and had good entrapment efficiency (48.2 ± 1.0%). The entrapped TDF was

most likely present in the amorphous form in the NPs. The accelerated stability studies showed no significant change in the different parameters estimated for the duration of the study. The *in vitro* release studies showed the ability of the designed NPs to provide controlled release of TDF. The cytotoxicity studies indicated the non-toxic nature of the designed NPs. The mucoadhesion studies performed (both *in vitro* and *ex vivo*) showed that the designed NPs had the ability to adhere to the intestinal mucous membrane. The esterase inhibition studies showed the ability of the designed NPs to provide metabolic protection for TDF in the presence of esterases. The *ex vivo* everted gut sac studies showed the ability of the NPs to be taken up by active endocytic pathways predominantly via clathrin-mediated uptake, the CS NPs increased the flux of TNF equivalents by 3.6 fold when compared to free TDF. *In vivo*, pharmacokinetic studies in male Wistar rats showed that NPs could improve oral bioavailability of TDF by 380% when compared to free drug. Therefore, it was concluded that the designed NPs were promising dosage forms to improve oral bioavailability of TDF.

For the preparation of PLGA based NPs, o/w emulsification followed by evaporation method was found suitable. The hybrid-design approach was found suitable to identify the critical variables and understand the interaction effects of the critical variables on PS and EE%. Experimental results showed that the optimized TDF loaded PLGA NPs were near spherical in shape with a PS of 218 nm and with good EE% (57%). The DSC and pXRD studies indicated that TDF most likely existed in the TDF loaded PLGA NPs in amorphous form. The NPs were stable in accelerated conditions for three months. The *in vitro* release studies showed that the drug release was both dissolution and diffusion dependent. The cytotoxicity studies indicated that the designed NPs decreased the cell viability only at very high concentrations making the NPs safe for administration to animals for testing. The *in vitro* esterase inhibition studies indicated that PLGA based NPs could provide metabolic protection for TDF when exposed to intestinal esterases, but PLGA inherently did not have any esterase inhibition property. This

indicated that the protection provided is primarily due to the entrapment of TDF within the NPs. From the *ex vivo* uptake studies using everted gut sac model, it was found that TDF loaded PLGA NPs were taken up by both clathrin and caveolae-mediated endocytic pathways. However, the role of clathrin-mediated uptake was more prominent. From the *in vivo* oral pharmacokinetics study in male Wistar rats, it was evident that oral bioavailability of TDF after incorporation into PLGA NPs improved by 5.8 folds compared to free drug. In conclusion, PLGA based NPs seemed to be promising drug delivery systems that could significantly ($P < 0.05$) enhance the oral bioavailability of TDF.

6.2 Future scope and directions

In both the cases, the developed nanocarrier systems were stable under accelerated conditions. A significant improvement in oral bioavailability of TDF was noticed. However, PLGA based nanoparticles showed a higher degree of oral absorption enhancement of TDF when compared to CS based nanoparticles. The significant improvement in oral bioavailability was attributed to protection of entrapped TDF from intestinal esterase metabolism and improvement in both active and passive uptake of TDF from the GIT.

Appendix

LIST OF PUBLICATIONS (From Thesis Work)

1. **Shailender Joseph,** Punna Rao Ravi, Paramita Saha, Srividya Myneni. Oral pharmacokinetic interaction of ester rich fruit juices and pharmaceutical excipients with tenofovir disoproxil fumarate in male Wistar rats. *Xenobiotica*, 2016; DOI: 10.1080/00498254.2016.1269375

2. Punna Rao Ravi, **Shailender Joseph,** Uday Sai Ranjan Avula and Shruthi Anthireddy. Development and validation of a simple and sensitive LC assay for determination of tenofovir in rat plasma and its application in pharmacokinetic studies. *Acta Chromatographica*, 2015; 27: 597–612.

LIST OF PUBLICATIONS (Outside Thesis Work)

1. Punna Rao Ravi, Rahul Vats, **Shailender Joseph,** and Nitin Gadekar. Development and validation of simple, rapid and sensitive LC-PDA ultraviolet method for quantification of nebivolol in rat plasma and its application to pharmacokinetic studies. *Acta Chromatographica*, 2015; 27: 281–294.

WORKS UNDER COMMUNICATION (From Thesis Work)

1. Effect of Ester Rich Fruit Juices on the Oral Pharmacokinetics of Tenofovir Disoproxil Fumarate in Male Wistar Rats. *Iranian Journal of Pharmaceutical Sciences*. **Status: Under Review.**

2. Chitosan nanoparticles for the oral delivery of tenofovir disoproxil fumarate: Formulation optimization, characterization and ex vivo and in vivo evaluation for uptake mechanism in rats. *Drug development and Industrial Pharmacy*. **Status: Under Review.**

3. Tenofovir disoproxil fumarate loaded PLGA nanoparticles for enhanced oral absorption: Effect of experimental variables and in-vitro, ex-vivo and in-vivo evaluation. *Colloids and surfaces. B: Biointerfaces*. **Status: Under Review.**

LIST OF CONFERENCE PRESENTATIONS (From Thesis Work)

1. **Shailender Joseph,** Paramita Saha, Avantika Dalvi, Srividya Myneni, Punna Rao Ravi. "Tenofovir disoproxil fumarate loaded PLGA nanoparticles for enhanced oral absorption: Effect of experimental variables and in vitro, in vivo and ex vivo evaluation" at PEAR-2017, JNTU, Hyderabad.

2. **Shailender Joseph,** Mrinalini Reddy, Keerthi Priya Odapalli, Punna Rao Ravi. "Oral pharmacokinetic interaction of ester rich fruit juices and pharmaceutical excipients with tenofovir disoproxil fumarate in male Wistar rats" at ICCD3–2017, BITS-Pilani, Pilani Campus.

3. Srividya Myneni, **Shailender Joseph,** Keerti Priya, Punna Rao Ravi. "Effect of pharmaceutical excipients on intestinal permeability of ester prodrug tenofovir disoproxil fumarate" at 66th IPC, Hyderabad.

4. **Joseph S.,** Avula U.S.R., Anthireddy S., Ravi P.R. "Development and validation of novel and sensitive LC assay for determination of tenofovir in rat plasma and its application in pharmacokinetic studies" at 65th IPC, Delhi.

LIST OF CONFERENCE PRESENTATIONS (Outside Thesis Work)

1. **Shailender Joseph,** Sekar VasanthaKumar, R.N. Saha "Design and study of levofloxacin oral controlled release formulations" at CTPS-2011, BITS-Pilani, Hyderabad.

2. Sekar Vasantha Kumar, **Shailender Joseph,** Rashid Ali, R.N Saha "Immediate release tablets of risperidone using superdisintegrants: formulation and evaluation". Presented the work in 62nd IPC, Manipal.

WORKSHOPS

1. 8th PAGIN workshop on "Data Analysis using NONMEM" at The Advanced Centre for Treatment, Research and Education in Cancer (ACTREC) Mumbai held from 1st–3rd August 2016.

2. "Revolution drug development in India and pharmacometrics training" organized by population approach group of India (PAGIN) held from 22nd – 24th July 2015 at PSG institute of medical sciences and research, Coimbatore.

3. Participated and presented a mock research proposal in a workshop on global health "3rd Winter Institute of Global Health" which addressed the challenges faced in healthcare delivery worldwide, jointly organized by BITS-Pilani, Hyderabad campus and Apollo institute of medical sciences and research on 17th – 25th of January, 2015.

Biography of Prof. Punna Rao Ravi

Prof. Punna Rao Ravi is working as Associate Professor in Department of Pharmacy, BITS-Pilani, Hyderabad Campus. He obtained his B.Pharm, M.Pharm and PhD degrees in Pharmaceutical Sciences from BITS-Pilani University, Rajasthan. He has been working as a faculty member in BITS-Pilani since year 2000. He has many publications in reputed international and national peer-reviewed journals and has presented papers in scientific conferences both in India and abroad. He has successfully completed government sponsored research projects and is expecting more grants from scientific funding agencies.

Biography of Mr. Shailender Joseph

Mr. Shailender Joseph has completed his B.Pharm and M.Pharm (with specialization in pharmaceutics) from BITS-Pilani, Pilani Campus, Rajasthan. Immediately after his M.Pharm he joined BITS-Pilani, Hyderabad campus as a full-time PhD scholar in July 2011. He has authored/co-authored research papers in renowned international peer-reviewed journals. He has also presented scientific posters/papers in reputed international and national conferences.

Digital Receipt

This receipt acknowledges that Turnitin received your paper. Below you will find the receipt information regarding your submission.

The first page of your submissions is displayed below.

Submission author:	Shailender Joseph
Assignment title:	Tenofovir Disoproxil Fumarate
Submission title:	Study on Pharmacokinetic and Nan…
File name:	00_Thesis_merge.pdf
File size:	7.36M
Page count:	211
Word count:	53,369
Character count:	263,163
Submission date:	04-May-2017 08:17AM
Submission ID:	809325355

Study on Pharmacokinetic and Nanocarrier Formulation Approaches for Improving the Oral Bioavailability of Tenofovir Disoproxil Fumarate in the Effective Treatment of HIV/AIDS

THESIS

Submitted in partial fulfilment
of the requirements for the degree of
DOCTOR OF PHILOSOPHY

by

SHAILENDER JOSEPH

ID. No. 2011PHXF019H

Under the Supervision of

Prof. PUNNA RAO RAVI

BITS Pilani
Pilani | Dubai | Goa | Hyderabad

BIRLA INSTITUTE OF TECHNOLOGY AND SCIENCE
PILANI (RAJASTHAN) INDIA
2017

Study on Pharmacokinetic and Nanocarrier Formulation Approaches for Improving the Oral Bioavailability of Tenofovir Disoproxil Fumarate in the Effective Treatment of HIV/AIDS

THESIS

Submitted in partial fulfilment

of the requirements for the degree of

DOCTOR OF PHILOSOPHY

by

SHAILENDER JOSEPH

ID. No. 2011PHXF019H

Under the Supervision of

Prof. PUNNA RAO RAVI

BITS Pilani

Pilani | Dubai | Goa | Hyderabad

BIRLA INSTITUTE OF TECHNOLOGY AND SCIENCE

PILANI (RAJASTHAN) INDIA

2017

Chapter 6

Conclusions

6.1 Conclusions

TDF having diester linkages in its structure is susceptible to esterases which decreases its oral absorption. There are many ingredients rich in ellagitannins and polyphenols that have many ester based structures. We attempted to evaluate the impact of such food ingredients on the oral pharmacokinetics of TDF as the structures present in such foods may competitively inhibit the esterases and prevent the metabolism of TDF. This constituted the pharmacokinetic approach for enhancing the oral bioavailability of TDF.

Nanotechnology has become an integral part of drug delivery research. Nanotechnology based products have overcome several diverse limitations of existing drugs and hence expanded the therapeutic horizon of such molecules. By designing a suitable nanocarrier system, the delivery system can reach and maintain therapeutically beneficial drug levels and access body sites that are inaccessible with conventional formulations. In the current work, we attempted to design and optimize two polymeric nanocarrier systems for TDF to enhance its oral bioavailability, one nanocarrier system contained a polymer from a natural source and the other contained a synthetic polymer. This constituted the nanocarrier formulation approach for enhancing the oral bioavailability of TDF.

Development of robust analytical techniques is essential for food-drug interaction studies and formulation development. Therefore, analytical methods for the estimation of TDF, TMF and TNF were developed and extensively validated. The methods were found to be selective towards the analyte of interest and were successfully employed in the analysis of samples originating from different studies that were conducted. Methods to quantify the drug in the body fluids are essential pre-requisite for *in vivo* studies. Therefore, a bioanalytical method for analysis of TNF in plasma was developed and validated using HPLC. The bioanalytical method was successfully employed for quantifying TNF in biological samples originating from

pharmacokinetic studies conducted in rats. The method was found to be adequately sensitive and selective towards the drug.

The interaction studies of TDF with the pharmaceutical excipients shows that only C-EL could provide a significant metabolic protection of TDF from esterase metabolism but, none of the excipients could significantly alter the oral pharmacokinetic properties of TDF. The interaction study of TDF with FJs rich in ester based structures indicated that the FJs could inhibit the conversion of TDF to TMF by esterases. However, among the FJs tested CBJ, GFJ, PJ and RGFJ could consistently alter the oral absorption of TDF in the studies conducted. These observations suggest that the ability of the components of these FJs to prevent the metabolic process of TDF especially within the gut wall plays a crucial role in increasing the intestinal absorption of TDF. As more amount of the drug was present in the diester form, which has better permeability characteristics. These observations correlated well in all the studies i.e. *in vitro* esterase inhibition, *ex vivo* everted gut sac and *in vivo* oral pharmacokinetic studies. GFJ and PJ had the most impact on the oral absorption of TDF with a 150% and 99% increase in the AUC_{total} values.

NPs for TDF were prepared using CS and crosslinking it with STPP. CS is biodegradable and can load drugs having diverse physicochemical properties, hence was chosen as a Polymeric carrier for TDF during the design of NPs. To optimize the manufacturing conditions, a hybrid-design approach was used. This design comprised of a low-resolution screening design (Plackett–Burman design) and a higher resolution Box-Behnken design which is a part of response surface methodology. This unique approach helped in selection and optimization of few important factors from many possible factors that could affect the properties of the NPs. The optimized formulations were subjected to *in vitro, ex vivo* and *in vivo* evaluation. From the characterization results, it was found that TDF loaded CS NPs were spherical in shape with a PS of 156 ± 5 nm and had good entrapment efficiency (48.2 ± 1.0%). The entrapped TDF was

most likely present in the amorphous form in the NPs. The accelerated stability studies showed no significant change in the different parameters estimated for the duration of the study. The *in vitro* release studies showed the ability of the designed NPs to provide controlled release of TDF. The cytotoxicity studies indicated the non-toxic nature of the designed NPs. The mucoadhesion studies performed (both *in vitro* and *ex vivo*) showed that the designed NPs had the ability to adhere to the intestinal mucous membrane. The esterase inhibition studies showed the ability of the designed NPs to provide metabolic protection for TDF in the presence of esterases. The *ex vivo* everted gut sac studies showed the ability of the NPs to be taken up by active endocytic pathways predominantly via clathrin-mediated uptake, the CS NPs increased the flux of TNF equivalents by 3.6 fold when compared to free TDF. *In vivo*, pharmacokinetic studies in male Wistar rats showed that NPs could improve oral bioavailability of TDF by 380% when compared to free drug. Therefore, it was concluded that the designed NPs were promising dosage forms to improve oral bioavailability of TDF.

For the preparation of PLGA based NPs, o/w emulsification followed by evaporation method was found suitable. The hybrid-design approach was found suitable to identify the critical variables and understand the interaction effects of the critical variables on PS and EE%. Experimental results showed that the optimized TDF loaded PLGA NPs were near spherical in shape with a PS of 218 nm and with good EE% (57%). The DSC and pXRD studies indicated that TDF most likely existed in the TDF loaded PLGA NPs in amorphous form. The NPs were stable in accelerated conditions for three months. The *in vitro* release studies showed that the drug release was both dissolution and diffusion dependent. The cytotoxicity studies indicated that the designed NPs decreased the cell viability only at very high concentrations making the NPs safe for administration to animals for testing. The *in vitro* esterase inhibition studies indicated that PLGA based NPs could provide metabolic protection for TDF when exposed to intestinal esterases, but PLGA inherently did not have any esterase inhibition property. This

indicated that the protection provided is primarily due to the entrapment of TDF within the NPs. From the *ex vivo* uptake studies using everted gut sac model, it was found that TDF loaded PLGA NPs were taken up by both clathrin and caveolae-mediated endocytic pathways. However, the role of clathrin-mediated uptake was more prominent. From the *in vivo* oral pharmacokinetics study in male Wistar rats, it was evident that oral bioavailability of TDF after incorporation into PLGA NPs improved by 5.8 folds compared to free drug. In conclusion, PLGA based NPs seemed to be promising drug delivery systems that could significantly ($P < 0.05$) enhance the oral bioavailability of TDF.

6.2 Future scope and directions

In both the cases, the developed nanocarrier systems were stable under accelerated conditions. A significant improvement in oral bioavailability of TDF was noticed. However, PLGA based nanoparticles showed a higher degree of oral absorption enhancement of TDF when compared to CS based nanoparticles. The significant improvement in oral bioavailability was attributed to protection of entrapped TDF from intestinal esterase metabolism and improvement in both active and passive uptake of TDF from the GIT.